TOM VELDKAMP

QUATERNARY RIVER TERRACE FORMATION IN THE ALLIER BASIN, FRANCE.

a reconstruction based on sand bulk geochemistry and 3-D modelling.

Promotor: Dr. S.B. Kroonenberg
Hoogleraar in de geologie en mineralogie

A. Veldkamp

QUATERNARY RIVER TERRACE FORMATION IN THE ALLIER BASIN, FRANCE.

a reconstruction based on sand bulk geochemistry and 3-D modelling.

Proefschrift
Ter verkrijging van de graad van doctor
in de landbouw- en milieuwetenschappen
op gezag van de rector magnificus,
dr. H.C. van der Plas,
in het openbaar te verdedigen
op woensdag 18 december 1991
des middags te half twee in de Aula
van de Landbouwuniversiteit te Wageningen.

ISN: 5511 66.

"Niet alle tijdgenoten bewonen dezelfde tijd. Het verleden verandert voortdurend, maar slechts weinigen beseffen dat."

"In mijn hele heelal heb ik nooit een onverbiddelijke onveranderlijke natuurwet aangetroffen. Dit heelal vertoont uitsluitend veranderende verhoudingen die soms door een kort-levende bewustzijn als wetten worden gezien."
De gestolen verslagen van Leto II Atreides, in: God emperor of Dune, F. Herbert, 1981.

Op de voorkant van dit proefschrift staat een kopie van de oudste kaart van het studiegebied (Limagne). Deze werd gemaakt in 1560 door Florentin Simeoni.

Aan mijn ouders en Marga

STELLINGEN

1 Met bulkgeochemische karakterisering van fluviatiele sedimenten kunnen geochemische en fluviatiele processen kwantitatief en statistisch verantwoord worden gereconstrueerd.

Dit Proefschrift

Kroonenberg, S.B, Moura, M.L. & Jonker, A.T.J., 1988, Geochemistry of the sands of the Allier river terraces, French Massif Central, Geologie en Mijnbouw 66:297-311.

2 Geomorfologische processen kunnen beschrijvend worden gesimuleerd met behulp van 'finite state modelling'.

Dit Proefschrift

3 De aanwezigheid van vruchtbare landbouwgronden ('terre noire' Gachon, 1963) in de Limagne is het indirekte gevolg van deglaciatie gedurende het Laat Pleniglaciaal.

Dit Proefschrift

Gachon, L., 1963, Contribution à l'étude du Quaternaire récent de la Grande Limagne marnocalcaire: morphogenèse et pédogenèse, Annales agronomiques, vol 14, no hors série 1.

4 Het alluviaal-stratigrafisch model van Bridge & Leeder (1979) zou realistischer zijn als het rekening hield met fluviatiele versnijding als gevolg van opheffing.

Dit Proefschrift

Bridge, J.S. & Leeder M.R., 1979, A simulation model of alluvial stratigraphy, Sedimentology, 26:617-644

5 Aangezien de kennis omtrent de Kwartaire dynamiek van het klimaat veel nauwkeuriger is dan die van de tektoniek, vormt de laatste de meest beperkende factor voor realistische modellering van terrasvorming.

Dit Proefschrift

6 De uitgestrekte Keniaanse planatievlakken zijn niet gevormd door pediplanatie-processen zoals beschreven door L.C. King, (1962).

King, L.C., 1962, The morphology of the earth. Oliver and Boyd, London.

7 Doordat er steeds meer bodemkundig onderzoek plaatsvindt zonder of met te weinig veldwerk, bestaat het gevaar dat bodemkundigen steeds meer moeite hebben om op verschillende schaalnivo's 4-D te denken.

8 Zowel de informatica als de statistiek zijn slechts werktuigen binnen de geowetenschappen, iets wat steeds meer collega's lijken te vergeten.

9 Miall's omschrijving (1983) van de ideale fluviatiele specialist van de jaren tachtig als: 'A Quaternary sedimentologist with experience in petroleum geology and river engineering, a passion for hydraulics, statistics and scuba diving, a more than passing interest in tectonics and a lot of money for coring equipment, combined with a good knowledge of biostratigraphy, palaeomagnetism, geochemistry, petrology, pedology, palaeoclimatology and structural geology" is toch nog incompleet voor de jaren negentig door de opkomst van modellering als onderzoekstechniek.

Miall, A.D., 1983, Basin analysis of fluvial sediments. Spec. Publs Int. Ass. Sediment. 6: 279-286.

10 Judo is de weg naar het doeltreffendst gebruik van zowel lichamelijke als geestelijke kracht.

Jigoro Kano

11 Op een geologische tijdschaal gezien is het menselijk gedrag en handelen net zo voorspelbaar als dat van iedere andere levensvorm, omdat het voortbestaan van de soort de belangrijkste drijfveer is.

12 Lood zal een nog groter milieuprobleem worden in Frankrijk zolang de Fransen hun uitgesproken voorkeur behouden voor wijndrinken, jagen en autorijden.

13 Het is onwaarschijnlijk dat het huidige plateau van Gergovie ook daadwerkelijk de plaats is waar Julius Ceasar in 52 AD door de Galliers is verslagen.

Stellingen behorende bij het proefschrift van A. Veldkamp: **Quaternary river terrace formation in the Allier basin, France:** a reconstruction based on sand bulk geochemistry and 3-D modelling.

VOORWOORD

Met dit proefschrift worden vier interessante jaren bijna volledig gewijd aan onderzoek bekroond. Natuurlijk staan die vier jaar niet los van de voorafgaande 24 jaren in mijn leven. Ik wil dan ook allereerst mijn ouders bedanken voor hun stimulering gedurende mijn studie. Met name mijn middelbare schooltijd heeft hun helaas meer dan alleen voldoening geschonken. Vervolgens wil ik al die mensen bedanken die een rol hebben gespeeld in mijn wetenschappelijke ontwikkeling en niet hieronder worden genoemd. Het in dit proefschrift beschreven onderzoek is het resultaat van een gezamelijke inspanning wat tot uitdrukking komt in de namen van de co-auteurs van de opgenomen publicaties en manuscripten.

Salle Kroonenberg wil ik bedanken voor de grote vrijheid die hij mij gaf bij de invulling en uitvoering van het onderzoek. Zijn aanstekelijk enthousiasme en optimisme heb ik altijd als stimulerend ervaren.

Ik ben Mario Moura zeer erkentelijk want het was hij die mij heeft ingewerkt op het gebied van de zandgeochemie. Verder heb ik met veel plezier samen gewerkt met Toine Jongmans, Tom Feijtel, Igor Staritsky, Ab Jonker, Piet Oosterom, Alfred Stein, Ed Meijer en Nico van Breemen binnen het kader van het VF project Frankrijk (VF86-09 en VF89-71). Binnen dit project hebben vele studenten in de Limagne hun veldwerk uitgevoerd ik wil met name Paul Römkens, Loes Janssen en Margot Spreuwenberg bedanken voor hun bijdrage aan het geochemische onderzoek. Tijdens mijn veldwerk heb nuttige assistentie gehad van mijn broer Ed en niet te vergeten mijn ouders welke niet te beroerd waren om vele zandmonsters te zeven.

Ton Engelsma wil ik bedanken voor het gedogen van mijn labatorium aktiviteiten en Bram Kuijper en Jan Huiting voor het uitvoeren van de XRF analyses van mijn 500 zandmonsters. Jan van Doesburg was altijd bereid om van een onbekende mineraal een röntgendiffractogram te maken. In ben J. van der Plicht en Henk Heijnis van de Rijksuniversiteit Groningen erg erkentelijk voor het zorgdragen voor de ^{14}C en Th/U dateringen. Antje Weitz heeft zowel de Zusammenfassung als enige tekeningen gemaakt. Piet Versteeg en andere medewerkers van de tekenkamer Biotechnion

worden hartelijk bedankt voor het maken van de vele figuren in dit proefschrift. Verder wil ik mijn (ex)kamergenoten, medekoffiedrinkers en andere collega's bedanken voor de prettige en informele sfeer.

Stephan Vermeulen ben ik veel dank verschuldigd voor het mede ontwikkelen van het eerste rivierterrassen model gedurende de eindfase van onze studie. Waarbij we zeer plezierige begeleiding hebben gehad van Prof. Dr. A.J. Udink ten Cate en Prof. Ir M.S. Elzas van de vakgroep informatica. Gerda Lenselink en Meindert van den Berg zijn voor mij zeer plezierige collega's die altijd open staan voor diepgaande vakinhoudelijke discussies.

Jannick Legeat is thanked for his enthusiastic support and interest in my research in the Limagne.

Het Sportinstituut Wageningen wil ik danken voor de mogelijkheden om mijn agressie op een gekontroleerde manier te kunnen afreageren.

De Vakgroep Bodemkunde en Geologie wordt bedankt voor het beschikbaar stellen van een stationeringsplaats, ondanks beginproblemen heb ik mijn stationeringsperiode toch als prettig ervaren.

De gepresenteerde onderzoekingen werden gesteund door de Stichting Aardwetenschappelijk Onderzoek Nederland (AWON) met subsidie van de Nederlandse organisatie voor zuiver Wetenschappelijk Onderzoek (NWO), (Project no 751.358.009, Geochemie en sedimentpetrografie van rivierafzettingen in de Limagneslenk Centraal Massief, Frankrijk).

Totslot wil ik Marga mijn vrouw bedanken voor het regelmatig willen lezen, meedenken en aanhoren van mijn hersenspinsels.

PUBLICATIONS

The chapters 2.2 through 4.2 were of will be published as separate papers, with some modifications. These papers have been adapted and slightly revised to fit the format of this thesis. The following papers form the basis of this thesis:

2.2: Veldkamp, A. & Kroonenberg, S.B., (subm). The Late Quaternary terrace chronology of the Allier (Limagne, France). Quaternaire.

2.3: Veldkamp, A., & Jongmans, A.G., (subm). Trachytic pumice clasts in Middle Pleistocene Allier terrace deposits (Limagne, France): A chronostratigraphical marker. Quaternaire.

3.1: Veldkamp, A., & Kroonenberg S.B., (in press) The application of bulk sand geochemistry in Quaternary research. A methodological study of the Allier and Dore terrace sands (Limagne, France). Applied Geochemistry.

3.2: Veldkamp, A., & Feijtel, T.C., (in press) Parent material controlled subsoil weathering in the Allier terraces (Limagne, France). Catena.

3.3: Veldkamp, A. & Staritsky, I.G., (in press) Spatial variability in fluvial terrace sand composition at the Allier/Dore confluence (Limagne, France). Geomorphology.

3.4: Veldkamp, A., (subm) Climate controlled sediment fluxes in the Allier basin (Limagne, France) during the Late Quaternary. Quaternary Research.

4.1: Veldkamp, A., & Vermeulen, S.E.J.W., 1989, River terrace formation, modelling and 3-D graphical simulation. Earth Surface Processes and Landforms. Vol 14, 641-654.

4.2: Veldkamp, A., (in press). A 3-D model of fluvial terrace development in the Allier basin (Limagne, France). Earth Surface Processes and Landforms.

SUMMARY

The research presented in this thesis is focussed on a quantitative reconstruction of the effects of past environmental dynamics within a fluvial system. The study area is part of the Allier basin (Limagne) in the Auvergne, Massif Central, France.

The research was carried out in several stages. At first field work was carried out to determine the terrace stratigraphy and chronology in more detail. A new age estimate of the Fva (65 m above present river bed) is based on pumice clasts found in the terrace sediments. Younger terraces were dated with ^{14}C and Th/U disequilibrium methods. Fx terrace sediments (15 and 10 m above present river bed) were mainly deposited during the Late Weichselian, while the Fwb terrace sediments (25 m above present river bed) have most probably a Late Saalian age. Due to these new age estimates a revision of the existing Allier terrace chronology is necessary. This new chronology shows a large time gap between the deposition of the Fv and Fw terrace sediments.

Next, sands of various terrace units were collected and bulk geochemically measured with XRF. This bulk geochemical research allowed a statistically significant discrimination of different terrace levels. The processes which shape and shaped the actual sand geochemistry were successfully quantified. It was found that grain size has only a very limited effect on bulk geochemical variability while longitudinal sorting processes and weathering have a stronger impact on actual sediment composition. Although the effects of parent material controlled weathering in the Allier sands were successfully modelled, the older terrace sediments are unsuitable for paleoenvironmental reconstructions. Such a reconstruction was done for the Weichselian and Holocene terrace deposits at the Allier/Dore confluence. The sediment mixing behaviour of these rivers is estimated by calculating sediment mixing ratios. This reconstruction started with an investigation of spatial mixing effects of Allier and Dore sediments in time by means of mapping and geostatistics. Results suggest an environmental

control over the spatial variability of sediment mixing at this confluence in time. The reconstructed relative sediment fluxes of the Allier in time show a good correspondence with known past environments. Relative Allier sediment fluxes seem mainly climate controlled whereby large fluvio-glacial fluxes at the end of a glacial played a dominant role in the Allier system. These large sediment fluxes in the Allier system caused a strong rise in the Allier riverbed level contributing to the development of lake basins (Marais) in Grande Limagne.

Further a large scale and long term model of terrace formation was constructed using finite state modelling. This methodology allows the construction of a general 3-D terrace formation model containing as well quantitative as qualitative knowledge on fluvial systems. Finally, an adapted version for the Allier (LIMTER) is made incorporating all present knowledge on this system. LIMTER allows the formulation and evaluation of long term terrace formation scenarios for the Allier system. Simulation results suggest that terrace stratigraphy in the study area is mainly the result of the internal Allier dynamics and climatic change. Local tectonism caused the development of unpaired terraces while the general regional uplift played a dominant role in terrace formation and preservation in general.

The terrace research as presented in this thesis shows that it is well possible for any fluvial system to simulate the interaction climate/tectonism and fluvial dynamics. The for the Allier simulated dynamics, net sedimentation during and at the end of a Glacial and net dissection during an Interglacial has no general validity.

SAMENVATTING

Het onderzoek dat in dit proefschrift wordt beschreven heeft als hoofddoel om een kwantitatieve reconstructie te maken van de gevolgen van veranderende milieu-omstandigheden gedurende het Kwartair in een riviersysteem. Het studiegebied is het Allierstroomgebied (de Limagne) gelegen in de Auvergne, Massif Central te Frankrijk.

Het onderzoek is gefaseerd uitgevoerd. Allereerst is er voornamelijk veldwerk uitgevoerd om de terrassenstratigrafie en hun ontstaansgeschiedenis beter uit te zoeken. Zo werd een nieuwe leeftijdsschatting voor het Fv-terras (65 m boven huidige rivier) verkregen door de vondst van een bepaald type puimsteen in de terrassedimenten. De jongere terrassen zijn radiometrisch gedateerd met behulp van de koolstof 14 methode en de Thorium/Uranium niet- evenwichtmethode. Zo weten we nu dat de Fx-terrassedimenten gelegen tussen de 15 en 10 m boven de huidige rivier, vooral tijdens het Laat Weichelien zijn afgezet, terwijl het Fwb terras (25 m boven de huidige rivier) zeer waarschijnlijk een Laat Saalien leeftijd heeft. Als gevolg van deze nieuwe dateringen werd een revisie van de bestaande Allier terrassenchronologie noodzakelijk. Deze nieuwe chronologie heeft een groot tijdshiaat tussen de afzetting van de Fv en Fw-terrassedimenten.

Vervolgens zijn de zanden van de verschillende terrassen en terraseenheden bemonsterd en geochemisch gemeten. Dit bulkgeochemisch onderzoek laat een statistisch significant onderscheid zien tussen de verschillende terrasnivo's. Bovendien zijn hiermee de processen die de actuele terras-zandsamenstelling bepalen of bepaalden goed te kwantificeren. Het blijkt dat zandkorrelgrootte slechts een beperkte invloed heeft op de bulkgeochemische samenstelling terwijl stroomafwaardse sortering en verwering na afzetting een groter effect hebben of hadden op de huidige zandsamenstelling. Ondanks dat de verwering van de Allier terrassedimenten goed gemodelleerd kon worden, zijn de sedimenten van de oudere verweerde terrassen ongeschikt om milieuomstandigheden uit het verleden te reconstrueren. Een dergelijke reconstructie is wel gedaan aan

de Weichselien en Holocene sedimenten bij de samenvloeiing van Allier en Dore. Het sedimentmenggedracht van deze rivieren in het verleden is onderzocht door een zogenaamde sediment-mengratio te berekenen. Om deze reconstructie mogelijk te maken is eerst een onderzoek uitgevoerd naar de ruimtelijke variabiliteit van het sedimentmenggedrag met behulp van karteren en geostatistiek. De resultaten suggereren sterk dat ook de ruimtelijke variabiliteit van riviersedimenten gerelateerd is aan de rivierdynamiek. De gereconstrueerde relatieve sedimentfluxen van de Allier correleren erg sterk met milieuveranderingen in het verleden. Vooral klimaatsveranderingen lijken de sedimentstromen in de Allier sterk te hebben bepaald. Grote fluvio-glaciale sedimentstromen aan het eind van een lange koude periode (Glaciaal) zijn erg dominant geweest in het Allier systeem. Een indirekt gevolg van deze grote sedimentstromen is het ontstaan van meerbekkens in de Limagne door een sterke stijging in beddinghoogte als gevolg van de grote sedimentaanvoer.

Vervolgens is een grootschalig lange termijn model gemaakt met behulp van 'finite state' modelleren dat terrasvorming driedimensionaal simuleert. Door 'finite state' modelleren kan een model worden gemaakt dat zowel beschrijvende als gemeten kennis bevat. Dit algemene model is vervolgens voor de Allier aangepast (LIMTER). LIMTER is een conceptueel model voor het opstellen en evalueren van terrasvormings-scenario's binnen het Allier systeem. Simulatieresultaten laten zien dat de terrasstratigrafie in het studiegebied voornamelijk het gevolg is van interne fluviatiele dynamiek en klimatologische veranderingen in de tijd. Lokale tektoniek veroorzaakte het ontstaan van ongepaarde terrassen terwijl de algemene regionale opheffing een dominante rol heeft gespeeld bij de conservering van terrassen in de tijd.

Het in dit proefschrift gepresenteerde terrasonderzoek laat zien dat het goed mogelijk is in een fluviatiel systeem de interaktie klimaat/tektoniek en fluviatiele dynamiek semi-kwantitatief te reconstrueren. De voor de Allier gesimuleerde dynamiek van netto sedimentatie gedurende en aan het eind van een glaciaal gevolgd door netto interglaciale versnijding heeft geen algemene geldigheid.

RESUME

L'étude décrite dans cette thèse a pour objectif principal d'établir une reconstitution quantitative des conséquences dues aux changements climatiques durant le Quaternaire dans un bassin versant. La région étudiée est le bassin versant de l'Allier, la Limagne, située en Auvergne, dans le Massif Central.

L'étude a été effectuée en plusieurs phases. La première phase a été principalement une phase de travail sur le terrain, pour déterminer la stratigraphie des terrasses et la chronologie de leur formation. Une nouvelle estimation de l'âge de la terrasse Fv (65m au-dessus de la rivière actuelle) a pu être obtenue grâce à la découverte d'un certain type de pierre ponce dans les sédiments de la terrasse. Les terrasses plus récentes ont été datées par radiométrie à l'aide de la méthode du Carbone 14 et de celle du déséquilibre Thorium/Uranium. Nous savons ainsi que les sédiments de terrasses Fx qui se trouvent entre 10 et 15 m au-dessus de la rivière actuelle ont été déposés principalement vers la fin de la glaciation de Würm, alors que la terrasse Fwb (25 m au-dessus de la rivière actuelle) date très probablement de la fin de la glaciation du Riss. Cette nouvelle datation a nécessairement entraîné une révision de la chronologie existante des terrasses de l'Allier. La nouvelle chronologie révèle un grand intervalle entre les formations des sédiments des terrasses Fv et Fw.

Au cours de la deuxième phase, des échantillons des sables de différents groupes de terrasses ont été prélevés, et ont ensuite été soumis à une analyse géochimique. Cette analyse de l'ensemble des échantillons montre une différence statistique significative entre les différents niveaux de terrasses. En outre, elle permet de quantifier correctement les procédés qui déterminent ou ont déterminé la composition actuelle des sables des terrasses. Il s'avère que la grosseur des grains de sable n'a qu'une influence limitée sur la composition géochimique de l'ensemble des échantillons, alors que le tri et l'altération en aval qui se sont produits après la déposition, ont ou avaient plus d'effet sur la composition actuelle. S'il était tout à fait possible de

simuler l'altération des sédiments des terrasses de l'Allier, il s'avère que les sédiments de terrasses dégradées plus anciennes ne sont pas adaptés à la reconstitution des circonstances environnementales du passé. Une telle reconstitution a toutefois été exécutée pour les sédiments de la Glaciation de Würm et de l'Holocène déposés au confluent de l'Allier et de la Dore. Le schéma du mélange des sédiments de ces deux rivières dans le passé a été étudié en calculant ce qu'on appelle le taux de mélange des sédiments. Pour pouvoir effectuer cette reconstitution, il a d'abord fallu réaliser une étude de la variabilité spatiale du schéma de mélange des sédiments en s'aidant de la cartographie et de la géostatistique. Les résultats suggèrent que la variabilité spatiale des sédiments des rivières est liée à la dynamique de la rivière. La reconstitution des courants de sédiments relatifs de l'Allier montre une grande concordance avec les changements environnementaux du passé. Il semble que ce soient les changements climatiques qui aient principalement déterminé les courants de sédiments dans l'Allier. Dans le bassin de l'Allier, ce sont les grands courants de sédiments fluvio-glaciaires de la fin d'une longue période glaciaire qui ont été prédominants. Une conséquence indirecte de ces grands courants de sédiments est l'apparition de dépressions lacustres en Limagne due à une forte élévation du lit de la rivière résultant de l'important apport de sédiments.

Ensuite un modèle à long terme et à grande échelle a été élaboré à l'aide du modèle 'Finite State' pour la simulation en trois dimensions de la formation des terrasses. Grâce a cette méthode, il a été possible de créer un modèle qui pouvait inclure aussi bien les données descriptives que les données quantitatives. Ce modèle général a ensuite été adapté aux conditions de l'Allier (LIMTER). LIMTER permet la formulation et l'évaluation des scénarios de formation des terrasses de l'Allier. Les résultats de simulation montrent que la stratigraphie des terrasses de la région étudiée sont principalement la conséquence d'une dynamique fluviatile interne et de changements climatiques. La tectonique locale a occasionné l'apparition de terrasses non-couplées alors que le relèvement régional général a joué un rôle dominant dans la conservation des

terrasses à travers les âges.

La présente étude montre qu'il est tout à fait possible de reconstituer de façon semi-quantitative l'interaction entre climat/tectonique et dynamique fluviatile dans un système fluviatile. La dynamique, simulée ici pour l'Allier, de la sédimentation nette pendant et à la fin d'une période glaciaire, suivie de la dissection nette interglaciaire n'est pas valable dans tous les cas.

ZUSAMMENFASSUNG

Die mit dieser Promotionsschrift vorgestellte Untersuchung beschäftigt sich mit der quantitativen Rekonstruktion der Auswirkungen während des Quartärs veränderter Umweltbedingungen auf ein fluviales System. Das Untersuchungsgebiet ist Teil des in der Auvergne gelegenen Allierbeckens (Limagne), Massif Central, Frankreich.

Die Untersuchung wurde in verschiedenen Phasen durchgeführt. Zuerst erfolgten Geländearbeiten, die eine detaillierte Bestimmung der Terassenstratigraphie und -chronologie ermöglichten. Eine neue Alterseinstufung der Fva(Fv)-Terasse (65 m über dem heutigen Flussniveau gelegen) konnte aus dem Fund eines bestimmten Bimssteintypes in den Terassensedimenten abgeleitet werden. Jüngere Terassen wurden radiometrisch mit Hilfe der 14C- und der Thorium/Uranium-Ungleichgewichtsmethode datiert. Es konnte nachgewiesen werden, dass die Fx-Terassensedimente, die zwischen 10 und 15 m über dem heutigen Flussniveau liegen, hauptsächlich im Verlauf der späten Weichselvereisung abgelagert wurden. Dagegen lassen sich die Fwb-Terassensedimente, die 25 m über dem heutigen Flussniveau liegen, mit grösster Wahrscheinlichkeit als spät saaleeiszeitlich datieren. Auf Grund dieser neuen Datierungen wurde eine Revision der bestehenden Allierterassenchronologie notwendig. Die neue Chronologie zeigt eine grössere Zeitdifferenz zwischen der Absetzung der Fv- und der Fw-Terassensedimente.

Desweiteren wurden Sandproben verschiedener Terassen und Terasseneinheiten gesammelt und mittels Röntgenfluoreszensanalyse (RFA) geochemisch untersucht. Die Kenntnis der gesamten geochemischen Zusammenstellung der Sedimente erlaubt eine statistisch signifikante Unterscheidung der verschiedenen Terassenniveaus. Ausserdem lassen sich hiermit die Prozesse, die die aktuelle Terassensandzusammenstellung bestimmen bzw. bestimmten, gut quantifizieren. Es zeigte sich, dass die Korngrösse der Sande nur begrenzten Einfluss auf deren gesamte geochemische Komposition hat, wogegen longitudinale Sortierungsprozesse und Verwitterung nach der Sedimentation grösseren Einfluss auf die heutige Sandzusammenstellung haben

bzw. hatten. Trotzdem der Verwitterungsverlauf der Allierterassensedimente gut modelliert werden konnte, eignen sich die Sedimente der älteren, verwitterten Terassen nicht, um die Paläomilieubedingungen zu rekonstruieren. Eine derartige Rekonstruktion erfolgte für die weichselzeitlichen und holozänen Terassenablagerungen des Allier/Dore Zusammenflusses. Das in der Vergangenheit gezeigte Sedimentmischungsverhalten dieser Flüsse wurde mittels Schätzung der Sedimentmischungsverhältnisse berechnet. Diese Rekonstruktion wurde durch eine Untersuchung der räumlichen Variabilität der Sedimentmischungseffekte der Allier und der Dore im Zeitverlauf ermöglicht. Dabei wurden Kartierungen und geostatistische Arbeitstechniken benutzt. Die Ergebnisse suggerieren, dass die räumliche Variabilität der Sedimentmischung im Zeitverlauf am Zusammenfluss stark von der zeitlichen Flussdynamik abhängig ist. Die rekonstruierten relativen Sedimentströme der Allier im Verlauf der Zeit korrespondieren gut mit bekannten Umweltdynamikenen der Vergangenheit. Der relative Sedimentstrom in der Allier scheint stark von klimatischen Veränderungen bestimmt zu sein. Die am Ende langer Vereisungsperioden auftretenden, grossen fluvio-glazialen Sedimentströme spielen eine dominante Rolle im Alliersystem. Eine indirekte Folge dieser grossen Sedimentströme ist das Entstehen der Seenbecken (Marais) in der Limagne, die durch starke Steigung der Strombetthöhe infolge starker Sedimentanfuhr gebildet werden.

Weiterhin wurde ein grossmasstäbiges Langzeitmodell der Terassenbildung mit Hilfe des 'finite state' Modellierungsansatzes erstellt. Diese Methode erlaubte es, die Terassenbildung dreidimensional zu simulieren, wobei sowohl quantitative als auch qualitative Informationen über fluviale Systeme verwendet werden. Im Anschluss daran wurde eine angepasste Version für das Alliersystem erstellt (LIMTER), dass alle verfügbare Information über dieses spezielle, fluviatile System enthält. Mit Hilfe von LIMTER können für das Alliersystem für lange Zeitspannen Terassenbildungsscenarios formuliert und evaluiert werden. Die Ergebnisse der Simulationsläufe zeigen, dass die Terassenstratigraphie im Untersuchungsgebiet hauptsächlich das Produkt interner Dynamiken im fluvialen Alliersystem sowie klimatischer Veränderungen ist. Lokale

Tektonik verursachte das Entstehen ungepaarter Terassen, wogegen allgemeine regionale Hebung eine dominante Rolle bei der generellen Erhaltung der Terassen bis in die rezente Zeit gespielt hat.

Die in dieser Promotionsschrift vorgestellte Untersuchung zeigt deutlich, dass es gut möglich ist, in einem fluviatilen System die Interaktion zwischen Klima und Tektonik einerseits und fluviatiler Dynamiken andererseits semiquantitativ zu rekonstruieren. Die für das Alliersystem simulierte Dynamik, als deren Charakteristiken überwiegende Sedimentation während und am Ende einer Vereisung und überwiegende Relief-verschneidung während der Interglaziale definiert werden, hat keine Allgemeingültigkeit.

CONTENTS

Chapter 1 **INTRODUCTION**

The global environment is subject to constant changes. Lately these global climatic changes have received much attention from the media. There is great and growing concern about the global environment, such as the accelerating increase in global greenhouse gases (CO_2, CH_4, CFC's etc) which may lead to a new global climate which will be warmer and more turbulent with associated sea level rise, etc. Other concerns are less well understood, irritant problems like ozone holes, increase ground level u.v. radiation, acid rain, all of which may have profound influence on ecosystems and biomass productivity.

In order to understand the future we have to study the past. A way to understand potential impacts of such global changes is to study analogue situations in the past. When one is interested in the nearby future one has to study short term variations in the past as proposed during the latest INQUA congress in Beijing. If one wants to get a more complete picture of the overall mechanisms of the global environmental changes one has to study paleoenvironmental dynamics on a geological time scale. Such overall studies can give important clues about the possible human impact on the earth environment.

The best studied past environments up to now are the deep sea, the polar environment (ice cores) and the eolian continental situation (löss sections in China). These past environments are stored in long continuous sediments which represent long time series up to more than 2.4 million years ago. The direct effects of these global changes on the fluvial system are still poorly understood. The fluvial system in dynamic equilibrium is able to adjust itself to changes of external variables by changing its internal variables like channel depth and width, river roughness, mean velocity, channel form, and slope (Schumm, 1977; Dawson & Gardiner, 1987). River terraces are an essential part of the fluvial system and are former abandoned floodplains which are found as elongated plateaus along valley slopes above the present river bed. Their formation can be looked upon as a result of

changes in equilibrium, caused by variation in external variables (Dury, 1970; Léger, 1983). Three driving forces behind terrace formation are frequently cited: changes in climate, tectonism and base level. Both climate and tectonism play a significant role in terrace formation as almost no terraced valley is known without any change in both factors during the Quaternary. Base level changes have only importance in fluvial reaches between actual coasts and the shelf edges.

River terraces provide long, but fragmentary, continental records of changing geo-environments. From a morphometrical point of view terraces are quite simple features but from a sedimentological point of view they are very complex. Each terrace unit is made up of several stacked often incomplete sedimentary cycles, representing alternating depositional and erosional stages. The resulting terrace stratigraphy provides a relative chronology to which other geological, geomorphological or palaeohydrological events can be related (Dawson & Gardiner, 1987). Unfortunately the character of the fluvial record makes it impossible to give a continuous long term registration of the paleoenvironment. A multi-disciplinary approach is thus necessary to study the past dynamics of a fluvial system.

During the last ten years the number of palaeohydrological investigations increased considerably. Fluvial dynamics during the Late Quaternary have been studied by Starkel (1983), Dawson & Gardiner (1987), Gregory et al. (1987) etc. These studies used terrace sedimentology, stratigraphy, morphology, and radiometric datings as research methodologies. During geochemical investigations of fluvial sands in France (Kroonenberg et al., 1988) and The Netherlands (Moura & Kroonenberg, 1990) it was found that bulk geochemical sand composition can also serve as an excellent indicator of both sedimentary processes and long-term changes in sediment composition as a result of climatic and uplift history.

Another aspect of fluvial systems is that they are so complex, and develop on such long time spans, that laboratory experiments and real system measurements (e.g. Schumm et al., 1977) can only partly reveal part of their functioning. Computer simulation is

increasingly recognized as a novel way to understand the way geomorphic systems work (e.g. Anderson, 1988). Especially process oriented geomorphologists tend to model their measured processes more and more. On the other hand the need for models describing less well known and defined systems is also growing. A simulation purely focussed on river terrace formation was done by Boll et al. (1988). Their qualitative 2-D model is unfortunately unsuitable for quantitative applications.

The research presented in this thesis is focussed on a quantitative reconstruction of the effects of past environmental dynamics within a fluvial system. At first, river terrace sediments are investigated with bulk sand geochemistry and these quantitative results are used as inputs for a model simulating river terrace formation in a fluvial system as a function of climatic changes and vertical crustal movements.

The study area is a part of the Allier basin (Limagne) in the Auvergne, Massif Central, France. In this area many basic geomorphological data were already collected for a project of the Agricultural University Wageningen (VF86-90). The study area was thought as very suitable for this kind of research because the Allier and it tributaries have many terraces and relatively much of the Quaternary history is known due to the eventful volcanic history.

The research was carried out in three stages. A stage with mainly field work to sample and determine the terrace stratigraphy and chronology in more detail. A second phase with analyzing and processing sand bulk geochemical data, and a third and final stage dedicated to modelling the Allier Quaternary terrace formation.

This thesis contains eight papers which are all revised and edited to one format. The original papers are listed below.

The order of chapters is according to the three named stages.

Stage one. In chapter 2, the study area is briefly introduced

(2.1), followed by new observations and insights of the Allier Quaternary terrace stratigraphy and chronology (2.2, 2.3).

Stage two. Chapter 3, describes the application of bulk sand geochemistry as a tool in Quaternary terrace research (3.1), followed by a model of the impact of weathering in the Allier terrace sands (3.2). Fluvial dynamics and sand geochemistry are linked in section 3.3 and 3.4 where the spatial, longitudinal and time related dynamics of sediment fluxes in the Allier during the Late Weichselian are reconstructed.

Stage three. The complete integration of the current knowledge on long term dynamics of fluvial systems in general and the Allier system particularly is made in chapter 4. In section 4.1 a modelling methodology and the evolving conceptual 3-D model on fluvial terrace formation are discussed. In section 4.2 an adapted and extended model for the Allier system is presented and evaluated.

Finally, in chapter 5 a synthesis is made. The usefulness and validity of the research methodologies are discussed and evaluated followed by a regional evaluation.

Chapter 2

STUDY AREA AND THE ALLIER TERRACE CHRONOLOGY

The study area is situated in Central France and comprises the Allier drainage basin. The Allier drains the Limagne rift valley and the surrounding Hercynian crystalline Massif Central. The Allier basin has many different terrace levels witnessing former flood plain levels. One of the earliest papers on the Allier terraces in the Limagne graben dates back to 1917 (E. Chaput). Detailed information on all previous investigations on the Allier terraces can be found in J-F Pastre's thesis (Pastre, 1987).

2.1 STUDY AREA

Most information in this chapter is derived from review books. More details on the general geological setting can be found in Autran & Peterlongo (1980) and in Jung (1971). The geology of the study area is excellently mapped at a 1:50.000 scale by the BRGM (Bureau de Recherches Géologiques et Minières). The following rather detailed maps served as basis of the field investigations Vichy XXVI-29, Maringues XXVI-30, Thiers XXVI-31 , Clermont-Ferrand XXV-31. The general geological setting is shown in Fig 2.1.1. and the studied terraces are shown in Fig. 2.1.2.

The oldest parts in the Massif Central are Late Precambrian and Caledonian high grade metamorphic rocks as gneisses and granulites. The majority of the metamorphic rocks in the Massif Central were metamorphosed during the Hercynian orogeny. The majority of the rocks are gneisses and granites, but also Palaeozoic sedimentary rocks and acid volcanic rocks are locally found.

After the Hercynian orogeny prolonged denudation seems to have dominated. Some residual flint occurrences suggest Mesozoic sedimentation in the Massif Central but more substantial evidence is still lacking. During the Tertiary when the Alpine orogeny started, many grabens opened up in the Massif central like the Rhône, Loire and Limagne graben.

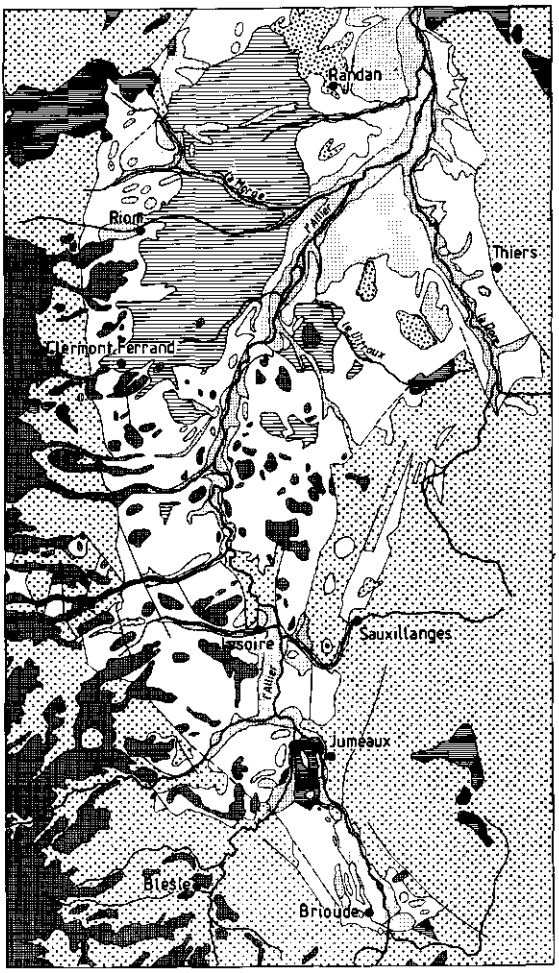

Figure 2.1.1. General geological setting of the study area

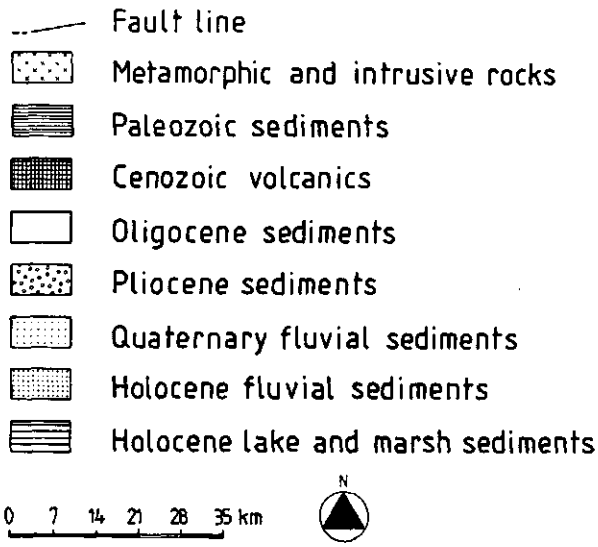

The sedimentary infill of these tectonic depressions started immediately. The Limagne rift valley which mainly developed during the Oligocene, was filled with marls, chalks, sands and clays during the Oligocene and Miocene. Meanwhile volcanism started along the active faulting zones from Miocene onwards to recent times. Cantal volcanism reached it climax between 9 and 6 million years ago, while the Mont Dore volcano had its most active phase between 3 and 1 million years ago. Late Quaternary and Holocene volcanism took place in the Chaîne des Puys.

2.1.1. The Allier and Dore basins

This study is mainly focussed on the terraces of the Allier and Dore rivers near their confluence (Fig 2.1.2). The Dore, draining the crystalline Forez, is a major Allier tributary. Other major tributaries are the Allagnon, draining the Cantal and Cézallier, and the Couze Pavin and Couze Chambon draining the Mont Dore region.

The Allier basin covers a surface of 14310 km^2 and has a mean annual discharge of 147 m^3/s. At the Allier Dore confluence the upstream Allier basin covers approximately 9000 km^2 while the Dore basin surface comprises 1250 km^2. The mean Allier discharge

at this confluence is 98 m^3/s and the mean Dore discharge 18 m^3/s (Pastre, 1987).

The Allier basin is underlain by both volcanic (22%) and crystalline basement rocks (58%), the Dore basin predominantly by crystalline basement (72%). Additionally, mainly basement-derived Oligocene sediments occur in both basins, 20% and 28% respectively.

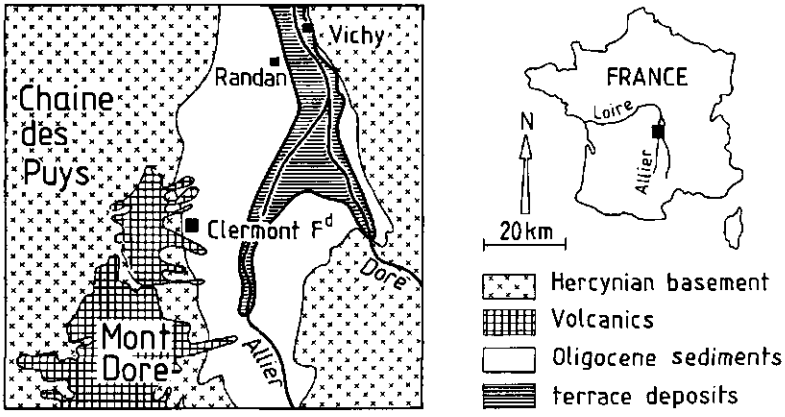

Figure 2.1.2. The studied Allier and Dore terraces.

The two basins differ also in geological history. Whereas the higher parts of the Allier basin, notably the Cantal and Mont Dore volcanoes, were subjected to severe glaciation (Veyret, 1980; Kieffer, 1971), the Dore basin has been largely free from glaciers, except for a very small part of the Forez (Etlicher et al. 1987).

Both rivers have about eight main terrace levels, numbered from Z (present river bed) to S (oldest terrace level). Including the different sub levels at least 14 different levels (Z, ZY, Y, YX, Xb, Xa, Wb, Wa, Vb, Va, Ub, Ua, T, S) can be distinguished.

The Allier terrace deposits are gravelly and sandy sediments poor in clay. The gravel composition reflects the different lithologies within the Allier basin. This composition is not linear correlated with basin lithology, the volcanic components

usually predominate while the Oligocene rocks are usually rare. Common heavy minerals of the Allier terraces are augite, green and brown hornblende, olivine, mica's and opaques (Van Dorsser, 1969; Rudel, 1963; Pelletier, 1971; Pastre 1986; Tourenq, 1986). The opaque component which can comprise more than 50% of the fine sand fraction, is predominantly composed of basaltic rock fragments (Kroonenberg et al., 1988). Larue (1977) studied the downstream changes in gravel petrology and Tourenq (1986) studied changes in heavy mineral content of the Allier terraces. Their results do not match well and are not comparable as they studied different specific fractions of the Allier sediments.

The heavy fraction of the Dore terrace sands (Van Dorsser, 1969; Pelletier, 1971; Tourenq, 1986; Van Wijck, 1985) consists essentially of mica's, tourmaline, zircon, opaques and augite. The occurrence of augite indicates some volcanic influence, but as volcanic bedrock is absent in the Dore basin, these minerals must originate from wind-blown ashes.

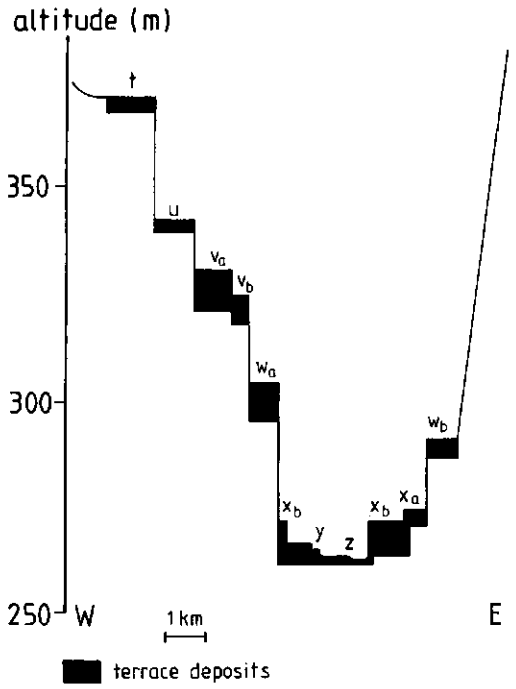

Figure 2.1.3. **The schematical cross section of terraces at Randan.**

2.1.2. Fluvial terrace formation in the Allier basin

As this study focuses on the fluvial Allier dynamics during the Quaternary a short overview of the current knowledge will be presented. Two major investigations were carried out on the fluvial sediments of the Allier terraces. Larue (1979) made the first thorough investigation on chrono-stratigraphy based on sediment composition while Pastre (1987) focussed on the heavy sand mineral assemblies in order to correlate and date the different terrace deposits by relating sand mineralogy with the mineralogy of dated eruptions. Both Larue and Pastre studied the whole Allier basin.

One of the most complete terrace sequences in the Allier basin is found near Randan (Clozier et al., 1980). This chronosequence displays at least ten terrace levels, shown schematically in the cross-section of Fig. 2.1.3. The oldest terrace level in this sequence, T is thought to be about 2 million years old (Pastre, 1987).

There are two existing terrace chronologies (Fig. 2.1.4.) one established by Larue (1979) and one by Pastre (1986, 1987). Both authors used indirect ways of correlating terraces with a certain age.

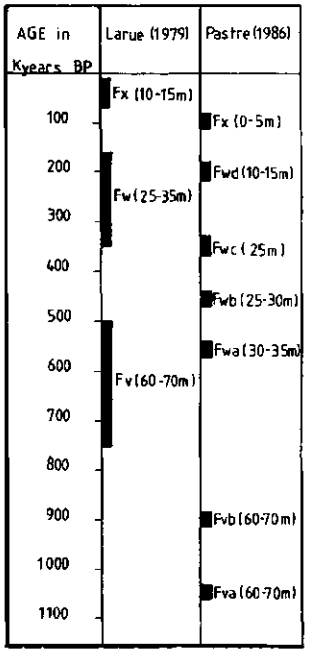

Figure 2.1.4. The two existing terrace chronologies

The typical sequence of terraces present in the Allier valley shows that accumulation and vertical erosion alternated repeatedly during the general valley deepening. Very similar terrace sequences are found along the Rhine, Meuse and Thames (Van den Berg, 1989; Van Straaten, 1946; Brunnacker & Boenigk, 1983; Andres, 1989; Mc Gregor & Green, 1978).

The mechanism of terrace formation is usually sought in three major external factors, climate, tectonism and base level. As the exact terrace formation mechanism for the Allier terraces is unknown each factor is considered.

Climate

Terrace sediment composition and alteration indicate that most of the Allier terrace deposits cumulated during and at the end of glacials. The alternations between cumulation and incision are therefore ascribed primarily to climatic causes (Raynal, 1984; Texier & Raynal, 1984; Bout, 1963; Kroonenberg et al., 1988).

Tectonism

The contribution of tectonism to terrace formation in the Allier basin is obvious from the tendency towards valley deepening throughout the Quaternary. The total amount of valley deepening at Randan since the Quaternary and consequently the probable amount of gradual uplift is about 150 m. Except gradual neotectonic uplift, which still takes place (Giot et al., 1978), some terrace sequences and longitudinal profiles suggest a tectonic fault component (Larue, 1979; Giot et al., 1978).

Base level

A direct or indirect influence of sea level variations on the erosion and sedimentation in the Allier basin appears not to have been possible as there is an area of continuous Quaternary deposition between the study area and the sea in the Paris basin and the lower Loire basin.

In general it can be concluded that climate and tectonism are the main external factors which have determined Quaternary terrace formation in the Allier basin.

2.2 THE LATE QUATERNARY TERRACE CHRONOLOGY OF THE ALLIER.

A. Veldkamp & S.B. Kroonenberg

Abstract

The Late Quaternary terrace chronology of the Allier has been reconstructed by means of terrace litho-stratigraphy with Th/U disequilibrium and ^{14}C datings. The terrace level at 25 m above present riverbed (Wb) near Coudes has a Late Saalian age. The two Weichselian terrace levels Xa and Xb (20 and 10 m) have at least four different litho-stratigraphical units, a Middle Pleniglacial, two Late Pleniglacial and a Younger Dryas unit respectively. The oldest Holocene terrace sediments have Atlanticum ages. The timing of Allier incision and sedimentation during the Late Weichselian seems mainly climatic related. Major fluvioglacial sediment fluxes from the melting glaciers on the Mt. Dore and Cantal at the end of the Late Pleniglacial caused a strong rise of Allier riverbed level. This rise of approximately 20 m in the Limagne contributed to formation of lakes like Marais de Ravel and the Grand Marais.

2.2.1. Introduction

Within lower Allier terraces major differences in sediment composition are known to occur (Kroonenberg et al., 1988; Larue, 1977). The major difference between the present riverbed and the Weichselian terrace (X) is the higher amount of basaltic fragments in the X terrace sands. This difference has partly a climatic origin as the Late Weichselian sediments are thought to have a fluvioglacial origin from melting glaciers in volcanic areas (Bout, 1963; Kroonenberg et al., 1988).

A previous bulk geochemical study (Kroonenberg et al., 1988) of Allier sands showed that basaltic rock fragments determine the TiO_2, Fe_2O_3, MgO, CaO and P_2O_5 content in the Allier sediments. Changes in bulk geochemical sand composition are well illustrated by CaO content, concentrated in the basaltic rock fragments, K_2O content, concentrated in crystalline rock fragments, and Na_2O concentrated in sodic plagioclase. CaO and K_2O contents are virtually independent of grain size because their host minerals are found in almost all grain size fractions and Na_2O is enriched in the finer sand fraction due to selective abrasion (Veldkamp, 1990).

In this chapter a new and more elaborated Late Quaternary

terrace (chemo)litho-stratigraphy is presented with new ^{14}C and U/Th datings allowing a more precise time setting of the Allier fluvial dynamics during the Late Quaternary.

2.2.2. Materials and methods

The various lower terrace levels have been thoroughly investigated by studying all available exposures along terrace scarps and in gravel/sand pits. Based on these sedimentological field observations and measured bulk geochemical sand composition a new litho-stratigraphy was made.

Sampling methodology and laboratory treatments and measurements of the sands were done according to Kroonenberg et al. (1988). The bulk element concentrations of SiO_2, TiO_2, Fe_2O_3, Al_2O_3, MnO, MgO, CaO, Na_2O, K_2O and P_2O_5, were measured with X-ray fluorescence spectroscopy. Mean bulk geochemical composition of each sampled sand layer is plotted for each described key section.

Special attention was paid to lithological discontinuities associated with paleosols and kryoturbated sediments/paleosols. The litho-stratigraphy was elaborated at those sites where datable materials were found. Sediments were dated with ^{14}C on organic rich samples, and by both ^{14}C and Th/U disequilibrium datings (Kroonenberg et al., in prep) of travertines. There are three main groups of terraces, from old to young, W, X and XY. The different terraces levels are indicated by an a or b (Wb and Xa) and the different litho-stratigraphical units by roman figures (X_{IV} and Wb_I). The studied W terrace is the Wb level which is found at 25 m above the actual Allier, The studied X levels, Xa and Xb, are found at 20 and 10 m respectively, while the ZY level starts at 7 m down to the present Allier.

2.2.3. Terrace litho-stratigraphy

Wb terrace sediments

The ages of the W terrace levels (25 to 45 m above river level) are still uncertain. A stratigraphical, palynological and sedimentological study at Pont-du-Château of Raynal et al. (1981) made them conclude that the Wa (45m) terrace sediments were most

probably deposited during the Cromerian glacial. They observed reworked ash layers in the studied Wa sediments. The mineralogy of these ash layers strongly resembles the characteristics of an ash layer used as a chronostratigraphic marker by Debard & Pastre (1988). This green clinopyroxene rich ash was given an age of approximately 300,000 years B.P., thus indicating that a younger age is more likely.

Near the Allier/Couze Chambon confluence at Coudes the 25 m terrace is well exposed along the RN 9. At this key section terrace sediments are found in a former gully incised in granite. The sediments have a maximum thickness of about 10 m and two main units can be distinguished (Fig. 2.2.1.). The lower unit, the Wb_I sediments, are poorer in volcanic clasts (less MgO and more K_2O) than the overlying WbII sediments. Wb_I sediments are slightly alterated before they were buried with Wb_{II} sediments. Both Wb litho-stratigraphic units are impregnated with travertine from nearby former springs.

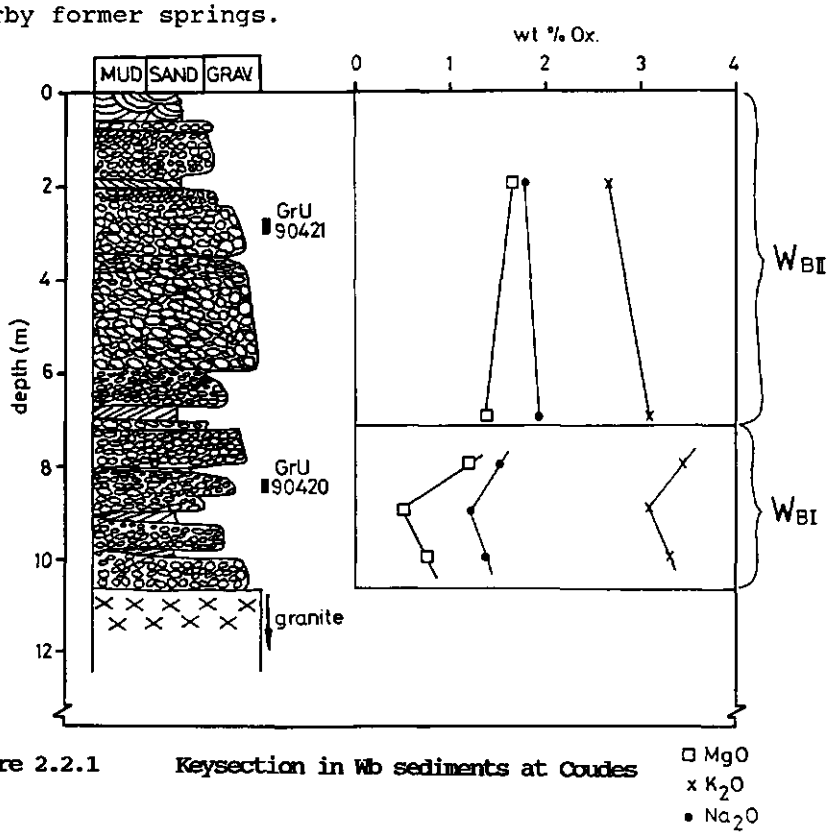

Figure 2.2.1 **Keysection in Wb sediments at Coudes**

The 25 m terrace level was originally dated as Late Weichselian based on fossils and artefacts found on and in the travertine capping of this terrace (Daugas & Tixier, 1978). Although both terrace units were originally thought to have a Weichselian age, radiometric dating showed otherwise.

The travertine impregnating both Wb units at Coudes was dated with the non-equilibrium Th/U method giving an age of 119,000 ± 13,000 (GrU-90420) for the Wb_I, and 93,000 ± 5000 GrU-90421) for Wb_{II} travertine.

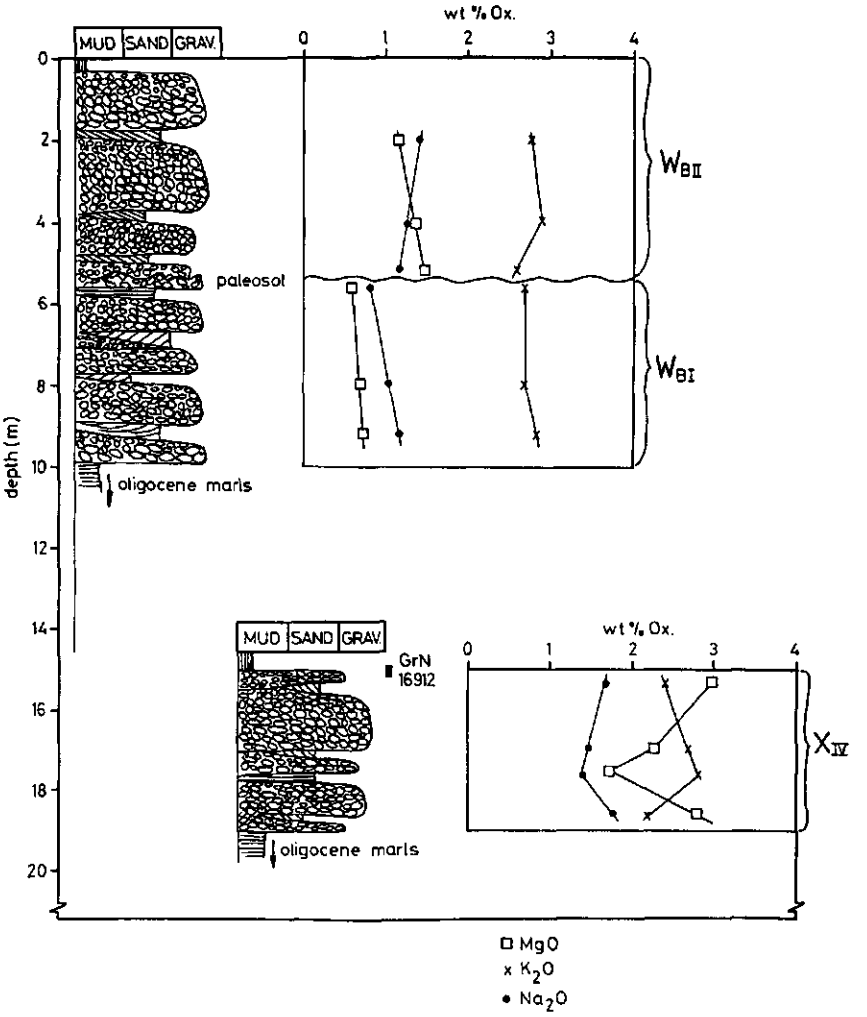

Figure 2.2.2 **Keysection in Wb sediments at Longues**

As the travertine shows no stratigraphical discontinuity between the two units, it must have been deposited after the Wb_{II} sediments. The Wb_{II} sediments are almost unaltered before travertine impregnation started indicating that these sediments are only slightly older than the oldest travertines. The travertines give therefore only the minimum age for the Wb_{II} sediments. As the Wb sediments were already deposited and in case of the Wb_{I} unit also altered before travertine impregnation took place these units are thought to have at least Saalian ages. Travertines impregnating terrace sediments of the 50 m terrace have Th/U ages up to 160.000 ± 10.000 (GrU-90418) years BP, indicating that travertine deposition took place also place during the Saalian. These older travertines suggest also that the Wb_{II} sediments are not much older than the Late Saalian travertines cementing them.

At Longues another terrace level at ±25 m above river terrace level is found. This terrace level displays a similar litho-stratigraphy (Fig. 2.2.2.) as the Coudes key section. The Wb_{I} sediments are also poorer in volcanic clasts (less MgO and more K_2O) than the overlying WbII sediments. The underlying Wb_{I} sediments are altered and locally kryoturbated before they were buried with Wb_{II} sediments. The kryoturbated paleosol clearly evidences a major time lag between the deposition of the two Wb units. At Longues the terrace sediments are also impregnated and covered with travertines. The travertines capping of the Wb terrace sediments at Longues were preliminarily dated by Kroonenberg et al. (1989), with the non-equilibrium Th/U method, giving Middle Weichselian ages as minimum ages for the Wb sediments.

The distinguished Wb terrace litho-stratigraphy is schematically shown in Figure 2.2.3., by two key-sections, one at Coudes and one at Longues. The general characteristics of the terrace litho-stratigraphy are described below.

Wb_{I} and Wb_{II}: Based on the similarities in litho-stratigraphy, bulk geochemistry and geographical position, the two Wb sites lie only 7 kilometres apart, the Wb terrace sediments are thought to

belong to the same terrace units and to have Saalian ages. The Wb_{II} sediments are not much older than 120,000 years while the Wb_{I} sediments are thought to have an age between 160,000 and 120.000 years.

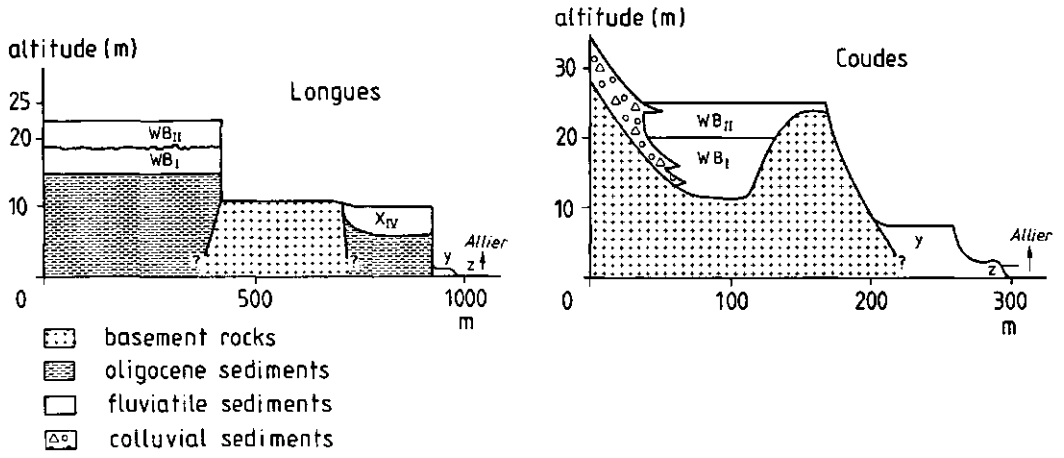

Figure 2.2.3 **Schematical litho-stratigraphy**

X terrace sediments

For the younger X and Y terrace levels, fragmentary palaeontological, palynological, archaeological and ^{14}C datings evidence that they were formed during the Weichselian and Holocene (Rudel, 1953; Lambert et al., 1980; Raynal, 1984). An important key section of the X terraces is situated at Les Jarrauds (Fig 2.2.4.), where all four Weichselian litho-stratigraphical units are found nearby. The highest terrace level is found at approximately 20 m above present riverbed. This terrace level, Xa, consists of two litho-stratigraphical units, a gravelly top unit which is characterized by high basaltic (high MgO and low K_2O content) sand and gravel content (X_{III}). This unit is locally overlying a more sandy unit relatively poor in basaltic fragments (X_{II}). At the transition to the lower Xb terrace level the Oligocene clays surface. The Xb terrace (10 m

above present river) has also two main litho-stratigraphic units. On top again relatively basaltic rich sediments (X_{VI}) overlie a basaltic poorer sediment (X_I). Sometimes the basaltic poor X_{II} sediments are found between X_I and X_{IV} sediments indicating that the X_I sediments are the relative oldest X sediments. The lower sediments (X_I) are altered and locally a paleosol is found at the contact with the overlying (X_{II}, X_{III} and X_{IV}) sediments. An organic rich clay layer at the base of the (X_I) unit was ^{14}C dated at 29,560 ± 330 years B.P. (GrN-17242), revealing a Middle Pleniglacial age. A colder climatic environment was suggested by the pollen content of this layer (Tuffery, 1986).

The four distinguished units are also found at other sites. The general characteristics of these four Late Weichselian units are schematically shown in Fig. 2.2.5. and described below.

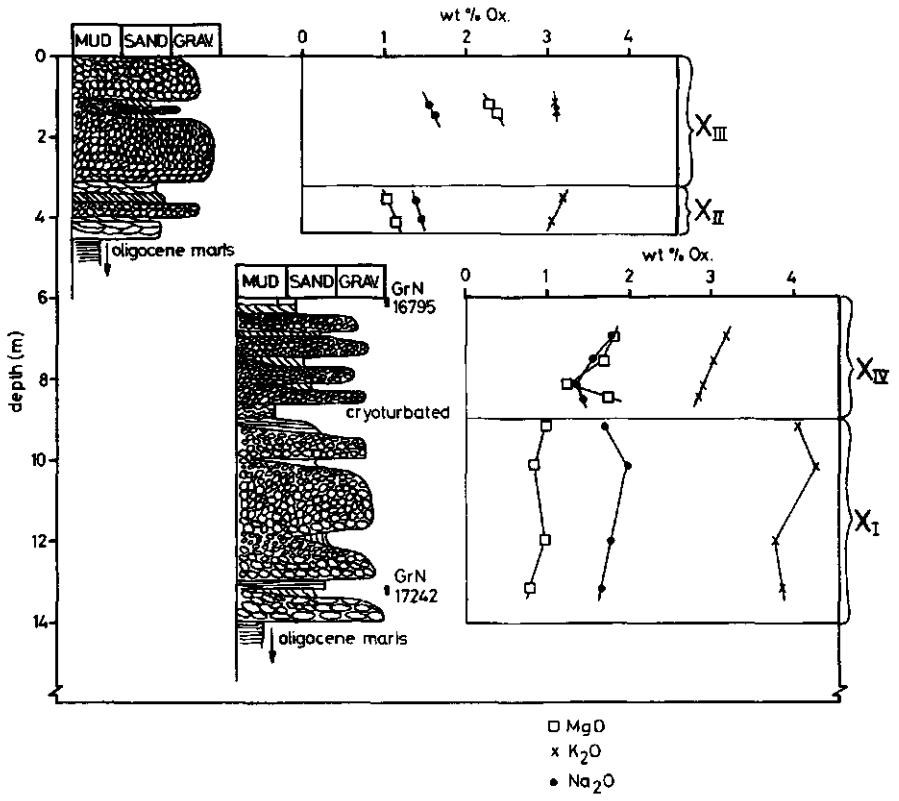

Figure 2.2.4. Key section at Les Jarrauds

X_I: This litho-stratigraphic unit, XW according to Kroonenberg et al. (1988), consists of gravelly sediments relatively poor in volcanic components. The thickness changes from almost 20 m to less then 3 m. This unit is an altered and strongly dissected relict of a former terrace level at about ±20 m above present river level. The X_I lithological unit is found in both X terrace levels (Xa and Xb).

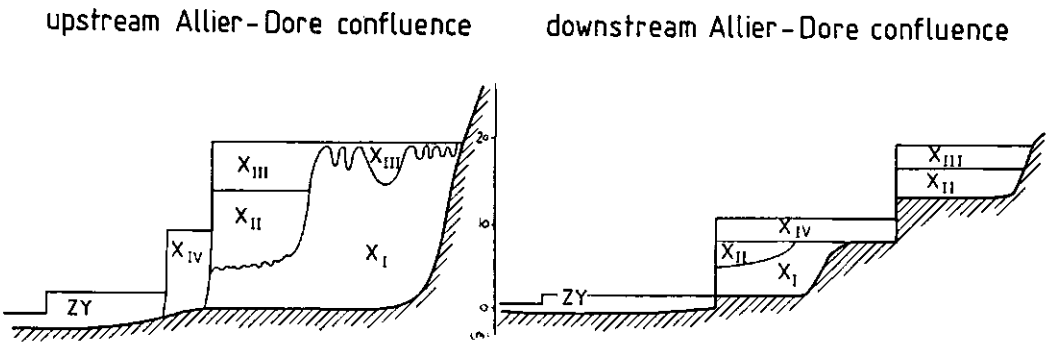

Figure 2.2.5 **Schematical litho-stratigraphy northern section**

South of Maringues and West of Le Bas Lachamp uneroded remnants of this 20 m terrace are found, the upper one to two metres of the X_I sediments are commonly disturbed by kryoturbation and frost wedges (Fig 2.2.6. and 2.2.7.). A kryoturbated clay layer in the upper two metres of this unit (Fig. 2.2.6.) West of La Bas Lachamp has an ^{14}C age of 16,585 ± 250 years B.P. (GrN-17243) giving a minimum age for the X_I sediments and a maximum age of the last major kryoturbation activity in the X_I sediments.

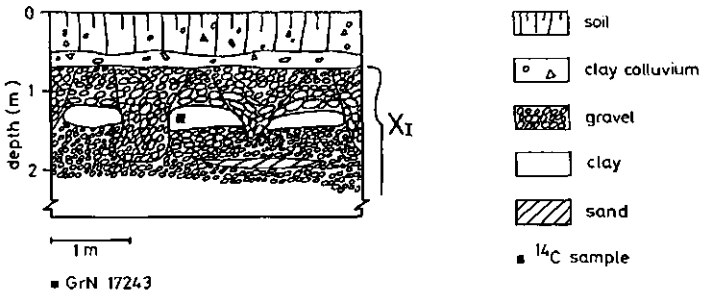

Figure 2.2.6 **Kryoturbation of the top X_I sediments at Las bas Lachamps**

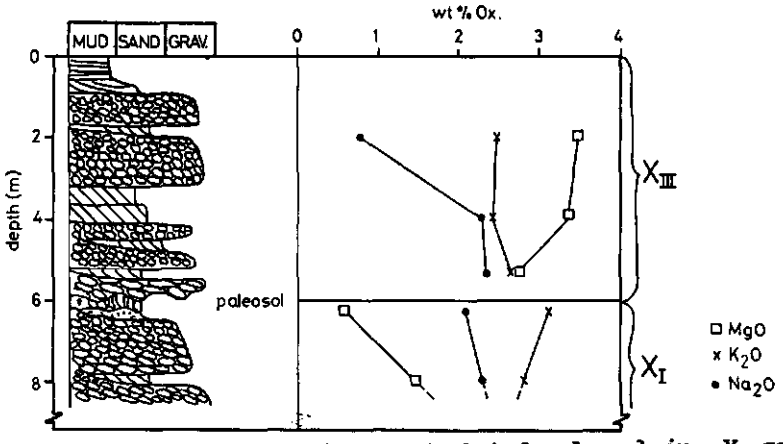

Figure 2.2.7 **X_{III} overlying kryoturbated paleosol in X_I sediments at Culhat.**

X_{II}: This lithological unit, the crystalline X terrace according to Larue (1977), predominantly consists of sandy sediments with a low volcanic content. These sediments occur very locally on top the X_I and below the X_{III} and X_{IV} sediments, and have a limited thickness of three to less than one metre. This unit is found in terrace level Xa as well as in Xb. The sediments are unaltered and no pollen or other datable materials were found in these sediments.

X_{III}: This litho-stratigraphic unit usually forms the top layer of the Xa terrace level (± 20 m above river level), and consists of gravelly sediments very rich in volcanic components. The X_{III} sediments are overlying both the X_I and X_{II} units. The volcanic rich sediments, which lack any datable material, are closely related to deglaciation in the upper Allier basin and have a

fluvio-glacial origin (Bout, 1963; Kroonenberg et al., 1988). The X_{III} sediments did locally bury some strongly kryoturbated paleosols in the X_I sediments (Fig 2.2.5.) indicating a maximum age of the X_{III} sediments of approximately 16,500 years B.P. (age of buried kryoturbated clay in paleosol in X_I sediments).

Correlation between the Late Weichselian chronology in the Artière basin and the Allier sediments showed that the age of the X_{III} unit is between 11,500 and 41,000 years B.P. (Lenselink et al., 1990). The pre-Alleröd age of the X_{III} sediments was confirmed by the observation near Lempdes that X_{III} sediment are buried by the same trachy-andesitic Alleröd ash as dated in the Ravel and Artière basin (Kroonenberg et al., 1987; Lenselink et al., 1990; Juvigné, personal communication). The X_{III} sediments were thus deposited between 16,500 and 11,500 years B.P..

X_{IV}: This litho-stratigraphic unit is the top layer of the Xb terrace level (±10 m above river level) and consists of gravelly and sandy sediments rich in volcanic components (Fig 2.2.8.). An organic clay block of a buried paleosol at the basis of the X_{IV} sediment unit (Fig 2.2.8.) at St Yorre has an ^{14}C age of 11,380 ± 100 years B.P., (GrN-16793). Another buried paleosol developed in the top layer of the X_{IV} sediments at Les Granvaux buried by a local sand fan has an age of 7310 ± 70 years B.P.(GrN-16795). The X_{IV} sediments were thus deposited between 11,380 ± 100 and 7310 ± 70 years B.P..

At Longues another terrace ±8 m above river level is found which resembles the X_{IV} unit as described in the northern section. It consists of gravelly and sandy sediments rich in volcanic components (much MgO and less K_2O), impregnated and capped with travertine. This level was dated by means of a correlation with a nearby dated archaeological site by Raynal (1984) as Younger Dryas. We dated organic matter of a palaeosol in the top sediments buried by half a metre pure travertine. The organic matter has an ^{14}C age of 9,630 ± 90 BP (GrN 16912), this Early Holocene age of post depositional organic matter confirms the Younger Dryas age of the X_{IV} sediments. But the $CaCO_3$ in the same sample was ^{14}C dated at 25200 ± 900 years B.P. (GrN-16912).

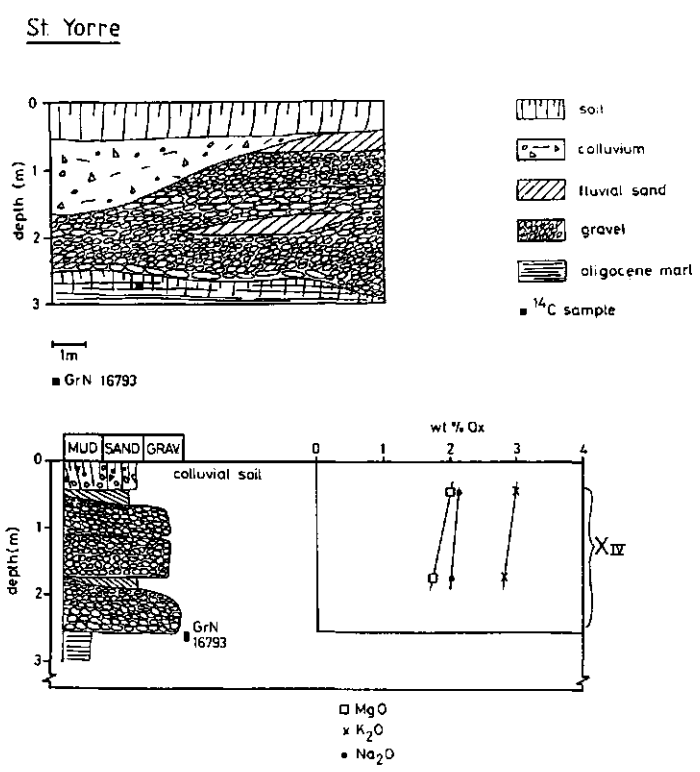

Figure 2.2.8 **Keysection in X_{IV} sediments at St Yorre**

As the $CaCO_3$ was precipitated in and around the dated organic matter, the $CaCO_3$ should be younger then the organic matter. These contradicting ages made us conclude that the dated $CaCO_3$ contained 'fossil' carbonates probably originating from the nearby Oligocene limestones.

ZY: This unit consists of at least three different terrace levels with predominantly sandy sediments, relatively poor in volcanic components. The oldest dated Holocene sediments from gullies incised in the X_{IV} sediments have a ^{14}C age of 6,230 ± 100 years B.P., (GrN-16794). A similar age was found for the oldest Holocene terrace level (Lambert et al., 1980).

2.2.4. A regional reconstruction of the Late Quaternary Allier dynamics

Our reconstructed chronology starts in the Saalian (Riss) when Wb_I and Wb_{II} sediments were most probably deposited. As no more details are known of these sediments, they cannot be correlated 7with any climatic event or environment. Our dated chronology of the Allier sediments allows only a tentative reconstruction of the Allier dynamics during the last 30,000 years (Fig 2.2.9.) . As standard the oceanic deep sea curve is used (Hays et al., 1976; Kominz et al., 1979) and matched with the continental chronologies of Les Echets (De Beaulieu et al., 1984) and Grande Pile (Woillard, 1978; Woillard & Mook, 1982). More regional sedimentological and palynological studies (De Beaulieu et al., 1982; Juvigné et al., 1988; Raynal et al., 1984; Reille & De Beaulieu, 1988) served as extra checks.

The litho-stratigraphy (Fig 2.2.9. fifth column) starts during a Middle Pleniglacial interstadial when the Allier was probably incised to the present river level.

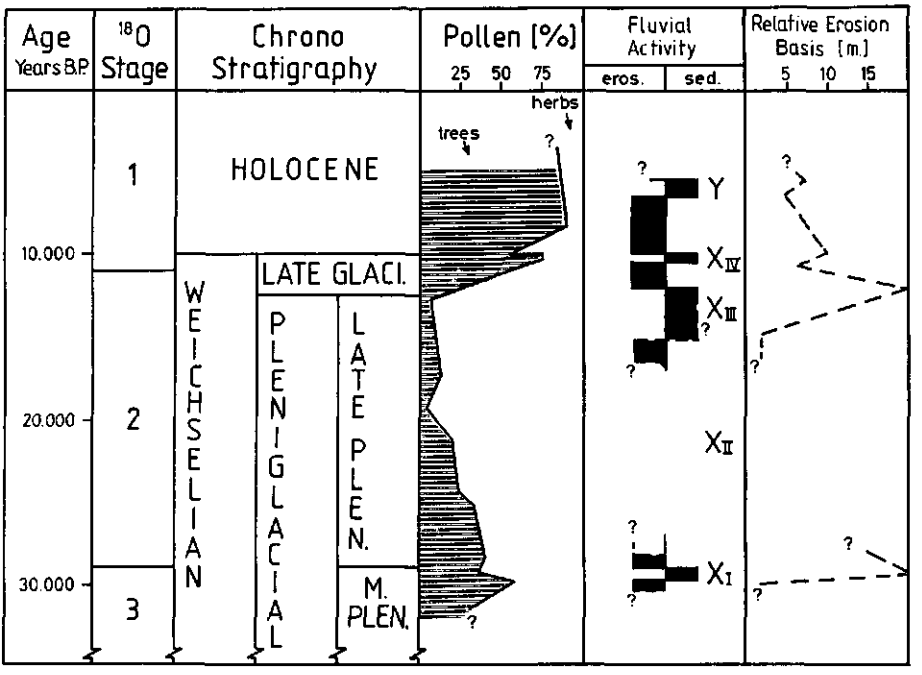

Figure 2.2.9 **The Late Weichselian chronology of the Allier**

When the X_I sediments were deposited during the Middle Pleniglacial the riverbed level rose up to 20 m above present river level. These X_I sediments were locally at least 15 m dissected and altered during the subsequent Late Pleniglacial before deposition of the X_{II} sediments. During the Late Pleniglacial known as the coldest episode during Weichselian the glaciers had their maximum extension and a dry tundra existed in the Limagne (Veyret,1980; De Beaulieu et al., 1982; Raynal, 1984). Under this severe climate the strong periglacial deformation of the upper X_I sediments took place. Within this environment local deposition of the volcanic poor X_{II} sediments took place. This cold period ended at the end of the Late Pleniglacial triggering a large fluvio-glacial sediment flux from the volcanic areas. This climate improvement which took place in several thousands of years, resulted in the deposition of the gravelly volcanic rich sediments of unit X_{III} (Bout, 1963; Kroonenberg et al., 1988). Their deposition caused a rise of 20 m of the river bed level and must have happened during catastrophic floods causing an infill of the palaeo-Auzon valley (Lenselink et al., 1990) and lake formation in the lower tributaries (Morge, Litroux, Buron etc) in the Limagne. X_{III} sediment were probably 15 m dissected during Bölling and Alleröd, after which the X_{IV} sediments were deposited during the colder Younger Dryas. These Late Glacial sediments were dissected during the Early Holocene. The oldest record of fluvial Holocene deposition in the Allier starts in the Atlanticum.

The X_{III} sediments and lake formation in the Limagne

Oval shaped semi-closed depressions (locally called 'marais'), several kilometres in diameter, occur in the lower parts of the Limagne rift valley. Within these marais lake sediments are found (Gachon, 1963). The top altitude of the X_{III} unit coincides with the altitude of the upper lake sediments in the Limagne. Their geographical relation is visualized in Fig 2.2.10. As the lake sediments, like the X_{III} sediments, overlie a kryoturbatic surface their deposition seems related. The X_{III} sediments originating from large sediment fluxes are thought to have served as a

barrier for the local tributaries causing lake development in the Limagne. These minor Allier tributaries in the Limagne could never compensate a sudden rise in riverbed level of 20 m by sedimentation due to their limited sediment supply. As the oldest lake sediments have an age of 12,370 ± 230 years B.P. (GrN-12891) (Kroonenberg et al., 1987) the X_{III} sediments are thought to be deposited between 16,585 ± 250 and 12,370 ± 230 years B.P..

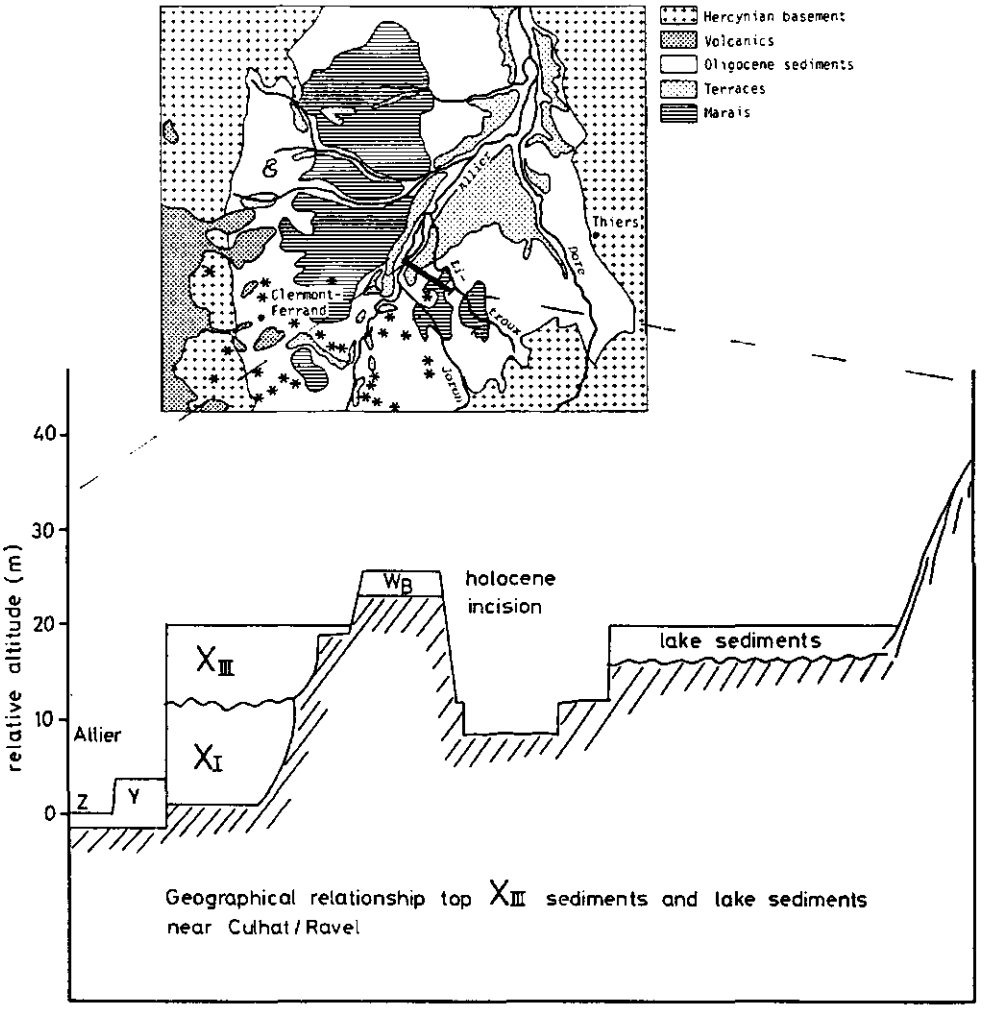

Figure 2.2.10 **Schematical morphological relation between the top of the Xa terrace level and lake sediments.**

Kroonenberg et al. (1987) explained lake development by thermokarst due to permafrost degradation a process which may have contributed to the actual lake basin morphology. But it are the large sediment fluxes during the end of the Late Pleniglacial which are thought to have caused lake formation in the Limagne.

2.2.5. Climatic and fluvial dynamics in the Allier basin

The regional reconstruction of the Allier dynamics during the Late Weichselian as in Fig. 2.2.9., allows the postulation of a simplified model for the relationship between climatic and fluvial dynamics in the Allier basin.

Climatic environment	Fluvial activity
Glacial	Deposition of sediments with a relative low volcanic content (< MgO and > K_2O). The older surface terrace sediments are kryoturbated.
Transition from Glacial to interglacial	Deposition of coarse volcanic rich (> MgO and < K_2O) fluvio-glacial sediments. A strong rise in river bed level due to the large sediment flux from melting glaciers.
Inter-glacial	Predominantly incision with temporary deposition of sandy sediment with a low volcanic component (< MgO and > K_2O).

This simplified model has some resemblance with a model where the general textural characteristics of terrace sediments are related to climatic environments (Texier & Raynal, 1984). Our

terrace litho-stratigraphic reconstruction also shows that the Interglacial Holocene terrace sediments have a finer texture than the coarse Glacial and Late Glacial sediments. But within our model the most important changes in the Allier system are sediment composition changes induced by glacier melting on the Mt. Dore and Cantal at the end of the Late Pleniglacial, a factor not considered in the simpler model of Texier and Raynal (1984).

2.3 TRACHYTIC PUMICE CLASTS IN MIDDLE PLEISTOCENE ALLIER TERRACE DEPOSITS: A CHRONOSTRATIGRAPHIC MARKER.

A. Veldkamp & A.G. Jongmans

Abstract

Trachytic pumice clasts with similar characteristics as pumice of the Sancy volcano at Neschers have been found at different sites in the 65 m (Va) terrace of the Allier, implying a maximum age for this terrace level of 800,000 years. Micromorphology of an intercalated paleosol and kryoturbatic features indicate that Va sediments have known at least one glacial/interglacial cycle before dissection of the Va level took place. By using the pumice clasts as a stratigraphic marker a reconstruction of the longitudinal profile of the Va level was made. This reconstruction shows that the Randan region has been relatively uplifted, while the Lezoux section has been subsided after dissection of the Va level.

2.3.1. Introduction

Fluvial terraces are commonly correlated on account of their relative altitude or sediment composition. In the Allier basin (Limagne, France., Fig. 2.3.1.), a first detailed terrace correlation was made for the geological map of Maringues (Jeambrun et al., 1980). The distinguished terrace levels were based on their relative altitude and general sediment composition. As in most other fluvial systems the stratigraphy of the Allier terraces is far from uniform. In the Allier section South of Clermont Ferrand which was studied by Van Dorsser (1969), it was almost impossible to demonstrate differences in heavy mineralogical sand composition for the different terraces. Pastre (1987) who extensively studied the sand mineralogy of the different Allier terrace sediments adapted the existing terrace classification almost purely based on sand mineralogy. He also established the chronology and ages of the terrace sands by correlating their heavy mineral composition with the mineralogy of known major volcanic events.

We studied the Va (Jeambrun et al., 1980) terrace of the Allier, which has an altitude of approximately 65 m above present river bed, along a stretch of 40 km, from Clermont Ferrand near the village of Beauregard l'Evêque to Vichy (Fig. 2.3.1.).

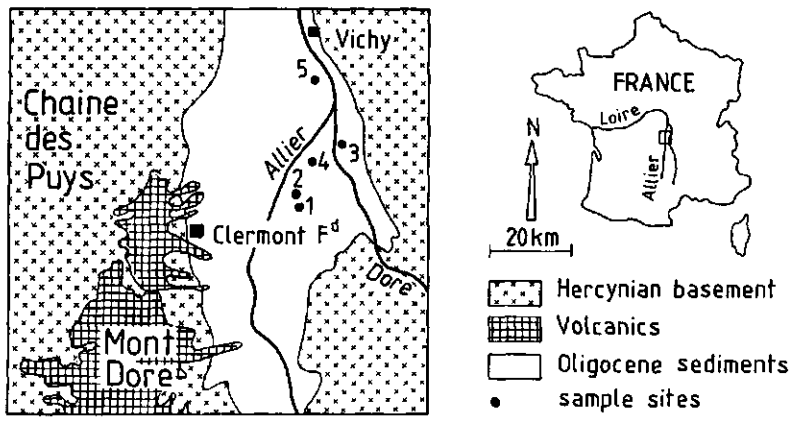

Figure 2.3.1. Map with sample sites

The average Va gravel composition, 50% basalts, 5% granites, 5% metamorphic rocks and 40% quartz, reflects the different lithologies within the Allier basin (Larue, 1977; Bout, 1963; Van Dorsser, 1969). Mineralogical sand compositions are given by Van Dorsser (1969), Rudel (1963), Pelletier (1971), Pastre (1987) and Tourenq (1986) and bulk geochemical compositions by Kroonenberg et al. (1988) and Veldkamp & Kroonenberg (1989). The age of the Va terrace was established at one million years based on sand mineralogy (Pastre, 1987) .

It was Pastre (1987) who observed pumice clasts at one site in the Va terrace level (at Saint-Sylvestre-Pragoulin, Pastre, 1987, p. 500). We found more pumice clasts in the sandy units of the Va terrace level at five widely separated sites. By comparing the pumice characteristics we conclude that this pumice originates from a single trachytic source eruption from the Sancy volcano approximately 800.000 years ago, implying a considerable younger maximum age for the Va terrace level as given by Pastre (1987).

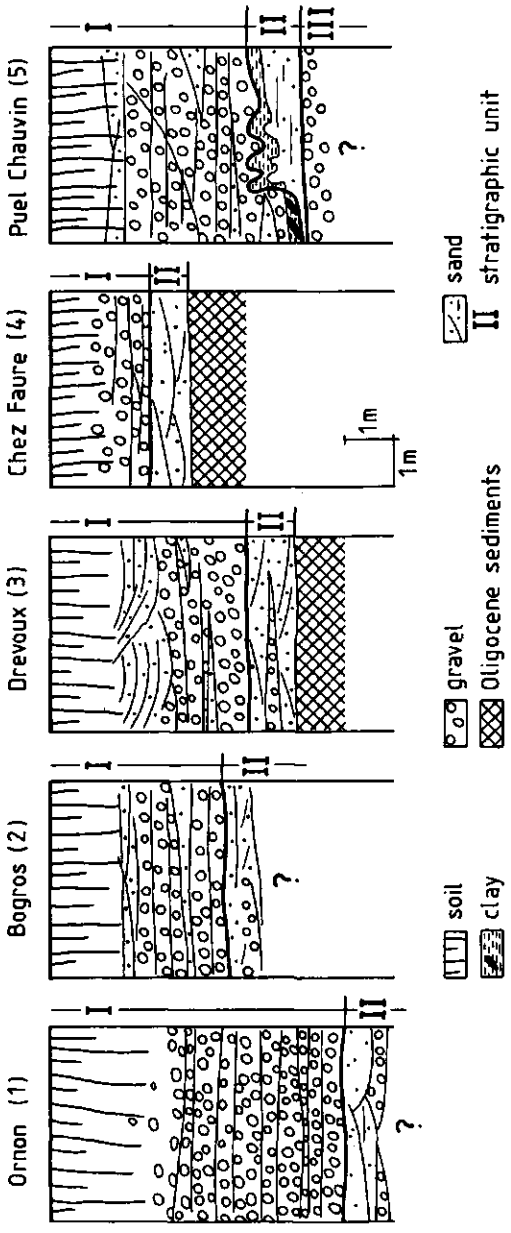

Figure 2.3.2. Terrace stratigraphy of sampled sites in Fva terrace

From five profiles in the Va terrace undisturbed samples were taken (Fig. 2.3.1., 2.3.2. and Table 2.3.1) for mineralogical and micromorphological examination. To enable a more detailed reconstruction of the Va terrace in terms of chronology and climatic environment, a kryoturbated paleosol was studied in more detail. Thin sections (10*10 cm) were made and described following the terminology of Bullock et al. (1985). Mineral countings (n=150) were performed in these thin sections.

site name	X-coor.	Ycoor.
Ornon	528.8	5078.8
Bogros	527.9	5079.7
Drevoux	535.5	5085.7
Chez Faure	532.0	5085.9
Puel Chauvin	533.2	5096.4

Table 2.3.1. **Map coordinates of sample sites.**

2.3.2. Stratigraphic marker

Terrace stratigraphy

The stratigraphy of the Va terrace sediments is based on field observations and micromorphological examinations. Four different lithological units are distinguished, from top to bottom.

Unit I, occurs in all 5 profiles and commonly consists of a 4 m thick gravel unit in which basaltic clasts dominate. Unit I facies indicate a braided gravel river. A planosol (FAO, 1974) has been developed in the upper two metres of all profiles (Feijtel et al., 1988).

Unit II, underlies unit I and predominantly consists of sands with many trachytic rock fragments and pumice fragments. Unit II facies suggest a sandy braided system. This unit has an average thickness of 1 metre. The pumice fragments are rounded and found

in clayey and loamy units or as pure pumice layers of several centimetres in major sand bodies. The best location to study the pumice macromorphologically is in the gravel pit near Ornon where pumice layers are exposed at the pit floor near the groundwater table.

Unit III, underlies unit II, and consists of basalt rich gravel. This unit of at least half a metre is only found in the Puel Chauvin profile. The facies of this unit suggest a similar river type as with the unit I, a braided gravel river.

Unit O, consists of Oligocene clayey sediments which form the base for all the Va terrace sediments. This unit is only well exposed in two excavations.

2.3.3. Pumice

In thin sections of all the five profiles the pumice fragments are fine grained hypocrystalline to holohyaline, with varying content of phenocrysts of feldspar (predominantly K-feldspar and albite, 20-500 μm), biotite, green and brown clinopyroxenes, brown amphibole, sphene (20-200 μm), and opaque minerals (20-40 μm). The pumice shows a vesicular texture with numerous spherical to ellipsoidal shaped holes, discontinuous wavy laminated oriented in a longitudinal section (Photos I and II in Fig. 2.3.3.). The pumice has a trachytic chemical composition and shows in-situ alteration and clay neoformation within the fragments (Veldkamp & Jongmans, 1990).

2.3.4. Correlation of pumice with dated Sancy eruptions

Micromorphological and mineralogical (Table 2.3.2.) observations of the Va pumice show a uniform composition and texture of the pumice fragments from the different sample locations.

The occurrence of one type of pumice in similar stratigraphic units at more than hunderd kilometres from the eruption centre (Sancy volcano) suggests that the Va pumice can be correlated to one major eruption, and can be used as stratigraphic marker.

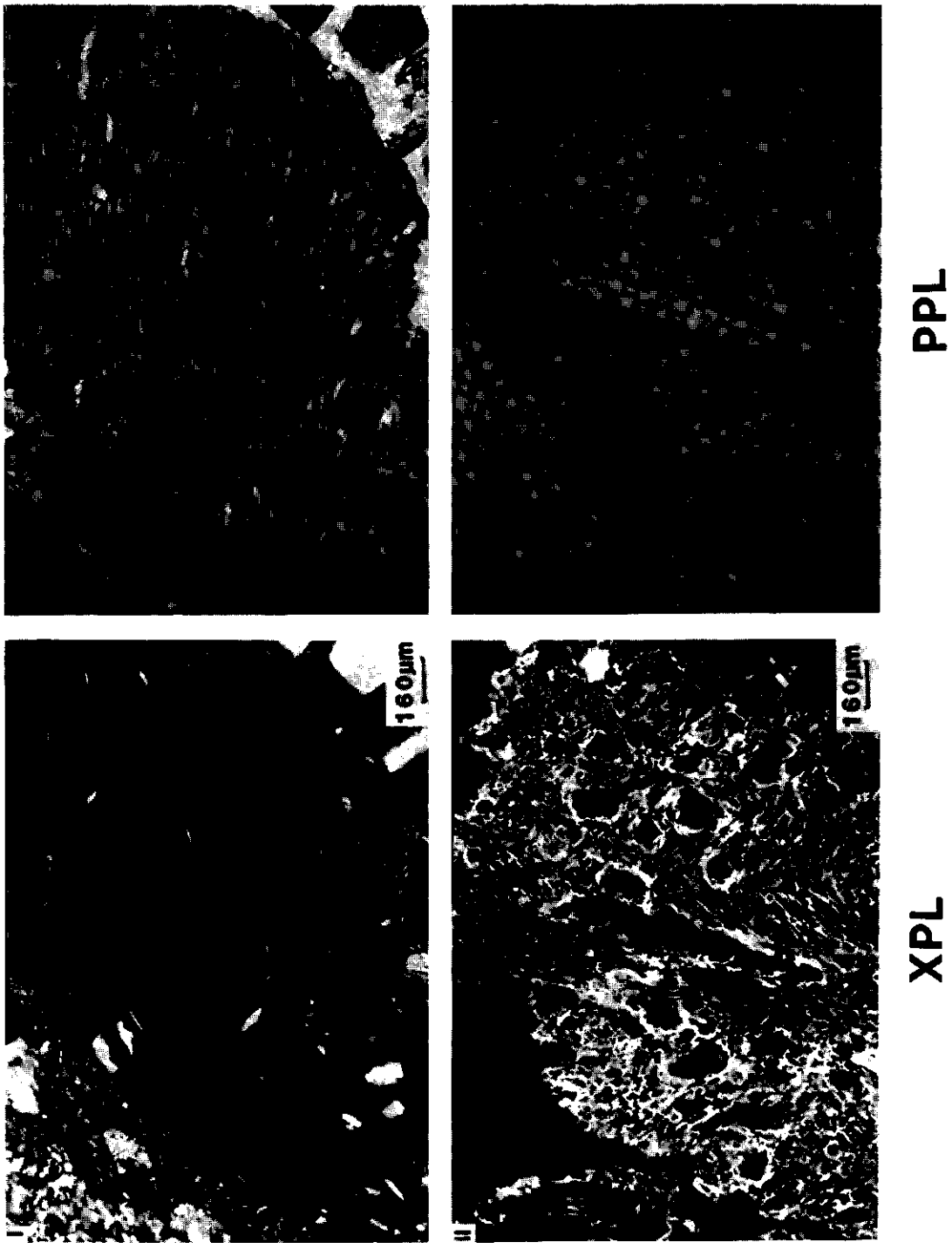

Figure 2.3.3. Pumice fragment of Neschers (Photo I) and pumice fragment from unit II of Ornon (Photo II).

Only a few major trachytic volcanic phases are known as possible source for the pumice clasts, the ignimbrite of Rioubes (±900,000 years BP) and the ignimbrite of Neschers (±800,000 years BP) (Besson et al., 1977; Chambaudet & Couthures, 1981; Ly, 1982; Pastre, 1987).

Mineral	Fva pumice Ornon	Fva pumice Puel Chauvin	Neschers pumice (Pastre, 1987)	Rioubes pumice (Pastre, 1987)
Zircon	1.0%	0.5%	0.5%	0.2%
Sphene	18.5%	20.0%	23.0%	24.0%
Brown amphibole	6.0%	8.0%	8.0%	2.0%
Green clinopyroxene	65.0%	64.5%	63.5%	68.8%
Brown clinopyroxene	6.0%	5.0%	3.5%	-
Apatite	1.5%	0.5%	1.5%	2.8%
Other	2.0%	1.5%	-	2.2%

Table 2.3.2. **Percentage of heavy minerals in Fva pumice (Ornon and Puel Chauvin), Neschers pumice and Rioubes pumice.**

Heavy mineral composition of the pumice fragments in the Ornon and Puel Chauvin profiles are compared with the two potential source types in Table 2.3.2. Biotite content was excluded to facilitate comparison. The occurrence of brown clinopyroxene in the Va pumice excludes the trachytic ignimbrite of Rioubes as source eruption. As there is a fairly good similarity between the Va and Neschers pumice composition, the Va pumice fragments are thought to belong to the Neschers generation. Consequently the age of the pumice containing sediments (unit II) can be considered at about 800,000 years. This maximum terrace level age is partly in accordance with the chronology of Larue (1979), but is much younger than the age estimate of Pastre (1987).

2.3.5. Paleoenvironment

Micromorphology of paleosol

The Puel Chauvin profile near Randan displays all stratigraphic units including a kryoturbated clayey band in unit II. The less weathered and kryoturbated parts show that the clayey layer was originally a fine layered sediment. The clayey band has a distinct angular blocky structure in a greyish (10 YR 5/1) clayey groundmass, indicating the formation of a well developed physicogenic structure. Channels, surrounded by porostriated b-fabrics and the occurrence of loose continuous excremental infillings suggest root and faunal activity. Walls of vughs and chambers demonstrate predominantly lenticular prints, indicating a former growing of euhedral masses of lenticular crystallaria, possible gypsum, in these voids (Porta & Herrero, 1990). Such gypsum formation is known from other paleosols in the Massif Central (Pierre, 1989).
Occurrence of yellow non laminated isotropic and greenish yellow anisotropic speckled oriented clay coatings (Feijtel et al., 1989; Jongmans et al., 1990) in the sandy parts of unit II indicates weathering of the pumice fragments and neoformation of clay. Since the described weathering features are not noticed in de overlying deposits of unit I it can be concluded that before unit II was kryoturbated and buried by unit I, a paleosol was formed in the sediments of unit II.

The main soil forming processes in this paleosol were in-situ weathering of pumice and trachytic rock fragments, neoformation of clay, biological activity and solution of crystallaria. These processes suggest that after and probably during the pumice deposition, a temperate climate prevailed. This environment with an interglacial signature was followed by a cold climatic period during which peri-glacial conditions caused the observed strong kryoturbation of the upper parts of unit II.

The other four profiles have also weathering features in their unit II sediments. But the absence of distinguishable differences

between weathering features in unit I and unit II makes the recognition of other paleosols difficult.

2.3.6. Terrace chronology Va

During deposition of the Weichselian terrace sediments the majority of the basaltic gravels were deposited at the end of a glacial as a result of glacier melting on the higher parts in the Allier basin (Bout, 1963; Kroonenberg, et al., 1988). Assuming similar depositional mechanisms for the Va terrace sediments the gravelly basaltic rich unit I is thought to be deposited at the end of a glacial period too. After deposition, dissection took place under more temperate climatic conditions, causing the formation of the Va terrace level.

On account of these observations and assumptions the following tentative chronology for the events of the Va sediments can be reconstructed :

- Fluvial deposition of pumice rich sandy sediments (unit II) took place around 800.000 years ago. The roundness of the trachytic fragments and pumice clasts indicate that these sediments have been fluvially transported before sedimentation. The deposition of these sandy sediments seems not directly related to climatic environment.
- After deposition, these sediments were weathered under temperate conditions (paleosol unit II).
- Next, climate shifted to periglacial conditions during which a strong kryoturbation of the existing soil took place (kryoturbated paleosol unit II). At other sites the unit II sediments were partly or completely eroded.
- At the end of a glacial period the remaining kryoturbated paleosol was covered by basalt-rich gravels (unit I).
- These sediments were incised under more temperate conditions causing the formation of the Va terrace level.

As the Va terrace sediments were subjected to at least one glacial/interglacial cycle, dissection of the Va level must have taken place considerably later than 800.000 years.

2.3.7. Tectonic implications

Using the pumice clasts as a chronostratigraphic marker a more reliable reconstruction of the longitudinal Va terrace profile can be made then on the base of topography alone. In order to reconstruct the longitudinal Va profile, the surface altitude of the studied profiles from the 1:25.000 topographical maps were used (Fig. 2.3.4.). The pumice layers are indicated individually. The pumice site described by Pastre (1987) downstream of Puel Chauvin is shown as well. Based on its similar stratigraphic position we include this apparently identical pumice marker horizon in our reconstructed longitudinal profile. The Oligocene/terrace sediment boundary is very irregular and therefore not considered. The profile of the actual Allier river bed is very regular in the studied Allier section, and therefore a relative longitudinal Va profile is presented (Fig. 2.3.4.).

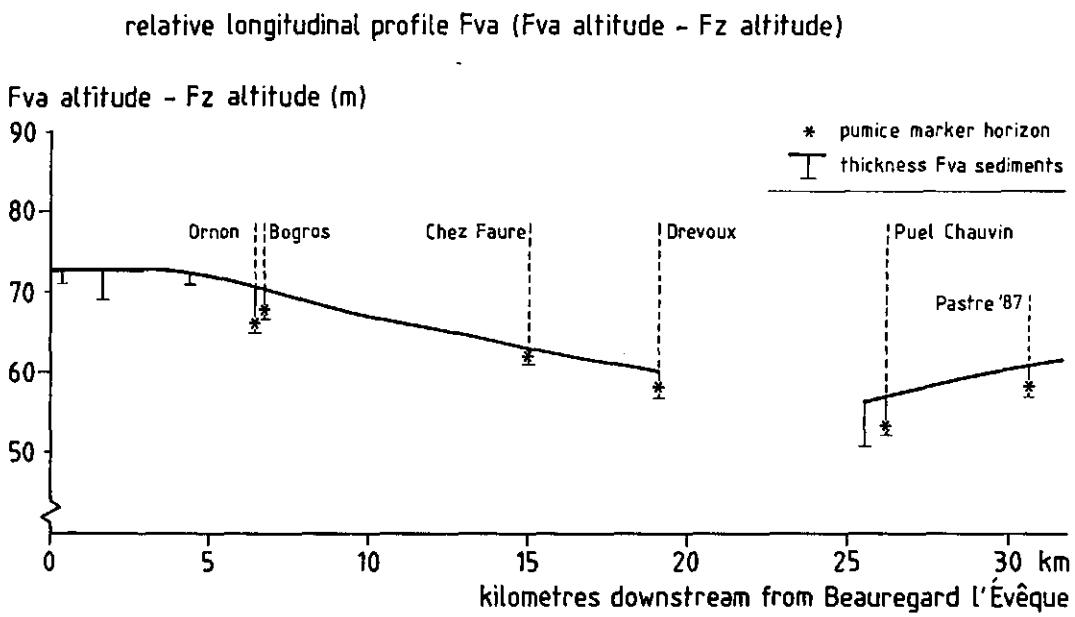

Figure 2.3.4. **Longitudinal profile of the relative altitude of the Fva terrace level.**

Near Clermont Ferrand the Va terrace level runs parallel to the actual riverbed, but more downstream the relative altitude decreases steadily. This gradual decrease in relative altitude in the longitudinal profile was also reported by Giot et al., (1978). North of the Allier/Dore confluence, the relative altitude of the Va terrace increases steadily. The scale and changes in the relative altitude clearly indicate that postdepositional tectonic disturbance of Va sediments took place. The Randan region has been uplifted while the Lezoux region has been subsided after dissection of the Va level. These vertical movements seem simultaneous and related to rift fault movements in the Limagne rift valley. Similar tectonic uplift was proposed by Larue (1979), who explained the course diversion of the Morge, an Allier tributary, by tectonism. The Va terrace of the Morge is found along the old course, while Fw is the oldest terrace level along the actual Morge, suggesting an uplift of the Randan region after the Va and before the W sediment deposition. Along the Allier irregular longitudinal profiles are only found for the V and older terraces, while the W and younger terraces show a very regular longitudinal profile. Our observations, confirm those of Larue (1979) and Giot et al., (1978) indicating a regional tectonic disturbance after the incision of the Va (< 800 ky) level and before deposition of W terrace sediments.

2.3.8. Conclusions

Pumice of the Neschers generation serves as a chronostratigraphic marker in the Allier Va terrace level. Va terrace sediments were subjected to at least one glacial/interglacial cycle before dissection of the Va level took place. A geographical reconstruction of the Va terrace level with the stratigraphic marker confirms that the Randan region has known a relative uplift and the northern Lezoux section a subsidence, after dissection of the Va terrace level.

Chapter 3

SAND BULK GEOCHEMISTRY

As Quaternary research is more and more interested in the quantitative aspects of major environmental changes it will be necessary to develop new quantitative methods. A way to determine quantitative paleohydrological changes is by studying the changes in bulk composition of fluvial sediments (Kroonenberg, 1990). As it is rather cumbersome to derive a bulk composition from the mineralogical composition of separate fractions and point-counting of thin sections is time consuming, it was decided to measure bulk sand composition geochemically.

3.1 THE APPLICATION OF BULK SAND GEOCHEMISTRY IN QUATERNARY RESEARCH. A METHODOLOGICAL STUDY OF THE ALLIER AND DORE TERRACE SANDS.

A. Veldkamp & S.B. Kroonenberg

Abstract
The bulk geochemistry of unconsolidated sands of river terraces in two drainage basins of contrasting geology in the Limagne rift valley, France, has been studied. Data processing and interpretation was done with multivariate statistics, notably factor analysis. In the Allier basin, underlain by volcanic rocks and crystalline basement, the abundance of basaltic rock fragments causes significantly higher bulk concentrations of TiO_2, Fe_2O_3, MgO, CaO, P_2O_5, V, Cr, Ni, Zn, Sr, Zr and Nb. In the Dore basin, underlain by crystalline basement alone, sands have a significantly higher SiO_2, K_2O, Rb and Pb content, originating from quartz, K-feldspars and mica's. Comparison between different terrace levels shows the impact of weathering and changes in supplied sediment composition over time. Approximately 65% of the total variance in the basaltic element content in the Allier terrace sands can be explained by the combined effect of parent material and weathering. The effect of grain size on sediment composition is only significant for Al_2O_3, Na_2O and Rb content in the Allier and for TiO_2, Fe_2O_3 and Nb content in the Dore sands. Approximately 60% of the total variability in these elements is grain size related. These data show that bulk geochemical studies of Quaternary terrace sands can provide valuable data complementary to traditional sedimentary petrographic research. They also indicate that data obtained during mineral exploration are potentially applicable in Quaternary research.

3.1.1. Introduction

Fluvial terraces result mainly from a complex interplay of changes in climate, tectonism and base level (Green and Mc

Gregor, 1987; Boll et al., 1988; Veldkamp and Vermeulen, 1989). These external factors are directly or indirectly reflected in the composition of the resultant sediments. Sediment composition is also controlled by local factors, such as sorting processes, post depositional weathering etc. Major changes within a fluvial system do not only change sediment granulometry and mineralogy but also the quantity of sediment delivered to the river. The total sample composition quantitatively reflects such changes. As Quaternary research is more directed toward the quantitative aspects of major environmental changes it will be necessary to determine such changes by studying the bulk composition of fluvial sediments (Kroonenberg, 1990). It is rather cumbersome to derive a bulk composition from the mineralogical composition of separate fractions or from time consuming point-counting of thin sections. Therefore we decided to measure bulk sand composition geochemically.

Although it is a common practice in exploration geochemistry to sample only one size fraction from stream sediments in order to obtain measurable and comparable results (Plant et al., 1988), we use geochemical measurements for bulk sand samples of all size fractions.

As a case study the Allier and Dore basins in the Massif Central were selected as two basins having different basin geology and consequently different sand compositions.

3.1.2. Materials and Methods

The Allier was sampled in 14 locations (total of 57 samples) by Kroonenberg et al. (1988), along a section between the confluences with the Couze Chambon in the south and the Dore in the north. The sample locations are situated in the present bed (Z) and four different terrace levels (Y, X, W, V) (Figure 3.1.1). Along a stretch of 30 km along the Dore river, 43 sand samples were taken at 12 sites from the same terrace levels as sampled along the Allier. The Dore was sampled from the confluence with the Allier up to its emergence from the rift valley scarp. In order to include the effect of sorting, 2 - 6 samples of different grain size distribution were taken from each

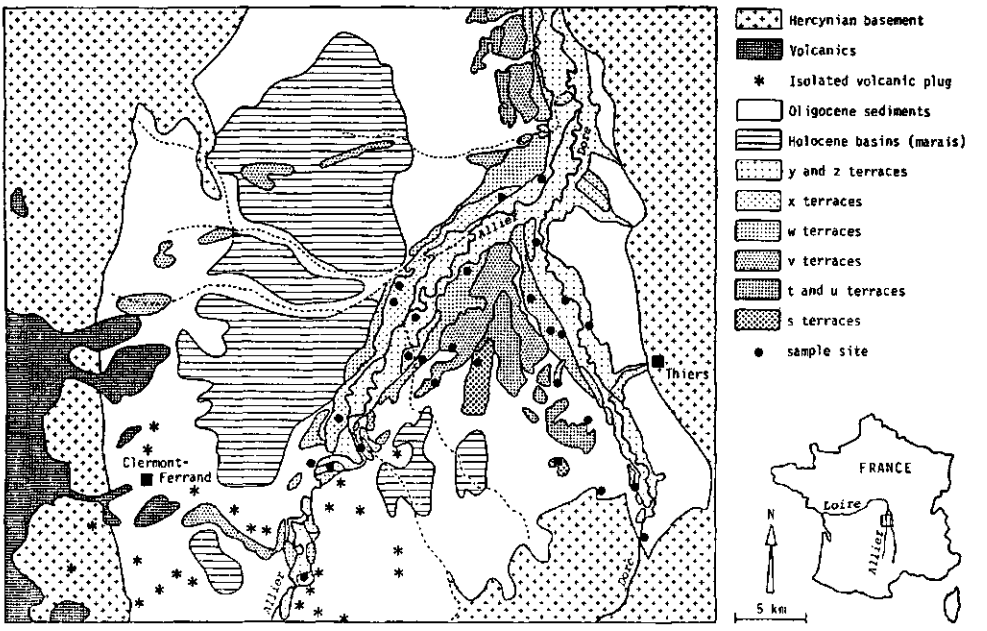

Figure 3.1.1. **Geological sketch map and sample locations in the Allier and Dore basins.**

sampling spot.

Three physical parameters were considered during sampling: RELALT (altitude relative to the present river bed), UPSTR (upstream distance from confluence Allier/Dore) and MEDIAN (median of grain size of analyzed samples). This was done in an attempt to evaluate the importance of lateral and downstream sorting and postdepositional weathering irrespective of the impact of climatic change and tectonism. Care was taken to sample sand from foreset laminae in small-scale cross-bedded sets, in order to avoid concentrations of heavy minerals in horizontally laminated lag deposits. Samples were taken as deep as possible to avoid effects of soil formation.

In the laboratory, detailed granulometrical analyses were carried out for 13 fractions. The <16 μm, <0.053, 0.053-0.075, 0.075-0.106, 0.106-0.15, 0.15-0.212, 0.212-0.3, 0.3-0.425, 0.425-0.6, 0.6-0.85, 0.85-1, 1-2, 2-4.8, >4.8 (mm) fractions were determined. The median grain size was determined from cumulative frequency plots. Median grain sizes ranged from 210 μm to 2000

3μm. Part of the sample, was separated with a sample splitter. Organic matter, calcium carbonate, free iron and all material <16 μm was removed by standard methods. This allowed direct comparison of chemical composition with optically determinable mineralogy and allowed us to avoid the effect of accumulated secondary products. Organic matter and manganese coatings were destroyed with H_2O_2 and 'free' iron was extracted with Na-dithionite-EDTA at pH 4.5. Although the clay content was measured, the fraction < 16 μm was not geochemically analyzed. In few cases this fraction (< 16 μm) amounted to more then a few percent by weight of the total sample.

After pretreatment, 0.6 g of the sample was separated with a micro-sample splitter, fused with 2,4 lithium tetraborate and analyzed. The major elements SiO_2, TiO_2, Al_2O_3, Fe_2O_3, MgO, CaO, Na_2O, K_2O and P_2O_5 and minor elements V, Cr, Ni, Cu, Zn, Ga, Rb, Sr, Zr, Nb, La, Ba and Pb were measured with X-ray fluorescence spectroscopy on a Philips XRF assembly. The system was calibrated using USGS geochemical standards as listed by Abbey (1980, p. 16). The mean, maximum and minimum bulk concentrations of the elements in Dore and Allier samples are listed in Table 3.1.1.

Statistical treatments were performed with SPSSpc (Norusis, 1986). The significance of differences in mean element abundances between the Allier and Dore groups were tested by a Students t-test. The interpretation of this complex multi-variable data set was carried out using factor analysis. Factor analysis examines the interrelationships among the variables (elements) in an effort to find a new set of variables (factors) fewer in number than the original set of variables, which express that which is common among the original variables (Dillon and Goldstein, 1984). A factor analysis is presented as a matrix giving the factor loadings of each variable. A factor loading indicates the relative contribution of a variable to the factors made; the larger the loading the more important the variable in the interpretation of the factor. The factors are rotated with a varimax rotation, to allow better group identification and interpretation. Multiple linear regression analysis was done with the stepwise methodology.

Var.	LLD	Dore			Allier		
		Mean	Minimum value	Maximum value	Mean	Minimum value	Maximum value
SiO_2	.007	81.09	69.42	89.00	74.95	63.01	85.02
TiO_2	.01	0.14	0.02	0.53	0.78	0.27	1.78
Al_2O_3	.075	10.15	5.25	16.36	11.63	7.84	15.61
Fe_2O_3	.003	0.65	0.13	1.91	3.27	0.82	7.87
MgO	.01	0.30	0.06	0.95	1.60	0.22	4.60
CaO	.0014	0.26	0.01	0.98	2.07	0.49	5.38
Na_2O	.01	1.68	0.28	3.42	2.23	1.50	3.63
K_2O	.006	4.32	3.21	5.22	2.88	1.92	3.80
P_2O_5	.01	0.06	0.03	0.13	0.19	0.06	0.44
V	4	25	5	57	99	22	232
Cr	14	10	10	10	33	10	148
Ni	2	2	2	2	21	2	82
Zn	1	7	1	85	26	1	76
Ga	4	11	5	18	12	8	16
Rb	1	147	106	197	105	54	218
Sr	1	146	75	208	282	149	531
Zr	2	63	7	349	112	33	215
Nb	4	5	3	18	11	5	21
Ba	36	657	446	802	676	506	879
La	7	18	6	73	22	6	68
Pb	1	20	10	29	11	10	29
sand fractions:							
<4.8	0.1	11.0	0.5	35.5	2.0	0.1	13.1
2-4.8	0.1	18.2	0.5	38.5	3.6	0.1	23.0
1-2	0.1	15.9	1.0	28.0	11.9	0.1	47.9
0.85-1	0.1	14.8	1.0	31.0	5.6	0.1	16.2
0.6-0.85	0.1	10.5	1.0	32.0	17.3	0.5	41.8
0.425-0.6	0.1	7.3	1.0	28.0	18.1	1.5	51.9
0.3-0.425	0.1	5.5	0.8	17.0	16.8	2.6	43.2
0.212-0.3	0.1	2.8	0.5	19.0	12.4	0.8	47.0
0.15-0.212	0.1	1.8	0.5	29.0	7.1	0.1	35.5
0.106-0.15	0.1	0.9	0.5	6.0	3.0	0.1	22.9
0.075-0.106	0.1	0.8	0.5	4.5	1.0	0.1	12.4
0.053-0.075	0.1	0.8	0.5	4.5	0.4	0.1	5.4
<0.053	0.1	0.9	0.5	5.5	0.6	0.1	7.6

Table 3.1.1 **Means, maximum and minimum values of major and minor elements and grain size classes of the Dore (32 samples) and Allier (49 samples) sands. SiO_2 to BaO and in weight percentages of oxides, Rb to Nb in weight ppm of the elements, size fractions (mm) in %.**

3.1.3. Results

Mean bulk geochemical composition of the Allier and Dore sands is given in Table 3.1.1. The average amounts of TiO_2, Al_2O_3, Fe_2O_3, MgO, CaO, Na_2O, P_2O_5, V, Cr, Ni, Zn, Sr, Zr and Nb are higher for the Allier sands whereas SiO_2, K_2O, Rb and Pb are higher for the Dore sands. The differences in mean element abundances between the Allier and Dore data are given in Table 3.1.2. In spite of high standard deviations, the differences between the elemental composition of sands from both rivers are significant with the exception of Ga, Ba and La.

As it is difficult to interpret and compare the raw Allier and Dore bulk sand compositions, a factor analysis with componential extraction was done for each basin (Table. 3.1.3). The input data set for each basin included not only the bulk geochemical composition but also the physical parameters RELALT, UPSTR and MEDIAN.

	Allier		Dore		
Var.	Mean	Standard Deviation	Mean	Standard Deviation	T-test 2-Tail Prob.
SiO_2	74.95	5.52	81.09	4.47	.000
TiO_2	0.78	0.40	0.14	0.11	.000
Al_2O_3	11.63	1.61	10.15	2.49	.003
Fe_2O_3	3.27	1.75	0.65	0.45	.000
MgO	1.60	1.13	0.30	0.24	.000
CaO	2.07	1.26	0.26	0.26	.000
Na_2O	2.23	0.31	1.68	0.87	.001
K_2O	2.88	0.39	4.32	0.37	.000
P_2O_5	0.19	0.10	0.06	0.03	.000
V	99	49	25	11	.000
Cr	33	37	10	0	----
Ni	21	19	2	0	----
Zn	26	23	7	15	.000
Ga	12	2	11	3	.079
Rb	105	30	147	23	.000
Sr	282	92	146	35	.000
Zr	112	51	63	64	.000
Nb	11	4	5	3	.000
Ba	676	60	657	69	.187
La	22	15	18	15	.273
Pb	11	4	20	5	.000

---- = below detection limit, st. dev. = 0.

Table 3.1.2 Comparison of the mean element concentrations of Allier and Dore by Students t-test. SiO_2 to P_2O_5 in weight percentages of oxides, V to Pb in weight ppm of the elements.

var.	Allier Fact 1 58.3%	Fact 2 13.8%	Fact 3 6.1%	Com.	Dore Fact 1 51.6%	Fact 2 11.4%	Fact 3 8.3%	Com.
Rel. alt.			0.72	0.63	0.93			0.87
UPST	0.50			0.50				0.05
Median		-0.79		0.63		-0.55		0.41
SiO_2	-0.87			0.98	-0.83			0.98
TiO_2	0.96			0.96		0.79		0.90
Al_2O_3		0.76		0.93	0.87			0.95
Fe_2O_3	0.96			0.95	0.74	0.52		0.88
MgO	0.95			0.94	0.77			0.86
CaO	0.94			0.95	0.83			0.93
Na_2O		0.80		0.76	0.94			0.95
K_2O	-0.55	0.61		0.84			0.81	0.73
V	0.91			0.89		0.59		0.58
Cr	0.84			0.84	--	--	--	
Ni	0.87			0.76	--	--	--	
Ga		0.59		0.55	0.77			0.80
Rb		0.82		0.79			0.83	0.83
Sr	0.91			0.91	0.93			0.91
Zr	0.89			0.93		0.90		0.88

Table 3.1.3 **Factor analysis including physical parameters, bulk geochemistry Allier and Dore sands.**

Interpretation of Allier data

The Allier sand data set can be described by three significant factors (Table 3.1.3), together explaining 78.2% of total bulk geochemical variance (cf. Kroonenberg et al., 1988).

Factor 1

Factor 1 explains 58.3% of the total variance, contains the variables UPSTR, TiO_2, Fe_2O_3, MgO, CaO, Ni, Cr, V, Sr, Zr, $-K_2O$ and $-SiO_2$. The contributing elements are known to occur in many different minerals of the Allier sands, notably olivine, augite, amphiboles, calcic plagioclase and Fe-Ti opaque minerals. The distribution of the elements between these minerals can be established in an approximate way from general crystal-chemical considerations and published mineral analyses from other sites.

Olivine, augite, amphiboles and plagioclases are common constituents of alkali basaltic rocks such as abound in the Central Massif. Well-rounded fragments of dense alkali-basaltic lavas, with a specific gravity around 3 g/cm^3, form the bulk of the heavy fraction of the Allier sands, and may constitute up to 50% by weight of the total sediment (Kroonenberg et al, 1988). It can be expected that this alkali-basaltic fraction strongly determines the variance in geochemical properties of the Allier sands. Therefore Factor 1 is interpreted as an alkali basaltic factor. The positive factor loading of UPSTR might indicate a downstream backlagging of alkali basalt grains due to density sorting as reported by Davies et al. (1978).

Factor 2

Factor 2, explaining 13.8% of the total variance, includes the variables, MEDIAN, K_2O, Na_2O, Al_2O_3, Rb and Ga. The contributing elements are fractionated by alkali feldspars and mica's (K, Na, Si, Al). Rb substitutes for K especially in mica's, and Ga for Al. Therefore these micro-elements are logical constituents of this factor.

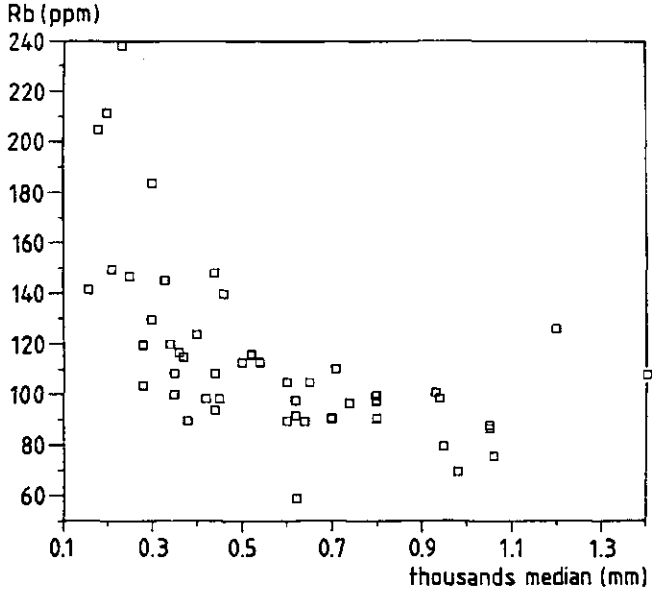

Figure 3.1.2. **Bivariate plot of Rb (ppm) with Median of grain size distribution of Allier sands. Data points are indicated by terrace symbols.**

As these minerals may be derived both from the crystalline basement as from acid volcanic rocks, factor 2 is interpreted as an alkali feldspar-mica factor without further specification. The negative MEDIAN factor loading indicates that variation at single sample sites by lateral sorting is probably related to the specific hydraulic properties of mica's and feldspars. This is well illustrated by Figure 3.1.2, in which Rb as a typical mica element is plotted against MEDIAN. Mineralogical analysis of samples of different grain size confirm these relations (Kroonenberg et al., 1988).

Factor 3

Factor 3, which explains 6.1% of the total variance, only contains RELALT. This suggests that bulk geochemical variation between terrace levels is partly independent from other variables, and probably reflects long-term changes in sediment supply.

Summarizing, the factor analysis indicates that variance of bulk geochemical properties of the Allier terrace sands is mainly due to an alkali basaltic component, which shows some longitudinal sorting, and to a lesser extent to local lateral sorting effects, especially of mica's and feldspars, and long-term changes in sediment composition.

Interpretation of Dore data

The Dore data are also grouped into three significant factors explaining 71.3% of the total variance (Table 3.1.3).

Factor 1

Factor 1, explains 51.6% of the total variance, and contains RELALT, Al_2O_3, Fe_2O_3, MgO, CaO, Na_2O, Ga, Sr, and $-SiO_2$. This factor includes elements which are known to be found in plagioclases, amphiboles and augite as major rock-forming minerals. The positive RELALT loading indicates a decrease of the factor 1 elements in the higher Dore terraces (Figure 3.1.3). As the altitude criterium can be directly used as an age criterium, the RELALT factor loading indicates a decrease of the factor 1 elements with increasing age.

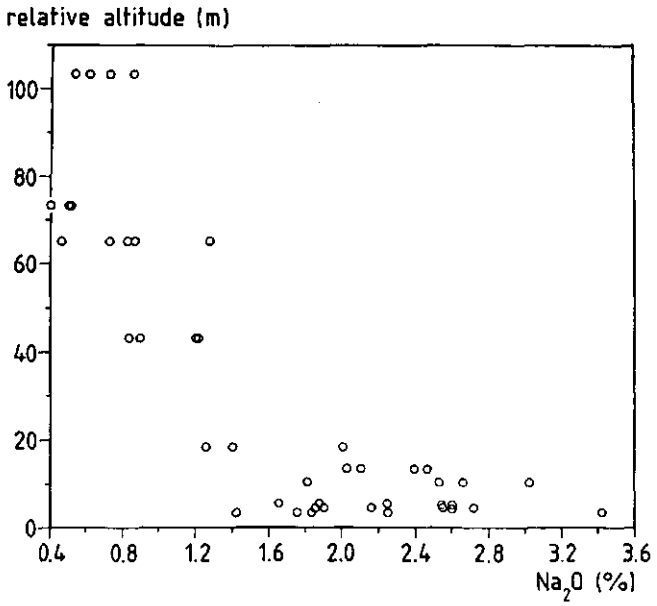

Figure 3.1.3. Bivariate plot of Na_2O (wt%) with relative altitude of Dore sands.

Since most elements of factor 1 are known as mobile with respect to weathering and predominantly occur in easily weathered minerals (Bear, 1964, Wedepohl, 1970) factor 1 can be considered as a weathering factor.

Factor 2

Factor 2, explaining 11.4% of the total variance, contains the variables MEDIAN, TiO_2, Fe_2O_3, Zr and Nb. These elements are common in stable heavy minerals like magnetite, ilmenite, rutile and zircon. The interpretation of Factor 2 as a stable heavy mineral factor is supported by the negative MEDIAN loading, as these minerals are commonly concentrated in the finer sand fractions (Figure 3.1.4).

Factor 3

Factor 3, explaining 8.3% of the total variance, includes the elements K_2O, Rb, Ba, and Pb. These elements are fractionated by K-feldspars and mica's. Rb, Ba and Pb can substitute for K in these minerals. If these elements originate from mica's alone, a strong negative MEDIAN factor loading and Rb dependence would

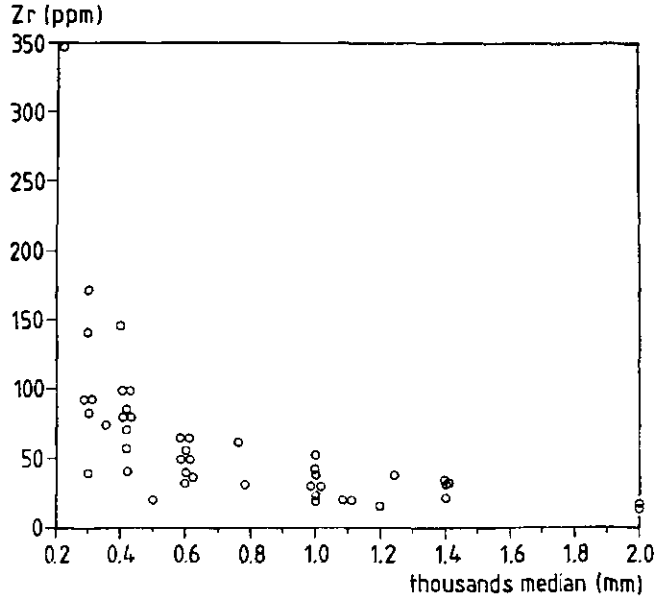

Figure 3.1.4. **Bivariate plot of Zr (ppm) with Median of grain size distribution of Dore sands.**

have been expected. However, as the median and Rb factor loadings are less than 0.5, the contribution of K-feldspar to Factor 3 is probably different from the influence of the mica component. Factor 3 is interpreted as a stable light mineral factor, related to crystalline rock fragments and fragments of large K-feldspar megacrysts from coarse porphyritic biotite granites common in the Dore drainage basin.

In summary, the Dore factors yield different conclusions then the Allier factors. The main part of the total variance of the geochemical properties reflects progressive weathering of the unstable minerals with increasing age of the sands. 11.4% of the total variance is caused by sorting of heavy minerals, while 8.3% of the total variance is determined by varying amounts of mica's and K-feldspars.

3.1.4. Regression with grain size data

Grain size and weathering are the main factors governing local bulk composition for both Allier and Dore sands. In order to

better assess the impact of these factors their effects were quantified by means of multiple linear regression.

Both Allier and Dore sands show approximately 10% of their total bulk geochemical variance is related to the median grain size of the sand sample. In three Dore grain size classes most measurements are below detection limit, and consequently have no normal distribution, these fractions, 0.053-0.075, 0.075-0.106 and 0.106-0.15 (mm), are excluded from further analysis and interpretation.

For each grain size related element a multiple linear regression model was made. From the twelve grain size classes, classes were selected with stepwise methodology as independent variables (Dillon and Goldstein, 1984).

Both Allier and Dore sands resulted in three significant models (at the 0.05 level). The standardized regression coefficients (Betas) and coefficients of determination (R^2) of the regression models are presented for each model (Table 3.1.4).

Elements (wt%)	R^2	fraction (mm)	Beta1 (-)	fraction (mm)	Beta2 (-)	fraction (mm)	Beta3 (-)
Allier:							
Al_2O_3	0.63	(0.212-0.15)	0.77	(0.85-0.6)	-0.27		
Na_2O	0.56	(0.212-0.15)	0.39	(0.85-0.6)	-0.69		
Rb	0.60	(0.212-0.15)	0.73				
Dore							
TiO_2	0.66	(0.15-0.106)	0.67	(0.6-0.425)	0.38	(0.075-0.053)	0.37
Fe_2O_3	0.55	(0.3-0.425)	0.40	(<0.053)			
Nb	0.78	(0.212-0.15)	0.79	(0.6-0.425)	0.31	(<0.053)	0.44
Zr	no significant model at the 0.05 level						

Table 3.1.4 **Multiple linear regression models for grain size related elements, model fit (R^2) and standardized regression coefficients for the grain size fractions selected with step wise methodology.**

A multiple regression on extracted components from the grain size data of both Allier and Dore samples resulted is similar regression models with comparable model fits, indicating that the role of collinearity is very limited.

3.1.5. Regression modelling of weathering effects

The Dore terrace sequence is strongly affected by weathering as reflected in almost 52% of the total geochemical variability. The weathering effect is not so apparent in the Allier sands. As Allier and Dore are both situated in the Limagne rift valley, Allier and Dore terraces should have experienced similar climatic conditions and hence a similar weathering trend.

The Allier data show that both clay content and content of factor 1 elemental ("basaltic") oxides (MgO for example) of the sands have a rather erratic behaviour within and between terrace levels (Figure. 3.1.5). This implies that neither basalt (parent material) nor clay (weathering product) content are simply related to terrace age, as might be expected in a chronosequence. Despite their unpredictable behaviour, "basaltic" oxides and clay content have an inverse semi-logarithmic relation (Figure. 3.1.6), suggesting a relationship between parent material and weathering.

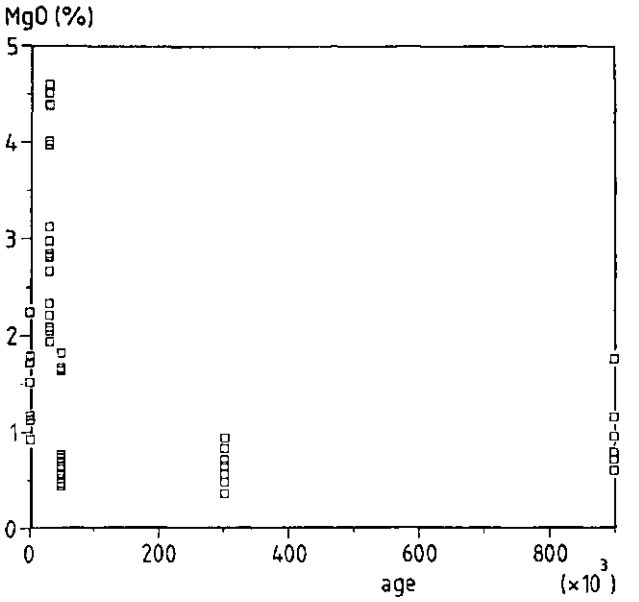

Figure 3.1.5. **Measured Mg (Ox wt%) and age relationship (according to PASTRE, 1986) in years in the Allier terrace sands.**

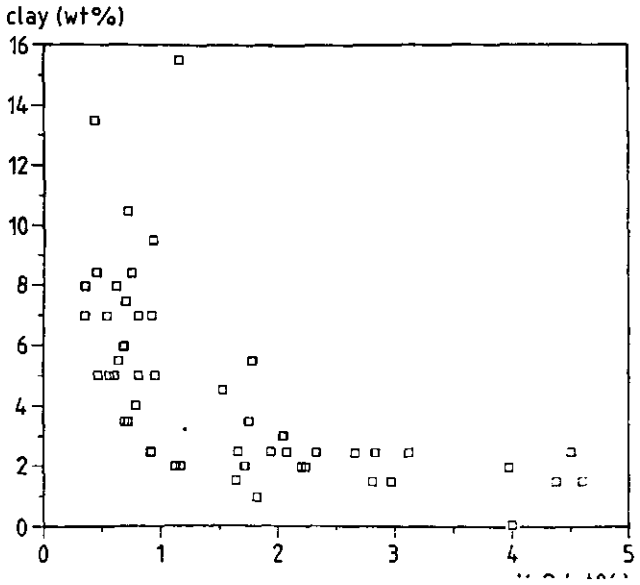

Figure 3.1.6. **Measured Mg (Ox wt%) and Clay (wt%) relationship for the subsoil fluvial sands of the Allier.**

In order to determine the effect of parent material in the Allier chronosequence a multiple regression analysis was carried out. Results showed actual Mg content with the independent contributions of (1) a clay formation factor, (2) a parent material factor and (3) their interaction factor.

The clay content seems related to the actual Mg content by a semi-logarithmic relationship and is transformed by a natural logarithm ln(CLAY (wt%)) (Figure. 3.1.6).

As independent parent material factor only the downstream compositional sorting variability of alkali basaltic rock fragments can be included (cf. Davies et al., 1978; Kroonenberg et al.,1988).

The interaction term is ln(CLAY) . UPSTREAM. A high contribution of this term will indicate a strong relationship between weathering and parent material composition.

In this way the following multiple regression model can be established to predict actual Mg content in MgO wt%.

$$Mg = Const + B_1 UPSTREAM + B_2 \ln(CLAY) + B_{1,2}(UPSTREAM \cdot \ln(CLAY))$$

The regression model is significant at the 0.05 level. Model fit expressed by the coefficient of determination (R^2) was 0.71. Similar regression models were made for the other basaltic elements Ti, Fe, Mn, Ca and P. All these regression models were significant at the 0.05 level and have model fits of about 0.65 (Table 3.1.5).

Elements	R^2	$Beta_1$	$Beta_2$	$Beta_{12}$
TiO_2	0.59	0.19	0.70	-0.64
Fe_2O_3	0.60	0.23	0.74	-0.64
MnO	0.63	0.09	0.68	-0.55
MgO	0.71	0.26	0.78	-0.75
CaO	0.66	0.29	0.75	-0.80
P_2O_5	0.60	0.30	0.74	-0.76

Table 3.1.5 **Multiple linear regression models for basaltic elements, model fit (R^2) and standardized regression coefficients. wt% basaltic element = B_0 + B_1*ln(wt%CLAY) + B_2*UPSTREAM(km) + $B_{1,2}$*ln(wt%CLAY)*UPSTREAM(km)**

The good model fits and the high loading of the parent material/weathering interaction term show that the Allier sand composition is strongly affected by parent material controlled weathering. A result also found for gravel weathering in the Allier terraces (Veldkamp et al., 1990).

3.1.6. Discussion

The results show that several regional and local factors have a significant contribution to the actual bulk sand composition in the Allier and Dore drainage basins. The most important local factors are sorting processes and postdepositional weathering. The factors provenance and changes of sediment composition in time have a more regional character and are of interest for Quaternary research. The origin of the variability in bulk geochemistry will be discussed individually for each factor and

finally the value of the bulk geochemical methodology will be discussed in the conclusions.

Provenance

It was shown that TiO_2, Al_2O_3, Fe_2O_3, MgO, CaO, Na_2O, P_2O_5, V, Cr, Ni, Cu, Zn, Zr, and Sr levels are significantly higher in the Allier sediments, whereas SiO_2, K_2O, Rb and Pb levels are significantly higher in the Dore sediments. These element abundances are evidently related to differences in sand provenance. The Dore sands derived from crystalline basement only, have higher levels of elements from quartz, K-feldspars and mica's (factor 3), while the Allier sands derived from both volcanic rocks and crystalline basement have higher amounts of elements of volcanic origin (factor 1). The occurrence of heavy minerals derived from volcanic ash in the Dore basin reported by various authors (Pelletier, 1971; Van Wijck, 1985; Etlicher et al., 1987), is not demonstrably reflected in the bulk geochemistry of the Dore sands.

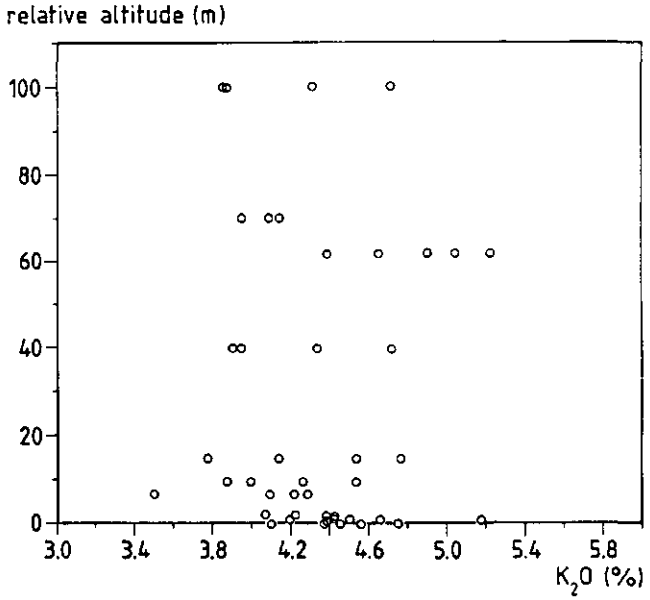

Figure 3.1.7. **Bivariate plot of K_2O (wt%) with relative altitude of Dore sands.**

Changes in sediment composition with time

The emergence of relative altitude as an independent factor in the Allier terraces is most probably caused by major changes in sediment supply or composition with time. Bout (1963) and Kroonenberg et al. (1988) proposed a relationship between climate (glaciated Cantal and Mt Dore) and sediment type (basalt content), large amounts of basalt are supplied to the Allier terrace sediments during a melting phase of the glaciers. Pastre (1986) suggested that not climate but volcanism is responsible for the sediment differences between the various terrace levels. In the largely unglaciated Dore basin where volcanism is absent, no such changes have been observed, as shown by the K_2O-Altitude diagram of Figure 3.1.7.

Sorting processes

The heavy mineral factor of the Dore and the alkali feldspar/mica factor of the Allier are grain size related and depend upon the local paleo-discharge during sedimentation. For both fluvial systems the local lateral sorting component is about 10% of the total variance in bulk geochemical characteristics. The sediments of Allier and Dore differ mainly in the elements for which grain size dependent relations are found (Allier: Al_2O_3, Na_2O, K_2O and Rb; Dore: TiO_2, Fe_2O_3, Nb and Zr). The main causes for these differences are probably the contrasting provenance. The standardized regression coefficients (Betas) of the multiple regression models, show high positive Betas for finer fractions and negative Betas for the coarser fractions. This suggests that the grain size related elements are predominantly present in the finer sand fractions.

This observation can easily be explained by the following processes and causes. Rb, a typical mica element, tends to concentrate in the fine sand fractions, due to the specific shape related hydraulic properties of mica's. Na_2O and Al_2O_3, originating from feldspars, are often reported to be more abundant in the finer sand fractions, due to selective abrasion (Riezebos, 1971; Basu, 1976; Odom et al., 1976; Davies et al., 1978; Potter, 1978; Pettijohn et al., 1987).

The enrichment of Ti, Zr, Nb and La (stable heavy minerals) in the finer Dore sands is related to the well known and often observed relationship of specific settling velocity with high densities and small primary grain sizes of these minerals.

The UPSTR factor loading of 0.5 in the main Allier factor, shows that there is a decrease of alkali-basaltic fragments downstream. Because no important tributaries occur in the region sampled, the downstream decrease can be explained by density sorting or by physical breakdown during transportation (Davies et al. 1978). A density sorting effect is supported by the large average bulk density of the alkali-basaltic fragments which is about 3 (g/cm^3). The susceptibility of those fragments to physical breakdown is illustrated by the well-rounded shape of most alkali-basaltic grains. It is not certain which effect predominates.

Postdepositional weathering

In the Dore basin factor analysis indicates that the amount of mobile elements (Factor 1) decreases with terrace altitude, indicating progressive weathering of unstable minerals. Plots of individual Factor 1 elements against relative altitude (e.g. Na; Figure. 3.1.3) corroborate this. Mica-feldspar (Factor 3) elements such as K plotted against relative altitude (Figure. 3.1.7) show no significant change. This observation substantiates the relative immobility of K in the Dore sands.

In the Allier basin, however, no weathering trend is directly discernable from factor analysis, in spite of the high amount of easily weatherable volcanic material in the sediment and the many weathering phenomena (Jongmans et al., 1991). But multiple regression modelling of the weathering effects in the Allier bulk sand composition showed that the variability of the present "basalt" content is strongly related to parent material controlled weathering. The regression models of weathering for MgO and CaO have the best fit (highest R^2) probably because they have easy weatherable mineral sources (olivine and Ca-plagioclases), in contrast to the other "basaltic" elements which

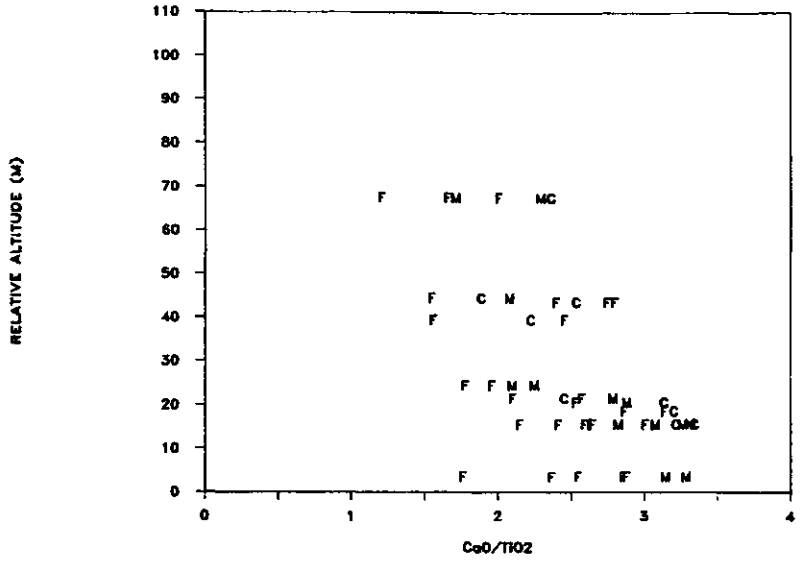

Figure 3.1.8. Bivariate plot of decreasing CaO/TiO2 with relative altitude of Allier sands. Data labels indicate median of grain size distribution, C = coarse, 900–2000 μm; M = medium, 600–900 μm; F = fine, 210–600 μm.

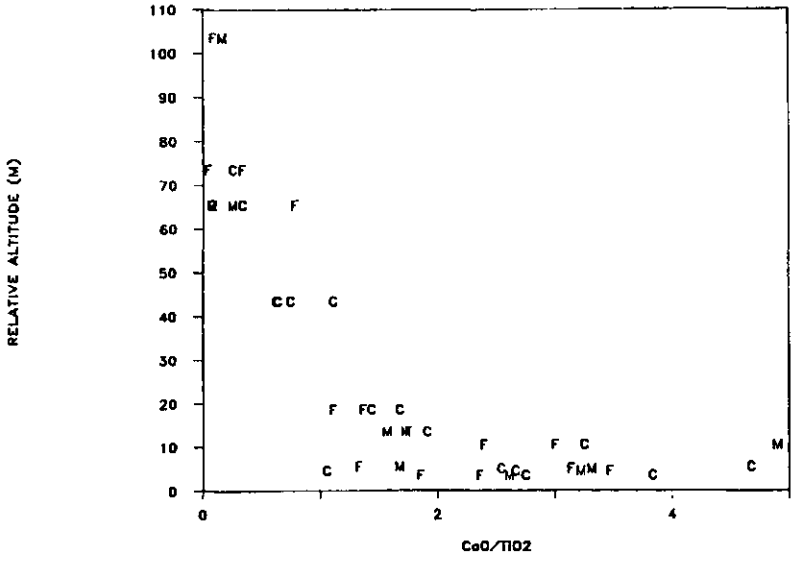

Figure 3.1.9. Bivariate plot of decreasing CaO/TiO2 with relative altitude of Dore sands. Data labels indicate median of grain size distribution, C = coarse, 900–2000 μm; M = medium, 600–900 μm; F = fine, 210–600 μm.

have more weathering resistant basaltic mineral sources, like heavy opaque minerals. The regression models have an average coefficient of determination of 0.65, indicating that about 65% of the total geochemical variability in actual "basaltic" elements content can be ascribed to the combined effect of parent material and clay neoformation.

Empirical weathering indices for Allier sediments (Ca/Ti; Figure. 3.1.8; Kroonenberg et al., 1988) and for Dore sediments (Figure. 3.1.9) show similar trends. Apparently the great fluctuations in the amount of basaltic rock fragments supplied to the Allier strongly influenced the gradual loss of mobile elements by weathering. On the contrary, the geochemical composition of the Dore sediments remained essentially constant with time.

Conclusions

What knowledge was obtained from our approach to analysis sands bulk geochemically? The main advantage as we see it is the easy quantification of bulk sediment composition allowing statistical processing of the data, facilitating the identification and quantification of sediment composition determining factors.

The local grain size and weathering factors were easily determined and quantified. The grain size factor has apparently only a limited impact on the bulk sand composition in the studied areas, only a few specific elements and probably some minerals too are strongly grain size determined.

Post depositional weathering which strongly controls the present Dore terrace sediment composition, is also prominent in the Allier sands where it is strongly related with sediment composition. The external factors which are of more interest for Quaternary research seem to play only a major role in the Allier basin. A significant factor was found which was interpreted to display climatic or volcanic induced changes in sediment composition.

The added value of the bulk geochemical approach is

illustrated by the fact that in both fluvial systems more than 50% of the variability in bulk geochemistry is due to components which are often neglected in routine sedimentary petrography, i.e. rock fragments and light minerals. This also indicates that bulk sediment geochemistry can result in new and additional data of interest in Quaternary research. However, the interpretation of geochemical factors can only be done if the sand mineralogy is known. Therefore, sediment bulk geochemistry is complementary to sedimentary petrology, but cannot replace it.

3.2 PARENT MATERIAL CONTROLLED SUBSOIL WEATHERING IN A CHRONOSEQUENCE, THE ALLIER TERRACES.

A. Veldkamp & T.C. Feijtel

Abstract
The chronosequence in the Allier terraces is subject to erratic changes in parent material composition with time. Approximately 65% of the total variance in the basaltic elements content in the Allier terrace sands can be explained by the combined effect of parent material and time related neoformation of clay in the subsoil. It is shown that parent material composition, as a function of transport distance, strongly influences weathering rate in the Allier terrace chronosequence. In order to evaluate parent material controlled weathering effects a process model simulation was made based on an exponential decrease of MgO and neoformation of clay. Long term simulations with this model suggest that parent material controlled subsoil weathering is significant for sediments with easy weatherable fragments. After prolonged weathering the role of parent material decreases and becomes untraceable in strongly weathered materials.

3.2.1 Introduction

River terraces are often used as chronosequences to study rates of weathering and soil formation. Such chronosequences are selected in order to keep soil-forming factors other then time constant (Stevens & Walker, 1970). However, the assumption of constancy of parent material for terrace sediments is often not very realistic (Kroonenberg et al., 1990). In many terrace sequences of major rivers, like the Rhine and Meuse, the composition of the supplied sediments changed with age as a result of uplift and incision in time (van Straaten, 1946; Brunnacker & Boenigk, 1983). Within such chronosequences the terrace sediment maturity commonly increases with age as a result of both postdepositional weathering and changes in parent material. When such chronosequences are studied it is always difficult to separate the role of time and parent material in chronosequence weathering. As it can be expected that parent material strongly determines weathering within a chronosequence we have focussed our study on the role of parent material in chronosequence weathering.

We studied the Allier terrace sequence (Massif Central, France),
a chronosequence with irregular changes in sediment composition

in time (Kroonenberg et al., 1988). Such a chronosequence is expected to separate the effects of parent material and time related subsoil weathering.

The goal of this chapter is to determine and quantify the effect of the original sediment composition on the actual terrace sand composition in the Allier chronosequence. Further it is tried to determine the control of parent material on subsoil weathering in a chronosequence by means of process modelling with a theoretical model.

3.2.2 Materials and methods

Allier terraces (fig. 3.2.1) are numbered according to French usage from Z (youngest) to S (oldest). Along a stretch of 40 km along the Allier river sand samples were taken from the present bed (Z) and from sand and gravel pits in 4 different terrace levels (fig. 3.2.1) at Y= 5 ky, X= 15 and 30 ky, W= 300 ky and V= 900 ky (Pastre, 1986; Raynal, 1984).

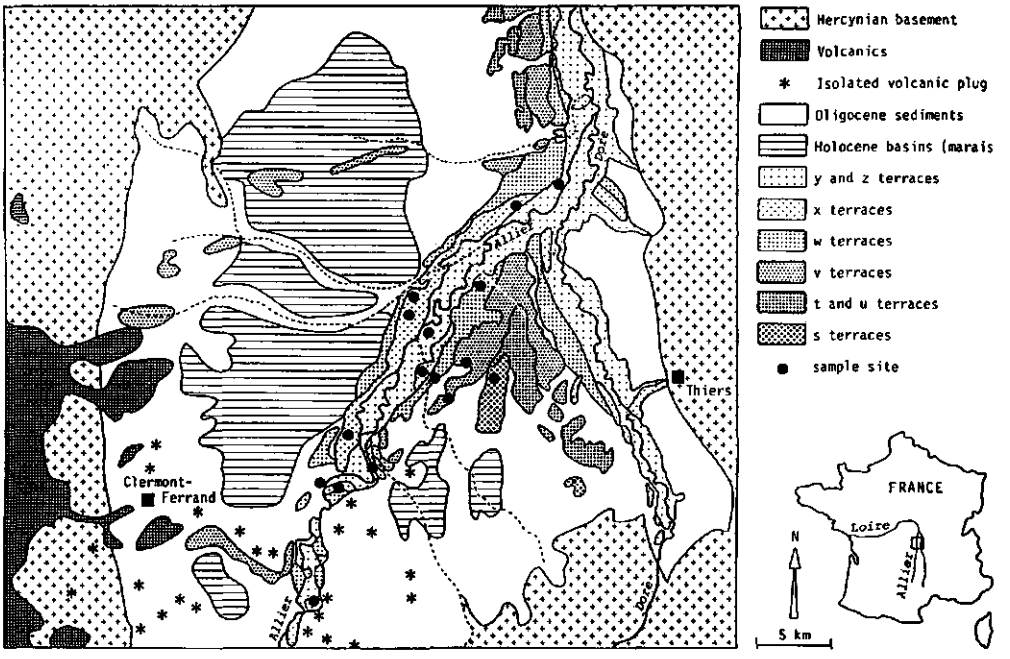

Figure 3.2.1 **Map of the survey area, showing the Allier and its terraces.**

At each sampling site 2-6 samples of different grain size distribution were collected, amounting to a total of 49 samples.

Care was taken to sample as much as possible sand from foreset laminae in small-scale cross-bedded sets, in order to avoid concentrations of heavy minerals in horizontally laminated lag deposits. Samples were taken as deep as possible (subsoil) to avoid effects of soil formation. In the laboratory, detailed granulometric analyses were done (15 fractions). To compare chemical composition with optically determinable mineralogy and to avoid the effect of secondary products, organic matter, calcium carbonate, free iron and all material <16 μm were removed from a representative sub-sample, separated by means of a sample splitter. Organic matter was destroyed with H_2O_2 and 'free' iron was extracted with Na-ditionite-EDTA at pH 4.5. Although the clay and fine silt content was measured, the decantated fraction < 16 μm was not analyzed geochemically.

After this pretreatment, 0.6 g of the sample was separated with a micro-sample splitter, fused with 2,4 g lithium tetraborate and analyzed. The major elements Si, Ti, Al, Fe, Mg, Ca, Na, K and P were analyzed with X-ray fluorescence spectroscopy on a Philips XRF assembly. The system is calibrated using USGS geochemical standards as listed by Abbey (1980, p. 16).

In order to determine whether parent material has a significant contribution to the actual terrace sediment composition of the Allier chronosequence a multiple regression analysis is carried out (Dillon & Goldstein, 1984) with the SPSSpc package (Norisus, 1986).

The following step in our approach is to evaluate the possible effects of parent material controlled weathering by means of a theoretical process response model. Modelling was done in accordance with chemical kinetics. A simplified parent material controlled weathering model was made where basalt containing sediment is weathering under certain strict assumptions. As basis for this model a spread sheet model of Feijtel & Meijer (1990) was used who used a similar modelling approach as Levine &

Ciolkosz (1986).

3.2.3 Results and discussion

Regression modelling on bulk geochemical data

Geochemical variability of the Allier sands is largest in Ti, Fe, Mn, Mg, Ca and P, as a result of varying amounts of basaltic rock-fragments. Also weathering effects, on which this study focuses, are most conspicuous in the basaltic elements (Kroonenberg et al., 1988; Jongmans et al., 1991; Veldkamp & Kroonenberg, 1989). The mean, maximum and minimum concentrations of these elements (Ox wt%) of the fraction between 16 μm and 2000 μm are listed in Table 3.2.1.

Var.	Mean	Minimum value	Maximum value	Standard Deviation
TiO_2	0.81	0.24	1.78	0.42
Fe_2O_3	3.36	1.16	7.87	1.82
MnO	0.04	0.01	0.10	0.03
MgO	1.63	0.36	4.60	1.19
CaO	2.10	0.49	5.38	1.34
P_2O_5	0.19	0.07	0.44	0.10
Clay	4.6	0.1	15.5	3.3

Table 3.2.1 **Means, minimum, maximum and standard deviations of bulk basaltic elements and clay contents of 49 Allier sand samples. Element values are in oxide weight percentages, fraction < 16 μm in weight percentage.**

Previous research showed that the basaltic element variability in the Allier sands is independent of changes in sampling depth and grain size (Kroonenberg et al., 1988; Veldkamp, 1990). The lack of correlation between basalt content and median is explained by the fact that reworking, concentration and depletion of basaltic grains take place simultaneously in sands of all different granulometric characteristics. The insignificant role of sampling depth for each terrace level indicates that all samples were taken deep enough to avoid direct soil formation effects.

The fact that the local site factors, grain size and sampling depth, have no significant contribution to the variability in basaltic elements, makes these elements suitable to study regional weathering effects in the Allier chronosequence.

Weathering of basaltic sand particles in Allier sediments results in an overall loss of Ti, Fe, Mn, Mg, Ca and P in the sand fraction, and an increase of the amount of clay in the terrace (Pastre, 1986; Feijtel et al., 1988; Jongmans et al., 1990). Changes in basaltic fragments content are well illustrated by Ca and Mg content, because they originate from the easier weatherable minerals in these fragments. We use Mg as representative element for basaltic particles in our study. Weathering of basaltic sand particles is therefore described in this paper as a decrease in Mg content and an increase in clay content in the bulk sample, though strictly speaking clay formation is not necessarily the result of the weathering of Mg-bearing minerals.

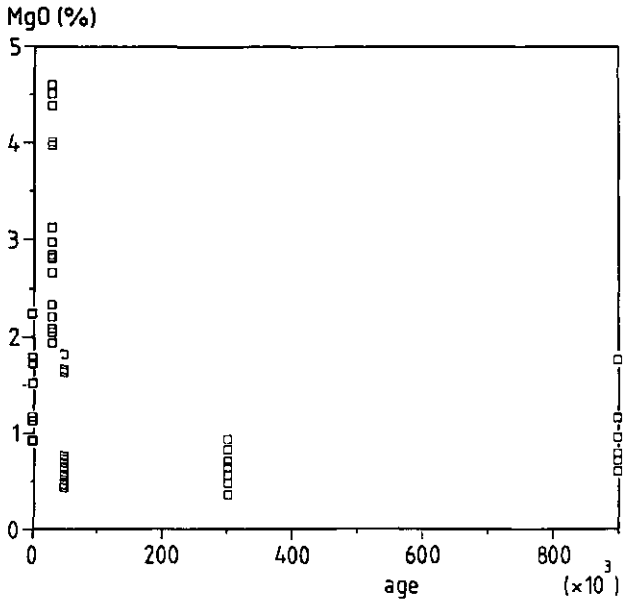

Figure 3.2.2 **Measured Mg (Ox wt%) in the Allier terrace sands with age (age according to Pastre, 1986) in kyears.**

Our data show that both Mg and clay content of the Allier terrace sands show a rather erratic behaviour within and from one terrace level to another (fig. 3.2.2). This implies that neither Mg nor clay content are simply related to terrace age, as might be expected in a chronosequence. Despite their unpredictable behaviour, Mg and clay content have roughly seen an inverse semi-logarithmic relation (fig. 3.2.3), suggesting a relationship between parent material and weathering.

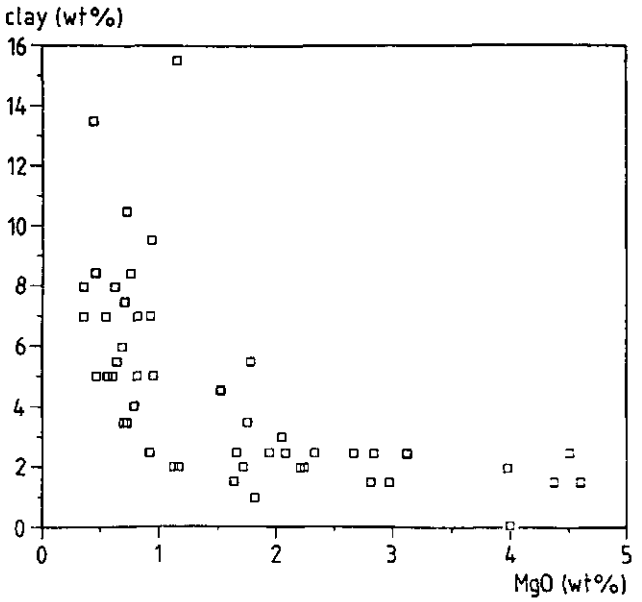

Figure 3.2.3 **Measured Mg (Ox wt%) and Clay (wt%) relationship for the subsoil fluvial sands of the Allier.**

In order to determine the parent material effect in the Allier chronosequence a multiple regression analysis is carried out, predicting the actual Mg content with the independent contributions of (1) a clay formation factor, (2) a parent material factor and (3) their interaction factor.

(1) The clay content seems related to the actual Mg content by a semi-logarithmic relationship (fig. 3.2.3) and is transformed by a natural logarithm ln(CLAY (wt%)).

(2) As independent parent material factor the downstream compositional sorting variability of alkali basaltic rock fragments is included (cf. Davies et al., 1978). Within the studied Allier section the downstream decrease of basaltic grains is almost linear (Kroonenberg et al.,1988). This trend is caused by downstream density sorting and by selective wear of the softer basaltic particles in comparison to harder quartz and feldspar grains. This is the only known variability in original parent material composition which is still traceable. Of course other factors like provenance and volcanism have determined variability in parent material but these factors cannot be reconstructed quantitatively any more. The sorting effect is expressed as UPSTREAM, the distance in kilometres upstream from a chosen point in the Allier.

(3) The interaction term is the product of the independent contributions of clay formation and parent material, ln(CLAY) . UPSTREAM. This term gives an indication of the interaction between the two terms and is used as an independent variable. A high contribution of this term to the regression model will indicate a strong relationship between parent material and weathering.

In this way the following multiple regression model can be established predicting actual Mg (in MgO wt%) content.

$$Mg = Const + B_1 UPSTREAM + B_2 ln(CLAY) + B_{1,2}(UPSTREAM \cdot ln(CLAY)). \quad (1)$$

The regression model was significant at the 0.05 level. Model fit expressed by the coefficient of determination (R^2) was 0.71. Predicted Mg contents plotted with age (fig. 3.2.4) show a good correspondence with measured Mg content with age (fig. 3.2.2). Further analysis of the residuals of the regression model did not reveal any new relationship. A plot of the residuals with age (fig. 3.2.5) shows that there are some differences for the different terrace levels. The X terrace has mainly positive residuals while the Z terrace has mainly negative residuals. These differences suggest different individual terrace

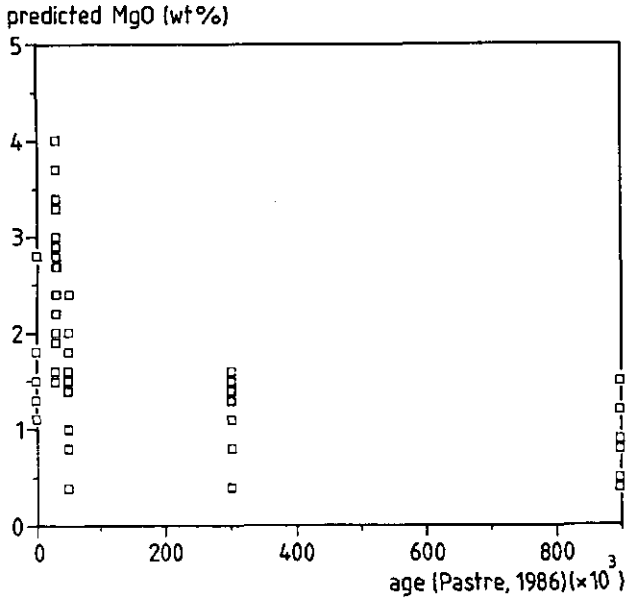

Figure 3.2.4 **Predicted Mg (Ox wt%) with age (according to Pastre, 1986) in kyears.**

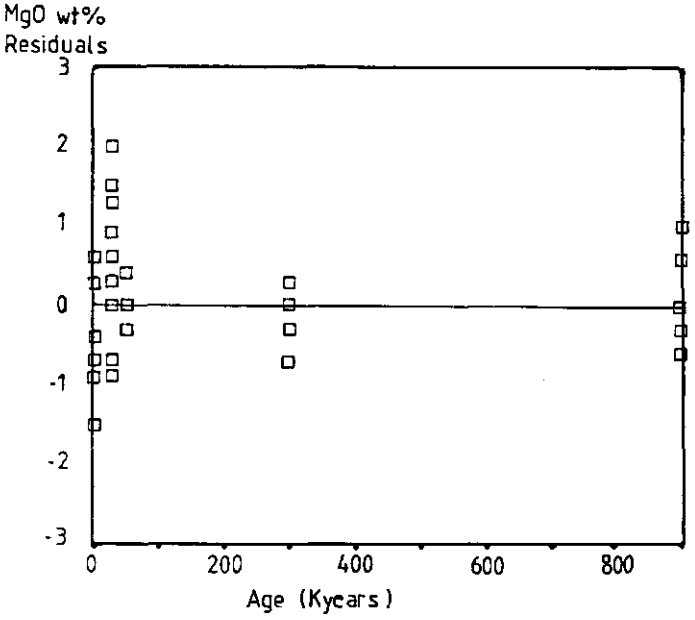

Figure 3.2.5 **Residuals of regression model with age (according to Pastre, 1986) in kyears.**

characteristics which are most probably caused by factors not considered in the regression model such as provenance and volcanism.

Similar regression models were made for Ti, Fe, Mn, Ca and P. All these regression models were also significant at the 0.05 level and have good model fits (Tab. 3.2.2).

Elements	R^2	$Beta_1$	$Beta_2$	$Beta_{12}$
Ti	0.59	0.19	0.70	-0.64
Fe	0.60	0.23	0.74	-0.64
Mn	0.63	0.09	0.68	-0.55
Mg	0.71	0.26	0.78	-0.75
Ca	0.66	0.29	0.75	-0.80
P	0.60	0.30	0.74	-0.76

Table 3.2.2 **Multiple linear regression models for basaltic elements, model fit (R^2) and standardized regression coefficients for the function:**
wt% basaltic element = B_0 + B_1.ln(wt%CLAY) + B_2.UPSTREAM(km) + $B_{1,2}$.ln(wt%CLAY).UPSTREAM(km)

The regression models for Mg and Ca have the best fit (highest R^2) probably because they have easy weatherable mineral sources (olivine, augite and Ca-plagioclases). The regression models have an average coefficient of determination of 0.65, indicating that about 65% of the total geochemical variability in actual basaltic elements content can be ascribed to the combined effect of parent material and clay neoformation.

As it is inappropriate to interpret the regression coefficients (B) as indicators of relative importance of variables, the dimensionless standardized regression coefficients (Betas) are calculated (Tab. 3.2.2). They allow a comparison between the contribution of each independent variable. These standardized regression coefficients indicate a relative large contribution of the interaction term (high negative values) to the overall model. This result indicates, as already suggested by fig. 3.2.3, that weathering product and parent material are strongly interrelated. This means that parent material significantly determines weathering rate within the Allier chronosequence, a result which agrees with the common knowledge on weathering.

Theoretically Modelling of parent material controlled weathering

In most chronosequences weathering products increase in a non linear manner with time, and primary minerals decrease correspondingly (Goldich, 1938; Hay, 1960; Ruxton, 1968; Lowe, 1986). The resulting exponential or semi-logarithmic equations are thought to be in accordance with chemical kinetics (Yaalon, 1975).

We also tried to model in accordance with chemical kinetics. We made a parent material controlled weathering model where basalt containing sediment is weathering under certain strict assumptions. Each assumption is listed and its validity for the Allier chronosequence is pointed out. The weathering process model is based upon the following nine assumptions:

(1) Weathering is decomposition of primary minerals, leaching losses and clay neoformation.

(2) Weathering is confined to basaltic rock fragments.
This assumption is corroborated for the Allier sediment by Jongmans et al. (1990,1991), who reported the volcanic fragments as major source for coatings of secondary weathering products. Although differential weathering susceptibility of the various basaltic minerals is observed (Veldkamp et al., 1990), the process simulation model treats the basaltic fragments as a whole.

(3) The model is only valid for subsoil sand deposits. i.e. interstratal or vadose zone weathering.
This assumption is included to obviate the need for considering vertical profile development in the upper few metres within individual terraces. This assumption is justified for the Allier sediments to some extent as no significant effect of sampling depth has been observed (Kroonenberg et al.,1988).

(4) The model is valid for one million years only.
This is the approximate age of the oldest sampled Allier terrace (Pastre, 1986).

(5) Constant weathering in time.

As it is too speculative to include climatic changes within the simulation model, the effects of weathering are considered to be constant and cumulative. Strictly speaking this assumption is not correct in the Allier basin. During the last million years the region has known many climatic changes which certainly affected water quality and temperature (permafrost) of the vadose zone (Bout, 1963; Veyret, 1978).

(6) No net clay illuviation or eluviation.
This assumption is supported by the fact that our samples originate from sediments (beyond 2-3 meters) where no distinct change in total clay content has been observed in the Allier terraces (Jongmans et al., 1991).

(7) Primary clay content is constant (2 wt %).
Many terraces are stratigraphically complex, with primary variations in clay content which are not taken into account within the model.

(8) Chemical composition of basalt and clay is constant.
This assumption if of course also incorrect for a real system. The average compositions are based on measurements in the Allier sequence given by Jongmans et al. (1991).

(9) Neoformation rate is not hampered by availability of other elements than Mg. Although most Mg is usually lost to the groundwater it is assumed that only Mg is limiting in respect to the neoformation rate.

Different simulations with changing initial compositions (basalt content) allow an evaluation of a real chronosequence like in the Allier basin. The model is tuned by adapting the rate parameters of both dissolution and neoformation processes (k_1 and k_2) to obtain comparable basalt and clay quantities as measured in the Allier terraces. Clay and MgO contents of the older terraces and the unweathered sands were used As standard reference values. This trial and error tuning was done because no comparable subsoil longterm weathering rates and rate parameters are known. Most weathering rates are based on detailed studies under well defined conditions. Studies which may give

comparable weathering rates as used in our model are catchment studies. These studies have the disadvantage that they register only actual weathering environments which are probably not the same as longterm weathering rates. The used dissolution rate of Mg (7×10^{-5} kg MgO/(ha yr)) is not directly comparable with any known dissolution rate. When this dissolution rate is recalculated into a geochemical denudation rate a value is obtained (2×10^{-3} kg MgO/(ha yr)) which is a factor 10^4 to 10^5 less then measured values in the catchment studies as published in Colman & Dethier (1986). This large difference is mainly caused by the assumption that all Mg is build in clay minerals. In reality most weathered MgO seems to dissolve in the ground water.

Parent material controlled weathering is incorporated in the model by making the rate parameter of neoformation (K_2) dependent on the amount of unweathered basalt (M(b)).

The simulation results of this theoretical and very simplified model have conceptual validity only because no realistic conditions are simulated. Only possible effects of parent material controlled weathering are simulated.

The basic quantitative assumption is that:
Mg (basalt) in sand fraction (a wt. %Mg) --> Clay (b wt. %MgO)

The equations used:

$$\text{Dissolution}_{(t)} = K_1 \cdot M(b) \qquad (2)$$

$$K_1 = k_1 - a \exp(t) \qquad (3)$$

Where:
- $M(b)$ = Mass available primary Mg (kg MgO/ha)
- K_1 = Rate parameter in kg MgO/(ha yr)
- k_1 = 7×10^{-5} kg MgO/(ha yr) for Mg
- a = scale correction factor, 5×10^{-6} kg MgO/ha for Mg
- $\exp(t)$ = time dependence of dissolution in $(yr)^{-1}$

$$\text{Neoformation}_{(t)} = K_2 \cdot M(d) \quad (4)$$

$$K_2 = k_2/M(b) \quad (5)$$

Where $M(d)$ = Mass available dissolved Mg (kg MgO/ha)

K_2 = Rate parameter in kg MgO/(ha yr)

k_2 = 2 (kg MgO)^2/(ha^2 yr) for Mg. kg and ha are squared because K_2 (equation 5) has kg MgO/(ha yr) as units.

$M(b)$ = Mass available primary Mg (kg MgO/ha)

In order to run the model a specific volume of sediment with a 'realistic' primary compositions were chosen.

Thickness of sediment layer (fixed) = 10 cm
Initial bulk density of sediment layer = 1.5 g/cm^3
Initial basalt content in sediment = 42 wt% (S_0), 35 wt% (S_1), 30 wt% (S_2), 25 wt% (S_3)
Mg content in basalt = 8 wt% MgO
Mg content in clay = 1.9 wt% MgO

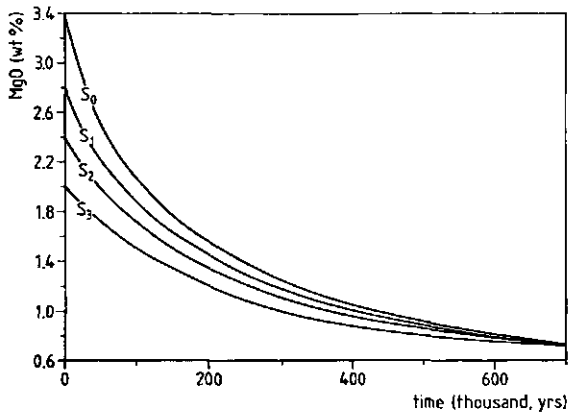

Figure 3.2.6 **Decrease of bulk sediment Mg (Ox wt %) content with time, for four simulations with the process model.**

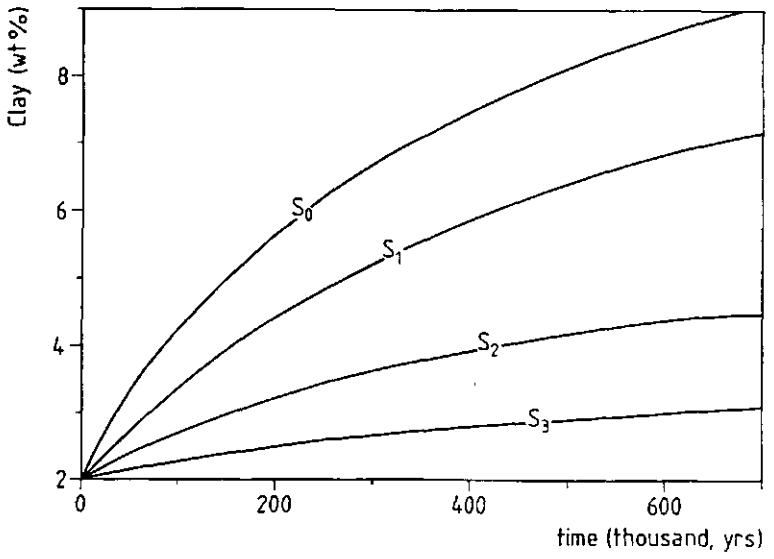

Figure 3.2.7 Increase of neoformed clay (wt%) in time, for four simulations with the process model.

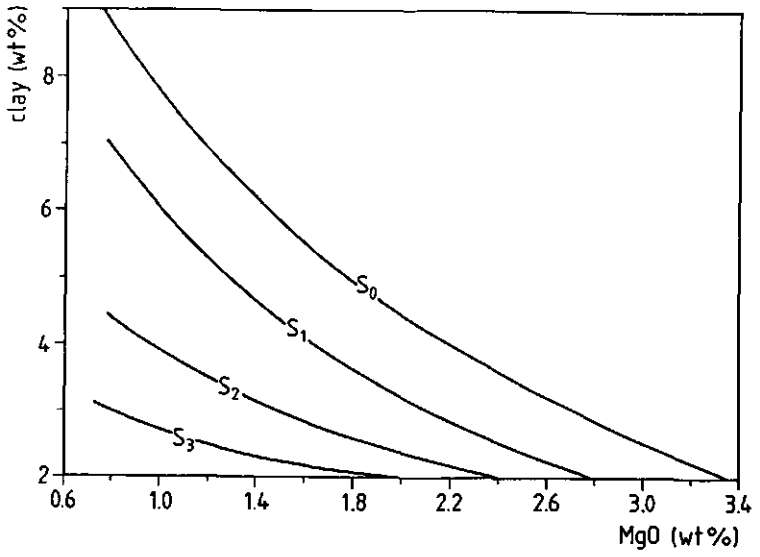

Figure 3.2.8 Total weathered basalt (Mg in Ox wt%) with total new formed clay (wt%), for four simulations with the process model.

The simulation results, which should be viewed qualitatively only, are presented in figs. 3.2.6 and 3.2.7. Figure 3.2.6 shows the decrease of bulk Mg concentration, as a measure of the decreasing basalt content in time. Four simulations (S_0 to S_3) are represented with each having a different initial MgO (basalt) content of the sediment. These different simulations show that sediments with a relative large content of basalt have faster weathering rates than sediments with lower basalt content under similar conditions. It is also illustrated that after prolonged weathering all terraces remain with comparable basalt contents. Figure 3.2.7 showing the increase in clay content during the four weathering simulations, illustrating the stronger increase in clay content of the sediments rich in easily weatherable components. The curves of Fig. 3.2.7 also show a large increase in clay content at the start of basalt rich sediment (S_0) weathering, indicating a high rate of clay formation at the start of that simulation. After prolonged weathering the rate of clay formation decreases and the difference in original sediment composition remains only traceable by the amount of neoformed clay, an unfortunately unmeasurable variable in a real chronosequence. The ultimate weathering stage will be a complete alteration of the basalt particles into clay. Such a stage is reported from the Caquetá basin in the Colombian Amazons, where strong tropical weathering erased all differences in provenance leaving only thick clay soils (Kroonenberg et al., 1990). Fig. 3.2.8, showing the Clay-Mg relations, displays qualitatively comparable relationship as the measured curve of fig. 3.2.3. Although the resulting Clay/Mg curves are not matching the measured effect, it illustrates that this type of relationship is most probably the result of parent material controlled weathering.

The simulation results suggest clearly that parent material composition has especially a strong weathering effect in sediments rich in basaltic particles. After prolonged weathering, more than a 0.5 million years in the model, the basaltic fragment content decreases and differences in initial parent material (S_0 to S_3) are almost erased leaving a chronosequence with very small

differences in MgO content between the different terrace levels.

3.2.4 Conclusions

The analysis of the Allier terrace chronosequence showed that parent material can strongly determine weathering within a chronosequence. The effects of parent material composition should therefore not be underestimated in the study of other chronosequences.

Long term simulations with a simplified theoretical process model of parent material controlled weathering indicate that parent material controlled weathering is only prominent in 'young' sediments with many easy weatherable fragments. Sediments with many weatherable components will show faster weathering rates than sediments with less weatherable components. After several 100 thousands of years of simulated weathering the differences in weathering rate due to the parent material decrease and becomes finally untraceable in very old deeply weathered chronosequences. The differences in initial parent material composition remain theoretically traceable by the total amount of neoformed clay during weathering, but, unfortunately this is an impossible measurable variable in real chronosequences.

3.3 SPATIAL VARIABILITY IN FLUVIAL SAND COMPOSITION AT THE ALLIER/DORE CONFLUENCE.

A. Veldkamp & I.G. Staritsky

Abstract

Spatial sand compositional variability in Allier (Limagne, France) terrace sediments is investigated and compared with spatial trends in the present river bed caused by sediment transport processes. In the actual Allier riverbed complete sediment mixing at the confluence with its tributary the Dore is delayed for approximately one kilometre, while the Younger Dryas terrace sands at this confluence display a delay of several kilometres. Geostatistics allow a discrimination of mixed and unmixed sediments within the same floodplain thus allowing better representative sampling for palaeohydrological research. The delay of complete sediment mixing at a confluence as displayed in sediment composition may be related to the amount of river channels and their sinuosity and floodplain width during deposition.

3.3.1 Introduction

River junctions are points of significant changes within a fluvial system. The site at which two rivers meet is marked by highly complex three-dimensional patterns of flow and sediment transport and deposition. The riverbed morphology reflects the complex flow dynamics and distinctive patterns of sediment transport within the confluence, which are largely controlled by junction angle and the ratio of the discharges between the confluent channels (Mosley, 1976; Best, 1986; Bathurst, 1988). Experimental results of Best (1986, 1988) and Roy & Bergeron (1990) showed that sediments from the tributary channel are preferentially concentrated along a distinct pathway and deposited in separate bars, displaying delayed sediment mixing.

Within palaeohydrology it is generally known that terrace sediments near former confluences have a complex spatial composition, displaying both local and regional variability. The local variability is mainly caused by sediment mixing processes of the main and tributary sediment flows, and the regional variability predominantly caused by past environmental changes. Because the palaeohydrologist is commonly interested in fluvial dynamics related to paleoenvironmental changes, samples near confluence terraces are commonly avoided (Green & McGregor, 1986). It is difficult to discern mixing effects from more

regional effects because there is only limited knowledge on the quantitative effects of sediment mixing. This limitation is due in part to the discrepancy between the short term experiments in well controlled shoots or brooklets and the long term macro scale studies in palaeohydrology.

In order to better understand the large scale sediment mixing at a confluence, the spatial effects of such mixing are investigated. The goal of this chapter is to discern in the Allier riverbed and its associated terrace the spatial compositional variability component caused by the mixing of two distinct sediment flows.

This study will focus first on the spatial mixing characteristics in the present riverbed. Subsequently the spatial compositional trends of terrace sands are investigated and compared with the riverbed sands of the same river allowing a more reliable interpretation of the sediment mixing effects.

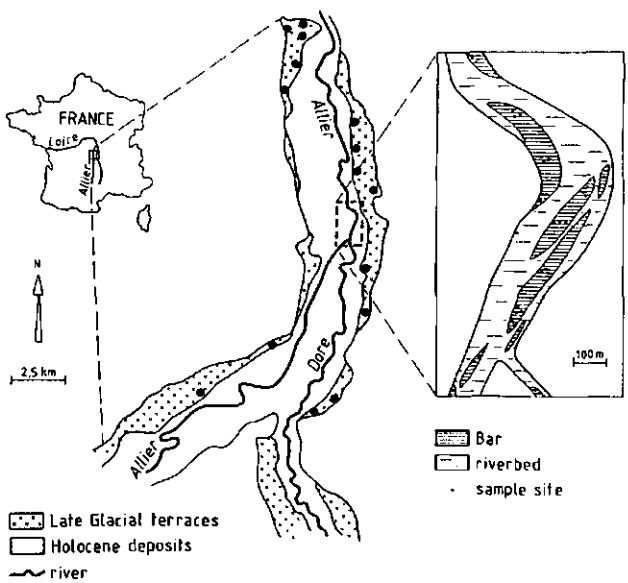

Figure 3.3.1 **Study area with sample sites in Allier riverbed and Younger Dryas terrace.**

3.3.2 Study area

The study area (Fig. 3.3.1) includes the actual riverbed of Allier river and its Younger Dryas terrace (Xb) (10 m above present riverbed), at the confluénce with a major tributary, the Dore. Previous bulk geochemical studies (e.g. Kroonenberg et al., 1988) in chapter 3.1 showed that basaltic rock fragments cause significantly higher levels of TiO_2, Fe_2O_3, MgO, CaO and P_2O_5 in the Allier sediments, whereas the Dore sands are characterized by significantly higher SiO_2 and K_2O levels, originating from quartz, K-feldspars and mica's. Changes in bulk geochemical sand composition are well illustrated by CaO content, concentrated in the basaltic rock fragments, and K_2O content, concentrated in crystalline rock fragments. Ca and K contents are virtually independent on grain size because their host minerals are found in almost all grain size fractions (Veldkamp, 1990).

A major difference between the present riverbed and the Younger Dryas terrace sediment composition is the higher amount of CaO (basaltic fragments) in the terrace sands. This difference has a climatic origin as the Younger Dryas sediments have a fluvioglacial origin from melting glaciers in volcanic areas (Bout, 1963; Kroonenberg et al., 1988). The actual riverbed sediments are relative poor in volcanics as they have no extra volcanic addition from melting glaciers.

3.3.3 Materials and methods

Sampling procedures and measurements

Sand samples were taken from bars in one kilometre riverbed at the actual Allier/Dore confluence (Fig. 3.3.1) yielding a total of 45 sample sites.

As the investigated river bars are predominantly gravelly, almost each sand bar in the investigated river section was sampled. The Younger Dryas Allier terrace near the Allier/Dore confluence was sampled along a stretch of 15 km in sand and gravel pits amounting to a total of 67 samples at 16 sites (Fig. 3.3.1).

At every sample site 1-4 samples of different grain size

distributions were collected, to incorporate a possible grain size effect due to local sorting processes during sedimentation (Veldkamp, 1990). Sand bulk element concentrations of SiO_2, TiO_2, Al_2O_3, Fe_2O_3, MnO, MgO, CaO, Na_2O, K_2O and P_2O_5, were measured with X-ray fluorescence spectroscopy. Detailed sampling methodology, laboratory treatments and measurements were done according to Kroonenberg et al. (1988).

Spatial variability procedures

Changes in sand composition at the Allier/Dore confluence are described by longitudinal profiles showing the average sand compositions of the sample sites on the right and left side of the river. Spatial variability is quantified with both geological clustering and geostatistics. In geological clustering it is assumed that a relationship exists between spatial sediment composition and geomorphological units, such as gravel bars in the present riverbed and terrace units as mapped (Fig 3.3.1) for the Younger Dryas terrace level. Within the geostatistical approach the spatial dependence is characterised by means of semi-variograms.

In geological clustering the mean sand composition is determined for each individual sampled geomorphological unit. The unit compositions are classified into three composition classes. The significance of differences in composition class is determined by means of multiple comparisons according to the Tukey method assuming independence between the distinguished units (Dillon & Goldstein, 1984).

Geostatistics starts with calculation of semi-variograms, after which the nuggets and slope angles for the spatial dependencies are estimated (Journel & Huijbregts, 1978; Stein et al., 1989). To investigate whether variables change more rapidly in one direction than in another direction, directional semi-variograms were used. Kriging was used (Burgess et al., 1981) to predict values at a regular grid which is used in turn for the computerized construction of maps.

3.3.4 Results and discussion

Present riverbed

Descriptive statistics of the present riverbed sands are given in Table 3.3.1. Longitudinal profiles of mean CaO and K_2O contents (Fig. 3.3.2) in the present riverbed show the downstream changes in sand composition of the river bars on the right and left side and in the centre of the river. After about one kilometre downstream there is no clear difference between the three distinguished bar types. These trends suggest delayed sediment mixing of the right and left bank side riverbars, while the bars in the river centre display a mixed sand composition.

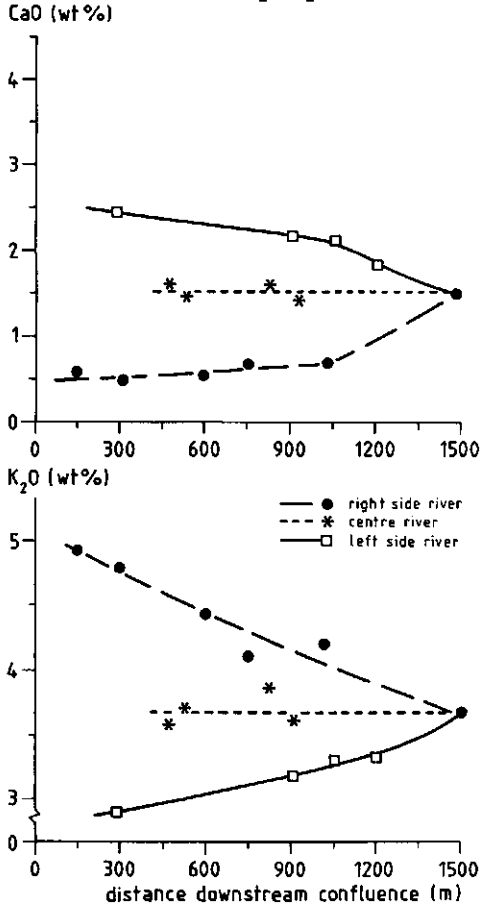

Figure 3.3.2 **Longitudinal trends of mean CaO and K_2O contents of the riverbars in the middle (M) and on the left (L) and right (R) river bank side of the Allier.**

Element (wt%)	All bars mean	std	Allier bars mean	std	Dore bars mean	std	Mixed bars mean	std
SiO_2	77.40	3.68	73.54	3.72	78.75	3.28	76.58	2.60
TiO_2	.51	.31	.98	.40	.40	.23	.52	.12
Al_2O_3	10.86	1.21	11.11	1.23	10.66	1.10	11.17	1.34
Fe_2O_3	2.27	1.49	4.43	1.99	1.68	1.06	2.38	.59
MnO	.03	.02	.06	.03	.02	.02	.03	.01
MgO	.98	.49	1.69	.31	.74	.43	1.10	.19
CaO	1.26	.54	2.06	.28	.94	.43	1.50	.17
Na_2O	1.44	.20	1.49	.13	1.39	.20	1.54	.20
K_2O	3.68	.56	3.03	.28	3.99	.50	3.23	.16
P_2O_5	.14	.05	.21	.05	.11	.05	.16	.02

Table 3.3.1 **Descriptive statistics present riverbed.**

Geological clustering

The mean CaO and K_2O river bar concentrations were classified into three classes (Fig. 3.3.3). The unmixed Allier sands are rich in CaO (>2 wt%) and poor in K_2O (<3 wt%), while sands with a Dore signature have opposite bulk geochemical characteristics, poor in CaO (<1 wt%) and rich in K_2O (>4 wt%).

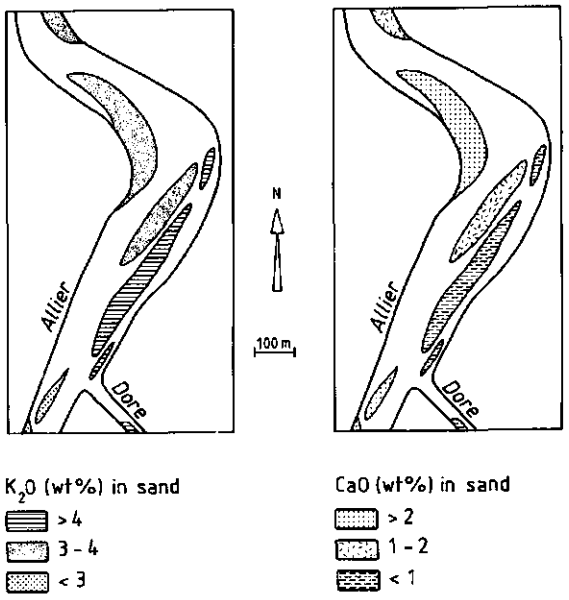

Figure 3.3.3 **Geological clustering maps of sand composition in river bars at Allier/Dore confluence.**

Dore sands are found in the Dore and along the eastern (right) river bank of the Allier, while along the opposite western bank sands with typical unmixed Allier characteristics are found. A river bar in the middle of the Allier has sand with a mixed origin (CaO 1-2 wt%; K_2O 3-4 wt%) illustrating the existence of sediment mixing at and downstream the Allier/Dore confluence.

Spatial variability

Since semi-variograms were expected to differ in two directions, parallel to the river and perpendicular to it, two directional variograms were compiled for the variables studied (Staritsky, 1989). No significant anisotropic spatial variability was found, however. The two directional semi-variograms of the CaO and K_2O content are equal, indicating that there is no relationship with the flow direction of the river (broken lines in Fig. 3.3.4 and 3.3.5). This rather surprising effect is probably due to the sharp bend of the river causing each directional semi-variogram to have a component parallel and perpendicular to the flow direction.

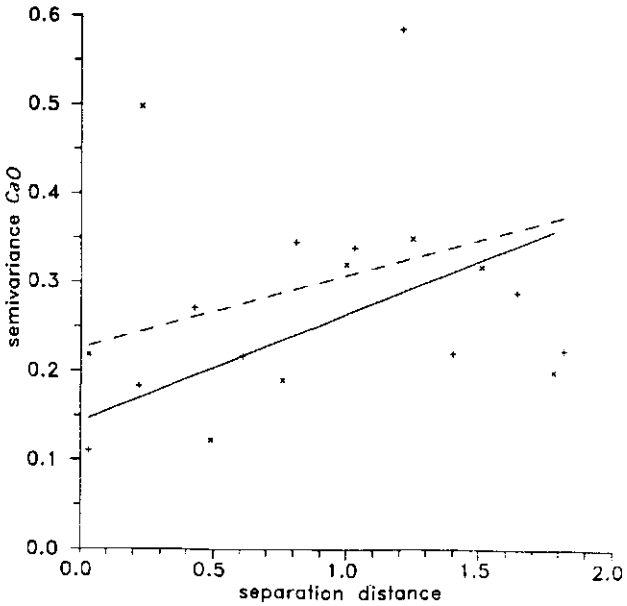

Figure 3.3.4 CaO Semi-variograms of the spatial dependence of the sand composition in the present riverbed (- - - - - -), and semi-variogram of flow direction with adapted grid cells (_____), illustrating dependence of variability with flow direction.

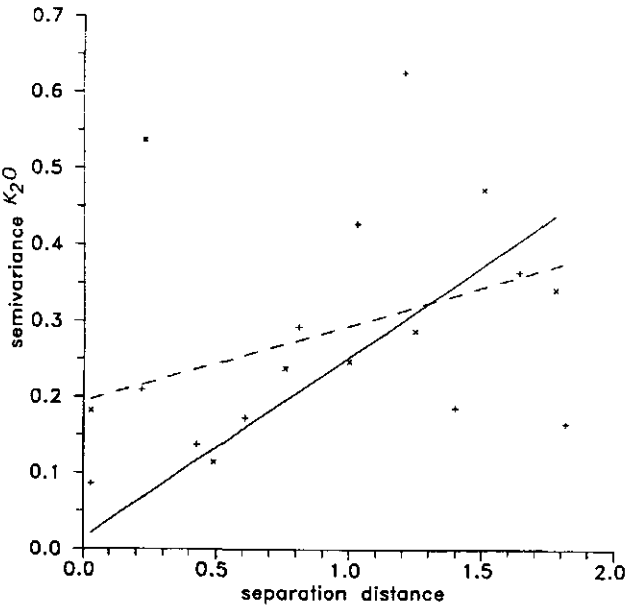

Figure 3.3.5 **K_2O Semi-variograms of the spatial dependence of the sand composition in the present riverbed (- - - - - -), and semi-variogram of flow direction with adapted grid cells (_____), illustrating dependence of variability with flow direction.**

To investigate this statement a semi-variogram along the flow direction was made using a transformed grid with grid lines parallel to the Allier (continuous lines in Fig. 3.3.4 and 3.3.5). These semi-variograms have high variability at short distances which is caused by the projection of both river sides on a grid parallel to the flow direction. The new semi-variograms have a much stronger spatial dependence for the larger distances than the semi-variograms of the actual grid cells, indicating that there exists, as expected, a directional dependence of the spatial sand compositional variability in a river.

With the semi-variograms (---------) of Fig. 3.3.4 and 3.3.5, maps of the predicted CaO and K_2O content are made with an isotropic kriging procedure. These maps show the spatial variability of CaO and K_2O content within the gravel bars in the riverbed (Fig. 3.3.6). The standard deviation of the prediction errors are all around 0.5 wt%. Downstream from the confluence the bars situated in the middle of the Allier display a mixed composition, while typical Dore and Allier sand bars remain along the edges of the riverbed.

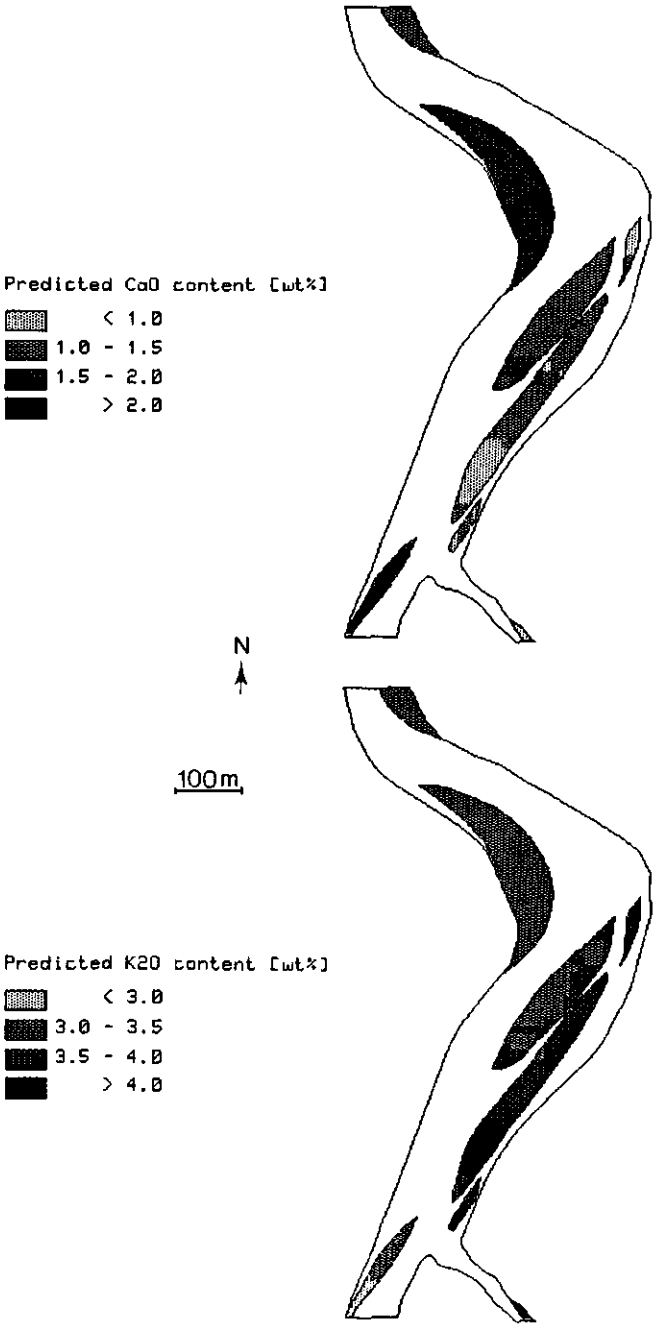

Figure 3.3.6 Maps of the general sand compositional trends in present riverbed.

This is in agreement with the maps of Fig. 3.3.3. The more downstream situated bars have a more homogeneous composition illustrating a more thoroughly mixed character. The kriged maps show more details of the changes in sand composition within the sand bars. They also do show the delayed sediment mixing in more detail compared to Fig. 3.3.3.

Origin of spatial variability

Spatial sand compositional variability in the present riverbed is clearly caused by the sediment mixing at the Allier/Dore confluence (Church & Kellerhals, 1978; Best, 1986; Bathurst, 1988). The observed compositional trends clearly show delayed sediment mixing as observed by other confluences (Komura, 1973; Best, 1986).

Sands with a mixed composition are found in the bars in the centre of the Allier and at the first major river bend (Fig. 3.3.3 & 3.3.6), thus indicating that sediment mixing starts immediately but a complete mixing is delayed for at least one kilometre in the present Allier riverbed. This delay of sediment mixing is most prominent for the bar sediments along the riverbed edge. This implies that terrace sediments are more likely to display a maximum delay of complete sediment mixing during their deposition.

Younger Dryas terrace

Downstream changes in mean terrace sand composition on the right and left river bank (Fig. 3.3.7) show differences for the two populations. Only many kilometres downstream the presumed former confluence, differences between the right and left bank terrace units diminish, suggesting a delayed sediment mixing of at least ten kilometres. Spatial variability within the Younger Dryas terrace is determined only by means of geological clustering due to the limited amount of sample sites (n=16). The units used are the different terrace units from the geological map. The sampled terrace units (Fig. 3.3.1) are classified according to their mean sand geochemical composition.

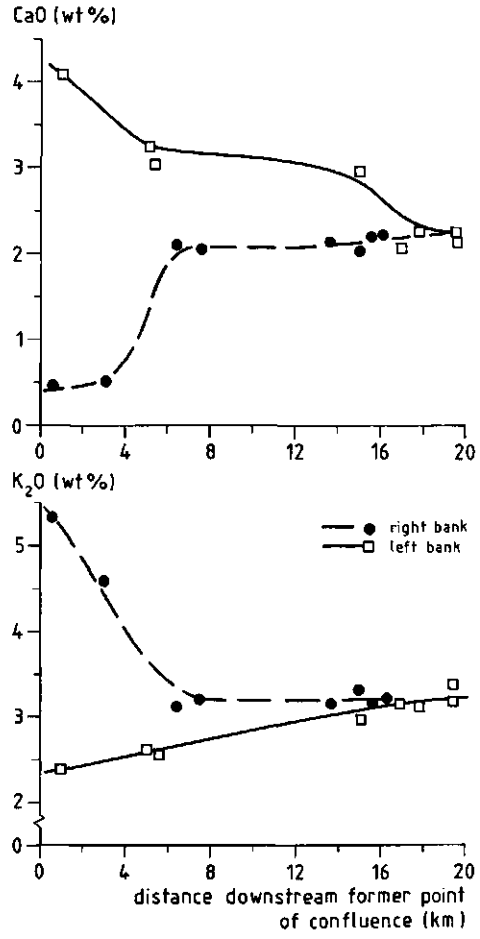

Figure 3.3.7 **Longitudinal trends of mean CaO and K_2O contents of terrace units on the left (L) and right (R) hand side of the Allier.**

The mean CaO and K_2O content of the units is divided into three classes shown on maps of spatial CaO and K_2O trends (Fig. 3.3.8). The Allier sediments are rich in CaO (>3 wt%) and poor in K_2O (<3 wt%) while Dore sands display opposite characteristics. Sands with Dore characteristics (CaO <2 wt%; K_2O >4 wt%) are found along the eastern valley slope a few kilometres downstream the presumed former Allier/Dore confluence. The occurrence of volcanic fragments in these sediments indicates that some mixing with Allier sediments took place before deposition.

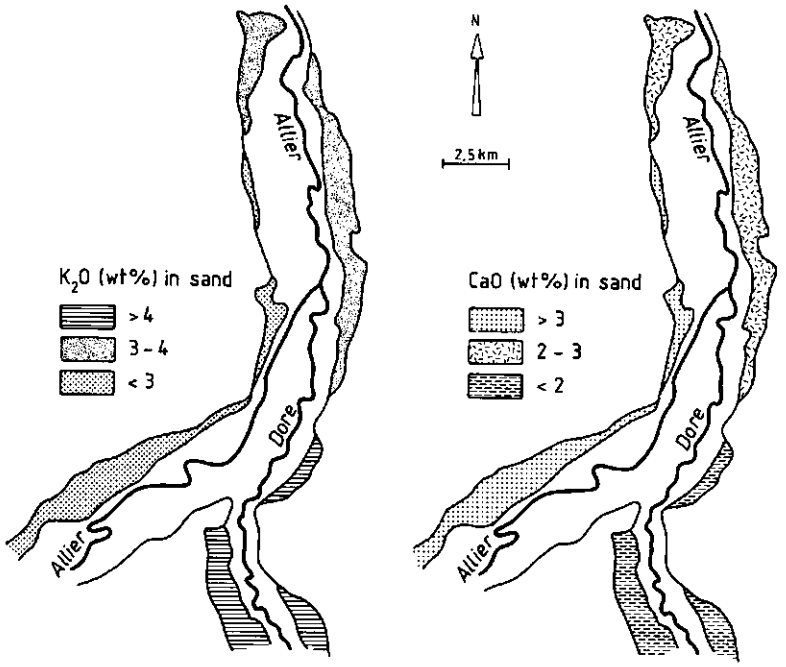

Figure 3.3.8 Geological clustering maps of sand composition in Younger Dryas terrace sediments at Allier/Dore confluence.

Sediments with strong Allier characteristics are found along the opposite western valley slope to about 10 km downstream of the presumed former Allier Dore junction.

Comparison of spatial compositional trends of present riverbed and terrace sands.

Although the sediment compositional pattern (Fig. 3.3.8) found in the Younger Dryas terrace sands is only tentative, the resemblance with the present riverbed (Fig. 3.3.3 and 3.3.6) is

strong. In both Younger Dryas and present Allier sediments an elongated body of Dore like sediment is found along the eastern Allier valley slope, downstream the confluence. It seems likely that this has a similar origin, delayed sediment mixing at a confluence.

The most striking difference between the Younger Dryas and present sediments is the scale difference in spatial variability. This difference may originate from the differences in fluvial system characteristics during deposition. Younger Dryas sediments were deposited by an Allier with a more braided character than the present more meandering river (Bout, 1963). These differences in fluvial system behaviour include differences in river sinuosity floodplain width and amount of channels. Sediment mixing in the actual Allier is maximally delayed to the first river bend. A river with a higher sinuosity can be expected to display a shorter delay in complete sediment mixing. This trend becomes more complicated when different channels occur in the floodplain. Sediment mixing at a confluence with different channels will show a longer delay than in one channel. From aerial photographs it can be seen that the Dryas Allier has known more channels. During the Younger Dryas the Dore mixed with the Allier channels one by one contributing to sediment mixing delay of several kilometres. The actual Dore flowing several kilometres parallel to the Allier is still occupying a former Allier channel.

3.3.5 Conclusions

The strong resemblance of the spatial compositional distribution within the present riverbed and the Younger Dryas terrace indicates that sediment mixing at the Allier Dore confluence strongly determined the spatial sand compositional variability in the Younger Dryas terrace. This result supports the general idea of the impact of former confluences on terrace sediment composition. The scale difference in spatial variability between the Younger Dryas and present Allier sediments suggests that changes in fluvial dynamics caused major changes in the

spatial variability of fluvial sediment composition at this confluence.

The large regional differences between fluvial sediment variability of Younger Dryas and present sediments indicate that sediment mixing in large scale systems is much more complicated than in small scale experiments. Therefore more macro scale research at confluences is needed to allow a more reliable palaeohydrological interpretations.

Quantitative determination of the spatial compositional variability in terrace sediments allows discrimination of the mixed and unmixed sediments within the same terrace level thus facilitating the selection of suitable sample sites for further regional palaeohydrological research. Geological clustering allows a first and quick discrimination of the sediment types but a more accurate discrimination can be obtained from a geostatistical approach which needs more sample sites.

3.4 CLIMATE CONTROLLED SEDIMENT FLUXES IN A FLUVIAL SYSTEM: A RECONSTRUCTION OF THE ALLIER BASIN DURING THE LATE QUATERNARY.

A. Veldkamp

Abstract

Longitudinal trends in bulk composition of Holocene and Late Weichselian terrace sands of the Allier (Central France) show that sand composition is mainly determined by longitudinal sorting and tributary sediment fluxes. These fluxes are mainly related to basin lithology and environment. The past changes in bulk geochemical composition of Allier sands as found in terrace sediments at a confluence are used to reconstruct the past sediment flux dynamics. The good match between the reconstructed Allier sediment flux dynamics and known environmental changes in it basin during the last 30.000 years indicates that the methodology of calculating sediment mixing ratios is a promising quantitative tool for paleoenvironmental reconstructions.

3.4.1 Introduction

Sediment composition within a fluvial system is the result of both internal factors such as transport mechanism and relative grain resistance during transport, as external factors such as source area and tributary dilution (Cameron and Blatt, 1971; Basu, 1976; Davies et al., 1978). These external factors can be related to present and past relief, source rock and climate by studying the longitudinal variation in fluvial sand composition (Franzinelli and Potter,1982; Knighton, 1982; Ichim and Radoane, 1990).

In palaeohydrological research it is often attempted to reconstruct past environments. Fluvial sediments are studied in order to establish the external factors determining sediment characteristics. Such studies do usually not rely on the longitudinal variation but on the interpretation of the stratigraphy of fluvial deposits (Starkel, 1983; Mitchell and Gerrard, 1987). There are many ways to relate sediment properties to hydrological regime and environmental conditions during deposition. A successful approach is estimating palaeodischarge peaks from maximum grain size (Maizels, 1986), thus allowing the registration of large scale changes within a fluvial system. In general the tendency in fluvial terrace research is to rely on sediment characteristics such as grain size and composition mostly combined with more or less fragmentary palynological and

paleontological data.

Climatic change, uplift and other major events in a drainage basin do not only bring along changes in the granulometrical and mineralogical composition, but also in the quantity of sediment delivered to a stream. These effects may greatly differ from one tributary to another within the same drainage basin. One tributary may carry sediment from deglaciating mountain ranges, another may show admixture of contemporaneous volcanism. Such events can be detected qualitatively e.g. by heavy mineral analyses, but the effect on the bulk composition of the fluvial sediments is rarely studied. Yet the study of bulk sediment composition is a way to quantify fluxes of sediment of different composition in a drainage basin.

When changes in bulk sediment composition at a confluence are measured it is possible to reconstruct the former sediment mixing process at this confluence by calculating the ratio of the two sediment fluxes which mixed at this confluence during deposition (mixing ratio). Environmental changes in a basin which cause changes in sediment supply can potentially be registered by the mixing ratios of tributaries and the main river at their confluences. It are these sediment mixing ratios which have the potential to monitor environmental changes in the fluvial sedimentary record quantitatively.

In this study the proposed concept of measuring the bulk composition of fluvial sediments in order to reconstruct the sediment flux dynamics is applied on the Allier river terraces in Central France. At first the effects of tributaries on the longitudinal sediment composition of the main river (Allier) are investigated. The climatic dynamics are evaluated by comparing Late Weichselian and Holocene sand compositions. After this regional study a more detailed study of the time related sediment mixing dynamics is made by focusing on one confluence.

The sediment bulk measurements are limited to the sands only,

because sands facilitate representative sampling and they are suitable sediments for reconstructing fluvial dynamics (Potter, 1978; Pettijohn et al., 1987). Bulk sand composition is measured geochemically because mineralogical and petrographical analysis is rather cumbersome to derive the bulk composition. Previous bulk geochemical analysis of fluvial sands showed that bulk geochemistry is a suitable tool to characterize the compositional variability of fluvial sediments (Kroonenberg et al., 1988; Moura and Kroonenberg, 1990; Veldkamp and Kroonenberg 1989).

Only the younger terraces are sampled because the older terrace sediments are already so strongly weathered (Veldkamp and Feijtel, 1990) that the original sediment composition cannot be reconstructed.

The study area

The study area (Fig. 3.4.1 and 3.4.2) includes the Late Weichselian terraces of the Allier. This study starts with the investigation of two relative young terrace deposits along a stretch of 100 kilometres (Fig. 3.4.1).

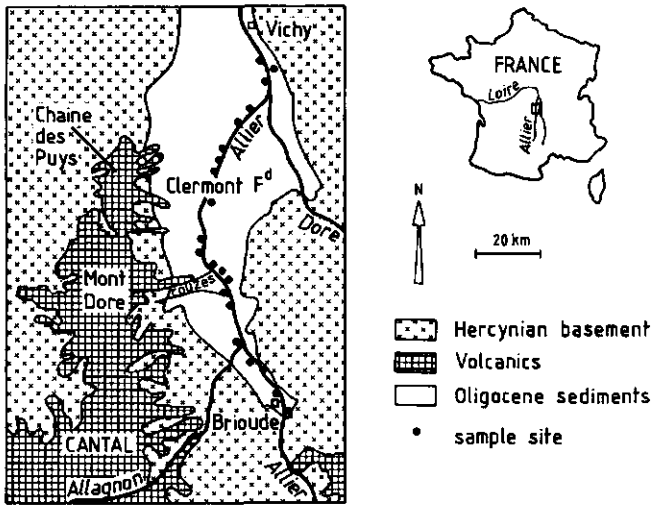

Figure 3.4.1 **Allier drainage basin and sample sites along a stretch of 100 km. for the longitudinal variability along Allier.**

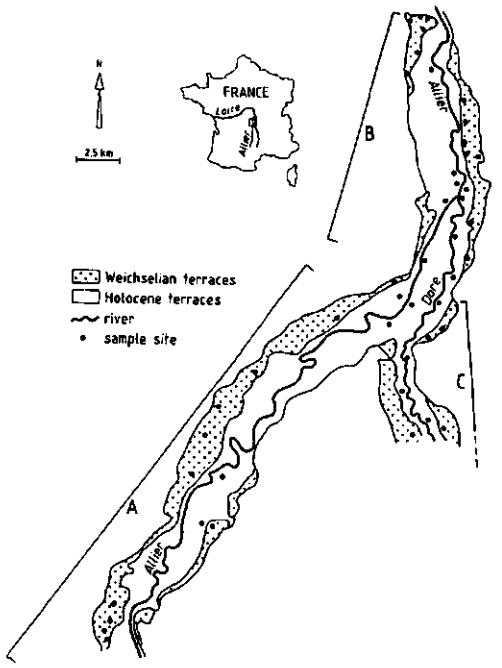

Figure 3.4.2 **Study area with sample sites at the Allier/Dore confluence for a study of sediment flux changes at this confluence. The sampled sands are devided into three groups, the Allier sands upstream (A) and those downstream (B) the Allier/Dore confluence and the Dore sands (C).**

(1) The Late Weichselian terrace level (X_{III}), approximately 15 m above present river level, characterized by a large volcanic component (Xa on geological map) (Clozier et al., 1980).
(2) The Holocene level (ZY), 0 to 5 m above present river, has sediments with a considerably smaller amount of volcanic components than the Late Weichselian deposits (Kroonenberg et al.,1988; Tourenq, 1986).

After this regional study a more detailed study of sediment flux dynamics is carried out at the Allier/Dore confluence where very contrasting sediments mix (Fig. 3.4.2).

The Late Weichselian terraces of the Allier are characterized by two levels at 20 and 10 m above present river level respectively. They have at least four different litho-stratigraphical units (Fig. 3.4.3), A Middle Pleniglacial (X_I), two Late Pleniglacial (X_{II} and X_{III}) and a Late Glacial (X_{IV}) unit respectively (Veldkamp and Kroonenberg, 1991). The X_{IV} units was incised during the Pre-Boreal and Boreal, because the oldest known Holocene sediments have Atlanticum ages indicating that most Holocene sediments are relatively recent.

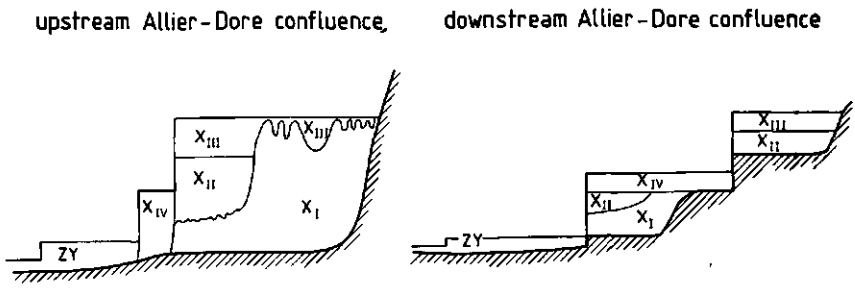

Figure 3.4.3 Schematic stratigraphy of Late Quaternary Allier terraces at the Allier/Dore confluence. The different terrace units have approximately the following ages base on ^{14}C datings:

X_I	30,000 - 29,000	y B.P.
X_{II}	25.000 - 16.500	y B.P.
X_{III}	16.500 - 12.500	y B.P.
X_{IV}	11.000 - 10.000	y B.P.
ZY	< 7000	y B.P.

3.4.2. Materials and methods.

To study the regional longitudinal variation of the Allier sand samples were taken from the Holocene (ZY) and Late Weichselian terrace (X_{III}) along a stretch of almost 100 km (Fig. 3.4.1). Sampling amounted to a total of 38 and 46 samples for Holocene and Late Weichselian terraces respectively. At each sampling site 2-6 samples of different grain size distributions were collected (both fine and coarse sand samples), to incorporate a possible grain size effect. Grain size effects are caused by the depletion or enrichment of certain minerals like heavy minerals, mica's and feldspars in specific fractions (Strakhov, 1969). Previously bulk geochemical investigations of the Allier sands in the section between the Dore and Couze Chambon showed that this grain size effect determined approximately 10% of the total geochemical variability (Kroonenberg et al., 1988). The grain size related sand oxides in the studied Allier section, mainly Na_2O and Al_2O_3, are so well correlated with grain size that they can be reasonably predicted from grain size data (Veldkamp, 1990).

Near the Allier/Dore confluence extra sand samples were taken along a stretch of 30 km of the Allier river in the different Late Weichselian and Holocene litho-stratigraphical units (Fig. 3.4.2). The sampled sands are divided into three main sampling groups (Fig. 3.4.2), the Allier sands upstream (A) and those downstream (B) the Allier/Dore confluence, and the Dore group (C). The effects of spatial mixing (Best, 1988) and longitudinal sorting effects (Davies et al., 1978) were taken into account (Veldkamp and Staritsky, in press, section 3.3). Sampling amounted to a total of 176 samples (X_I=39, X_{II}=22, X_{III}=50, X_{IV}=65) from Late Weichselian stratigraphic units and 54 from Holocene deposits.

Sampling methodology and laboratory treatments and measurements were done according to Kroonenberg et al. (1988) as described in chapter 3.1..

Statistical treatments were performed with SPSSpc (Norusis, 1986). Mean bulk geochemical composition of the terrace sands upstream (A) and downstream (B) the Allier/Dore confluence are listed in Table 3.4.1 and 3.4.2. The average Dore sand (C) composition (Tab. 3.4.3) is known from previous research (Veldkamp and Kroonenberg, 1989).

3.4.3. Results and discussion

Regional variation in sand bulk geochemical longitudinal profiles

Bulk geochemical longitudinal profiles of Allier sands showed that geochemical variability is determined by three major element groups. These groups were also found by the first exploratory investigation by multivariate statistics (Kroonenberg et al., 1988). The first group is characterized by the oxides, TiO_2, Fe_2O_3, MnO, MgO, CaO and P_2O_5, which are related to different abundances of basaltic rock fragments. The second group, Na_2O and Al_2O_3 has a variability related to grain size, and the third group represents variability of the acid crystalline mineral group (K_2O and SiO_2) which is mainly due to differences of K-feldspars, quartz and crystalline rock fragments.

terraces Element	ZY	X_{IV}	X_{III}	X_{II}	X_{I}
SiO_2	72.57	70.50	67.51	77.54	78.09
TiO_2	0.97	1.08	1.35	0.60	0.53
Al_2O_3	10.84	11.53	12.13	10.49	11.02
Fe_2O_3	4.36	4.83	5.78	2.41	1.87
Na_2O	1.50	1.57	1.93	1.77	2.04
MgO	1.93	2.85	3.16	1.07	1.03
CaO	2.42	3.62	3.89	1.65	1.53
K_2O	2.82	2.68	2.56	2.98	2.57

Table 3.4.1 **Mean oxide contents upstream Dore/Allier confluence.**

terraces: Element	ZY	X_{IV}	X_{III}	X_{II}	X_{I}
SiO_2	76.25	74.31	68.87	78.86	76.61
TiO_2	0.60	0.85	1.23	0.37	0.56
Al_2O_3	11.19	10.99	12.22	11.09	11.74
Fe_2O_3	2.68	3.66	5.56	1.45	2.38
Na_2O	1.53	1.40	1.56	1.60	1.48
MgO	1.16	1.74	2.48	0.59	0.69
CaO	1.50	2.32	3.52	0.94	0.98
K_2O	3.41	3.32	2.87	4.02	3.85

Table 3.4.2 **Mean oxide contents downstream Dore/Allier confluence.**

terraces: Element	ZY	X_{IV}	X_{III}	X_{II}	X_{I}
SiO_2	77.99	79.49	81.31	81.31	82.08
TiO_2	0.18	0.15	0.15	0.15	0.25
Al_2O_3	11.83	11.27	10.19	10.19	10.04
Fe_2O_3	0.81	0.76	0.73	0.73	0.90
Na_2O	2.25	2.25	1.70	1.70	1.03
MgO	0.40	0.38	0.33	0.33	0.32
CaO	0.44	0.39	0.22	0.22	0.19
K_2O	4.50	4.11	4.23	4.34	4.22

Table 3.4.3 **Mean oxide content Dore terrace.**

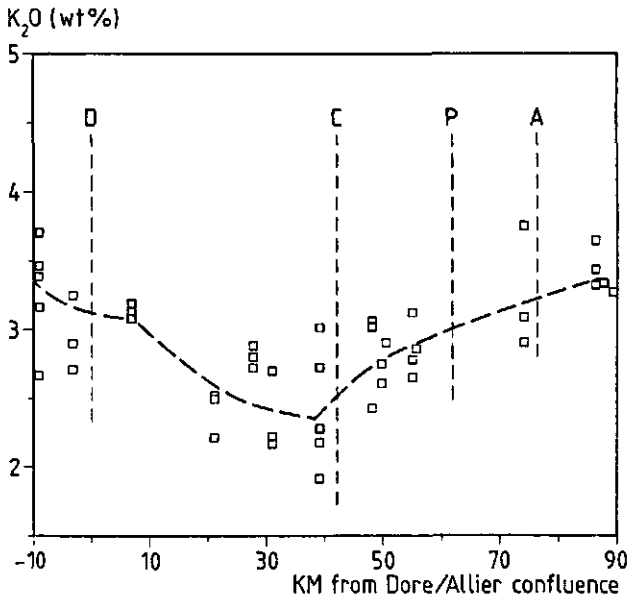

Figure 3.4.4 K_2O (wt%) longitudinal profile (km) from Brioude to Vichy Late Weichselian terrace sand. Allier flow direction is from right to left. The main tributaries are indicated by vertical lines and symbols, A=Allagnon, P=Couze Pavin, C=Couze Chambon, D=Dore.

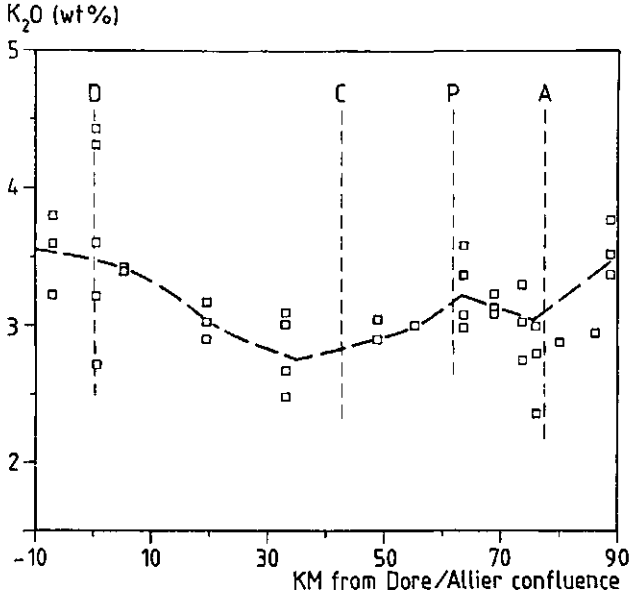

Figure 3.4.5 K_2O (wt%) longitudinal profile (km) from Brioude to Vichy present riverbed sand. Allier flow direction is from right to left. The main tributaries are indicated by vertical lines and symbols, A=Allagnon, P=Couze Pavin, C=Couze Chambon, D=Dore.

One oxide of each group is presented in two longitudinal profiles, one for the Holocene and one for the Late Weichselian sands. K_2O (Fig. 3.4.4 and 3.4.5) represents the acid crystalline component, Na_2O (Fig. 3.4.6 and 3.4.7) the grain size related component and MgO (Fig. 3.4.8 and 3.4.9) the basic volcanic component in the Allier sands. The main tributaries are indicated in each longitudinal profile as vertical lines and symbols, A=Allagnon, P=Couze Pavin, C=Couze Chambon, D=Dore. The Allier flow direction is from south to north (right to left in the profiles of Fig. 3.4.4 to 3.4.10). The changes in general trend as indicated by the broken line are based on average changes in bulk concentrations for the concerning oxide.

K_2O trends

Longitudinal K_2O contents (Fig. 3.4.4 and 3.4.5) indicate gradual changes in sediment composition in both Holocene and Late Weichselian sands. The Allier bulk sand composition shows a relative decrease in K_2O (and SiO_2) content at each tributary draining predominantly volcanic areas such as the Allagnon (A), the Couze Pavin (P) and the Couze Chambon (C). The Dore (D), draining an crystalline area, causes an increase of K_2O content in the Allier sands. The differences of K_2O concentrations between the Late Weichselian and Holocene trends are very slight. It can be observed that the K_2O concentration levels in the Holocene sands are generally higher than in the Late Weichselian sands, illustrating the higher acid crystalline component in these sands.

Na_2O trends

The Na_2O (and Al_2O_3) bulk concentration trends (Fig. 3.4.6 and 3.4.7), predominantly representing changes in the albitic endmember of plagioclase (Kroonenberg et al., 1988) and grain size effects, show a large variance. This can be attributed to the sampling strategy to select samples with different grain size distributions (Veldkamp, 1990). Nevertheless, the Na_2O curve shows major tendencies at tributaries which seem independent from grain size such as the strong increase of Na_2O (and Al_2O_3)

fig 3.4.6

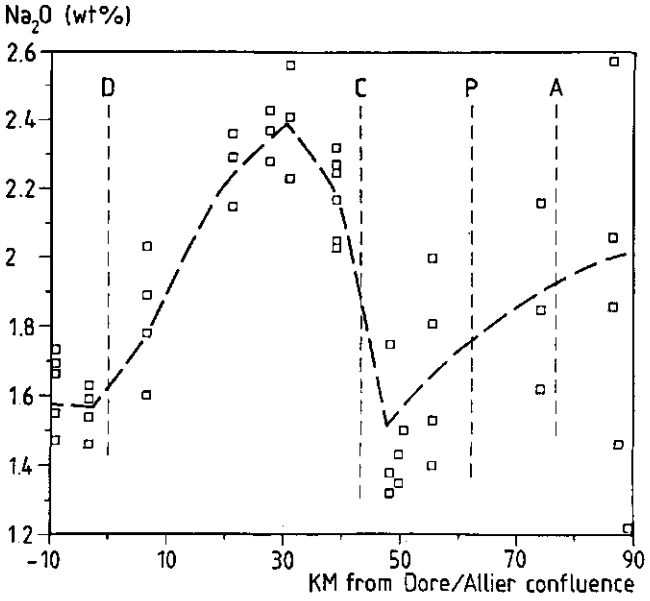

Figure 3.4.6 **Na_2O (wt%) longitudinal profile (km) from Brioude to Vichy Late Weichselian terrace sand. Allier flow direction is from right to left. The main tributaries are indicated by vertical lines and symbols, A=Allagnon, P=Couze Pavin, C=Couze Chambon, D=Dore.**

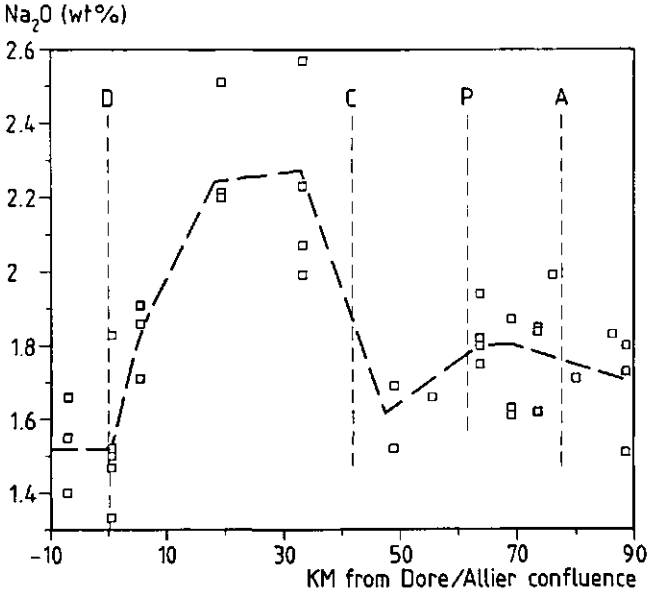

Figure 3.4.7 **Na_2O (wt%) longitudinal profile (km) from Brioude to Vichy present riverbed sand. Allier flow direction is from right to left. The main tributaries are indicated by vertical lines and symbols, A=Allagnon, P=Couze Pavin, C=Couze Chambon, D=Dore.**

concentrations at the Allier/Couze Chambon confluence. The Na_2O trends south of the Couze Chambon only show a slight general decrease downstream. Further downstream, north of the Couze Chambon there is a stronger decrease in Na_2O concentrations. These decreasing trends downstream seem independent from the tributaries and are probably related to the longitudinal sorting effect caused by backlagging of 'heavy' grains and the breakdown of grains during transport as described by Cameron and Blatt (1971) and Davies et al. (1978).

The profiles for the Holocene and Late Weichselian sands show a strong resemblance. They have approximately equal trends and similar bulk concentration levels. The resemblance of the Na_2O (and Al_2O_3) trends for the Holocene and Late Weichselian sands is probably only related to the specific origin of Na_2O. The Couze Chambon basin contains the majority of the acid volcanic deposits of the Mont Dore, like the trachytic ignimbrite of Neschers. These acid volcanic deposits are well known sources of albite. This can explain the sudden change in Na_2O content in both the Holocene and Late Weichselian longitudinal profiles. Apparently no major changes in provenance occurred from Late Weichselian to recent times.

MgO trends

The bulk concentrations of basic volcanic elements like MgO in the Late Weichselian (Fig. 3.4.8) and Holocene (Fig. 3.4.9) show different trends. In the Late Weichselian sands (Fig. 3.4.8) from Brioude downstream, there is an increase in MgO content at confluences (Allagnon and the Couzes) draining the higher volcanic areas which were glaciated during Late Weichselian (Veyret, 1980). A strong increase in MgO concentration resembling the Na_2O trend, is found at the confluence of the Couze Chambon and the Allier. Further downstream, the high MgO contents of the Late Weichselian terrace at Pont du Château (km 35 in Fig. 3.4.8) clearly reflect high content of volcanic components (Bout, 1963). This section shows a large spread in MgO content.

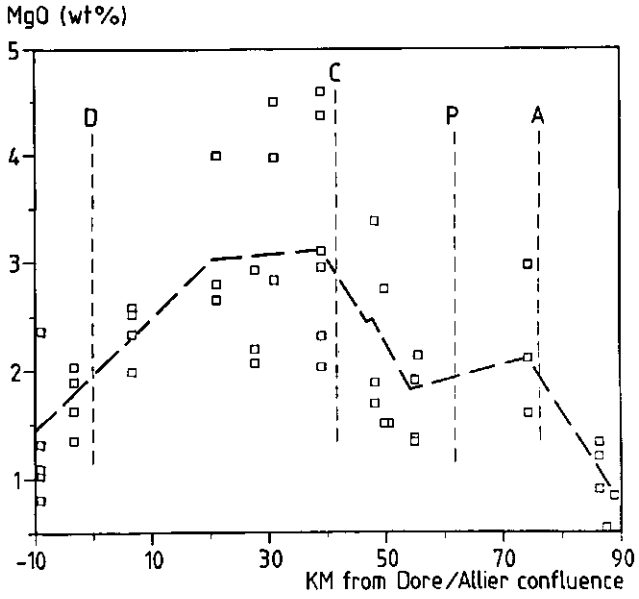

Figure 3.4.8 **MgO (wt%) longitudinal profile (km) from Brioude to Vichy Late Weichselian terrace sand. Allier flow direction is from right to left. The main tributaries are indicated by vertical lines and symbols, A=Allagnon, P=Couze Pavin, C=Couze Chambon, D=Dore.**

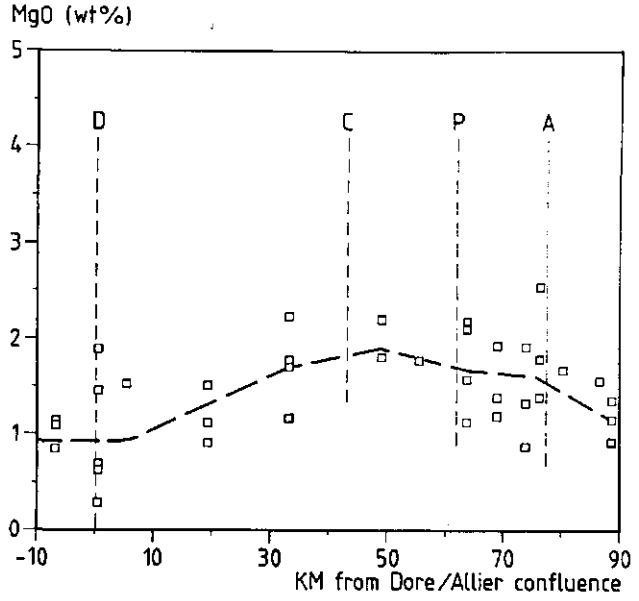

Figure 3.4.9 **MgO (wt%) longitudinal profile (km) from Brioude to Vichy present riverbed sand. Allier flow direction is from right to left. The main tributaries are indicated by vertical lines and symbols, A=Allagnon, P=Couze Pavin, C=Couze Chambon, D=Dore.**

Further downstream down to the Dore confluence the longitudinal sorting effect causes a decrease in MgO concentrations downstream, as reported by Kroonenberg et al. (1988). The Dore tributary causes a dilution of basic volcanic particles with abundant crystalline material, resulting in MgO concentration levels which are almost equal to those at Brioude.

In the Holocene sands MgO concentrations (Fig. 3.4.9) change with less sudden changes at the confluences. The amount of MgO in the Allier sands gradually increases at the Allagnon, Couze Pavin and Couze Chambon, and decreases at the Dore confluence. A longitudinal sorting effect seems also be detectable between the Couze Chambon and the Dore. Both longitudinal profiles have comparable trends but the amplitude of the Late Weichselian curve is much larger than that of the Holocene one.

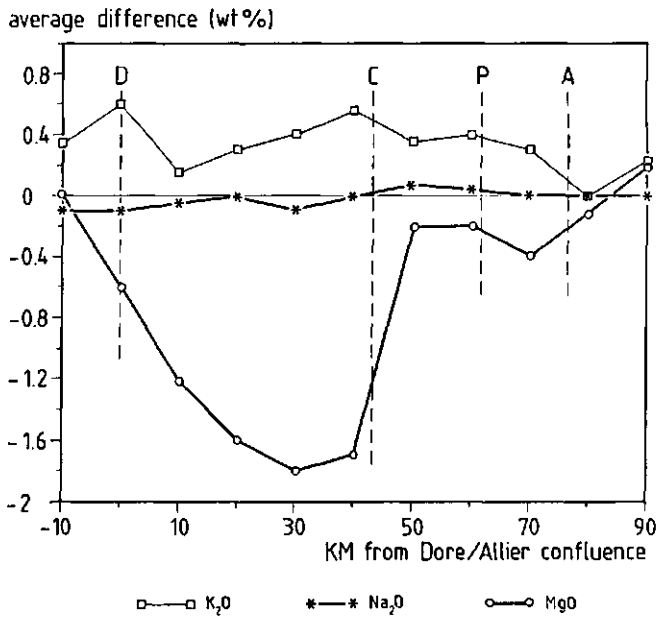

Figure 3.4.10 **Longitudinal profile (km) of average differences (wt%) of K_2O, Na_2O and MgO concentrations between Holocene and Late Weichselian sands (Average Holocene - Average Weichselian). Allier flow direction is from right to left. The main tributaries are indicated by vertical lines and symbols, A=Allagnon, P=Couze Pavin, C=Couze Chambon, D=Dore.**

A comparison of the Late Weichselian and Holocene sand composition

Both Late Weichselian and Holocene sands show the effect of sediment mixing at confluences. MgO mainly of volcanic origin increases in the Allier sands at the Allagnon, Couze Pavin and Couze Chambon confluences at the expense of K_2O. K_2O from crystalline basement rocks increases only at the Dore confluence.

The differences between oxide contents in the Late Weichselian and Holocene deposits are visualised by plotting the longitudinal trends of the calculated average difference of (K_2O_{hol} - K_2O_{weich}), (Na_2O_{hol} - Na_2O_{weich}) and (MgO_{hol} - MgO_{weich}) (Fig. 3.4.10). The difference between the average Holocene and Late Weichselian Na_2O concentrations are almost zero. Holocene sands are richer in K_2O and poorer in MgO than the Late Weichselian sands. The most striking change from Late Weichselian to Holocene is the relative large negative value for (MgO_{hol} - MgO_{weich}) at and downstream the Couze Chambon/Allier confluence (Fig. 3.4.10). Apparently much relatively basalt-rich material was supplied to the Allier in Late Weichselian times by the Couze Chambon (Fig. 3.4.8), but this supply ceased during the Holocene (Fig. 3.4.9). This change can obviously not be due to basin lithology or longitudinal sorting. Possible causes for these changes are either climatic changes or Late Weichselian basic volcanism (Bout, 1963; Kroonenberg et al., 1988).

Causes for diverging longitudinal trends

Bout (1963) related the volcanic rich Late Weichselian sediments to a melting phase of the glaciers. His theory is supported by field evidence (Kroonenberg et al., 1988) and by the observation that tributaries related to glaciated areas cause a stronger increase in MgO content in the Late Weichselian sands compared to the Holocene sands (Fig. 3.4.10).

Pastre (1986) and Tourenq (1986) both name volcanism as the major factor causing the relative high volcanic content of the Late Weichselian sediments. The volcanic history of the Allier basin indicates that during the Late Weichselian active volcanism

of the Chaîne des Puys took place indeed. Around 27.000 B.P. the Tartaret volcano at the bottom of the Couze Chambon valley emitted a 28 km long basalt flow downstream (Raynal and Daugas, 1984; Raynal et al., 1985). However, no Late Weichselian volcanism is known in the other major tributaries, the Allagnon, Couze Pavin and Dore basins. Therefore, only the relatively large volcanic component at the Couze Chambon in the Late Weichselian sands may be related to the volcanic activity of the Tartaret volcano.

On the other hand there are many Holocene volcanoes known in the Allier, Couze Chambon and Couze Pavin basins (Camus et al., 1983). The trachytic maar of Lac Pavin (5990 ± 115 B.P.; Juvigné and Gewelt, 1987) is the most recent volcanic activity in the Allier basin. Nevertheless, Holocene volcanism did not result in any notable increase in the volcanic component in the Holocene Allier sands. Apparently active volcanism had no direct impact on sand composition.

Therefore Bout's (1963) theory on a paleoclimatic origin for the Late Weichselian increase in volcanic components is more likely. Whereby the role of Late Weichselian volcanism in the Couze Chambon basin cannot be completely excluded. At the end of the Late Pleniglacial melting of glaciers in the higher volcanic areas must have resulted in the release of a considerable quantity of volcanic-rich fluvioglacial sediments. After the glaciers had molten away the fluvioglacial flux from the Allagnon, Couze Pavin and Couze Chambon stopped and the steady base flux of crystalline components became automatically more important during the Holocene.

The preceding evaluation of the longitudinal changes in bulk geochemical sand composition from Late Weichselian to Holocene indicated that not volcanism but climatic changes played the most important role in determining fluvial sand composition. This result implies that climatic changes within the Allier system can be studied from changes and trends in fluvial sand composition. As bulk sand composition was measured it is also possible to reconstruct the past sediment flux dynamics which caused the

measured changes in sediment composition. Now paleoenvironmental changes within the Allier basin can be measured both qualitatively as quantitatively.

As a case study sediment mixing at one confluence the Allier/Dore confluence was studied because at this confluence two very contrasting sediment types mix and mixed.

3.4.4. Sediment mixing at the Allier/Dore confluence

As argued in the introduction may a mixing ratio give a direct indication of the sediment mixing history. This ratio used as a measure of the relative contributions of both Allier and Dore to sediment mixing. The following procedure was used to determine the ratios of the two fluxes which mixed at the Allier/Dore confluence.

The significance of differences in mean oxide content for each litho-stratigraphical unit (Table 3.4.1 and 3.4.2) was determined by means of multiple comparisons according to the Tukey method. The significance of change in mean Allier sediment composition at the Allier/Dore confluence was determined by students t-tests for each stratigraphical unit, using the SPSSpc package (Norusis, 1986). Mean SiO_2, TiO_2, Fe_2O_3, MgO, CaO and K_2O content are significant different (at the 0.05 level) for the ZY, X_{IV}, X_{III} and X_{II} units, while the X_I unit differs only significantly from the other terrace units in MgO, CaO and K_2O content. Therefore only MgO, CaO and K_2O contents are used further as trend oxides for sediment compositional changes of the Allier during the last 30,000 years. The compositional dynamics are plotted as bulk chemo-stratigraphy of the sediment groups upstream (A) and downstream (B) the Allier/Dore confluence in Figure 3.4.11. The composition of the litho-stratigraphic units upstream (A) and downstream (B) the Allier/Dore confluence show different trends in time.

It is obvious that the oxides of basaltic origin MgO and CaO have complementary trends with the crystalline K_2O (Kroonenberg et al., 1988). The oldest Late Weichselian sands (X_I and X_{II}) are relatively poor in volcanic oxides MgO and CaO and rich in acid crystalline K_2O.

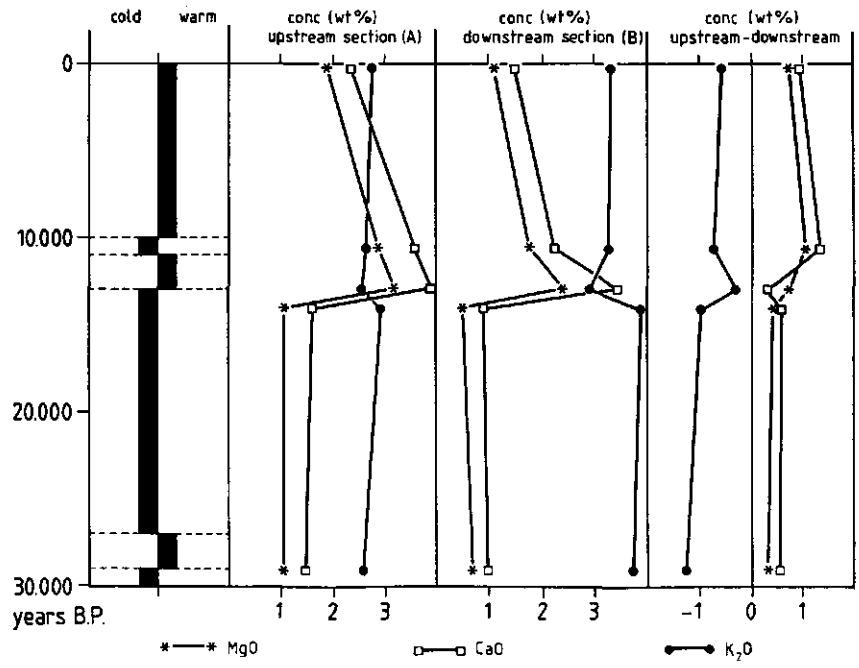

Figure 3.4.11 **Correlation of changes in bulk sediment composition with climate at the Allier/Dore confluence.**

The X_{III} sands have opposite characteristics, they are very rich in MgO and CaO and poor in K_2O. In the X_{IV}-unit sands the CaO and MgO contents are slightly lower (K_2O higher) than in the X_{III} sands. The basaltic oxide content decreases further in the Holocene (ZY) sands.

Within each Allier terrace unit mean MgO, CaO and K_2O contents also show significant changes at the Allier/Dore confluence. The MgO and CaO content decrease at the confluence while the K_2O content increases in all Allier terrace units. These relative changes are visualized in Figure 3.4.11, where the changes in (Ox wt%) CaO, MgO and K_2O content (Upstream Ox wt% - Downstream Ox wt%) of the Allier sands are plotted against age. The general compositional trends of Fig. 3.4.11 confirm the picture of a main

stream with volcanic rich sediment (Allier) which is diluted by a volcanic poor sediment (Dore). This dilution effect is very small for the X_{III} sands (Upstream Ox wt% - Downstream Ox wt% are small) and large for the X_{II} sands.

Mixing ratio

The mass ratio of the Allier and Dore sands which mixed at the confluence (sand mixing ratio) can be calculated for different oxides (bulk Ox wt %) and time periods. This is done by the following formula:

$$\text{Sand mixing ratio} = \frac{(\text{Ox wt\% Allier downstream} - \text{Ox wt\% Dore})}{(\text{Ox wt\% Allier upstream} - \text{Ox wt\% Allier downstream})}$$

Sand mixing ratio's of terrace units are only calculated for those oxides which show a significant change at the confluence (Table 3.4.4). A sand mixing ratio >1 indicates a larger and a ratio <1 a smaller Allier sand contribution to the Allier/Dore sediment mixing than the Dore. Differences in calculated ratios (Tab. 3.4.4) should be carefully reviewed.

terrace Element	ZY	X_{IV}	X_{III}	X_{II}	X_I
SiO_2	0.47	1.36	9.15	1.86	ns
TiO_2	1.14	3.04	9.00	0.96	ns
Al_2O_3	ns	ns	ns	ns	ns
Fe_2O_3	1.11	2.48	21.95	0.75	ns
Na_2O	ns	ns	ns	ns	ns
MgO	0.99	1.23	3.16	0.54	1.09
CaO	1.15	1.48	8.9	1.01	1.44
K_2O	1.85	1.23	4.38	0.31	0.29
Average	1.12	1.80	9.42	0.91	0.94

ns = no significant change at confluence

Table 3.4.4 Mixing ratios at Allier/Dore confluence.

A difference between a ratio of 2 and 10 equals the difference between a ratio of 0.5 and 0.1, and with a large or small mixing ratio the estimation error increases strongly. Both effects contribute to the large variability in mixing ratios within each terrace unit. Therefore only average sand mixing ratios are used in this research.

The average sand mixing ratios (Table 3.4.4) in time, illustrating general sand mixing dynamics of Allier and Dore are shown in Figure 3.4.12.

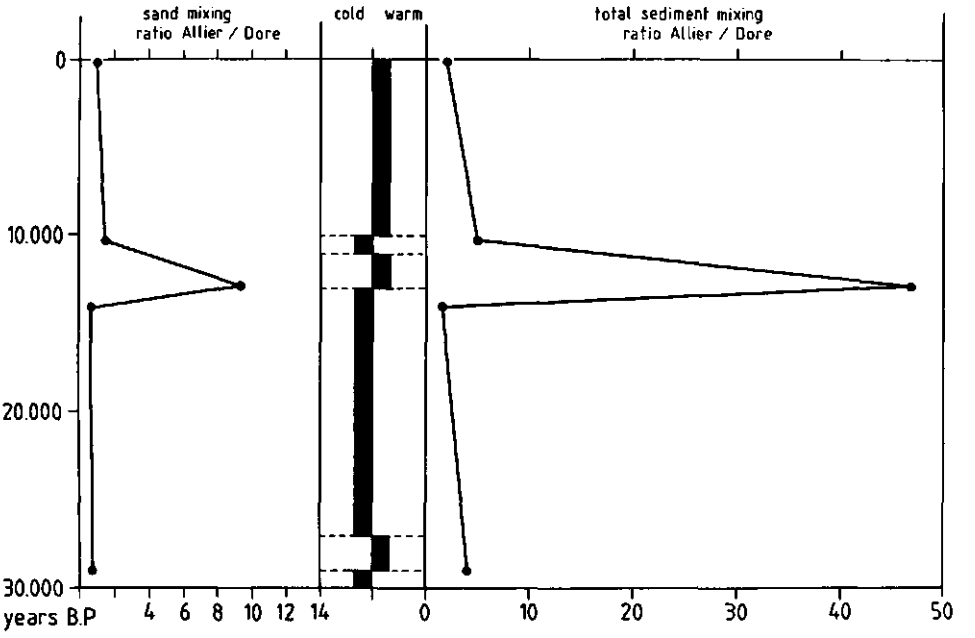

Figure 3.4.12 **Changes in sand and total mixing ratio's in time at the Allier/Dore confluence.**

Striking is the large mixing ratio of the X_{III} sands suggesting a very large sediment flux in the Allier. During deposition of X_{II} sediments the Dore contributed 1.7 times more sand than the Allier, whilst the Allier contributed about 6 times more sand than the Dore when the X_{III} sediments were deposited.

Mixing ratios for Fe_2O_3 and TiO_2 are usually higher than the mixing ratios of MgO and K_2O for the same terrace units (Tab. 3.4.4), suggesting an oxide dependence of the mixing ratio. These higher ratio's point to an enrichment of the minerals containing Fe and Ti, the heavy minerals. It is generally known that heavy minerals tend to concentrate at confluences (Schumm, 1977). Further research is needed to see whether the mixing ratio has any value in detecting mineral enrichment (placers) at former confluences.

As both Allier and Dore have known changes in the amount of supplied sediment in time, their mixing ratio only records changes relative to each other. The actual compositional differences in the Dore terrace sands are mainly caused by post-depositional weathering which does not play a dominant role in the younger sediments studied in this research (Veldkamp and Kroonenberg, 1989). As there are no indications that the Dore has known any constrains in sediment supply in time, Dore sediments can be seen as a relative constant geochemical reference for the Allier sediment dynamics. As the Dore basin had no major changes during the last 30.000 years it can be assumed that the Allier/Dore mixing ratio predominantly reflects changes in Allier sediment fluxes.

The proportion of sand with respect to the total gravel, sand and clay content in the Dore is much higher then in the Allier. From the sampled gravel and sand pits estimates of the relative sand proportions of Allier and Dore deposits have been made (Table 3.4.5). Assuming that the terrace sediments give a good representation of the sediment fluxes that mixed during their deposition, the estimated proportions can be used to convert the average sand mixing ratio into a total sediment mixing ratio.

Terrace unit	Estimated sand contribution Allier/Dore	Total sediment mixing Allier and Dore
ZY	0.5	2.3
X_{IV}	0.33	5.4
X_{III}	0.2	47.1
X_{II}	0.5	1.8
X_{I}	0.2	4.7

Table 3.4.5 Total mixing ratios of sediments Allier and Dore

This mixing ration is the mass ratio of the bulk terrace sediments which actually mixed during deposition of each terrace units (Table 3.4.5).

The total mixing ratios of the X_I, X_{III} and X_{IV} sediments (Tab. 3.4.5, Fig. 3.4.12) increase considerably compared to the sand mixing ratio. The X_{III} sediments show a sediment flux of the Allier almost 50 times the Dore contribution during sediment mixing.

3.4.5. Sediment fluxes and climate

Mixing characteristics of Allier and Dore sediments suggest that sediment fluxes of the Allier, compared to the Dore sediments, show cyclic changes in time. The X_I sediments deposited at the end of the Middle Pleniglacial show a five time larger contribution of Allier than of Dore sediments. The local Late Pleniglacial sediments (X_{II}) yield a sediment mixing ratio which indicates an Allier contribution of only twice the Dore supply. This small mixing ratio may be explained by the periglacial environment and by the building up of extensive glaciers in the upper Allier basin storing large quantities of potential Allier sediments. Deglaciation during the end of the Late Pleniglacial released an enormous mass of fluvioglacial sediments into the Allier (X_{III}), causing the large sediment flux represented by the X_{III} sediment mixing ratio. This large sediment flux (about fifty times the Dore contribution) was deposited during catastrophic events within a few thousand years. Evidence of the catastrophic character of the X_{III} deposition is given by Lenselink et al. (1990). Sediments deposited during the short

colder interval of the Younger Dryas (X_{IV}) have a mixing ratio of about 5, similar as that of the X_I sediments. This is probably due to the fact that both cold intervals were too short for extensive glacier build up, but long enough for a major environmental change.

The reconstructed relative sediment fluxes of the Allier at the Allier/Dore confluence confirm the general idea as found by comparison of the Late Weichselian and Holocene longitudinal profiles, that sediment fluxes in the Allier basin are mainly a function of climate. The observed trend is that during periglacial and interglacial environments the Allier supplies only twice as much sediments as the Dore, only at the end of a glacial the relative Allier contribution increases strongly to five times the Dore supply. After a prolonged cold period during which extensive glaciers can built up in the headwaters of the Allier, very large sediment fluxes can be expected in the Allier as a result of glacier melting. These fluvioglacial sediment fluxes can increase to fifty times the Dore contribution.

The results suggest that there exists a correlation between the sediment flux magnitude and the duration and intensity of glacials. It would be interesting to investigate such quantitative relationships in areas with well known past environments.

3.4.6. Methodological evaluation

It has been shown that changes in bulk geochemical sand composition in a fluvial system can be applied in Quaternary research as a method to reconstruct paleohydrology in relation with paleoenvironmental changes. It is obvious that this methodology is only applicable in well dated fluvial systems.

Within the described case study it remains difficult to validate the assumption that the calculated mixing ratio's display mainly Allier dynamics instead of Dore dynamics or both. The reconstructed time related sediment fluxes are difficult to validate, they can be only compared to a relative sediment load curve for the last 15.000 years, based on interpretations of

concepts for Central European river valleys (Starkel, 1983). Although both curves are constructed by different methods, it can be observed that they show a fairly match for the 15.000 to 10.000 years BP interval, but the magnitudes of changes in both curves differ strongly. Fig. 3.4.12 has of course only local validity but illustrates that it is also well possible to reconstruct sediment flux magnitudes more directly and quantitatively than Starkel (1983) did.

The results suggest a quantitative relationship between sediment flux magnitude and paleoenvironment. When more reconstructions are made it may be possible to construct a continental sediment flux record which gives quantitative indications of the past glacials. Such a record would be complementary with the existing palynological records which give mainly accurate descriptions of the warmer paleoenvironments.

3.4.7. Conclusions

Longitudinal abrasion, sorting and tributary sediment fluxes mainly determine longitudinal trends in geochemical bulk composition of the Late Weichselian and Holocene Allier sands. Changes in tributary sand composition from Late Weichselian to Holocene seem predominantly caused by climatic changes, as volcanic activity or other changes in source terrain did not show any direct measurable effect. Sediment flux dynamics at the Allier/Dore confluence are reconstructed for the last 30.000 years by calculating mixing ratios from changes in bulk geochemical sediment composition in time. These reconstructed sediment fluxes correlate strongly with climatic changes during the last 30.000 years. Allier sediment supply seems to depend mainly on the type and duration of climatic episodes.

The surprising good correlation between the reconstructed Allier sediment fluxes and paleoenvironment suggests that the methodology applied is a promising technique in Quaternary research.

Chapter 4

LONG TERM MODELLING OF RIVER TERRACE FORMATION

Within geomorphology the use of long term models has increased strongly in recent years. As geomorphological theories have mostly been validated for small spatial and temporal scales only, they are not necessarily appropriate for the larger range of scales (Howes & Anderson, 1988). Constrains in the development of longterm geomorphological models are therefore mostly due to the interrelationships between conceptualization and scale (Anderson & Sambles, 1988). Especially longterm simulations are hampered by the lack of large scale quantified knowledge. There are two main reasons, for this poverty:

1) One can envisage short-term (high-frequency) variations nested within long-term (lower-frequency) variations (Bradley, 1985). As only short-term processes are measured in experimental studies we can only guess at the quantitative effects of the long term processes.
2) Depending on the scale at which an environmental system is viewed, there are different sets of laws which operate. This scale effect causes that process or system variables which are system dependent at higher order scales may become independent if the order of scale is reduced (Huggett, 1985). Due to these scale effects, extrapolation of experimental results to large scales will certainly lead to considerable errors (Schumm, et al., 1987; Howes & Anderson, 1988).

These scale gaps in geomorphology can only partly be filled by more research. According to Huggett (1985) there is not much that can be done about the scale problem; the important thing is to be aware of its existence. The scale problem illustrates that the description of the geomorphological system as a complex, inaccessible, scale dependent and inherently random natural system (Howes & Anderson, 1988), is well chosen. According to the same authors, there is an upper limit to the degree of numerical modelling which is possible for such systems. They found it necessary to consider alternative modelling strategies and

techniques for use in these situations (Howes & Anderson, 1988).

The aim of this chapter is to discuss a possible alternative modelling strategy for the geomorphological scale problems that arise with long term modelling. Instead of using unreliable quantitative relations in numerical modelling, additional qualitative descriptive modelling is proposed.

Scale dependent modelling

An important step in long term modelling is the determination of the scale dependent system variable hierarchy. The system and process variables are listed in hierarchy with increasing degrees of dependence. Depending on the time span involved, time may be either an extremely important independent variable or of relative little significance to a geomorphologic study (Schumm & Lichty, 1965).

Another scale modelling aspect is the source scale of the used numerical relationships in the model. This scale aspect can be determined by a systematic scale analysis. Such a scale analysis is based on the assumption that relationships can only be used in a model when they are applied on the same scale as on which the original measurements were done. The scale analysis can be done in a very similar way as the commonly applied unit analysis, except that not only the units should match but also their magnitude. Such a model scale analysis can be applied successfully for relative short time spans. On such scales, a model scale analysis should be incorporated as a standard procedure in geomorphological modelling.

Modelling over long time spans

When a scale analysis is strictly applied on longer time spans, thousands of years or even longer, it can be concluded that reliable quantitative modelling is actually impossible. Most knowledge on such timespans is descriptive and interpretative.

But it is the large time scale which attracts many geomorphologists as most landforms are the result of long term processes.

The scale problem is sometimes 'solved' by a number of assumptions. In such cases it is assumed that a short time span relationship can be extrapolated to a longer timespan. A very creative solution is given by Tetzlaff & Harbaugh (1989) who used 'compute-and-drift' and 'compute-and-stop' schemes to overcome long time spans. These schemes use short term calculations for longterm simulations. In case a direct application of such a relationship does not work out properly, a scale (tuning) factor is included to obtain more realistic results. It is obvious that this approach obscures the lack of knowledge and suggests a simple straight forward solution of the scale problem which certainly does not exist.

Another approach of long term modelling is to abandon the goal to make a full numerical model, as there is to less quantitative knowledge for that purpose. Consequently it is decided to use also the knowledge which is sufficiently available, qualitative descriptive relations. Modelling with both quantitative and qualitative relations can be done with finite state modelling (Zeigler, 1976).

Finite state modelling

A finite state model describes a system which can be in different states at different times. The basic principles of finite state modelling are to choose a finite sets of inputs, states and outputs, and to specify for each state combination one and only one transition to another state in case a change in state takes place.

A system behaviour can be represented as a finite state model in a scheme, flowchart or table, showing the system states and state transitions, including the conditions when changes of state take place. The state descriptions and transitions can be as well descriptive as quantitative.

The most uncertain and difficult part of finite state

modelling is extracting the qualitative information from literature. A major problem is that descriptive knowledge contains many uncertainties commonly indicated by words as, 'probably', 'may be', 'could be', 'is thought to', etc. When extracting the essential facts one has to generalize certain facts and relations. A way to support the extraction of this kind of knowledge is by keeping in mind that at the end of the modelling activities the model has to written down in a computer language, for instance PASCAL. When the simple and limited syntax of PASCAL is taken into account one can construct several 'rules' for knowledge extraction who facilitate finite state modelling. Two important rules are for example:

1) No uncertainties are allowed in the extracted relationships, a state or a relationship exists or does not exist (A state can only be true or false).
2) The reasoning and combining of information can only be done with use of AND, OR, THEN, UNTIL, CASE, FOR ... DO, IF ... ELSE, REPEAT ...UNTIL, WHILE ... DO etc. (Findlay & Watt, 1981).

As it is the task of linguists to develop such kind of rules, it is beyond the scope of this chapter and will therefore not be discussed in detail. But it becomes obvious that by applying this kind of modelling the computer is not only used as a calculator but also as a reasoning machine.

Because model states are unique and they have only one possible transition to another state, decision rules can be used to define these transitions. It are these decision rules who are directly programmable and can be looked upon as model thresholds. Although, Begin & Schumm (1984) showed that system thresholds are commonly gradual, they can be looked upon as abrupt on a large timescale, implying that finite state modelling is scale dependent.

Validity of finite state models

By using qualitative knowledge in finite state modelling the

validity of modelling is only on the conceptual level. Concepts and hypothesis can be tested and evaluated by simulations of certain scenario's. When the time scale is reduced the numerical portion increases, but the validity remains at the conceptual level.

Conclusions

Finite state modelling, allowing the application of qualitative descriptive relations in a model, is proposed as an alternative strategy for long term modelling in geomorphology. By this kind of modelling the computer is not only used as a calculator but also as a reasoning machine. Models made according to the finite state principle have only validy on the conceptual level and should display the actual state of knowledge on the subject. Even if it is possible to construct a complete numerical model, the strategy of finite state modelling can make the geomorphologist more aware of the limited validity of long term models.

4.1. RIVER TERRACE FORMATION, MODELLING, AND 3-D GRAPHICAL SIMULATION.

Veldkamp A. & Vermeulen S.E.J.W.

Abstract

A model on river terrace formation is presented, written in PASCAL and run on a VAX 8600. The model calculates the influence of a fluvial system on the relief of an area with macroscopical dimensions (10 km x 20 km x 0.5 km) over a period of 2.5 million years. Model input relies on uplift and alternations in discharge and sediment load as a function of climatic changes. The output of the model are 3-dimensional grid drawings which visualize the impact of uplift, discharge, and sediment load on a landscape. Model formulation is based on empirical information on fluvial systems, which was incorporated in the model by means of a slightly adapted way of finite state modelling in which decisions act as thresholds. The model is organized using two entities, 'River' and 'Landscape' with attributes that have values within a specific realistic domain. The model produces plausible (x,y,z) and (x,y,t) plots in the light of existing geomorphological theories. The described modelling procedure shows that it is possible to simulate river terrace formation three dimensionally with the use of empirical information.

4.1.1 Introduction

The fluvial system in dynamic equilibrium is able to adjust itself to changes of external variables by changing its internal variables like channel depth and width, river roughness, mean velocity, channel form, and slope (Schumm, 1977; Dawson & Gardiner, 1987). River terrace formation can be looked upon as a result of changes in equilibrium, caused by variation in external variables like climate, tectonic and base level (Dury, 1970; Léger, 1983). The natural systems are so complex, and develop on such long time spans, that even laboratory experiments (e.g. Schumm et al., 1977) can only partly reveal part of their functioning. Computer simulation is increasingly recognized as a novel way to understand the way geomorphic systems work (e.g. Anderson, 1988). Modelling and simulation comprise the activities involved in constructing a model of a real world system and simulating it on a computer (Elzas, 1978). To gain insight in river terrace formation, a simulation model was developed which graphically describes changes in a landscape due to changes of a fluvial system in time. This is an extension of the research on simulation of river terrace formation by Boll et al. (1988). Their model appeared to be unsuitable for three-dimensional

application, making a new approach necessary. To make an overall model construction possible some oversimplifications have to be made in those cases in which no accurate data or relations are available. The developed model consists of an algorithm of 575 lines written in PASCAL and runs on a VAX 8600. This algorithm is available on request. The model construction, its properties, and relations will be discussed first, followed by a simulation example with input and output.

4.1.2. Materials and methods

Model construction in this study started with the choice of a type of model which would best fit the objective to gain insight in terrace formation. Due to lack of accurate and detailed information, a macroscopical empirical description of fluvial systems was selected as a basis for model formulation. Subsequently, a discrete time model was constructed, which simulates generalities of terrace formation.

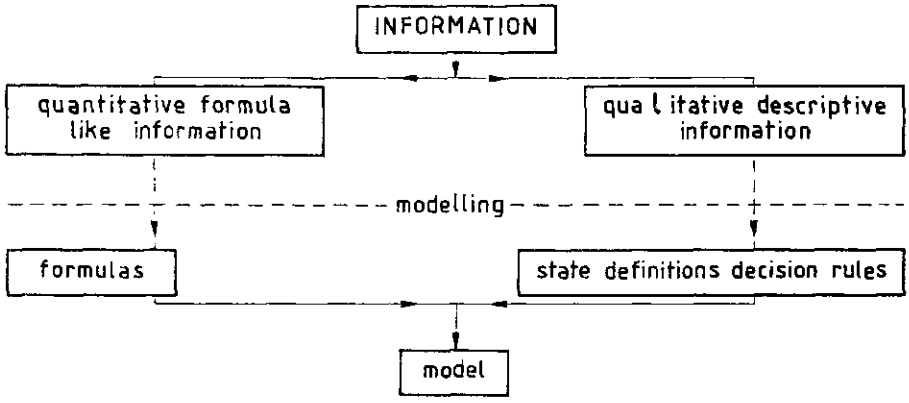

Figure 4.1.1 **Modelling with two groups of information**

4.1.3. Model construction

The information used in modelling can be divided into two major groups (Fig. 4.1.1): (1) quantitative, often empirical formulas, and (2) descriptive, qualitative knowledge. Since both types of information are indispensable for the model, the qualitative knowledge was incorporated as well, using finite state modelling methods (Zeigler, 1976), slightly adapted to our needs as described in the introduction of chapter 4. Grammatical analysis can be used to test the certainty and utility of descriptive information. Since no simplified grammatical analysis exists, a set of prohibition rules on Dutch grammar was stated and used in analyzing texts. Those prohibition rules are based on the simple and limited syntax of PASCAL (Findlay & Watt, 1978), and the sequential calculations of the central processing unit. Since we are no linguists the grammar rules used can be looked upon as very primitive implements only, and will therefore not be discussed in this paper.

States																								
Erosion	1	1	1	1	1	1	1	1	1	1	1	0	0	0	0	0	0	0	0	0	0	0	0	0
Channel form	M	M	M	M	M	M	B	B	B	B	B	B	M	M	M	M	M	M	B	B	B	B	B	B
Uplift	1	1	1	0	0	0	1	1	1	0	0	0	1	1	1	0	0	0	1	1	1	0	0	0
Resulting processes:																								
Incision	1	1	1	?	?	?	1	1	1	0	0	0	0	0	0	0	0	0	0	0	0	0	0	0
Bank-erosion	0	0	0	?	?	?	1	1	1	1	1	1	0	0	0	0	0	0	0	0	0	0	0	0
Deposition	0	0	0	0	0	0	0	0	0	0	0	0	1	1	1	1	1	1	1	1	1	1	1	1

M= Meandering channel
B= Braided channels (note meandering excludes braided and vice versa)
1= true
0= false
?= Unknown which erosion process will act.

Table 4.1.1 **Matching of states and the resulting deposition and erosion processes.**

In order to define the transition form one state to another, decision rules are used. The states of the model, which are only true or false, change at certain defined boundary conditions. Different states, are separated by thresholds and as such represent discontinuities is a system (Hugget, 1985). In the following example the state combinations of a fluvial system which result in a combination of incision and bank erosion or

deposition are listed in Table 4.1.1 (extracted from Schumm, 1977, 74-91). However, it has to be noted that other texts will yield other states. The question marks in Table 4.1.1 visualize gaps in knowledge about erosion under various uplift and channel form states. To fill up these gaps some assumptions were made. In the model the question marks were replaced by 'true'. An advantage of using finite state modelling for the qualitative knowledge is that the relations of Table 4.1.1 are easily translated into decision rules in PASCAL:

```
IF EROSION AND
     UPLIFT     AND MEANDER          THEN INCISION
     UPLIFT     AND BRAIDED          THEN INCISION AND BANK_EROSION
     NOT UPLIFT AND MEANDER          THEN INCISION AND BANK_EROSION
     NOT UPLIFT AND BRAIDED          THEN BANK_EROSION
IF NOT EROSION                       THEN DEPOSITION
                                (disregarding all other
                                conditions)
```

These rules can be incorporated in the model algorithm.

Model organization

When different textbooks are used, a well defined and formalized organization is needed. A hierarchical organization structure, similar to common data base organizations was chosen. Model organization, as presented in Table 4.1.2, was done with the use of entities and attributes. An entity was defined as an independent, commonly compound, unit in the object system. An attribute is a property, mark or characteristic usually variable of an entity in the studied object system. The entities defined, RIVER and LANDSCAPE are described by their attributes, each with values in a realistic domain. The interactions between the two entities are defined as PROCESSES. These processes are simplifications of the geological processes, and were directly programmed in the model algorithm. The LANDSCAPE relief was defined as an (x,y) matrix, with two stored values in each grid cell (100m x 200m): altitude z (m) and time of deposition t (ky). This matrix is used as the model output and makes GIS

Table 4.2.2

A. Time	:1 < Time <2500 (Ky)
B. Entities	
1. Entity: RIVER	
Attributes	Domain
1.1 Discharge	:20 < Discharge < 280 (m^3s^{-1})
1.2 Input_load	:0 < Input_load < 3.0 E^{-3} (m^3s^{-1})
1.3 Form	:meandering or braided
1.3.1 Width	:400 < Flood_plain_width < 1500 (m)
1.3.2 Maxload	:7.05E^{-5} < Maxload < 3.5E^{-3} (m^3s^{-1})
1.4 Erosion	:-2.1E^{-3} < Qerosion < 3.5E^{-3} (m^3ky^{-1})
2. Entity: LANDSCAPE	
Attributes	Domain
2.1 Quplift	:0 < Quplift < 0.4 (m/ky)
2.2 Relief x,y,z	:100 < x < 10000 (m) 100 < y < 10000 (m) 1 < z < 500 (m)
2.2.1 Valley_depth	:20 < Valley_depth < 500 (m)
2.2.2 Stratigraphy	:0 < stratigraphy < 2500 (ky)
2.4 Valley_width	:400 < Valley_width < 9500 (m)
C. Processes	
1 Uplift	:Uplift whole relief
2 Erosion	:Relief denudation, a relieff volume decrease
2.1	:Vertical erosion, denudation of the valley bottom.
2.2	:Horizontal erosion, denudation of the river banks.
3 Sedimentation	:built up of the relief, an relief volume increase

Table 4.1.2 Model organization

applications like the creation of single value maps possible. The selected relief magnitude, 10 km x 20 km x 0.5 km (x,y,z), size of middle scale rivers, reflects the macroscopical scale of the simulation. This also applies for the selected timespan of 2.5 million years (in time steps of 1000 years), due to the fact that most terraces in major river basins started to form at the beginning of the Quaternary. The domain limits, as used for each attributes (Tab. 4.1.2), were derived from published data on middle scale fluvial systems (Leopold et al., 1964). Climate and tectonics are external input variables for the model. Discharge and sediment load are input functions which were assumed to vary as a result of climatic change only.

4.1.4. Model Operation

At each time step (of 1 ky) a certain scenario is considered to compute model behaviour. Calculations of the volume to erode or deposit were followed by state determinations and calculations which determine the boundaries of relief changes and the processes which change the landscape. Discharge and input load are the input functions used to calculate the relief volume that changes during one time step. MAXLOAD, which is the maximum load at the current discharge, is calculated according to equation 1 derived from Boll et al., (1988).

$$MAXLOAD = L1 \times DISCHARGE^2 + L2 \times DISCHARGE + L3 \times DISCHARGE \quad (1)$$

with:

MAXLOAD	:	Maximum load	(m^3s^{-1})
L1	:	Suspended load factor	(sm^{-3})
L2	:	Dissolved load factor	(-)
L3	:	Bed load factor	(-)
DISCHARGE	:	Discharge	(m^3s^{-1})

L1, L2 and L3 are factors which represent respectively the dissolved, suspended and bed load component of the maximum load of a river. These factors have different values for a meandering

and a braided river and are used to tune the model. For a meandering river L1 = 2.2 x 10^{-8} (sm^{-3}), L2 = 3 x 10^{-6} (-) and L3 = 1.15 x 10^{-6} (-), for a braided river L1 = 1.9 x 10^{-8} (sm^{-3}), L2 = 3.2 x 10^{-6} (-) and L3 = 1.3' x 10^{-6} (-). One of the model assumptions is that at each timestep the river enters the landscape with input load and leaves it with the maximum load. This condition makes it possible to calculate the erosion or deposition quantity (Qerosion) with use of the mass balance of Equation 2.

$$QEROSION = MAXLOAD - INPUT\_LOAD \qquad (2)$$

with:

QEROSION	: Erosion or sedimentation quantity	(m^3s^{-1})
MAXLOAD	: Maximum load of the system	(m^3s^{-1})
INPUT_LOAD	: Input load	(m^3s^{-1})

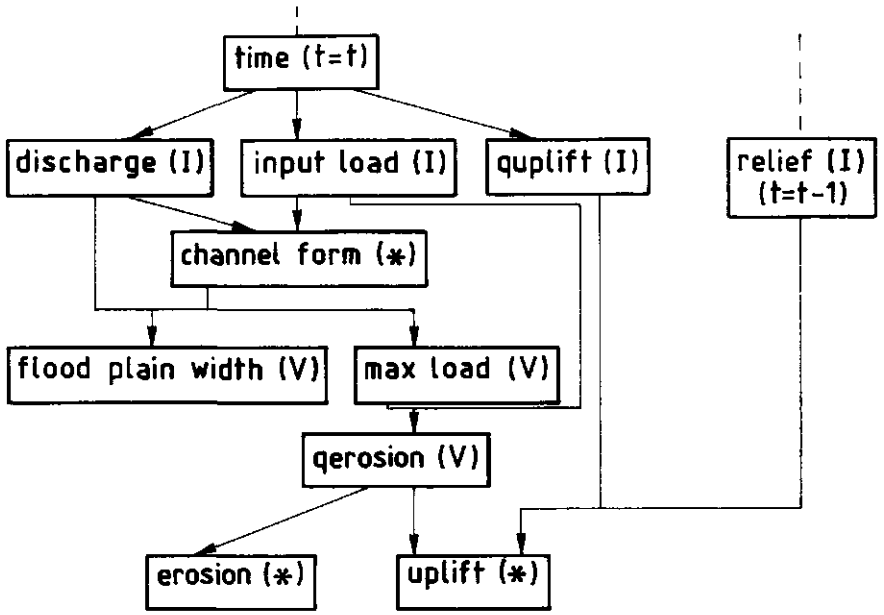

Figure 4.1.2 Flowchart of the model inputs (I), states (*) and variables (V).

The flowchart of Figure 4.1.2 shows how inputs, states and variables are used in the model. [Uplift], [Erosion] and [Channel form] are the states used to determine the process(es). [Uplift] becomes true when the fluvial system cannot compensate the uplift by erosion during one time step. [Erosion] is true when the calculations of the erosion quantity indicate a positive volume (QEROSION). The [Channel from] (meandering or braided) is determined by changes in discharge and input load, according to the following decision rules, which were indirectly derived from qualitative relations formulated by Schumm (1977, 135).

IF $Q_{t-1} < Q_t$ AND $LOAD_{t-1} > LOAD_t$ THEN MEANDERING IS TRUE

IF $Q_{t-1} < Q_t$ AND $LOAD_{t-1} < LOAD_t$ THEN $FORM_{t-1}$ IS TRUE

IF $Q_{t-1} > Q_t$ AND $LOAD_{t-1} > LOAD_t$ THEN $FORM_{t-1}$ IS TRUE

IF $Q_{t-1} > Q_t$ AND $LOAD_{t-1} < LOAD_t$ THEN BRAIDED IS TRUE

with:

Q_{t-1}	: Discharge of the preceding time step	(m^3s^{-1})
Q_t	: Discharge	(m^3s^{-1})
$LOAD_{t-1}$	: Input load of preceding time step	(m^3s^{-1})
$LOAD_t$	: Input load	(m^3s^{-1})
$FORM_{t-1}$	: Channel form of preceding time step	(-)

Floodplain width and valley slope are two model variables which act as boundaries between which relief changes take place. Since the valley slope calculations did not yield any visible changes, the slope was assumed constant (0.005 m m^{-1}). This insensitivity of valley slope is due to the relatively high minimum quantity to be eroded or deposited. The floodplain width for a braided river is not calculated, but comprises the whole width of the lowest level in a cross-section. Chorley et al., (1984,310) stated that it is likely that there exists a relation between meander wave length (Lambda) and valley width. In this study the relation 'floodplain width of a meandering river is 0.5 Lambda' is used. Equation (3) is derived from the sinuosity formula of a meandering river from Schumm (1977,115).

$$FLOOD\_PLAIN\_WIDTH = 0.5 \times 30 \times (DISCHARGE/0.028)^{0.5} \quad (3)$$

with:

FLOOD_PLAIN_WIDTH	: Flood plain width of a meandering river	(m)
DISCHARGE	: Discharge	(m^3s^{-1})

The model processes, i.e., (1) erosion, subdivided into incision and bank erosion, and (2) deposition, are used to distribute mass transport over the x and y-axis (for instance increase of z-values of grid cells because of sedimentation process), as indicated in Figure 4.1.3. The incision process reduces the z value of the grid cells in the lowest part of a cross-section with one unit, and bank erosion raises the width in the lowest part of the cross section with two units (Fig. 4.1.3).

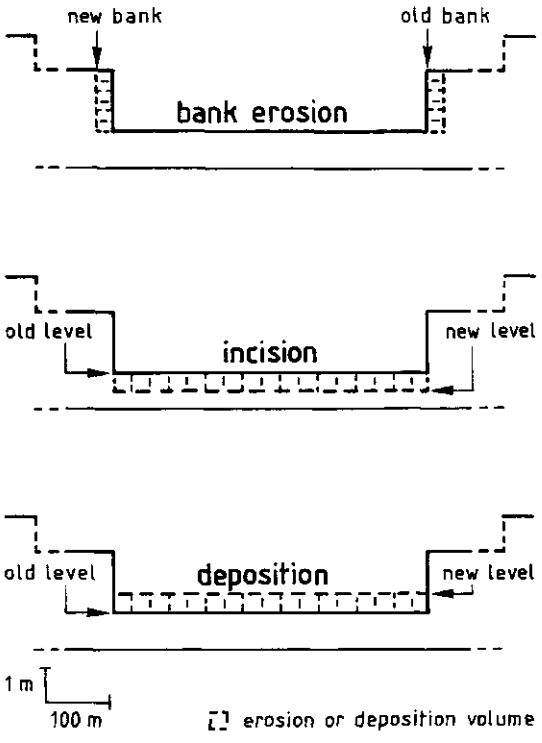

Figure 4.1.3 Model processes and their impact on a cross-section

4.1.5. Results

A simulation yielding illustrative results was selected to demonstrate the simulation procedure.

Input

Although the relationship between fluvial dynamics and climate behaviour depends on the nature of climatic change and the effects of such changes on discharge and sediment load (Lowe & Walker, 1984), a simple relation was assumed between temperature, discharge and sediment load change. A climatic cycle, consisting of a glacial and an interglacial period, was divided by Boll et al. (1988) into four phases, in which each have different discharge and sediment load characteristics. Direct sedimentological and paleoclimatical evidence in many natural terrace systems suggest that in glacial periods, sediment load increases as a result of reduced vegetation cover and hence increased lateral sediment supply to the river. In interglacial periods slope stabilization by vegetation and higher precipitation lead to increasing discharge. This more or less complementary relationship between discharge and sediment load is translated in the model as sinus and cosinus functions, respectively. In order to obtain a more refined climatic curve, the input functions of discharge and input load used are directly based on the widely accepted Milankovic curve (Imbrie & Palmer, 1979), which describes climatic changes in the Quaternary as a result of astronomical parameters. Consequently, discharge, Equation 4, is simulated as the sum of three SIN functions and input load, Equation 5, as the sum of three COS functions, of the earth orbit parameters periods of 23.000, 42.000 and approximately 100.000 years, as found in $d^{18}O$ curves by Hays et al. (1976).

$$\text{DISCHARGE} = \text{DAVE} + \text{DAMP} \times (\text{SIN}(2\pi \times \text{TIME}/100) + \text{SIN}(2\pi \times \text{TIME}/42) + \text{SIN}(2\pi \times \text{TIME}/23)) \quad (4)$$

$$\text{INPUT\_LOAD} = \text{INLAVE} + \text{INLAMP} \times (\text{COS}(2\pi \times \text{TIME}/100) + \text{COS}(2\pi \times \text{TIME}/42) + \text{COS}(2\pi \times \text{TIME}/23)) \quad (5)$$

with:

DISCHARGE	: Discharge	(m^3s^{-1})
DAVE	: Average discharge	(150 m^3s^{-1})
INPUT_LOAD	: Input load	(m^3s^{-1})
INLAVE	: Average input load	(0.005 m^3s^{-1})
DAMP	: Discharge amplitude	(130 m^3s^{-1})
INLAMP	: Input load amplitude	(0.0015 m^3s^{-1})
TIME	: Time	(ky)

The input function of tectonics in this simulation is a constant uplift of 0.1 m each 1000 years.

Output

Each 0.5 million years pictures are made of the landscape (x,y,z,t) data. Three-dimensional pictures are drawn with use of the computer package UNIRAS. The (x,y,t) pictures of Figure 4.1.5 were drawn manually. The (x,y,z) relief diagrams show the development and destruction of river terraces (Fig. 4.1.4). The uplift of the landscape as well as the incision of the valley are visible. The (x,y,t) diagrams indicate the time of deposition of the surface deposits, at the end of the simulation (2.5 million years) there are still deposits which were laid down during the first 0.5 million years (Fig. 4.1.5). Those remnants are only preserved at small high spots. Another visualization of the dynamic properties of the simulated example is shown in Fig. 4.1.6, which portrays the formation, reduction, and destruction of several terraces in one cross-section at y=18km, during the simulation process. Only some small terrace remnants remain in the cross-section. Besides graphical output, the number of the model states and processes which occur during simulation, is recorded (Tab. 4.1.3)..

The periods during which the model states remain constant, have an average duration of about 7 ky, with a minimum of 1 ky and a maximum of 19 ky. Figure 4.1.7 gives a detailed insight in terrace formation between 1.42 and 1.45 million years, caused by the sequence of model states and processes.

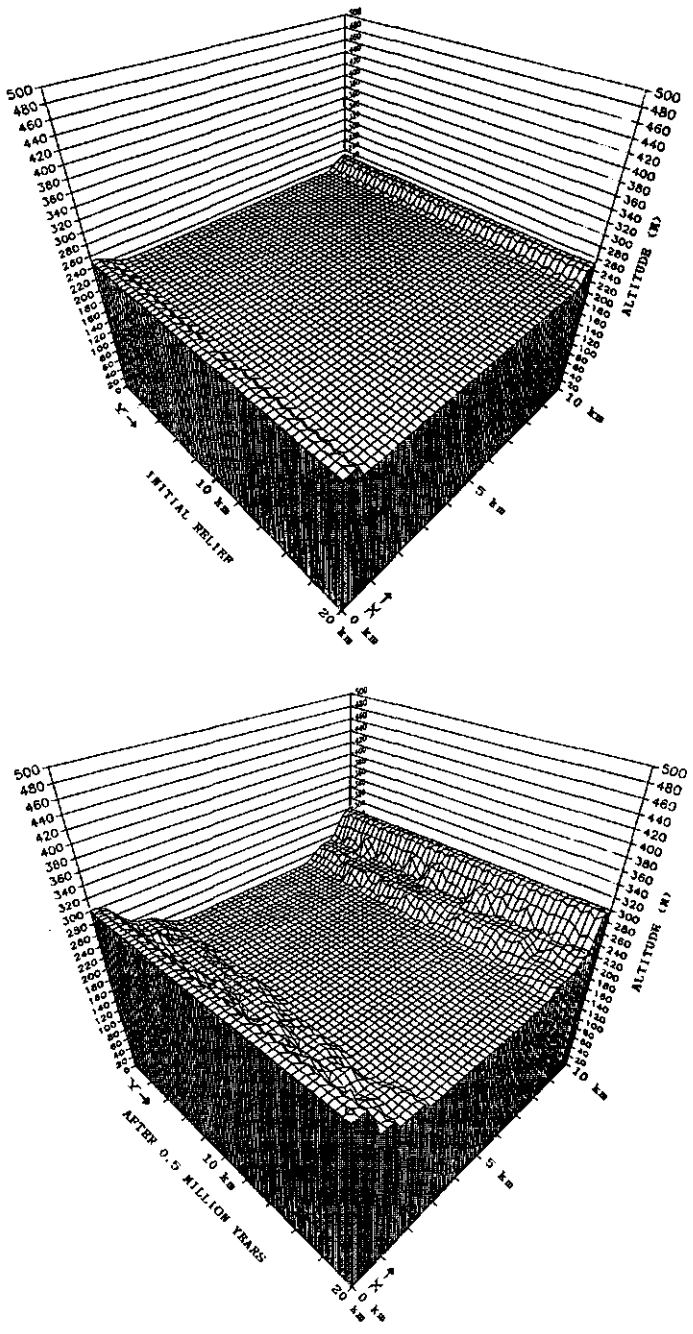

Figure 4.1.4 x,y,z relief pictures of the landscape development each 0.5 million years during the simulation.

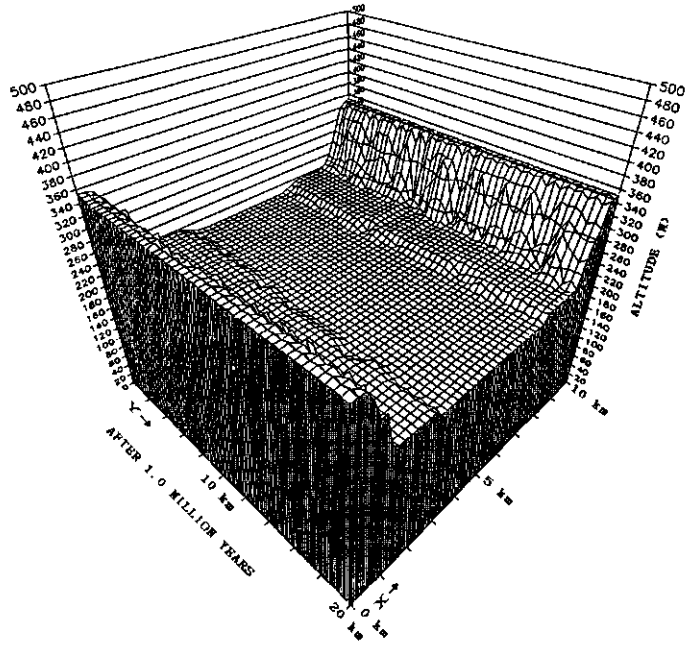
500
480
460
440
420
400
380
360
340
320
300
280
260
240
220
200
180
160
140
120
100
80
60
40
20
0
ALTITUDE (M)
Y
AFTER 1.0 MILLION YEARS
10 km
20 km
0 km
5 km
10 km
X

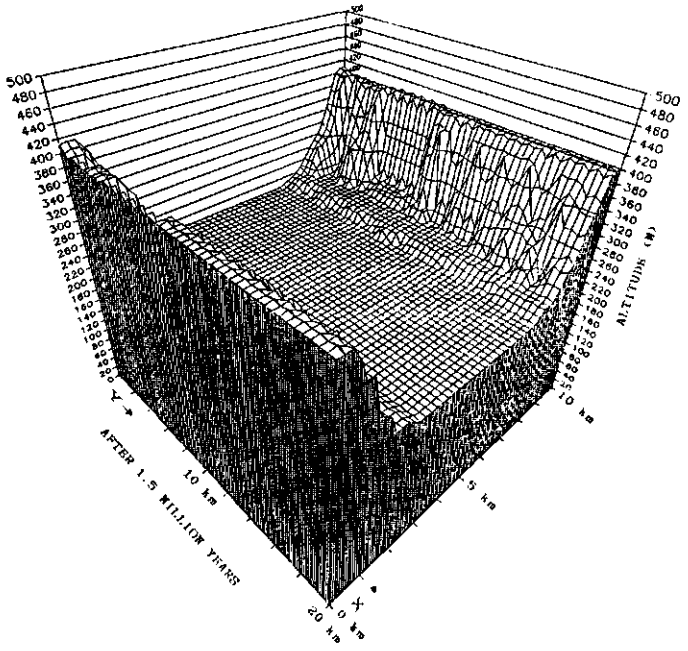
500
480
460
440
420
400
380
360
340
320
300
280
260
240
220
200
180
160
140
120
100
80
60
40
20
0
ALTITUDE (M)
Y
AFTER 1.5 MILLION YEARS
10 km
20 km
0 km
5 km
10 km
X

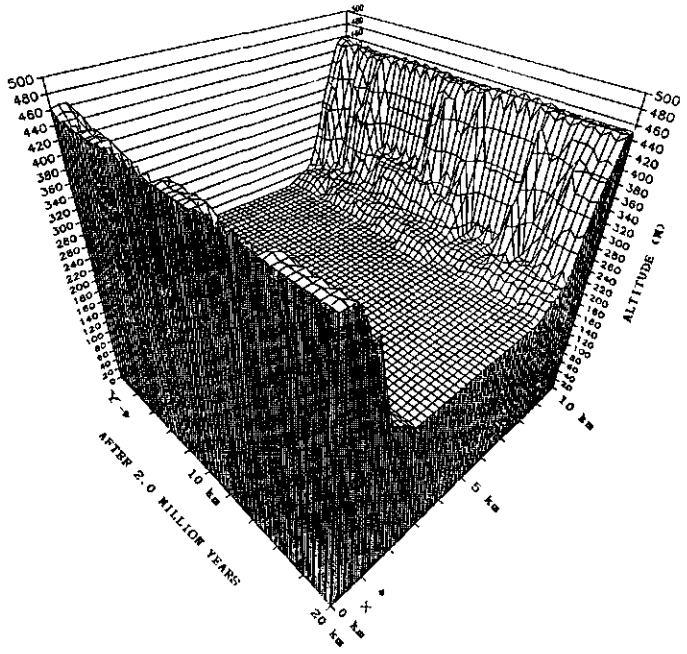
AFTER 2.0 MILLION YEARS
ALTITUDE (M)
Y
X
0 km
5 km
10 km
20 km

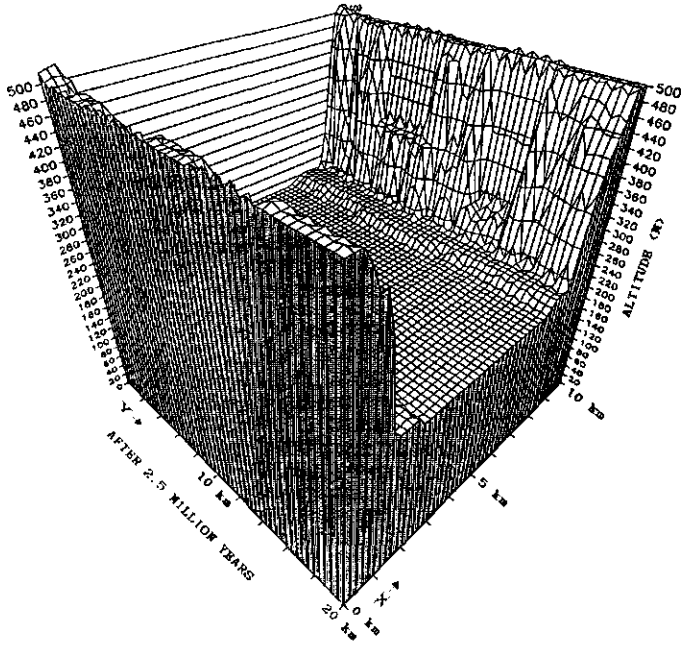
AFTER 2.5 MILLION YEARS
ALTITUDE (M)
Y
X
0 km
5 km
10 km
20 km

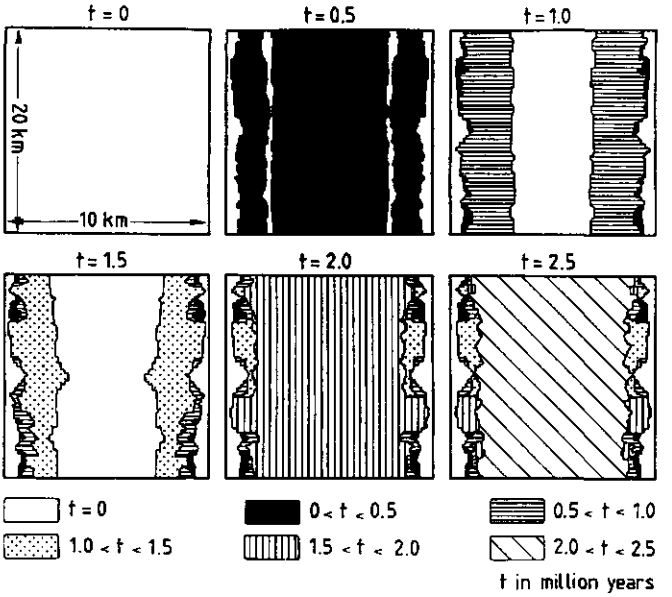

Figure 4.1.5 **x,y,t pictures, showing the time of deposition of the surface deposits each 0.5 million years during the simulation.**

Uplift	Erosion	Meandering	Incision	Bank-erosion	n_1
1	1	1	1	0	71
1	1	0	1	1	2
0	1	1	1	1	1044
0	1	0	0	1	674
1	0	1	0	0	43
1	0	0	0	0	70
0	0	1	0	0	104
0	0	0	0	0	492
n_2: 186	1791	1262	1117	1720	

1 = true
0 = false
n_1 = Frequency of time steps that a model state occurs (sum is 2500).
n_2 = Frequency of time steps that a state variable or process is true.

Table 4.1.3 **Frequencies of the model inputs, states, and outputs.**

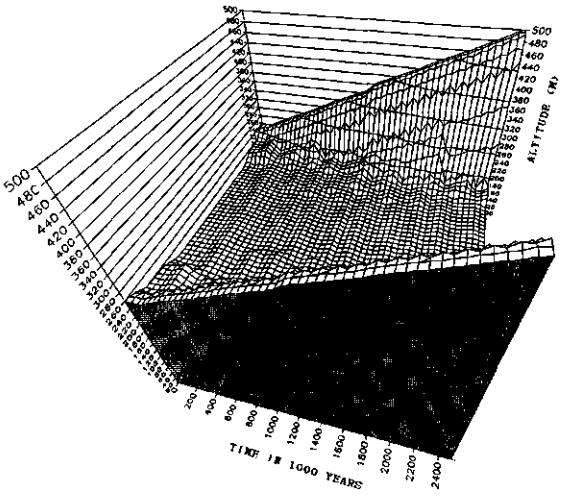

Figure 4.1.6 x,90,z picture, showing the development of one cross-section (y=90) during simulation.

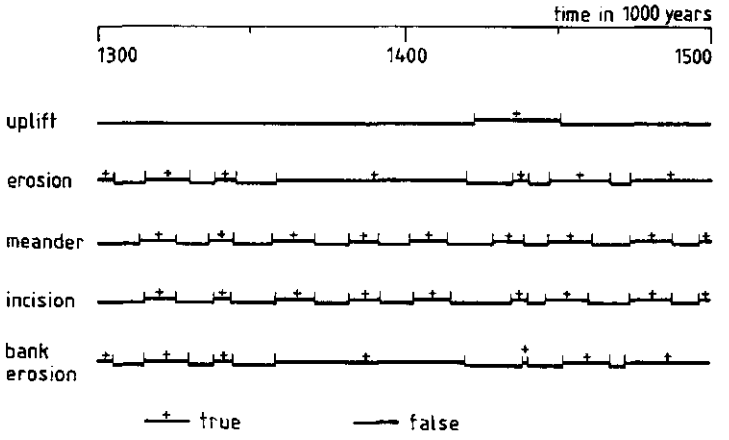

Figure 4.1.7 Model states and processes occuring between 1,3-1,5 million years during simulations.

A period of erosion (incision and bank erosion) is the two channel types interchanges with a period of sedimentation. Due to this sedimentation the fluvial system cannot compensate the uplift by incision, and the [Uplift] state becomes true. When sedimentation has stopped a meandering river immediately starts incising until the uplift is compensated. This incision (without bank erosion) causes a new terrace to develop. During the following time steps the new terrace decreases in width due to bank erosion.

Observing the simulation results it can be concluded that both intrinsic and extrinsic changes of state take place. When inside the system thresholds are crossed without changes in input variables, like uplift, an intrinsic change of state takes place. Whenever the system responds directly to external influences, extrinsic thresholds are crossed (Huggett, 1985; Schumm, 1977). Due to the simple model organization the input strongly determines the output causing the majority of the threshold crossings to be of extrinsic character. By changing model parameters other simulations were carried out. Simulations without uplift or with a constant uplift of more than 0.5 m/ky resulted in terraces which disappeared quickly after their formation.

4.1.6. Discussion and Conclusions

The observed differences in the various simulations have made it possible to formulate some conclusions concerning terrace formation in the described model. Within the simulated fluvial system model, terraces are formed by changes in discharge and sediment load. Commonly terraces are quickly eroded. At some specific input values, however, such as a constant uplift rate of 0.1 m/ky, some terrace remnants are preserved from being eroded. Both extrinsic and intrinsic changes of state can bring about terrace formation in the model. Although this model has not and cannot be validated, it produces plausible (x,y,z) and (x,y,t) plots in the light of existing geomorphological theories.

The described model and simulation show that it is possible to simulate river terrace formation and to graphically display

the results with use of both quantitative and qualitative information. The decision rules which are the result of finite state modelling, allowing the incorporation of qualitative relations. They act as thresholds and strongly determine the model output. This indicates that further model improvements could be found in extension of the used decision rules or refinements in states and state transitions. When the presented model is applied to a real system it can be used to formulate and analyze hypotheses of fluvial terrace formation. The methodology used is also applicable on many other geomorphic subjects, especially when not all information is or can be quantified.

4.2 A 3-D MODEL OF FLUVIAL TERRACE DEVELOPMENT IN THE ALLIER BASIN.

A. Veldkamp

Abstract
The combined effects of climate and tectonism on general terrace stratigraphy and valley asymmetry during the last half million years in the Allier system (France) are simulated by a 3-D conceptual model (LIMTER). This model allows the formulation and evaluation of long term terrace formation scenarios for the Allier system. Simulation results suggest that terrace stratigraphy in the study area is mainly the result of the internal Allier dynamics and climatic change. Local tectonism caused the development of unpaired terraces while the general regional uplift played a dominant role in terrace formation and preservation in general.

4.2.1. Introduction

River terraces are a fundamental part of fluvial landscapes. The existence and formation of terraces has been subject of research for many years because they provide a relative chronology to which other geological, geomorphological or palaeohydrological events can be related (Dawson & Gardiner, 1987). It has always been tempting to link Quaternary terrace chronologies with established chronologies of major Quaternary environmental changes, such as climatic and sea level oscillations, especially when other dating evidence is not available.

A first and well known generalization about the response of fluvial systems in semiarid to subhumid regions to slight shifts in climate was set forth by Huntington (1907, p. 358) and is called "Huntington's principle" (Fairbridge, 1968, p.1125; Bloom, 1978, p. 248). Huntington's principle, was established as a general model which many followed in constructing terrace chronologies, whereby glacials are thought to be characterized by aggrading braided rivers and the interglacials by incising meandering rivers. This generalization is now recognized as being exceedingly simplistic.

The other major generalization of a driving force behind terrace formation which is or was often applied concerns changes in base level. Such base level changes may be due to sea level

changes or epirogenetic movements. In Britain base level changes received much attention and the relative changes in sea-level were seen as a major external driving force for river-level changes (Green & Mcgregor, 1987). In continental Europe a climatic school dominated which applied base level changes due to tectonism as second important external variable (Brunnacker & Boeningk, 1983; Buch, 1987; Texier & Raynal, 1984). However, a perfect association of terrace depositional phases and incision episodes with climatic phases of certain base-levels is rarely possible, or even likely. Terraces are in fact very complex features, resulting partly from external factors and partly from the nature of response in the fluvial system itself. Rivers may make terraces without there necessarily being an external change (Schumm, 1977). Often the external model breaks down on a lack of detailed understanding of the processes operating within the fluvial system.

Stratigraphy offers a direct way to gain more insight in the internal dynamics of a fluvial system. The sediment properties, deposition conditions and their sequence can give detailed insight in former conditions within the fluvial system studied. Breaks or facies transitions within the sedimentary record often mark major environmental changes, indicating possible external forces controlling fluvial dynamics and terrace formation.

In general it has long been recognized that alluvial sedimentary successions are composed of two main facies groups. One group comprises sandstones and conglomerates the other group consists of, mudstones and siltstones (Bridge & Leeder, 1979). A similar alluvial sediment discrimination was made in fluvial terrace sediments by Texier & Raynal (1984) who correlate coarse sediments to glacial environments and fine sediments to interglacial environments. They belong to the climatic school as they linked the reviewed terraces with the major Quaternary climatic cycles.

A simulation of alluvial stratigraphy within one floodplain

under strict assumptions (Bridge & Leeder, 1979) showed that the internal dynamics can strongly determine the stratigraphical record. Tectonic movements had only a significant influence on the simulated successions if a preferred direction of tilting maintained. From this simulation and the correlations of Texier & Raynal (1984) it becomes obvious that if one wants to create a more realistic model of fluvial terrace formation the stratigraphical record has to be incorporated.

More effects of changes in fluvial dynamics can be viewed, when considering both geographical position of terraces and their stratigraphical record. The role of tectonism seemed only minor in the stratigraphical model of Bridge & Leeder (1979) but when similar movements are considered in a model including terrace formation more distinct results can be expected. Tectonic uplift is likely to cause vertical erosion of a river and thus abandoning of the floodplain, an effect not incorporated in their stratigraphical model.

In respect to tectonism river terraces are more valuable than stratigraphy because they give direct indications of former river gradients, and successive terraces show successive river positions. In areas of tectonic activity, valleys and their terraces may be asymmetrical, tilted or warped in various ways, giving valuable clues for interpretation of tectonic movements.

Models which describe fluvial system dynamics for longer time spans are sparse because most knowledge on fluvial systems is mostly based on short term, well controlled experiments (Gregory, 1983; Dawson & Gardiner, 1987). They are therefore usually based on the correlation of terraces with known major changes during the Quaternary. Most of these models are used for the interpretation of large terrace sequences.

Recently a quantitative but still conceptual, long term (2000 ky) macro scale (100 km^2) fluvial system model was constructed which simulates the development of fluvial terraces as the result of external and internal changes in the simulated fluvial system (Veldkamp & Vermeulen, 1989). This so-called coarse scale model

(Thornes, 1987) did not consider the effects on the fluvial stratigraphical record.

In this paper the combined effects of climatic change, tectonism and internal fluvial dynamics on alluvial stratigraphy and valley morphology are simulated using a comprehensive version of the existing 3-D fluvial terrace formation simulation model. As an exercise a plausible terrace development scenario is simulated for the Randan section in the Allier valley with the 3-D LIMTER (LIMagne TERraces) model. The program listing can be found as appendix II in this thesis.

4.2.2. Model characteristics

Model construction, organization and operation are described in a previous paper (Veldkamp & Vermeulen, 1989). Model organization was done with entities and attributes. An entity is an independent unit in the object system, the entities in this model are LANDSCAPE and RIVER. An attribute is a property, mark or characteristic of an entity, such as discharge for RIVER and Valley_depth for LANDSCAPE. Attributes have been constrained to lie in realistic domains for the Allier system. The LIMTER entities and their attributes are described in Table 1.
Interaction between the two entities are defined as erosion and sedimentation processes acting in timesteps of 1000 years.

These model processes are long term and large scale analogies of real erosion and sedimentation processes. They are artificially constructed processes reacting to changes in the 1000 years discharge/sediment load equilibrium which are defined as a function of climate. When the sediment input load exceeds the sediment transport capacity the difference is deposited (DEPOSITION = true), and in case the transport capacity exceeds the input load the difference is eroded in the simulated system (EROSION = true).

The quantity to erode or deposit in LIMTER is calculated from a sediment budget, but which processes act in the LANDSCAPE is determined by decision rules extracted from general literature on hydrology (Schumm, 1977).

A. Time	:1 < Time <800 (Ky)
B. Entities	
1. Entity: RIVER	
Attributes	Domain
1.1 Discharge	:1.58×10^{12} < Discharge < 9.47×10^{12} ($m^3 ky^{-1}$)
1.2 Input_load	:0 < Input_load < 9.46×10^{7} ($m^3 ky^{-1}$)
1.3 Form	: meandering or braided
1.3.1 Width	:0.15 <Flood_plain_width< 14.4 (km)
1.3.2 Maxload	:2.22×10^{6} < Maxload < 1.10×10^{8} ($m^3 ky^{-1}$)
1.4 Erosion	:-6.62×10^{7} < Erosion < 1.10×10^{8} ($m^3 ky^{-1}$)
2. Entity: LANDSCAPE	
Attributes	Domain
2.1 Quplift	:0 < Quplift < 0.4 (m/ky)
2.2 Quplift_unequal	:0 < Quplift_unequal < 0.05 (m/ky)
2.3 Relief x,y,z	:150 < x < 15000 (m) 150 < y < 15000 (m) 1 < z < 500 (m)
2.3.1 Valley_depth	:20 < Valley_depth < 500 (m)
2.3.2 Stratigraphy	:0 < stratigraphy < 1000 (ky)
2.3.3 sediment_composition	:1 < sediment_composition <= 4 (-)
2.4 Valley_width	:0.15 < Valley_width < 14.30 (km)

Table 4.2.1 Model organization

These decision rules are:

IF EROSION AND UPLIFT AND MEANDER	THEN INCISION
IF EROSION AND UPLIFT AND BRAIDED	THEN INCISION AND BANK_EROSION
IF EROSION AND NOT UPLIFT AND MEANDER	THEN INCISION AND BANK_EROSION
IF EROSION AND NOT UPLIFT AND BRAIDED	THEN BANK_EROSION
IF NOT EROSION	THEN DEPOSITION (disregarding all other conditions)

Whereby UPLIFT and NOT UPLIFT are system states indicating the impact of tectonic uplift. UPLIFT is true (NOT UPLIFT = false)

when the fluvial erosion is not able to compensate the LANDSCAPE uplift. MEANDER is true when the Allier is meandering while the BRAIDED state is true when the Allier is braiding. The impact of INCISION, BANK_EROSION AND DEPOSITION in a cross-section are shown in Fig. 4.1.3. Erosion processes are headward migrating along the longitudinal profile, while sedimentation migrates in downward direction. Irregular headward erosion during erosion of a meandering RIVER is caused by changes in the effective floodplain width during the simulation. The resulting irregular bank erosion causes a similar effect as a meandering river does.

During a simulation the volume to erode or deposit by the RIVER in the LANDSCAPE is calculated for each time step of 1 ky. These calculations are followed by state determinations and boundary calculations within which LANDSCAPE changes must take place. The LANDSCAPE is changed by modifying grid cells elevations in response to the acting process. The changed LANDSCAPE is stored in a geographical information system (GIS).

Terrace stratigraphy

Terrace stratigraphy was also incorporated within LIMTER. During the simulations the stratigraphy (sediment age and composition class) of the upper ten metres (grid cells) are stored. The sediment composition classes are derived from bulk geochemical sediment research of the Allier terraces. There are four sediment composition classes with the following characteristics:

Class 0, is the underlying bedrock;

Class 1, are sandy and clayey sediments with a low volcanic content which are deposited during interglacial periods in a meandering system;

Class 2, are predominantly sandy sediments with an intermediate volcanic content which are deposited in a braided system, during glacial periods;

Class 3 are gravelly sediments with a high volcanic content, which are deposited in a braided system at the end of

a prolonged glacial (> 10 ky).

4.2.3. Model Input

The inputs and outputs of the Allier system simulations are described after which simulation results are presented and discussed.

Climate

The Quaternary has known many astronomically controlled mondial changes in climate, which can be very satisfactory described by Milankovics curve (Berger, 1978). These climatic changes are directly registered in deep sea cores, ice cores and löss profiles giving indications of the relative amounts of water stored in ice masses, and changes in mondial circulations. Although the relationship between fluvial dynamics and climate behaviour depends on the nature of climatic change and the effects of such changes on discharge and sediment load (Lowe & Walker, 1984), a simple linear relation was assumed between caloric insolation (Berger, 1978), mean discharge and sediment load each 1000 years. During Glacials much water is stored in glaciers and drier continental climates prevail causing lower mean 1000 years discharges in rivers. Due to the drier and colder glacial environment the vegetation cover decreases causing an increase in sediment supply to fluvial systems. Interglacials yield the opposite picture, an increase in the mean 1000 years discharge and a complementary decrease in the 1000 years sediment supply. This simplified relationship between mean discharge and mean sediment load is partly supported by the changes in magnetic susceptibility as found in the long löss sections in China, indicating dry glacials and wet interglacials during the last 2.4 million years in this continental area (Heller & Wang, 1991). A similar condition can be expected in the Allier basin where the glaciers caused a permanent high pressure area during the glacials.

As model simulations require a climatic input with a constant reliability during the simulated time span a simplified

Milankovics curve was used as basic climatic input. Mean discharge each 1000 years is simulated as the sum of three SIN functions with the periodicities of the precession (23,000 years), obliquity (41,000 years) and eccentricity (96,000 years). As the sediment load is assumed to have a similar behaviour complementary to the 1000 years discharge it was simulated as the sum of the COS functions of the same three periodicities. Although these curves do not exactly match the climatic curves derived from deep sea cores and löss sediments, they sufficiently describe climatic changes during the Quaternary for our conceptual long term modelling purposes. The general assumption that there exists a simple straight forward relationship between Milankovics curve and both the 1000 years discharge and sediment load curves is of course a too strong oversimplification to have any realistic validity. It is obvious that a refinement of this assumption would improve the general validity of the model.

Except the difference in behaviour of the fluvial dynamics in a glacial and interglacial stadia the transition from a glacial to an interglacial environment was also taken into account. Bulk geochemical research showed also that changes in sediment flux magnitude and sediment composition are related to the intensity and duration of a climatic episode (Veldkamp, 1991). During prolonged glacials, large glaciers were built up on the higher parts in the Allier basin, the Cantal and the Mont Dore volcanoes (Veyret, 1978). When climatic conditions improved relative fast glacier melting caused the release of large quantities of coarse volcanic rich sediments into the Allier. During the Late Quaternary this extra sediment flux ranged from 2 to almost 50 times the Interglacial flux quantities.

The fluvioglacial sediment fluxes are incorporated within LIMTER as follows: when a glacial lasts longer than 10 ky an extra large (4 x normal flux) sediment flux with composition class 3, is released into the system at the transition to a new interglacial period. The flux magnitude of 4 is based on model tuning. The resulting alternating erosion and deposition states during the simulation are clearly illustrated by the cumulative erosion graph (Fig. 4.2.1).

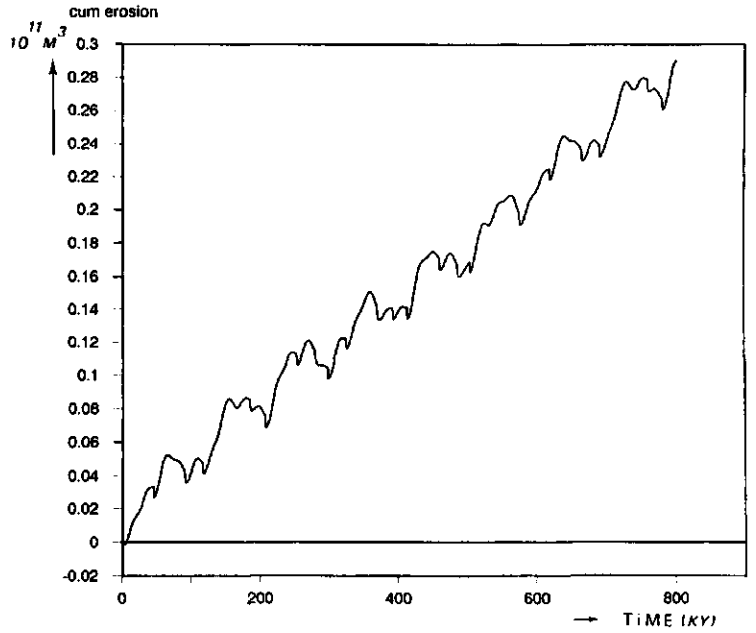

Figure 4.2.1 **Cumulative erosion curve, derived from changes in discharge/sediment load equilibrium during simulation of LIMTER. This curve illustrates the alternating erosion and sedimentation stages during simulations.**

Tectonism

Two different components of tectonism (Fig. 4.2.2) are incorporated in LIMTER. A component of gradual uplift of the whole simulated landscape (QUPLIFT), and an uplift component describing the difference in uplift rate of the landscapes on both sides of the Allier (QUPLIFT_UNEQUAL). The latter tectonic component assumes an active fault in the middle of the Allier valley, dividing the entity LANDSCAPE in two parts with different uplift rates. There is some field evidence which suggests the presence of such a faulting zone.

Because there is no proof that tectonism has known changing rates in the Allier basin in time, only simulations with constant gradual uplift are made. A simulation with a QUPLIFT of 0.1 m/ky and a QUPLIFT_UNEQUAL of 0.01m/ky will be shown.

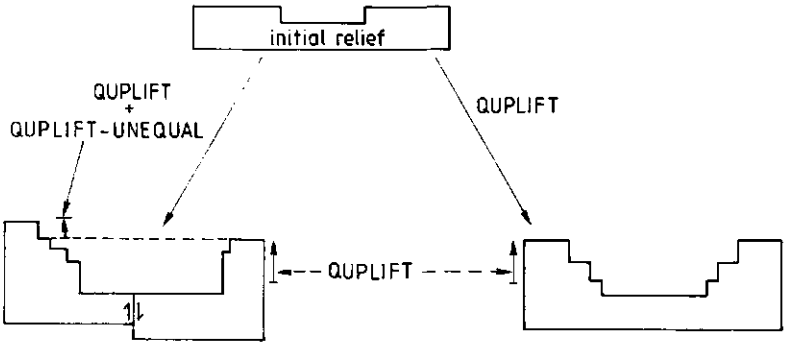

Figure 4.2.2 **Two tectonic components as input of the LIMTER simulation. Quplift is the general uplift of the modelled area, Quplift-unequal is the difference in uplift rate between the two valley sides, assuming an active fault in the middle of the valley parallel to the flow direction.**

Initial relief

The initial relief (Fig. 4.2.3.a) is also a model input. The simulated LANDSCAPE has a surface of 225 km^2 (15 x 15 km), a maximum altitude of 270 m and a minimum altitude of 240 m. The initial relief consists of a broad (valley_width is 7800 m), shallow (valley_depth is 30 m) valley. Terrace stratigraphy displays only age 0 and composition class 0 indicating that no fluvial sediments occur in the initial LANDSCAPE.

4.2.4. Model Output

The output of LIMTER is a raster GIS file with the LANDSCAPE altitudes and stratigraphy for each timestep. With these data, cross sections, maps, 3-D relief graphs, or 3-D graphs of one cross section development in time can be drawn.

4.2.5. Simulation results

A simulation with plausible realistic simulation results is presented in more detail. This simulation had the climatic and tectonic inputs as described by the model input. The LANDSCAPE development in time during this simulation is illustrated three-dimensionally in Fig. 4.2.3 for each 100 ky.

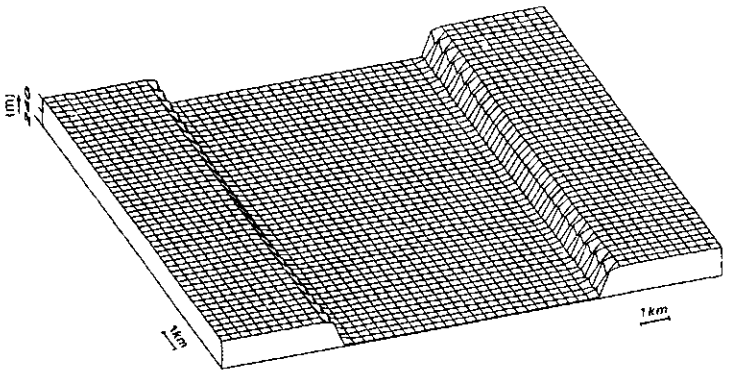

initial relief

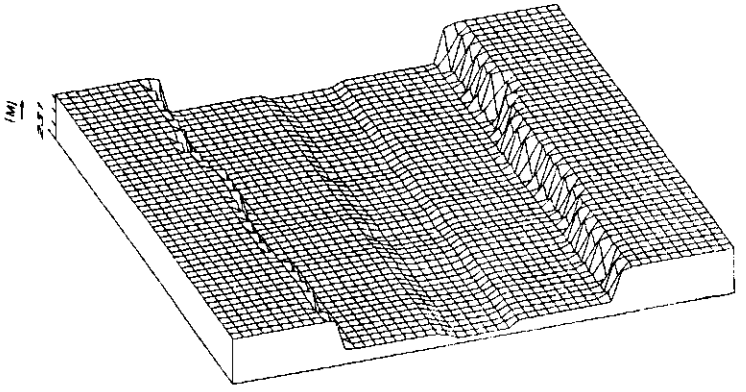

relief version D2 after 100 timesteps

Figure 4.2.3 3-D valley relief development during simulation, in timesteps of 100 ky. The effects of changing fluvial dynamics are illustrated by incision and terrace formation. Irregularities in the valley slopes are also caused by changes in fluvial dynamics during the headward erosion.

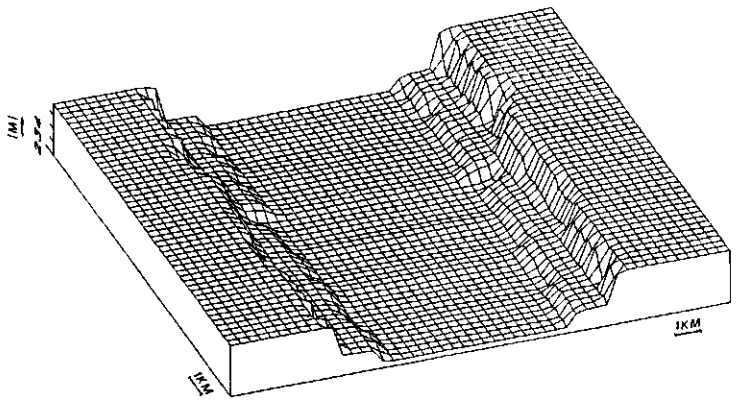

relief version D2 after 200 timesteps

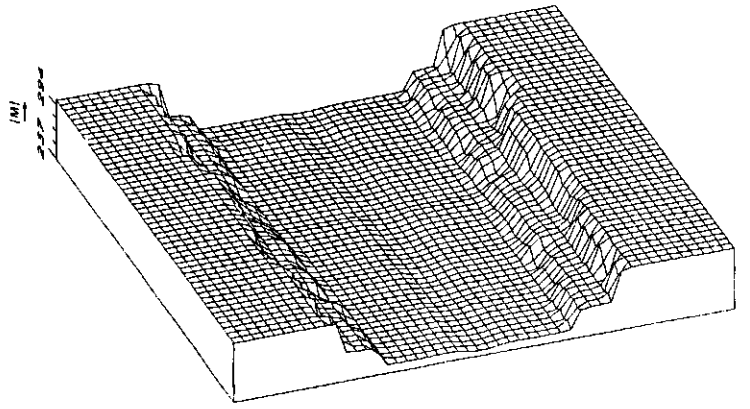

relief version D2 after 300 timesteps

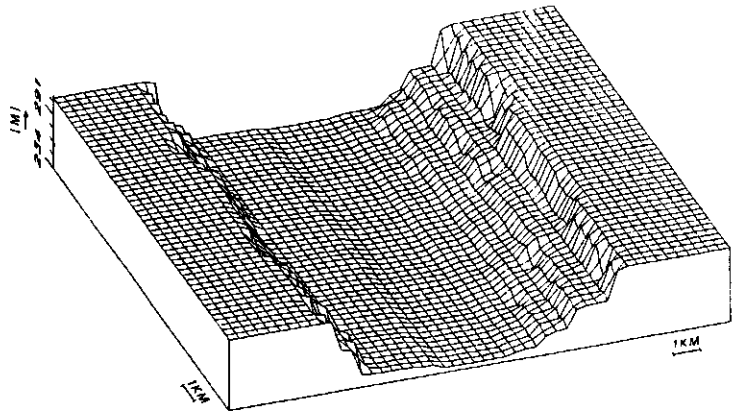

relief version D2 after 400 timesteps

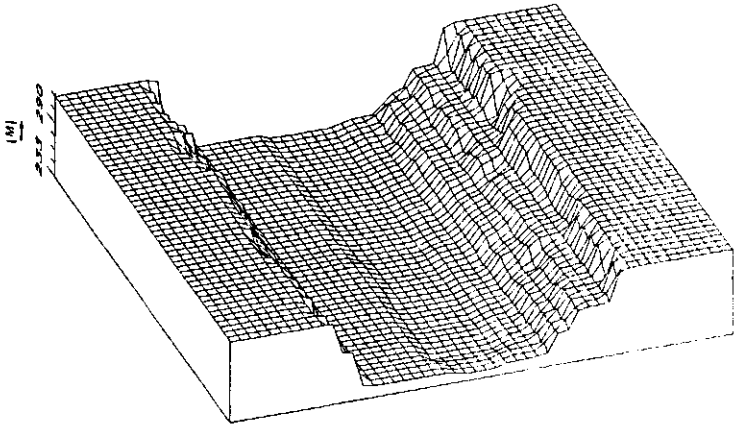

Relief version D2 after 500 timesteps

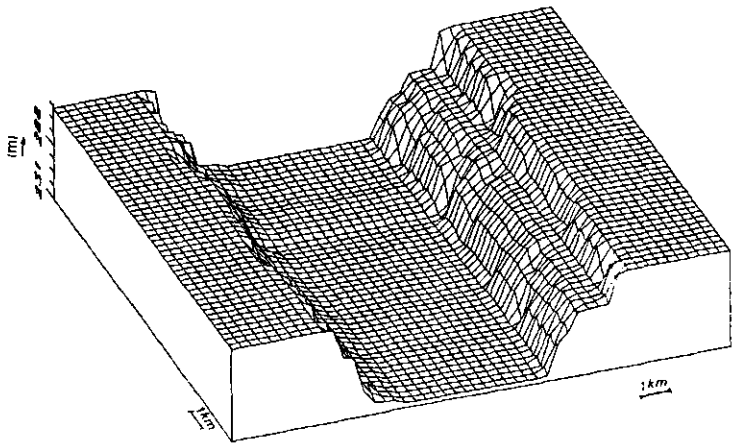

relief version D2 after 600 timesteps

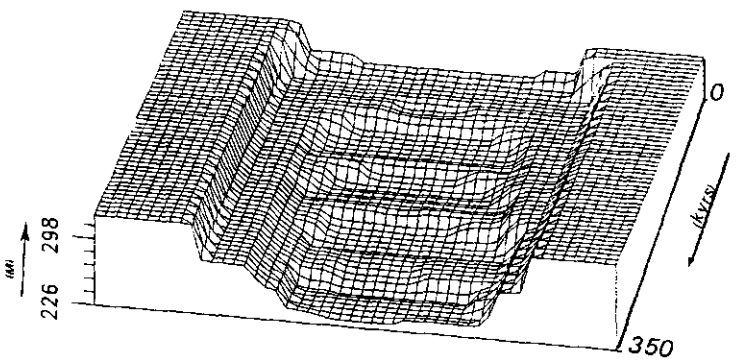

cross section in time version d2

Figure 4.2.4 **3-D graph of the development of one cross section in time. An asymmetrical terrace sequence develops as a result of distorted downgrading of the Allier system.**

Valley morphology

Simulations without tectonic uplift result in temporary terraces only, while large constant uplift rates (>0.3 m/ky) cause steep canyons without terraces, while uplift rates around 0.1 m/ky display many terraces. Simulations with gradual uplift of the LANDSCAPE as a whole result in paired terraces only. When a difference in uplift rate for both halves of the LANDSCAPE is introduced (QUPLIFT_UNEQUAL > 0), asymmetrical terrace sequences develop with both paired and unpaired terraces. Most terraces remain on the valley side with the highest uplift rate. Simulations with both general and unequal uplift components result in landscapes with comparable characteristics as the present Randan terrace sequence. To illustrate the incision and sedimentation dynamics in more detail a cross-section sequence in time is drawn in Fig. 4.2.4, showing relief changes during the first 350 ky of the simulation. Both figures clearly show the alternating incision and sedimentation of the Allier in time causing several different terrace levels. The effects of unequal uplift also become prominent during the simulation. An asymmetrical terrace sequence develops as a result of distorted downgrading of the Allier system.

During the simulations unpaired terraces develop only due to changes in unequal uplift. This result contrasts with the traditional view that unpaired terraces are generated by changes in internal factors such as a widely swinging meander belt which produces unpaired terraces during the slow lowering of a broad floodplain.

Terrace stratigraphy

Terrace stratigraphy displays the total effect of both sedimentation and erosion processes related to the sediment fluxes dynamics during simulation. Simulations without major changes in sediment flux due to climatic change resulted in thin sediment layers with a very simple stratigraphy. When the sediment composition and flux magnitude are related to climatic environment a very complex terrace stratigraphy develops.

Figure 4.2.5 A cross-section and terrace stratigraphy development during the last 100 ky of the simulation shown each 20 ky.

It is not surprising that the largest sediment fluxes (Class 3), i.e. those related to glacier melting, are relatively well preserved in the terrace stratigraphy. During these large fluvioglacial sediment fluxes the floodplain and the lowest terraces are buried by these sediments. This burial causes the formation of the 'standard' Allier terrace stratigraphy with relatively volcanic poor sandy units buried by volcanic rich gravelly units. This development can be seen in the cross-sections in Fig. 4.2.5., displaying the changes in both relief and stratigraphy (sediment age and composition). Six cross-sections illustrate the fluvial system dynamics during the last simulated 100 ky. The last cross-section shows the LANDSCAPE during an interglacial period like the present Allier and can directly be compared with the actual Randan cross-section.

Although the river has exhibited a meandering state many times, it is surprising that the typical interglacial sediments (Class 1) are rarely found in the stratigraphical record. This limited occurrence of meandering sediments is true for both the described simulation and the actual Randan terrace sequence. During LIMTER simulations interglacial sediments are deposited during each interglacial but they are almost always eroded during the same interglacial or the subsequent glacial. The limited occurrence of interglacial sediments in the sedimentary records seems to be due to the mainly eroding characteristics of a meandering Allier, the most common interglacial Allier state.

4.2.6. Evaluation of the simulated Randan terrace sequence

In Fig. 4.2.6. the cross-section after 520 timesteps (ky) is plotted together with the cross-section near Randan, allowing comparison of the LIMTER simulation results with the actual Allier system at Randan. It has to be realized that the Randan cross section in Fig. 4.2.6. is only a strong schematization of reality. The effects of mass movements on slopes and the dissection of terraces by minor tributaries are not included in the schematic cross-section. Because LIMTER has only conceptual value the correspondence between the model and the Randan

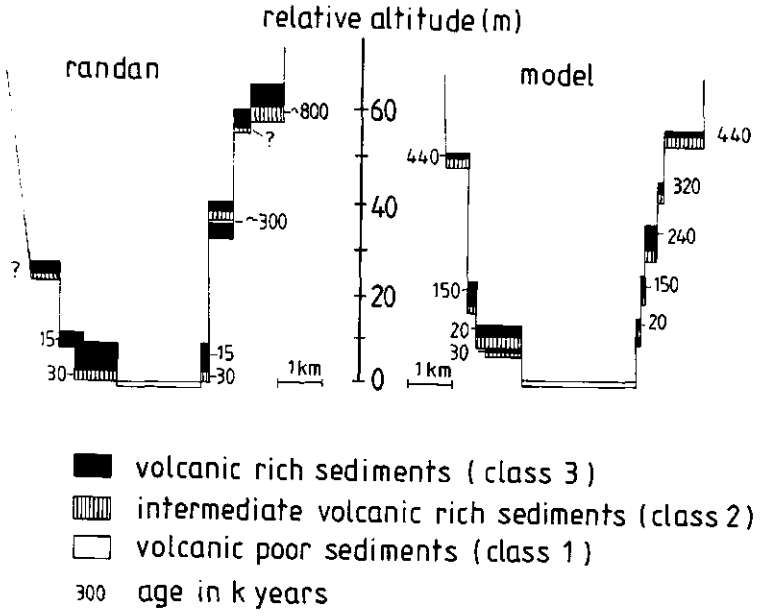

Figure 4.2.6 **Comparison of the Randan terrace sequence and the model output. Note the good correspondence between the younger terraces for model and reality.**

sequence should be reviewed qualitatively only. This implies that the rates for discharge, sediment load and uplift, have no validity outside the model, but they might give some indication of the order of magnitude these variables might have had in the Allier system.

The major points of correspondence between LIMTER output and the Randan sequence are the number of terraces, the general terrace stratigraphy, and the relative altitudes and distribution of the terraces on the valley slopes. Also clear differences exist between the model and reality. In LIMTER a relative age of 420 ky is found for the 65 m terrace (Va) while in reality this terrace level is thought to have an age of approximately 800 ky. This large age difference suggests that the incision rate in LIMTER was probably too fast compared with what actually took place in the Allier system. When the LIMTER is run for 800 ky a much deeper and steeper valley exists as the actual Randan sequence. On the other hand, the age difference between the younger terraces in the model and in the Allier is much smaller, suggesting a much better simulation of the Allier system during

the last few hundred thousands of years. This change in age correspondence between simulation results and reality suggests that the uplift rates near Randan changed during the Quaternary. Probably an almost stand still in uplift took place between 800 and 400 kyears BP. This interpretation implies that the model assumption of constant uplift rates is incorrect for the Randan terrace sequence. A change in tectonic activity is supported by some distorted longitudinal terrace profiles indicating regional tectonic activity between the formation of the V and W terrace levels (Larue, 1979; Giot et al., 1978).

Another striking difference between simulation results and reality is the complete lack of terrace remnants of the Va and Vb terraces on the eastern valley side in the Randan sequence. This discrepancy is difficult to interpret but it might also be related to the same tectonic events which caused the differences in terrace sediment age.

In general it is striking that relative simple model inputs can accomplish a complicated terrace sequence, including unpaired terrace levels and a relative complicated terrace stratigraphy. Despite the differences between LIMTER output and the Allier terrace sequence the simulation is thought to display a possible general scenario for the development of the actual Randan terrace sequence.

General applications of LIMTER

LIMTER has of course no validity outside the Allier basin because it was adapted to this unique system only. The impact of climate was simulated relatively straight forward by changes in the 1000 years sediment and discharge because the Allier system is strongly controlled by fluvio-glacial fluxes from glaciers in its headwaters (Veldkamp, 1991). It remains therefore to be seen whether this input assumption has any validity in a system without such a fluvio-glacial control during the Quaternary.

The hydraulically-based clastic sedimentation model of Tetzlaff and Harbaugh (1989) seems to allow a more straight forward interpretation of simulation results than LIMTER. LIMTER

calculates only an average impact each time step (1000 years) while they coped with longer timespans by the 'compute-and-drift' and the 'compute-and-stop' strategies. Although Tetzlaff & Harbaugh's basic assumptions seem realistic their complete numerical model has so many calculation operations that no reliable results can be expected. During each operation the calculation errors increase resulting in unreliable outputs. LIMTER has less realistic basic assumptions but has much less calculation operations reducing the calculation errors and limiting the computing power demands. It is obvious that both approaches have different advantages and disadvantages and are more or less complementary.

It is beyond any doubt that an elaborated model with a solid hydraulically-based foundation such as constructed by Tetzlaff & Harbaugh (1989), suggests a more general validity. But their numeric model is mainly focussed on quantified transport and deposition processes neglecting other complex dynamics in the fluvial system. The remaining problem is that such a model should be tuned to both sedimentary sequences as valley morphology (river terraces). The latter is the main goal of LIMTER while long term hydraulogically based models can only be tuned to sedimentary sequences. Another problem is to obtain a reliable long term input for such a hydraulogical model, because our oversimplified input assumption is unsuitable for such a model.

4.2.7. Conclusions

The long term simulations of an Allier like system with LIMTER suggest that the Allier terraces at Randan are mainly the result of the internal dynamics responding to both climatic and tectonic factors. The conceptual model (LIMTER) illustrates that in the Allier system tectonism may have played a dominant role in determining the terrace formation and preservation, while climatic dynamics seem to have strongly determined terrace stratigraphy by causing changes in composition and magnitude of sediment fluxes.

The simulated valley morphology is the result of the interaction of tectonic movements and fluvial dynamics. Unequal

uplift results in unpaired terraces and asymmetrical downgrading of the simulated river.

Chapter 5 **SYNTHESIS**

The main aim of this research was to establish a quantitative large scale reconstruction of the longterm Allier dynamics as a result of global environmental changes. Therefore a model was made simulating these long term dynamics. Model dynamics were based on the most commonly applied concept in fluvial palaeohydrology, the concept of dynamic equilibrium as postulated by Schumm (1977). Within a complex natural system such as a fluvial system a single event is thought to be able to trigger a complex morphological and/or sedimentological response as the various components of the system react to the change. Within a fluvial system in dynamic equilibrium, terrace formation may be concentrated into relatively short time periods of dynamic equilibrium associated with interglacial, interstadial or glacial conditions (Green & McGregor, 1987).

A key problem which has to be solved is to determine under which conditions thresholds are reached in a fluvial system. In the Allier system we found a rather straight foreward relationship whereby the Allier can be envisaged as oscillating between a cold-climate braided, terrace building condition during and at the end of a glacial and a more meandering, incision condition during the interglacials. The Allier threshold between deposition and incision is found at the transition from glacial to interglacial.

For NW Europe most investigators agree on a general cold deposition of most terrace sediments but their interpretation of the exact system dynamics involved in creating such deposits differ strongly (Starkel, 1983; Gibbard, 1988). Part of the Meuse (M.W. van den Berg, pers. comm.) and Thames basins (Dawson and Gardiner, 1987) are thought to have similar dynamics as found for the Allier. Starkel (1983) reports that the main phases of erosion in the Vistula and other European rivers were in late glacial and early interglacial times in as well meandering as braided systems. This insight is not shared by Gibbard (1988) who states that incision occurs when river run off is highly seasonal but when limited supplies of detritus are available, i.e.,

predominantly under cold climates.

A very plausible general statement, which we support, is made by Green and McGregor (1987) who state that different river systems react differently to similar environmental changes. They give two main reasons for such differences: the size of the river and the position of its basin in relation to the geographical pattern of the environmental variables that govern the behaviour of fluvial processes. According to them the differences between basins of similar order are caused by the fact that the amount of environmental change needed to bring a fluvial system to and across a critical geomorphological threshold for terrace formation is not the same in all environments.

By applying the concept of dynamic equilibrium a large scale model LIMTER was made simulating Quaternary Allier dynamics. Starkel (1983), Green & McGregor (1987) and Bull (1990) envisage at each phase a leading factor which pushes the whole system towards down cutting or aggradation leading to a new equilibrium between mean discharge and mean sediment load. A similar behaviour is found for LIMTER. A change in 1000 years discharge, 1000 years sediment load or uplift rate will usually trigger a system response of erosion or deposition.

LIMTER simulations show that terrace formation takes place in a model in dynamic equilibrium thus confirming the general validity of the Schumm's concept of dynamic equilibrium. LIMTER also demonstrates that both climate and tectonism play a significant role in terrace formation. But the main conclusion is that it is well possible to model such a complex and large scale system.

Methodology

The following methodologies were applied in this thesis: 1) bulk geochemical characterization of terrace sediments, 2) sediment flux reconstruction, and 3) finite state modelling. Although none of these tools is essentially new, the novelty is the way they were applied and combined in this research.

1 Bulk sand geochemistry

This research tool facilitates the discrimination and quantification of the impact of different factors and processes on terrace sand composition. The effects of provenance, weathering, grain size and fluvial transport could be satisfactory discerned and statistically modelled. Within the Allier and Dore sands, the role of grain size distribution was very limited due to the large amounts of rock-fragments in both sediment types. In sands with mainly mineral grains like in The Netherlands (Moura & Kroonenberg, 1990), grain size distribution plays a more important role in bulk geochemical variability. The effects of weathering are very dominant in the Allier terrace sands. It turned out that most of the original sand composition of terraces older than Weichselian was altered by weathering processes. Although it is possible to simulate this parent material controlled weathering, it remains impossible to reconstruct their original sediment composition a characteristic necessary for a paleoenvironmental reconstruction.

2 Sediment flux reconstruction

By extensively measuring the changes in sand bulk geochemistry at a major confluence, past sediment mixing can be characterized and quantified. This quantification can be used to reconstruct the past relative sediment fluxes within the studied system. To permit a reliable reconstruction of the past sediment mixing, spatial variability within the terrace sands was studied first. The sediment flux reconstruction could only be done with Weichselian and younger sediments because the effects of weathering processes are limited in these sediments. The good match of the reconstructed fluxes and the known past environment indicates that this methodology is a promising new tool in Quaternary research.

3 Finite state modelling

Although bulk geochemical studies of the Allier terrace sands yielded much new information of the large scale and long term Allier dynamics there still remains a considerable shortage in

large scale quantitative data. In order to bridge the gap between the limited quantitative and abundant descriptive knowledge on Quaternary terrace formation, finite state modelling was applied to construct a 3-D model simulating river terrace formation. The developed model (LIMTER) has therefore only conceptual validity because many used model relationships and functions are derived generalities from theoretical concepts and empirical measurements. The aim to establish a quantitative large scale model was therefore not completely met.

A main disadvantage of the used modelling methodology is that the model can never be validated because it is impossible to measure the long term dynamics of such a large scale system.

We saw that there exists a general agreement on the concept of dynamic equilibrium (Schumm, 1977). This concept is typical for Quaternary geology and geomorphology because it is dynamic and applicable on a long time span. Within such a concept the qualitative aspects of changes dominate. A fluvial system is described in terms of braided versus meandering and aggradation versus incision divided by thresholds, while the real fluvial system has both meandering and braided characteristics, and while deposition and incision usually take contemporaneously place.

Stratigraphic models (Bridge & Leeder, 1979; Tetzlaff & Harbaugh, 1989) simulating fluvial sedimentation originate from the field of sedimentology. These models are more focussed on the variability within sedimentary bodies and their hydraulic parameters. There are a few essential differences between the geomorphological and the sedimentological approach. The geomorphologist is mainly interested in where, when, how and under which conditions, sedimentation and erosion take place. The sedimentologist however, is mainly interested in the deposition process itself and less in when and where. That is why the models of Bridge & Leeder (1979) and Tetzlaff & Harbaugh (1989) have only limited tectonic or climate related inputs or processes. Their model relations are focussed on (sub)processes which have a direct effect on the sediment characteristics like discharge determining grain size distribution. But the more general aspects

of climatic and tectonic settings are often neglected in such models. These limitations find their origin in the scale difference between stratigraphic models and geomorphological models. The existing fluvial deposition models result in detailed stratigraphical output causing an overestimation of general model reliability. The geomorphological models like LIMTER result in more general and global outputs giving a better visualisation of the complex real world system. It are the geomorphological models with their more holistic approach which can give a better representation of the complex overall processes involved in shaping fluvial deposits. Although there is limited overlap in the interests of geomorphologists and sedimentologist it would enrich both disciplines when their modelling attempts would be more related.

Regional conclusions

The application of new combinations of research methodologies in the Allier basin resulted in some new regional insights. Because the Allier sediments now have been radiometrically dated with ^{14}C and Th/U methods a considerable revision of the existing Allier terrace chronology (Fig. 5.1) is necessary. This new chronology has some resemblance with Larue's (1979) chronology, who studied a much larger area. Pastre's (1987) chronology gives systematically much older ages for the terrace sediments, indicating that his methodology of linking the mineralogy of dated volcanics with sand mineralogy is not as accurate as he assumes.

The new chronology shows a large time gap between the deposition of the V and W terrace sediments. The LIMTER simulations clearly indicate that this must have a tectonic origin. It seems that the uplift of the Randan area and probably the Limagne graben as a whole, came to an almost standstill for a few hundred thousands of years during the Middle Pleistocene. LIMTER simulations also suggest differences in uplift rates of both sides of the Allier valley.

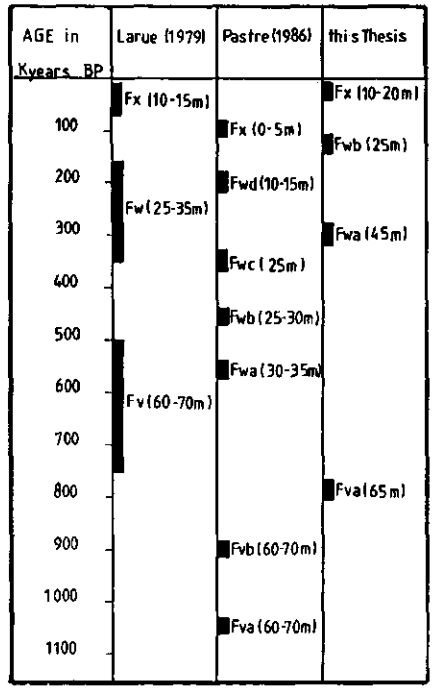

Figure 5.1 **The reconstructed terrace chronology**

Our paleo-environmental reconstruction shows that sediment flux dynamics in the Allier basin during the Late Quaternary and most probably the whole Pleistocene is strongly related to glacier dynamics on the Cantal and Mont Dore, and thus climate controlled. An indirect result of the strong climatical relationship of the past Allier dynamics is the development of Holocene lake basins (Marais) in Grande Limagne. These lakes are the result of a strong rise of the Allier riverbed level caused by enormous sediment supply due to glacier melting.

Further Research

Simulations of future scenarios with LIMTER suggest more incision and erosion of the current Y and X terraces during the next few thousands years. It is important to keep in mind that such simulations give only very general predictions in time steps of 1000 years. Because the future climate scenarios are still

under discussion and since LIMTER is strongly climate controlled and does not include human factors, it is not realistic to use LIMTER to simulate future scenarios. Only a more refined and improved version will be suitable for such predictive simulations.

The bulk geochemical methodology should be more often used as a quantitative large scale tool to gain insights in long term fluvial system dynamics. The technique of reconstructing sediment fluxes within a fluvial system can be more refined when it is applied on other fluvial systems. A way to make a more reliable past sediment flux reconstruction is to apply the same technique on several confluences within the same basin. In case of the Allier a study at the Sioule/Allier and Loire/Allier confluences combined with the Dore/Allier study would certainly result in a more accurate basin reconstruction.

It is possible to combine such confluence studies with a sediment budget study in the delta. The reconstructed relative sediment fluxes would allow a more quantitative reconstruction of the sediment source areas.

More research is needed to see whether finite state modelling can indeed contribute to better longterm modelling in geomorphology. It is therefore proposed to apply this technique to other macro-scale objects in geomorphology. Another rather successful attempt is already made by modelling coastal terraces as function of changing sea level and uplift (Veldkamp, in prep). The 3-D terrace model may gain more value by adapting it to different fluvial systems. This has been done for the Meuse system, a fluvial system in which the impact of glaciers is very limited compared with the Allier system (Veldkamp & van den Berg, subm).

Another way to improve LIMTER is to combine finite state modelling with the methodology of "fuzzy knowledge". The result would be a model with less firm decision rules allowing more realistic system states.

Although it is generally known that the current state of knowledge in geomorphology obstructs pure numerical modelling,

this should not hold up the efforts of trying it. Of course new methodologies have to be developed to measure large scale processes on the appropriate scale. Such efforts will hopefully reveal knowledge gaps, indicating where additional theorizing is necessary. Finite state modelling will allow to test/simulate newly developed concepts and theories.

It is a pity that as a result of increasing modelling activities the attention of geomorphologists shifted more to the short term processes. The fact that many global theories have their roots in the 19^{th} century indicates that theorizing on large scales in geomorphology has come to an almost stand still. Better balanced research activities will contribute more to the field as a whole, and will sooner lead to workable solutions of scale problems in geomorphology.

REFERENCES

Abbey, S., 1980, Studies in 'Standard samples' for use in the general analysis of silicate rocks and minerals. Part 6: 1979 edition of 'usable' values, Geol. Surv. Canada Pap 80-14:30 pp

Anderson, M.G., 1988, Modelling geomorphological systems. John Wiley & Sons Ltd, London.

Anderson, M.G. & Sambles, K.M., 1988, A review of the bases of geomorphological modelling. In: Anderson, M.G., (Ed), Modelling geomorphological systems. John Wiey & Sons Ltd, London.

Andres, W., 1989, The Central German upland, Catena supplement 15, p. 25-44.

Autran, A. & Peterlongo, J.M., 1980, Le Massif Central In: Géologie des Pays Européens, France, Belgique, Luxembourg. Dunod (Paris): 3-133.

Basu, A., 1976, Petrology of Holocene fluvial sands derived from plutonic source rocks: implications to paleoclimatic interpretation. Jour. Sed. Petr. vol 46, no.3 p. 694-709.

Bathurst, J.C., 1988, Flow processes and data provision for channel flow models, in: Anderson M.C. (Ed) Modelling geomorphological systems. John Wiley & Sons Ltd.

Bear, F.E., (Ed), 1964, Chemistry of the soil, 2 nd ed., Reinhold publishing corporation, New York

Begin, Z.B. & Schumm S.A., 1984, Gradational thresholds and landform singularity: significance for Quaternary studies. Quaternary research 21, 267-274.

Berger, A.L., 1978, Long-term variations of caloric insolation resulting from the Earth's Orbital elements. Quaternary Research 9, 139-167.

Besson J.C. & Ly, M.H., Cantagrel, J.M., De Goër De Herve A., et Vincent P.M., 1977, Une coulée de ponces post-Villafranchienne sur le versant oriental du Mont-Dore. C.R. Acad. Sc. Paris 284 Sér. D.P. 1875.

Best, J.L., 1986, The morphology of river channel confluences. Progress Phys. Geogr., 10(2), 157-174.

Best, J.L., 1988, Sediment transport and bed morphology at river channel confluences. Sedimentology, 35, p 481-498.

Bloom, A.L., 1978, Geomorphology, a systematic analysis of Late Cenozoic landforms, Prentice-Hall, Inc New York.

Boll, J., Thewissen, T.J.W., Meijer, E.L., and Kroonenberg, S.B., 1988, A simulation of the development of river terraces, Zeitschrift für Geomorphologie, 32, 31-45

Bout, P., 1963, Observations sur la basse-terrasse de l'Allier a Pont du Château. Actes du quatre-vingt-huitième congrès national des sociétés savantes. Clermont Ferrand.

Bradley, R.S., 1985, Quaternary paleoclimatology, methods of paleoclimatic reconstruction. Allen & Unwin, Boston.

Bridge, J.S. & Leeder, M.R., 1979, A simulation model of alluvial stratigraphy. Sedimentology, 26: 617-644.

Brunnacker, K. & Boenigk, W., 1983, The Rhine valley between the Neuwied basin and the Lower Rhenish Embayment. In: K. Fuchs et al., (Eds). Plateau Uplift, Springer Verlag, Berlin: 62-72.

Buch M.W., 1987, Spätpleistozäne und holozäne fluviale Geomorphodynamik im Donautal östlich von Regenburg - ein Sonderfall unter den mitteleuropäischen Flusssystemen?, Z. Geomorphologie N.F. Suppl.-bd 66, pp.95-111, Berlin.

Bull, W.B., 1990, Stream-terrace genesis: implications for soil development. Geomorphology, 3, p.351-367.

Bullock, P., Fedoroff, N., Jongerius, A., Stoops, G., and Tursina, T., 1985, Handbook for soil thin section description. Waine research publications, England, 150 pp.

Burgess, T.M., Webster, R., & McBratney, A.B., 1981, Optimal interpolation and isarithmic mapping of soil properties. IV sampling strategy. Journal of Soil Science, 32, 643-659.

Cameron, K.L. & Blatt H., 1971, Durabilities of sand size schist and "volcanic" rock fragments during fluvial transport, Elk Creek, Black hills, South Dakota, Jour. of Sed. Petr. Vol. 41, no. 2, p. 565-576.

Camus, G., De Goer, A., Kieffer, G., Mergoil, J., Vincent P.-M., 1983, Parc naturel regional des volcans d'Auvergne, Volcanologie de la Chaîne des Puys, A.R.P.E.G.E. imprimerie Moderne 15000 Aurillac.

Chambaudet, A., & Couthures, J., 1981, Datations pas traces de fission de gisements Plio-Pléistocène de la périphérie des Monts-Dore (Massif Central, France), C.R. Acad. Sc. Paris, t 293, sér II, pp67-71.

Chaput, E., 1917, Recherches sur les terrasses alluviales de la Loire et de ses principaux affluents. Thèse Annales de l'Université de Lyon nouv. série I, Façc 41. (from J.F. Pastre, 1987)

Church, M. & Kellerhals, R., 1978, On the Statistics of grain size variation along a gravel river. Can. J. Earth Sci., 15, p. 1151-1160.

Chorley, R.J., Schumm, S.A., and Sugden, D.F., 1984, Geomorphology, Methuen and Co Ltd New York.

Clozier, L., Fleury, R., Giot D., 1980, in: BRGM, Carte géologique de la France a 1/50 000, Maringues XXVI-30 Note explicative, Orléans, France

Colman, S.M. & Dethier, D.P., 1986, Rates of chemical weathering of rocks and minerals. Academic Press Inc.

Daugas, J.-P. & Tixier, L., 1978, Stratigraphie du Quaternaire récent et niveau archéologique protohistorique a Coudes (Puy-de-Dôme). L'Antropologie, T. 82 no. 3 pp.439-450.

Davies, D.K., Vessell, R.K., Miles, R.C., Foley M.G., Bonis S.B., 1978, Fluvial transport and downstream sediment modifications in an active volcanic region. In: Miall A.D., (Ed) Fluvial Sedimentology: Canadian Soc. of Petroleum petrologists, memoire 5, p.61-83.

Dawson, M.R. & Gardiner, V., 1987, River terraces, the general model and palaeohydrological and sedimentological interpretation of the terraces of the Lower Severn. in: Gregory, K.J., Lewin, J. & Thornes, J.B. (Eds), Palaeohydrology in practise, John Wiley & Sons Ltd, London.

Debard, E. & Pastre, J.-F., 1988, Un marqueur chronostratigraphique du Pléistocène moyen à la périphérie du Massif Central: la retombée à clinopyroxène vert du Sancy dans le site acheuléen d'Orgnac III (Bas-Vivarais, SE France), C.R. Acad. Sci. Paris, T.306, Série II, p.1515-1520.

De Beaulieu, J.-L. & Reille, M., 1984, A long Upper Pleistocene pollen record from Les Echets, near Lyon, France. Boreas, Vol. 13, pp. 111-132.

De Beaulieu, J.-L., Pons, A., et Reille, M., 1982, Recherches pollenanalytiques sur l'histoire de la végétation de la bordure nord du Massif du Cantal (Massif Central, France), Pollen et Spores, vol XXIV, no 2 p 252-300.

Dillon, W.R. & Goldstein, M., 1984, Multivariate Analysis, methods and applications. John Wiley & Sons, New York.

Drees, L.R. & Wilding, L.P., 1978, Elemental distribution in the light mineral isolate of soil separates. Soil. Sci. Am. J., vol. 42.

Dury, G.H., 1970, Rivers and river terraces, Macmillan, London.

Elzas, M.S., 1978, Systemen en modellen, Landbouwkundig tijdschrift 90-8a (in Dutch).

Etlicher, B., Janssen, C.R., Juvigné, E., Leeuwen, J.F.N., 1987, Le haut Forez (Massif Central, France) après le pleniglaciaire Würmien: environnement et tephra du volcan de la Nugère. Bulletin de l'association française pour l'étude de Quaternaire, 1987-4 229-239.

Fairbridge, R.W., 1968, Terraces, fluvial-environment controls, in: Fairbridge, R.W., (Ed), Encyclopedia of geomorphology: Reinhold Book Corp. New York, p 1124-1138.

F.A.O., 1974 Soil map of the world, 1:5000,000, Vol I Legend FAO UNESCO Paris, 59 pp.

Feijtel, T.C., Jongmans, A.G., Miedema, R., Van Breemen, N., 1988, Genesis of two planosols in the Massif Central France. Geoderma, 43: 249-269.

Feijtel, T.C., Jongmans, A.G., Van Doesburg, J., 1989, Identification of clay coatings in an older Quaternary terrace of the Allier, Limagne, France. Soil Sci. Soc. Am. J. 53: 876-882.

Feijtel, T.C. & Meijer, E.L., 1990, Simulation of soil forming processes. Syllabus of course with spreadsheets and exercises. Internal report Department of Soil Science and Geology, Agricultural University Wageningen, The Netherlands.

Findlay, W. & Watt, D.A., 1981, PASCAL, an introduction to methodical programming. Pitman publishing limited, London, second edition.

Franzinelli, E., & Potter, P.E., 1982, Petrology, chemistry, and texture of modern river sands, Amazon river system, Journal of Geology, vol.91, p.23-39.

Gibbard, P.L., 1988, The history of the great northwest European rivers during the past three million years. Phil. Trans. R. Soc. Lond. B318, 559-602.

Giot, D., Clozier, L., Fleury, R., 1978, Manifestions tectoniques quaternaires en Limagne d'Allier. Bull. du BRGM, section I, no 2, p. 150-155.

Goldich, S.S., 1938, A study in rock-weathering, Jour. of Geology, 46 .17-58.

Green, C.P. & McGregor, D.F.M., 1986, The utility of intercomponent ratios in the interpretation of stone count data, In: Bridgeland, D.R., (Ed), Clast lithological analysis, Quaternary Research Association, Technical guide no. 3, p. 83-93.

Green, C.P. & McGregor, D.F.M., 1987, River terraces: a stratigraphic record of environmental change. In: Gardiner, V., (Ed), 1986, International geomorphology 1986 Part I. John Wiley & Sons Ltd.

Gregory K.J., (Ed) 1983, Background to palaeohydrology. John Wiley & Sons Ltd, London.

Gregory, K.J., Lewin, J. & Thornes, J.B. (Eds), 1987, Palaeohydrology in practise, John Wiley & Sons Ltd, London.

Hay, R.L., 1960, Rate of clay formation and mineral alteration in a 4000 year-old volcanic ash soil on St Vincent, B.W.I., Am. Jour. of Science, vol. 258, p.354-368.

Hays, J.D., Imbrie, J., Shackleton, N.J., 1976, Variations in the earth's orbit, pacemaker of the iceages. Science 194, p 1121-1132

Heller, F. & Wang, J., 1991, Magnetism of Quaternary sediments: Löss in China. Special Proceedings, Review reports, for symposia of the XIII International congress INQUA Beijing, 1991, p 88-98

Howes, S. & Anderson, M.G., 1988, Computer simulation in geomorphology. In: Anderson, M.G., (Ed), Modelling geomorphological systems. John Wiley & Sons Ltd, London.

Hugget, R.J., 1985, Earth Surface systems, Springer-Verlag, Berlin, Heidelberg. 262 p.

Huntington, E., 1907, Some characteristics of the glacial period in nonglaciated regions. Geol. Soc. Amer. Bull. Vol 18, pp 351-388.

Ichim, I., & Radoane M., 1990, Channel sediment variability along a river: a case study of the Siret River (Romania). Earth Surface Processes and Landforms, vol. 15, 211-225.

Imbrie, J. & Palmer-Imbrie, K., 1979, Ice ages, solving the mystery. Enslow Publishers Hill Side, New Jersey.

Jeambrun, M., Dadet, P., Clozier., L., Fleury, R., et al., 1980, Carte Géologique de la France a 1:50.000 Maringues XXVI-30, Note explicative BRGM, Orléans 54p.

Jongmans, A.G., Van Doesburg, J., and Van Breemen, N., 1990, Micromorphology and mineralogy of weathering and neoformation phenomena in a Quaternary terrace sequence of the Allier, Limagne, France. Chemical Geology vol 84, no 1/4 p. 83-85.

Jongmans, A.G., Feijtel, T.C., Miedema, R., Van Breemen, N.. Veldkamp, A., 1991. Soil formation in a Quaternary terrace sequence of the Allier, Limagne, France. Macro and Micro morphology, particle size distribution, chemistry. Geoderma 49. p.215-239.

Journel, A.G. & Huijbregts, Chr. J., 1978, Mining Geostatistics. Academic press, New York, N.Y.

Jung J., Symposium 1971, Géologie, géomorphologie et structure profonde du Massif Central français; Plein Air Service éd., Clermont-Ferrand, 1 vol., 610 p., 154 fig.

Juvigné, E. & Gewelt, M. 1987, La narse d'ampoix comme téphrostratotype dans la Chaîne des Puys Méridionale (France). Bulletin de l'Association française pour l'étude de Quaternaire, 1987-1, p.37-49.

Juvigné, E., Milcamps, V., Delibrias, G. & Evin, J., 1988, Ages de traits polliniques et chronozonation du Tardiglaciare final et de l'Holocène dans le Massif Central (France), Mededelingen rijks geologische dienst vol. 42 p. 33-50.

Kieffer, G., 1971, Aperçu, sur la morphologie des regions volcaniques du massif central. Symposium J. Jung 1971 Clermont-Ferrand, p479-510.

Knighton, A.D., 1982, Longitudinal changes in the size and shape of streambed material: evidence of variable transport conditions. Catena vol. 9, 25-34.

Kominz, M.A.,Heath, G.R., Ku, T.L., Pisias, N.G., 1979, Brunhes time scales and the interpretation of climatic change. Earth Planet Sci. Lett. 45, p 394.

Komura, S., 1973, River-bed variations at confluences. Proceedings International symposium on river mechanics. International Association for hydraulic research.

Kroonenberg, S.B., van den Berg van Saparoea, R.M., Jonker A.T.J., 1987, Late glacial and Holocene development of semi-closed basins (Thaw lakes?) in the Limagne Rift Valley, French Central Massif, Geol. Mijnbouw 66:297-311.

Kroonenberg, S.B., Moura, M.L., Jonker, A.T.J., 1988, Geochemistry of the sands of the Allier river terraces, France. Geologie en Mijnbouw 67: 75-89.

Kroonenberg, S.B., van der Plicht, J., Vlaanderen, B. & Wassink, W., 1989, Th-U disequillibrium dating of travertine-impregnated Pleistocene Alluvial terraces in the Limagne Rift Valley, France. Busche, D., (Ed), Abstracts of paper and poster of second international conference on geomorphology., Geoöko plus 1, p. 162.

Kroonenberg, S.B., 1990, Geochemistry of Quaternary fluvial sands from different tectonic regimes. Volume 84, no 1/4 p 88-91.

Kroonenberg, S.B., Hoorn, M.C., Moura. M.L., & Veldkamp, A., 1990, Variability in bulk geochemistry of fluvial terrace sands, consequences for the study of weathering chronosequences. Pedologie XL-1 p 19-31.

Lambert. J., C. Orcel., J., Daugas & J. P. Raynal, 1980, Premiers resultats dendrochronologiques pour le Massif Central francais obtenus sur un bois fossilé de la basse terrasse de l'Allier a Joze (Puy-de-Dôme). C. R. Acad. Sc. Paris, t.290 série D p263-266.

Larue, J.P. 1977, étude du matériel différentes nappes alluviales de l'Allier., Extrait de la revue d'Auvergne tome 91-numero 3, Institut de Géographie LIV, Clermont-Reproduction, Aubiere.

Larue J.P., 1979, Les nappes alluviales de la Loire et de ses affluents dans le Massif Central et dans le Sud de bassin Parisien: étude géomorphologique. Thèse géographie, Clermont II, multigraphée 543 p., plus annezes: 30 cartes, 126 planches.

Léger, M., 1983, Signification dynamique et climatique des formations et terrasses fluviatiles quaternaires, Colloque de l'Associations française pour l'étude de Quaternaire. Paris, Deuxième sèrie 21 année no 17-18-19 /1 /2 /3.

Lenselink G., Kroonenberg, S.B. & Loison, G. 1990, Periglacial to Holocene paleo-environments in the Artière basin in the Western Limagne rift valley, Massif Central, France. Quaternaire 2, p.131-148.

Leopold, L.B., Wolman, M.G. & Miller, J.P., 1964, Fluvial processes in geomorphology. W.H. Freeman & Company, San Francisco.

Levine, E.R. & Ciolkosz, J., 1986, A computer simulation model for soil genesis applications. Soil Sci. Soc. Am. J. 50:661-667.

Lowe, D.J., 1986, Controls on the rates of weathering and clay mineral genesis in airfall tephras: a review and New Zealand case study. In: Colman S.M., Dethier, D.P., (Eds), Rates of chemical weathering of rocks and mineral, Academic Press, Inc New York.P.265-330.

Lowe, J.J. & Walker, M.J.C., 1984, Reconstructing Quaternary environments. Longman Group, New York.

Ly, M. H., 1982, Le plateau de Perrier et la Limagne du Sud: Etudes volcanologiques et chronologiques des produits Montdoriens (Massif Central français). Thèse III^{ème} cycle, Clermont Fd.

Maizels, J.K., 1986, Modelling of palaeohydrologic change during deglaciation, géographie et physique Quaternaire, vol XL no3, p.263-277.

McGregor, D.F. & Green, C.P., 1978, Gravels of the River Thames as a guide to Pleistocene catchment changes. Boreas, Vol 7., pp 197-203.

Mitchell, D.J., & Gerrard, A.J. 1987, Morphological responses and sediment patterns. in: Gregory, K.J., Lewin, J., and Thornes, J.B., Palaeohydrology in Practice. John Wiley & Sons Ltd, London.

Mosley, M. P. 1976, An experimental study of channel confluences, Journal of Geology vol 84, p.535-562.

Moura, M.L. & Kroonenberg, S.B. 1990, Geochemistry of Quaternary fluvial sediment in the southeastern Netherlands, Geologie en Mijnbouw, 69: 359-373.

Norusis, M.J., 1986, Advanced statistics SPSS/PC+ for the IBM/XT/AT SPSSinc, Chicago, USA.

Odom, I.E., Doe, T.W., Dott, R.H., 1976, Nature of feldspar-grain relations in some quartz-rich sandstones. Jour. Sed. Petr. vol. 46, no.4 p.862-870

Pastre, J.F., 1986, Altération et paleoaltération des minéraux lourds des alluvions Pliocènes et Pleistocènes du bassin de l'Allier (Massief Central, France) Assoc. Rf. Etude Quat. Bull. 3/4:257- 269.

Pastre, J.F., 1987, Les formations Plio-Quaternaires du bassin de l'Allier et le volcanisme regional (Massif Central, France). Thèse doctorat de l'Université Paris IV. 706 p.

Pelletier, H., 1971, Sur les minéraux lourds transparentes des alluvions anciennes et récentes de la Limagne, d'Auvergne. Thèse Fac. Sci. Clermont-Ferrand, 79 p.

Pettijohn, F.J., Potter, P.E., Siever, R., 1987, Sand and sandstone, second edition, Springer Verlag, New York, Berlin, Heidelberg.

Pierre, G., 1989, Les altérites fossilisees par des coulées de lave: valeur paleoclimatique et implications geomorphologiques; l'exemple de l'Auvergne, de l'Aubrac et du Velay. Thèse a l'université de Paris I Pantheon Sorbonne.

Plant, J.A., Hale, M., Ridgeway, J., 1988, Developments in regional geochemistry for mineral exploration. Trans. Inst. Min. Metall. (sect. B: Appl. Earth Sci) 97 p B116-B130.

Porta, J. & Herrero J., 1990, Micromorphology and genesis of soils enriched with gypsum, In: L.A., Douglas (Ed), Soil Micromorphology: a basic and applied science: proceedings of the VIIIth International working meeting of soil micromorphology, San Antonio, Texas July 1988, Elsevier p.321-339.

Potter P.E., 1978, Petrology and chemistry of modern big river sands., Journal of Geology, vol. 86 p. 423-449.

Raynal, J.-P., Paquereau, M.-M. & Daugas, J.-P., 1981, Stratigraphie - La formation fluviatile de Sainte-Martine (Pont-du-Château, Puy-de-Dôme), nouvelle séquence de Pléistocene Moyen d'Auvergne. C.R. Acad. Sc. Paris t. 292, Série II - p. 841-846.

Raynal, J.-P., 1984, Chronologie des basses terrasses de l'Allier en grande Limagne (Puy-de-Dôme, France). Bulletin de l'Association française pour l'étude du Quaternaire, 1.2.3., p.79-84.

Raynal, J.P., Daugas, J.P., Paquereau, M.M., Guadelli, J.L., Marchianti, D., Miallier, D., Fain, J., Sanzelle, S., 1984, Le maar de Saint-Hippolyte (Puy-de-Dôme, France), Datation pas thermoluminescence, flores et faunes fossiles, présence humaine, climatochronologie et dynamique du système paléo-lacustre. Rev. Sc. d'Auvergne, Vol. 50,

Raynal, J.P., Paquereau, M.M., Daugas, J.P., Miallier, D., Fain, J. & Sanzelle, S., 1985, Contribution à la datation du volcanisme Quaternaire du Massif Central français par thermoluminescence des inclusions de quartz et comparasion avec d'autres approches: implications chronostratigraphiques et paléoenvironementales. Bulletin de l'Association française pour l'etude de Quaternaire 1985/4 p.183-207.

Reille, M. & De Beaulieu, J.-L., 1988, La fin de l'Eémien et les interstades du Prewürm mis pour la première fois en évidence dans le Massif Central français pas l'analyse pollinique. C. R. Acad. Sci. Paris, t. 306, série II p. 1205-1210.

Riezebos, P.A., 1971, A contribution to the sedimentary petrological description of the Maas deposits in southern Limburg (The Netherlands), Geologie en Mijnbouw, vol. 50 (3), p.506-514.

Roy, A.G., & Bergeron, N., 1990, Flow and particle paths at a natural river confluence with coarse bed material. Geomorphology 3, p. 99-112.

Rudel, A., 1953, La faune Quaternaire des terrasses de l'Allier a Pont du Château. Rev. des Sc. Nat. d'Auv., pp 43-47.

Rudel, A., 1963, Les minéraux lourds des terrasses Quaternaires de Limagne d'Auvergne et les éruptions montdoriennes Soc. Geol. Fr. Bull. (7):468-469.

Ruxton, B.P., 1968, Rates of weathering of Quaternary volcanic ash in north east Papua. Trans. IX Int. Congr. Soil Sci, Adelaide, 4:367-376.

Schumm, S.A., 1977, The fluvial system, Wiley New York.

Schumm, S.A. & Lichty, R.W., 1965, Time, space and casuality in geomorphology. American Journal of Science, vol 263, p 110-119.
Schumm, S.A., Mosley, M.P. & Weaver, W.E., 1987, Experimental fluvial geomorphology. John Wiley, New York. 413 p.
Staritsky, I.G., 1989, Manual for the geostatistical programs SPATANAL, CROSS and MAPIT. Agricultural University Wageningen, Department of Soil Science and Geology, internal report.
Starkel, L., 1983, The reflection of hydrologic changes in the fluvial environment of the temperate zone during the last 15,000 years. In: Gregory, K.J., (Ed), Background to Palaeohydrology, John Wiley & Sons, London.
Stein, A., Bouma, J., Mulders, M.A.,, & Weterings M.H.W., 1989, Using spatial variability studies to estimate physical land qualities of a level river terrace, Soil Technology, 2, 385-402.
Stevens, P.R. & Walker, T.W., 1970, The chronosequence concept and soil formation. The quarterly review of biology, vol 45. p. 333-350.
Strakhov, N.M., 1969, Principles of lithogenesis, vol 2. Consultants Bureau, New York and Oliver & Boyd, Edinburgh.
Tetzlaff, D.M. & Harbaugh, J.W., 1989, Simulating clastic sedimentation. Computer methods in the geosciences. Van Nostrand Reinhold.
Texier, J-P., & Raynal, J-P., 1984, Les dépôts et terrasses fluviatiles d'aquitaine et du bassin de l'Allier. Bulletin de l'Association française pour l'étude du Quaternaire, 1.2.3., p. 67-71.
Thornes, J.B., 1987, Models for palaeohydrology in practice. in: Gregory, K.J., Lewin, J. & Thornes, J.B. (Eds), Palaeohydrology in practise, John Wiley & Sons Ltd, London.
Tourenq, J., 1986, Etude sedimentologique des alluvions de la Loire et de l'Allier des roches des bassins versants Doc. BRGM 108:108 pp.
Tuffery, C., 1986, Les formations alluviales récentes de l'Allier dans la région de Vichy: chronostratigraphie et évolution morphologique. thèse Institut de Géographie, Université de Clermont-Fd II.
Van den Berg, M.W., 1989, Toelichting op kaartblad, 59,60,61,62, Geomorfologische kaart van Nederland 1:50.000, Staring Centrum, Wageningen, Rijksgeologische Dienst, Haarlem. 33 p.
Van Dorsser, H.J., 1969, Etude geomorphologique dans une partie de la vallee de l'Allier dans la Grande Limagne Publ. ITC, Delft, Pays Bas, Ser.B 50:66 pp.
Van Straaten, L.M.J.U., 1946, Grindonderzoek in Zuid-Limburg. Meded. Geol. Sticht. Serie C-VI-2.
Veldkamp, A. & S.E.J.W. Vermeulen, 1989, River terrace formation, modelling, and 3-D graphical simulation. Earth Surface Processes and Landforms, vol 14, 641-654.
Veldkamp, A. & Kroonenberg, S.B., 1989, A comparison of the sand geochemistry of the Allier and Dore terraces, Limagne Rift Valley, France. in: Busche D., (Ed), Abstracts of papers and posters, second international conference on geomorpholoy, Frankfurt, Geoöko plus 1, vol 1, p 304.
Veldkamp A., 1990, Prediction of bulk chemical composition of fluvial sands from grain size data, Allier and Dore terrace sands Limagne Rift Valley, France. Chemical Geology vol 84 no 1/4 p 208-209.
Veldkamp. A. & Jongmans, A.G., 1990, Trachytic pumice weathering, Massif Central, France: geochemistry and micromorphology. Chemical Geology vol 84, no 1/4, p. 145-147.
Veldkamp, A. & Feijtel T.C., 1990, Regional weathering with bulk geochemistry: a case study for the Allier terrace sands, Limagne, France. Chemical Geology vol 84, nol/4 p 142-144.

Veldkamp, A. & Kroonenberg, S.B., 1991, The effects of a periglacial environment on the fluvial dynamics of the Allier during the Late Weichselian, Limagne, France. Abstract, Symposium periglacial environments in relation to climatic change Maastricht/Amsterdam 3-6 may. p.13-14.

Veldkamp, A., 1991, Reconstructing past sediment fluxes within a fluvial system: the Allier basin during the Late Quaternary. Abstract XIII INQUA, Beijing, China, p 368.

Veldkamp, E., Jongmans, A.G., Feijtel, T.C., Veldkamp, A. & Van Breemen, N., 1990, Alkali basalt gravel weathering in Quaternary Allier river terraces, Limagne, France. Soil Science Soc. of Am. Journal. 54: 1043-1048.

Veyret, Y., 1980, Quelques caracteres d'une moyenne montagne englacee, exemple des hautes terres cristallines et volcaniques du massif central français. Rev. de Géomorphologie dyn. 29, p.49-65.

Veyret, Y., 1978, Modelé et formation d'origine glaciare dans le Massif Central français, problèmes de distribution et de limites dans un milieu de moyenne montagne. Thèse de doctorat d'etat, Université de Paris I. 2 vol, 783 p.

Wedepohl, K.H. (Executive Editor), 1970, Handbook of geochemistry, Springer-Verlag Berlin, Heidelberg, New York.

Wijck van, H., 1985, Zware mineralen onderzoek Limagne Frankrijk, Internal report, Department of Soil science and Geology, Agricultural University Wageningen. (In Dutch).

Woillard , G.M., 1978, Grande Pile peat bog: a continuous pollen record for the last 140,00 years. Quaternary research, 9. 1-21.

Woillard, G.M. & Mook, W.G., 1982, Carbon-14 dates at Grande Pile Correlation of land and sea chronologies. Report in: Science, Vol 215, Jan. p. 159-161.

Yaalon, D.H., 1975, Conceptual models in pedogenesis: Can soil-forming functions be solved? Geoderma 14, 189-205.

Ziegler, B.P., 1976, Theory of modelling and simulation: An introductory exposition of concepts, Department of applied mathematics, The Weizmann institute Tehovot, Israel, Wiley, New York.

Curriculum vitae

Antonie Veldkamp werd geboren op 22 mei 1963 te Nieuwe Pekela. In 1981 behaalde hij het Atheneum-B diploma aan de scholengemeenschap St Michiel te Geleen. Hij studeerde vanaf 1981 Bodemkunde en Bemestingsleer (N33) aan de Landbouwuniversiteit waar hij in 1985 het kandidaatsexamen aflegde. Van maart 1985 tot april 1986 was hij werkzaam bij het TPIP project in Embu (Kenya) waar hij zijn praktijktijd en veldwerk voor twee hoofdvakken volbracht. Deze twee hoofdvakken, Geologie en Tropische Bodemkunde, werden vervolgens in Wageningen afgerond. De doctoraalstudie bestond verder nog uit een hoofdvak informatica. In september 1987 verkreeg hij het ingenieursdiploma met lof.

Vanaf januari 1988 tot januari 1991 was hij als Onderzoeker in Opleiding (OIO) werkzaam bij de stichting Aardwetenschappelijk Onderzoek Nederland (AWON) en gestationeerd bij de vakgroep bodemkunde en geologie van de Landbouwuniversiteit.

APPENDIX I

XRF analysis

X-ray fluorescence analysis (XRFS) is a standard analytical tool to obtain quantitative geochemical data. At the Department of Soil Science and Geology a method for determination of trace elements in glass beads of fused soil and sediment samples was developed (Kuijper & Meijer, 1987). A Sc tube is used to determine both macro and trace elements. In 1989 this method was replaced by another method wherby trace elements are measured with a Rhodium X-ray tube in combination with the measuring of the Compton scattered radiation (internal ratio method). The macro elements are still measured with a Sc tube.
The X-ray fluorescence intrumentation include a Philips PW1410 wavelength-dispersive spectrometer, LiF200 and LiF220 analyzing crystal, scintillation and gas flow-proportional counters and an automatic sample changer. More detailed instrumental information of the used method is given by Moura & Feijtel (1989).

A major disadvantage of the current methodology is that it is impossible to calculate the Lower Limit of Detection (LLD) for the trace elements. It is possible to estimate the LLD based on the standard reference sample which are used to calibrate the system. As LLD's estimated in this way still tend to give an under estimation of detection limits a more practical way to estimate the detection limits was used (Thompson & Howarth, 1978; Reimann & Wurzer, 1987; Reimann, 1988). The practical detection limit instead of the rather meaningless theoretical detection limit was estimated from 50 duplo's of the Limagne project sand samples (Tab I.1 & I.2).

Table I.1 Determination of practical detection limits for macro elements of the Allier and Dore sands. (50 duplos)

Element	Mean diff.	Std diff	Est. LD	line fit
SiO_2	0.64	0.71	~1.00	poor
TiO_2	0.07	0.06	<0.01	good
Al_2O_3	0.22	0.22	~0.01	average
Fe_2O_3	0.02	0.02	<0.01	good
MnO*	0.00	0.00	>0.01	no relationship
MgO	0.03	0.03	<0.01	poor
CaO	0.01	0.01	~0.01	poor
Na_2O	0.42	0.17	~0.01	average
K_2O	0.13	0.03	<0.01	good
P_2O_5	0.01	0.01	~0.01	poor
BaO*	0.01	0.01	~0.01	no relationship

* = not very reliable element
~ = difficult to estimate as only high concentrations occur in data set.

Table I.2 Determination of practical detection limits for trace elements of the Allier and Dore sands. (50 duplos)

Element	Mean	difference	criterion(%)	LD	line fit
Ba*	639	20	3	>800	nvt
Co*	29	7	29	>50	nvt
Cu*	<6	-	-	>6	nvt
Cr	51	2	5	4	poor
Ga*	14	2	11	>25	nvt
La	37	11	35	20	poor
Nb	8	2	35	6	poor
Ni	46	5	13	8	average
Pb	36	3	7	1	average
Rb	136	24	18	3	good
Sr	280	35	12	6	good
V	117	38	39	31	good
Zn	37	2	7	3	average
Zr	194	17	9	3	good

* = unreliable element

$$\text{criterion } p = \frac{|x - x'|}{x + x'} \times 2 \times 100\%$$

References

Kuijper, A.J., Meijer, E.L., 1987, Het meten van sporenelementen in boraatparaels met de Philips PW1404 rontgenspectrometer. Intern rapport, Vakgroep Bodemkunden en Geologie.

Moura M.L., Feijtel T.C., 1989, Analysis of trace elements using X-ray fluorescence system: application of the Rh-Compton correction method. Internal report Department of Soil Science and Geology.

Reimann, C., 1988, Reliability of geochemical analysis: recent experiences. In: MacDonald, D.R., & Mills, K.A., (Eds), Prospecting in areas of glaciated terrain 1988; The Canadian Institute of Mining and Metallurgy. p. 485-499.

Reimann, C., Wurzer F., 1987, Monitoring accuracy and precision, improvements by introducing robust and resistant statistics. Mikrochim. Acta 1986 II 31-42.

Thompson, M., & Howarth, R.J., 1978, A new approach to the estimation of analytical precision. Journal of geochemical Exploration, 9. p 23-30.

Bulk geochemical measurements of Allier and Dore sands used in this thesis are listed below. For each sample the following data are listed: sample number, location name, map coordinates (From 1:25.000 topographical maps), terrace code, absolute and relative altitudes (m), sampling depth (m), Distance upstream from actual Allier/Dore confluence (Upstr) in km, Median of grain size distribution, SiO_2, TiO_2, Al_2O_3, Fe_2O_3, MnO, MgO, CaO, Na_2O, K_2O, P_2O_5, BaO, V, Cr, Co, Ni, Cu, Zn, Ga, Rb, Sr, Zr, Nb, Ba, La, Pb.

ALLIER DATA

Sample	labnr	Location	x-coord	y-coord	Terrace	Alt	RelAlt	Depth	UpstrMedian		SiO2	TiO2	Al2O3	Fe2O3	MnO	MgO	CaO	Na2O
334	203	Tissonnieres	525.275	5081.000	Fz	293	0	0.00	19.3	280	74.18	0.70	12.13	3.05	0.04	1.52	1.78	2.51
335	204	Tissonnieres	525.275	5081.000	Fz	293	0	0.00	19.3	540	79.44	0.48	10.94	1.84	0.02	0.92	1.37	2.21
336	205	Tissonnieres	525.275	5081.000	Fz	293	0	0.00	19.3	740	78.87	0.55	10.07	2.20	0.03	1.13	1.73	2.20
337	206	Dallet	518.075	5069.000	Fz	315	0	0.00	33.0	160	71.70	0.75	13.55	3.36	0.04	1.79	1.77	2.57
338	207	Dallet	518.075	5069.000	Fz	315	0	0.00	33.0	350	78.55	0.48	11.26	2.08	0.02	1.17	1.38	2.23
339	208	Dallet	518.075	5069.000	Fz	315	0	0.00	33.0	420	76.29	0.90	10.11	4.31	0.06	1.72	1.58	1.99
340	209	Dallet	518.075	5069.000	Fz	315	0	0.00	33.0	640	75.97	0.73	10.43	3.41	0.05	2.24	2.40	2.07
AV431		Charnat 124	533.400	5089.200	Fz	278	0	0.00	8.0	300	70.31	1.11	11.87	5.15	0.07	2.11	2.33	1.65
AV432		Charnat 124	533.400	5089.200	Fz	278	0	0.00	8.0	400	73.19	0.66	10.96	3.31	0.05	2.21	2.31	1.51
AV433		Charnat 124	533.400	5089.200	Fz	278	0	0.00	8.0	1600	72.50	0.92	10.31	3.85	0.05	2.26	3.27	1.50
AV406		116	535.300	5091.500	Fz	277	0	0.00	6.8	1000	76.03	0.62	10.63	2.68	0.03	1.52	2.39	1.50
AV407		116	535.300	5091.500	Fz	277	0	0.00	6.8	800	77.14	0.47	10.90	2.10	0.02	1.04	1.60	1.54
AV408		116	535.300	5091.500	Fz	277	0	0.00	6.8	600	77.88	0.49	12.27	2.28	0.03	1.05	1.54	1.64
AV409		116	535.300	5091.500	Fz	277	0	0.00	6.8	250	71.34	0.66	12.65	3.22	0.04	1.61	1.95	1.73
AV410		117	535.000	5092.000	Fz	269	0	0.00	4.8	420	75.16	0.43	11.67	2.07	0.02	1.05	1.48	1.70
AV411		117	535.000	5092.000	Fz	269	0	0.00	4.8	1000	81.96	0.31	10.57	1.33	0.01	0.57	1.01	1.45
AV412		117	535.000	5092.000	Fz	269	0	0.00	4.8	300	73.17	0.53	12.21	2.62	0.03	1.29	1.73	1.78
AV413		118	535.600	5093.600	Fz	267	0	0.00	2.0	150	68.82	1.07	12.99	4.88	0.07	1.92	2.23	1.74
AV414		118	535.600	5093.600	Fz	267	0	0.00	2.0	400	72.51	1.11	11.29	4.90	0.07	1.82	1.97	1.51
AV399		112	536.500	5095.200	Fz	204	0	0.00	~0	900	74.06	1.01	10.11	4.37	0.07	1.91	2.21	1.33
AV400		112	536.500	5095.200	Fz	204	0	0.00	~0	400	67.15	1.83	11.14	8.71	0.12	2.17	2.12	1.48
AV401		112	536.500	5095.200	Fz	204	0	0.00	~0	800	76.27	0.68	9.77	2.76	0.03	1.54	2.42	1.43
AV402		113	536.500	5095.400	Fz	204	0	0.00	~0	500	77.44	0.42	11.25	1.95	0.02	1.01	1.42	1.60
AV403		113	536.500	5095.400	Fz	204	0	0.00	~0	500	73.93	0.57	11.94	2.54	0.03	1.29	1.76	1.69
AV404		113	536.500	5095.400	Fz	204	0	0.00	~0	250	71.28	0.62	13.37	3.04	0.03	1.36	1.76	1.82
AV415		a 119	536.800	5096.300	Fz	204	0	0.00	~0	550	77.46	0.38	10.74	1.68	0.02	0.92	1.33	1.54
AV416		a 119	536.800	5096.300	Fz	204	0	0.00	~0	900	77.78	0.53	9.35	2.34	0.03	1.25	1.72	1.31
AV417		a 119	536.800	5096.300	Fz	204	0	0.00	~0	200	73.03	0.61	13.02	2.94	0.03	1.38	1.82	1.79
AV418		b 119	537.000	5096.100	Fz	204	0	0.00	~0	300	73.52	0.51	13.20	2.38	0.03	0.96	1.56	1.87
AV419		b 119	537.000	5096.100	Fz	204	0	0.00	~0	800	80.33	0.38	9.72	1.59	0.02	0.73	1.24	1.34
AV420		b 119	537.000	5096.100	Fz	204	0	0.00	~0	100	68.77	0.84	14.12	3.87	0.05	1.64	2.26	1.79
AV421		120	536.500	5096.900	Fz	204	0	0.00	~0	1200	79.18	0.40	10.02	1.82	0.02	1.03	1.40	1.33
AV422		120	536.500	5096.900	Fz	204	0	0.00	~0	600	78.69	0.58	10.26	2.60	0.04	1.22	1.38	1.37
AV423		120	536.500	5096.900	Fz	204	0	0.00	~0	300	75.45	0.79	12.57	3.69	0.05	1.31	1.51	1.70
AV424		120	536.500	5096.900	Fz	204	0	0.00	~0	800	77.29	0.59	10.46	2.60	0.03	1.03	1.39	1.38
AV310		91	536.900	5096.000	Fz	204	0	0.00	~0	900	77.70	0.69	11.07	3.14	0.04	1.29	1.62	1.47
AV311		91	536.900	5096.000	Fz	204	0	0.00	~0	100	70.17	0.88	13.62	4.14	0.05	1.85	2.21	1.77
AV312		91	536.900	5096.000	Fz	204	0	0.00	~0	800	75.91	0.76	10.96	3.47	0.05	1.40	1.75	1.48
AV378		Charnat 106	536.800	5095.600	Fz	204	0	0.00	~0	450	79.53	0.36	11.05	1.12	0.01	0.45	0.80	1.49
AV379		Charnat 106	536.800	5095.600	Fz	204	0	0.00	~0	600	78.28	0.32	10.86	1.43	0.02	0.60	0.75	1.43
AV380		Charnat 107 w	536.800	5095.700	Fz	204	0	0.00	~0	600	73.95	0.90	10.89	3.84	0.06	1.44	1.54	1.48
AV381		Charnat 107 w	536.800	5095.700	Fz	204	0	0.00	~0	1200	80.71	0.20	10.14	0.78	0.01	0.38	0.61	1.31
AV382		Charnat 107 w	536.800	5095.700	Fz	204	0	0.00	~0	900	79.42	0.56	10.90	2.65	0.04	1.13	1.22	1.39
AV383		Charnat 107 e	536.700	5095.700	Fz	204	0	0.00	~0	1200	81.28	0.23	9.76	0.90	0.01	0.43	0.61	1.23
AV384		Charnat 107 e	536.700	5095.700	Fz	204	0	0.00	~0	1000	79.67	0.24	10.75	0.97	0.01	0.46	0.68	1.40
AV385		Charnat 107 e	536.700	5095.700	Fz	204	0	0.00	~0	500	79.73	0.24	11.48	0.60	0.01	0.28	0.68	1.52
AV386		Charnat 107 e	536.700	5095.700	Fz	204	0	0.00	~0	600	81.00	0.20	10.29	0.84	0.01	0.51	0.68	1.28
AV390		Charnat 109	536.900	5096.100	Fz	204	0	0.00	~0	1100	78.73	0.44	9.98	2.09	0.03	1.02	1.28	1.34
AV391		Charnat 109	536.900	5096.100	Fz	204	0	0.00	~0	800	80.51	0.38	10.81	1.69	0.02	0.87	1.19	1.42
AV392		Charnat 109	536.900	5096.100	Fz	204	0	0.00	~0	500	71.44	1.03	11.24	4.82	0.07	1.70	1.79	1.52
AV393		Charnat 110	536.700	5096.000	Fz	204	0	0.00	~0	1900	83.71	0.11	7.92	0.56	0.00	0.27	0.34	0.97
AV394		Charnat 110	536.700	5096.000	Fz	204	0	0.00	~0	900	76.98	0.41	11.15	1.79	0.02	0.91	1.38	1.56
AV395		Charnat 110	536.700	5096.000	Fz	204	0	0.00	~0	420	75.14	0.58	11.24	2.69	0.04	1.65	1.90	1.56
AV396		Charnat 111	536.700	5095.800	Fz	204	0	0.00	~0	150	72.21	0.84	12.70	3.75	0.05	1.47	1.81	1.75
AV397		Charnat 111	536.700	5095.800	Fz	204	0	0.00	~0	1200	80.10	0.41	9.77	1.74	0.02	0.75	0.99	1.24
AV398		Charnat 111	536.700	5095.800	Fz	204	0	0.00	~0	600	76.55	0.64	11.02	2.50	0.04	0.91	1.35	1.45
AV387		Charnat 108	537.000	5096.200	Fz	204	0	0.00	~0	1000	82.67	0.18	10.42	0.74	0.01	0.35	0.55	1.34
AV388		Charnat 108	537.000	5096.200	Fz	204	0	0.00	~0	400	74.88	0.63	11.56	2.75	0.04	1.29	1.35	1.50
AV389		Charnat 108	537.000	5096.200	Fz	204	0	0.00	~0	1300	83.67	0.15	9.75	0.65	0.01	0.29	0.42	1.14
AV104		Issoire Orbeil	521.800	5044.300	Fz	363	0	0.00	63.5	355	69.94	0.91	12.78	4.21	0.06	2.19	2.40	1.82
AV105		Issoire Orbeil	521.800	5044.300	Fz	363	0	0.00	63.5	710	72.00	0.87	11.77	4.06	0.06	2.11	2.21	1.75

Sample	K2O	P2O5	BaO	V	Cr	Co	Ni	Cu	Zn	Ga	Rb	Sr	Zr	Nb	Ba	La	Pb
334	3.03	0.17	0.06	163	26	61	26	<4	29	21	120	282	191	16	710	54	15
335	3.17	0.13	0.06	141	<14	64	10	<4	8	14	113	277	83	11	791	16	12
336	2.90	0.17	0.06	137	<14	52	10	7	16	12	97	291	99	10	731	<7	6
337	3.10	0.18	0.08	184	61	43	29	<4	40	17	142	262	262	20	765	49	10
338	3.01	0.12	0.06	104	<14	34	16	<4	15	17	109	244	88	9	705	9	10
339	2.68	0.13	0.06	259	74	53	32	5	43	13	99	234	171	16	646	<7	10
340	2.48	0.20	0.05	177	64	48	46	9	26	12	90	316	129	13	659	12	13
AV431	2.97	0.27	0.07	132	84	34	60	<6	59	14	102	241	256	18	538	66	60
AV432	2.92	0.22	0.07	63	69	26	56	<6	29	12	98	237	140	8	569	27	34
AV433	2.54	0.26	0.08	100	71	29	52	<6	22	12	80	354	135	4	575	27	32
AV406	2.82	0.21	0.08	69	46	30	48	<6	13	13	89	300	120	<2	622	14	32
AV407	3.10	0.16	0.08	44	32	33	44	<6	18	12	104	247	116	5	671	26	36
AV408	3.25	0.17	0.09	49	35	27	43	<6	16	18	114	250	123	7	660	40	36
AV409	3.28	0.22	0.08	74	58	31	53	<6	48	16	121	255	182	10	659	38	37
AV410	3.43	0.15	0.08	40	37	42	60	<6	25	14	117	241	115	5	673	<12	35
AV411	3.52	0.12	0.09	22	21	34	48	<6	4	11	112	225	91	4	756	<12	31
AV412	3.42	0.18	0.09	49	41	25	43	<6	33	15	119	250	162	10	677	34	34
AV413	3.17	0.25	0.08	130	82	33	54	<6	75	18	119	253	315	20	630	72	36
AV414	3.04	0.21	0.06	133	77	39	59	<6	52	14	104	219	213	10	521	42	28
AV399	2.74	0.15	0.07	133	107	33	55	<6	37	14	89	233	211	10	530	40	31
AV400	2.76	0.25	0.06	273	123	38	48	<6	108	15	95	217	410	22	468	84	33
AV401	2.77	0.22	0.07	66	44	20	39	<6	12	12	85	303	129	2	576	38	28
AV402	3.18	0.15	0.09	42	41	34	51	7	15	13	109	232	119	7	655	20	31
AV403	3.24	0.19	0.09	57	42	25	39	8	36	13	117	250	208	14	682	40	33
AV404	3.42	0.20	0.09	64	49	21	38	<6	41	17	132	253	180	14	665	33	40
AV415	3.43	0.14	0.09	47	29	32	47	<6	11	13	112	227	102	5	679	18	31
AV416	3.00	0.16	0.08	36	38	18	36	<6	4	12	95	244	99	3	637	26	27
AV417	3.44	0.20	0.08	57	57	29	57	<6	39	17	126	251	149	8	655	35	36
AV418	3.54	0.17	0.09	39	36	32	39	<6	20	14	126	256	152	10	694	17	38
AV419	3.16	0.14	0.08	50	27	42	50	<6	4	10	104	215	108	2	649	16	33
AV420	3.37	0.31	0.09	43	62	26	43	7	76	16	133	270	140	10	680	39	41
AV421	3.46	0.15	0.09	42	30	26	42	<6	3	11	113	223	99	5	696	19	33
AV422	3.29	0.15	0.08	51	51	37	51	<6	16	12	108	206	121	4	582	23	33
AV423	3.52	0.19	0.08	52	49	40	52	<6	46	14	126	218	249	14	598	51	39
AV424	3.44	0.14	0.07	43	43	28	43	<6	18	13	120	208	133	9	627	34	31
AV310	3.26	0.16	0.08	40	37	42	60	<6	25	14	117	241	115	5	673	<12	35
AV311	3.41	0.28	0.09	22	21	34	48	<6	4	12	112	225	91	4	756	<12	31
AV312	3.22	0.18	0.08	49	41	25	43	<6	33	15	119	250	162	10	677	34	34
AV378	4.25	0.04	0.08	25	24	40	44	<6	<3	14	163	179	156	10	633	19	35
AV379	4.30	0.10	0.09	34	27	42	45	<6	10	12	170	176	139	5	663	28	39
AV380	3.53	0.18	0.08	105	68	45	59	<6	43	14	130	199	227	16	577	57	37
AV381	4.35	0.09	0.09	14	16	36	45	7	<3	14	160	193	70	3	738	24	37
AV382	3.55	0.12	0.07	64	46	34	49	<6	25	14	128	201	120	<2	588	21	34
AV383	4.18	0.09	0.09	16	14	37	46	<6	<3	12	160	170	94	<2	652	13	38
AV384	4.31	0.08	0.09	15	17	37	45	<6	11	13	163	189	100	4	715	<12	39
AV385	4.31	0.03	0.08	18	13	37	45	17	<3	16	165	193	122	8	692	15	36
AV386	4.19	0.08	0.09	12	39	38	44	<6	<3	14	160	175	77	2	659	13	36
AV390	3.43	0.15	0.09	40	35	39	47	<6	16	13	119	210	165	9	671	36	33
AV391	3.54	0.14	0.08	31	26	40	49	<6	11	13	123	215	92	4	643	18	35
AV392	3.23	0.23	0.10	132	79	35	52	<6	58	13	111	217	380	27	706	115	33
AV393	3.84	0.06	0.08	<5	7	23	26	7	<3	11	138	150	61	<2	643	13	35
AV394	3.70	0.14	0.09	39	28	19	28	<6	<3	13	131	232	116	8	682	14	31
AV395	3.08	0.17	0.08	61	50	22	43	<6	21	14	109	237	134	7	581	28	34
AV396	3.57	0.20	0.08	93	60	22	42	<6	51	14	139	228	320	18	656	72	36
AV397	3.88	0.11	0.08	38	36	31	47	<6	5	11	140	198	95	7	618	20	35
AV398	3.63	0.08	0.08	66	59	30	37	<6	15	15	136	201	194	8	575	32	35
AV387	4.13	0.07	0.08	8	11	36	41	<6	<3	14	153	176	70	<2	686	<12	39
AV388	3.75	0.15	0.08	66	59	28	49	<6	33	14	148	198	222	7	611	37	40
AV389	4.33	0.08	0.09	<5	13	41	50	7	<3	12	167	166	70	<2	718	<12	39
AV104	3.08	0.26	0.07	150	82	92	60	12	92	13	128	304	382	22	1007	81	19
AV105	2.98	0.22	0.05	135	82	59	60	12	78	17	127	294	306	18	991	68	11

Sample	Tabnr	Location	x-coord	y-coord	Terrace	Alt	RelAlt	Depth	UpstrMedian	SiO2	TiO2	Al2O3	Fe2O3	MnO	MgO	CaO	Na2O
AV109		Les Gaves	517.300	5050.400	Fz	350	0	0.00	55.3 500	74.73	0.64	11.20	2.98	0.04	1.78	1.97	1.66
AV110		Les Gaves	517.300	5050.400	Fz	350	0	0.00	55.3 2000	67.06	1.31	11.43	5.98	0.09	3.53	4.38	1.76
AV116		Longues place	526.300	5057.300	Fz	349	0	0.00	48.7 1000	74.84	0.74	10.43	3.58	0.06	2.21	2.15	1.52
AV117		Longues place	526.300	5057.300	Fz	349	0	0.00	48.7 500	74.98	0.59	11.12	2.78	0.04	1.81	1.93	1.69
AV120		Crezin	521.200	5038.700	Fz	372	0	0.00	68.8 1000	77.96	0.45	10.32	2.11	0.03	1.20	1.45	1.63
AV121		Crezin	521.200	5038.700	Fz	372	0	0.00	68.8 2000	77.86	0.54	10.64	2.53	0.03	1.40	1.72	1.61
AV122		Crezin	521.200	5038.700	Fz	372	0	0.00	68.8 710	72.38	0.72	12.32	3.57	0.05	1.94	1.90	1.87
401	41	Chappe	528.300	5025.200	Fz	409	0	0.00	86.2 500	76.20	0.37	10.49	2.70	0.05	1.57	1.04	1.83
394	34	Jumeaux	526.200	5031.000	Fz	393	0	0.00	80.0 500	76.83	0.42	10.52	3.25	0.07	1.68	1.37	1.71
AV78		Azerat	529.300	5023.600	Fz	406	0	0.00	88.5 500	76.26	0.45	12.02	2.31	0.03	1.36	1.00	1.80
AV79		Azerat	529.300	5023.600	Fz	406	0	0.00	88.5 710	77.16	0.38	11.57	2.08	0.02	0.93	0.77	1.73
AV80		Azerat	529.300	5023.600	Fz	406	0	0.00	88.5 2000	78.12	0.45	11.07	2.37	0.03	1.16	0.93	1.51
AV68		Pont Pakowski	521.900	5035.300	Fz	390	0	0.00	73.5 710	75.71	0.57	11.57	2.68	0.03	1.34	1.47	1.84
AV69		Pont Pakowski	521.900	5035.300	Fz	390	0	0.00	73.5 250	72.54	0.68	11.77	3.49	0.05	1.93	1.92	1.85
AV70		Pont Pakowski	521.900	5035.300	Fz	390	0	0.00	73.5 1000	78.37	0.44	10.68	1.81	0.02	0.88	1.12	1.62
393	33	Saut de loupe	525.800	5034.000	Fz	393	0	0.00	76.0 600	71.13	0.99	10.75	4.52	0.06	2.55	2.82	1.99
AV17		St Yorre	535.500	5101.200	Fz	259	0	0.00	5.3 250	73.50	0.86	11.89	3.33	0.05	1.53	1.75	1.86
AV44		N Pont de Ris	536.500	5095.500	Fz	263	0	0.00	0.4 710	80.41	0.51	9.77	2.09	0.03	0.29	0.52	1.47
AV45		N Pont de Ris	536.500	5095.500	Fz	263	0	0.00	0.4 500	77.56	0.33	11.45	1.23	0.02	0.69	0.88	1.83
AV46		N Pont de Ris	536.500	5095.500	Fz	263	0	0.00	0.4 700	80.51	0.36	10.51	1.37	0.02	0.63	0.74	1.52
AV47		N Pont de Ris	536.500	5095.500	Fz	263	0	0.00	0.4 2000	72.57	1.79	9.19	7.01	0.10	1.46	1.53	1.33
AV94		Les cotes	514.500	5049.500	FzCC	383	0	0.00	46.0 355	68.20	1.19	13.34	4.30	0.06	1.81	3.43	2.24
AV95		Les cotes	514.500	5049.500	FzCC	383	0	0.00	46.0 710	72.17	1.44	11.22	5.25	0.07	1.69	3.07	1.77
AV98		Chidrac	511.400	5044.500	FzCP	452	0	0.00	63.5 1000	70.18	0.99	12.39	4.41	0.06	2.30	3.10	1.88
AV99		Chidrac	511.400	5044.500	FzCP	452	0	0.00	63.5 500	67.58	1.12	13.41	4.68	0.06	2.55	3.31	1.90
AV12		Pont de Ris	536.500	5095.500	Fyz	265	2	0.50	0.5 1000	73.27	1.48	9.89	5.64	0.08	1.90	2.10	1.50
AV15		Les Graviers	533.700	5105.200	Fyz	257	2	0.50	-7.0 710	79.01	0.64	9.59	2.53	0.04	1.10	1.42	1.55
AV106		Issoire Orbeil	521.800	5044.300	Fy	365	2	1.50	63.5 500	76.72	0.41	11.29	2.19	0.03	1.14	1.07	1.80
AV107		Issoire Orbeil	521.800	5044.300	Fy	365	2	0.80	63.5 355	71.86	0.63	12.89	3.22	0.04	1.58	1.61	1.94
395	35	NJumeaux	526.200	5031.200	Fy	400	7	1.80	80.0 850	77.99	0.20	11.36	1.28	0.01	0.57	0.30	1.75
396	36	NJumeaux	526.200	5031.200	Fy	400	7	2.80	80.0 1100	82.36	0.12	10.25	1.00	0.01	0.42	0.11	1.30
397	37	NChappe	527.800	5026.200	Fy	414	5	0.55	86.2 210	67.26	0.72	15.63	4.00	0.05	2.15	1.27	2.57
398	38	NChappe	527.800	5026.200	Fy	414	5	0.60	86.2 600	73.99	0.35	12.83	2.23	0.03	1.34	0.96	2.57
399	39	NChappe	527.800	5026.200	Fy	414	5	0.70	86.2 1000	75.91	0.32	11.43	1.97	0.02	1.21	0.81	2.06
400	40	NChappe	527.800	5026.200	Fy	414	5	0.80	86.2 1400	78.97	0.27	10.97	1.86	0.02	0.91	0.66	1.86
AV87		La tuilerie	522.200	5034.600	Fy	395	5	1.50	74.0 1400	56.79	2.58	13.56	9.67	0.14	4.99	6.38	2.16
AV88		St Blaise	522.800	5034.600	Fy	395	5	1.00	74.0 1000	63.38	1.84	12.91	7.27	0.10	4.13	4.41	1.85
AV118		Longues usine	516.000	5056.800	Fx4	365	15	1.50	49.5 710	74.82	0.62	11.36	3.13	0.04	1.52	1.34	1.43
AV119		Longues usine	516.000	5056.800	Fx4	365	15	1.50	49.5 2000	70.07	1.21	10.81	6.02	0.09	2.76	2.70	1.35
AV81		Les granges	521.900	5024.900	Fx4	410	10	2.00	87.3 1000	78.63	0.33	11.41	1.93	0.02	0.54	0.50	1.46
AV67		St Blaise	523.200	5034.500	Fx4	400	10	1.50	74.0 1000	69.38	1.69	12.09	7.47	0.09	1.62	1.81	1.62
AV29		Jarrauds	536.700	5099.300	Fx4	271	10	2.10	-3.5 1400	75.34	1.15	11.06	3.68	0.05	1.64	2.38	1.46
AV30		Jarrauds	536.700	5099.300	Fx4	271	10	2.20	-3.5 710	72.32	1.17	11.01	4.40	0.06	2.05	2.20	1.54
AV13		Jarrauds	536.700	5099.300	Fx4	271	10	2.00	-3.5 1000	75.49	0.75	11.14	2.90	0.04	1.36	1.71	1.59
AV14		Jarrauds	536.700	5099.300	Fx4	271	10	1.50	-3.5 1000	73.36	0.98	11.42	3.86	0.06	1.91	2.18	1.63
AV136		Les jarrauds A	536.200	5099.300	Fx4	270	9	2.50	-3.5 1500	71.84	1.03	11.18	4.43	0.05	1.92	3.00	1.52
AV158		Hauterive	534.000	5104.000	Fx4	265	10	3.70	-9.0 1400	68.61	1.33	11.55	5.10	0.07	2.85	4.35	1.68
AV159		Hauterive	534.000	5104.000	Fx4	265	10	3.70	-9.0 1400	70.31	1.31	10.58	5.19	0.07	2.71	3.66	1.46
AV160		Hauterive	534.000	5104.000	Fx4	265	10	3.50	-9.0 2000	69.55	1.40	10.67	5.66	0.08	2.99	4.07	1.49
AV161		Hauterive	534.000	5104.000	Fx4	265	10	3.00	-9.0 2000	73.75	1.01	10.43	3.93	0.05	2.18	3.04	1.38
AV28		Hauterive	534.000	5104.000	Fx4	265	10	3.00	-9.0 1400	74.01	1.19	10.60	3.92	0.06	2.37	3.52	1.66
AV174		Petit BArdins	537.500	5092.500	Fx4	271	10	3.00	3.0 1200	69.46	1.40	11.23	6.45	0.09	2.74	2.78	1.32
AV175		Petit BArdins	537.500	5092.500	Fx4	271	10	3.00	3.0 1600	71.35	1.25	10.97	5.54	0.07	2.32	2.87	1.24
AV176		Petit BArdins	537.500	5092.500	Fx4	271	10	3.40	3.0 1400	75.63	0.71	10.68	3.10	0.04	1.56	2.01	1.36
AV177		Petit BArdins	537.500	5092.500	Fx4	271	10	3.40	3.0 1700	76.66	0.75	10.94	3.25	0.04	1.51	2.05	1.41
AV197		St Yorre Sud	536.300	5100.100	Fx4	269	9	2.30	-4.5 1600	75.27	0.73	10.93	3.36	0.03	1.44	2.13	1.33
AV198		St Yorre Sud	536.300	5100.100	Fx4	269	9	2.30	-4.5 700	74.54	0.71	11.17	3.81	0.04	1.52	2.05	1.42
AV199		St Yorre Sud	536.300	5100.100	Fx4	269	9	2.30	-4.5 1500	75.45	0.71	10.85	3.61	0.03	1.23	2.11	1.28
AV200		St Yorre Sud	536.300	5100.100	Fx4	269	9	2.00	-4.5 750	75.43	0.66	11.50	3.04	0.03	0.98	1.97	1.49
AV202		St Yorre Sud	536.300	5100.100	Fx4	269	9	2.50	-4.5 900	72.37	1.01	11.29	4.16	0.05	1.89	3.42	1.41
AV204		St Yorre Sud	536.300	5100.100	Fx4	269	9	2.50	-4.5 1000	74.49	0.95	11.06	3.89	0.05	1.70	2.83	1.38

Sample	K2O	P2O5	BaO	V	Cr	Co	Ni	Cu	Zn	Ga	Rb	Sr	Zr	Nb	Ba	La	Pb
AV109	3.00	0.19	0.05	129	82	42	60	12	57	13	117	265	187	14	979	65	10
AV110	2.45	0.39	0.05	247	106	66	60	12	103	17	89	494	281	21	1003	84	16
AV116	2.90	0.19	0.05	117	82	49	60	12	96	9	110	275	102	12	923	50	17
AV117	3.05	0.19	0.05	86	82	70	60	12	74	10	117	269	116	11	794	26	25
AV120	3.09	0.13	0.06	73	82	50	60	12	36	12	114	234	93	12	879	36	13
AV121	3.23	0.17	0.07	53	82	39	60	12	44	13	114	274	128	13	904	37	21
AV122	3.13	0.20	0.06	103	82	46	60	12	78	13	141	261	266	17	976	75	19
401	2.95	0.12	0.06	111	82	54	60	10	25	14	100	182	203	15	670	30	8
394	2.88	0.15	0.07	125	82	30	60	10	41	17	91	226	101	10	690	13	106
AV78	3.52	0.15	0.07	68	82	43	60	10	32	18	151	176	154	15	886	63	29
AV79	3.77	0.10	0.07	68	82	55	60	10	25	16	147	190	59	10	868	59	24
AV80	3.37	0.12	0.07	68	82	52	60	13	30	18	128	182	99	12	933	58	14
AV68	3.03	0.14	0.06	89	82	55	60	12	23	18	119	248	108	13	869	39	22
AV69	2.75	0.18	0.05	112	82	46	60	15	51	16	109	256	185	16	940	79	15
AV70	3.30	0.12	0.07	59	82	61	60	10	31	12	110	226	75	11	961	35	19
393	2.36	0.23	0.05	236	82	51	60	18	55	15	68	356	187	19	629	42	18
AV17	3.42	0.19	0.08	113	82	49	60	14	28	14	151	260	336	21	1054	106	21
AV44	3.60	0.09	0.08	68	82	41	60	10	13	12	140	190	114	17	998	37	23
AV45	4.43	0.09	0.07	68	82	69	60	10	12	17	196	210	65	14	883	47	29
AV46	4.31	0.08	0.07	68	82	12	60	10	16	14	182	193	57	5	932	42	18
AV47	3.22	0.18	0.06	313	82	31	60	13	98	17	147	139	420	35	964	119	17
AV94	3.40	0.27	0.08	181	82	40	60	12	107	18	140	437	319	21	1079	69	31
AV95	3.12	0.24	0.05	235	82	38	60	12	98	13	127	380	318	21	1058	31	21
AV98	2.77	0.27	0.06	176	101	40	60	12	77	16	103	425	197	15	977	75	13
AV99	2.88	0.29	0.06	167	82	40	60	12	91	17	125	415	346	21	1068	87	15
AV12	2.72	0.19	0.04	224	91	115	60	10	12	12	102	276	216	17	819	42	22
AV15	3.22	0.13	0.06	88	82	35	60	10	17	14	119	255	98	13	851	39	16
AV106	3.58	0.14	0.07	68	82	44	60	12	39	13	146	205	146	12	879	75	18
AV107	3.37	0.20	0.07	80	82	43	60	12	73	15	147	240	287	16	979	82	18
395	4.46	0.08	0.07	68	82	52	60	10	12	15	170	154	44	6	769	20	20
396	4.65	0.06	0.11	68	82	49	60	10	12	17	146	164	49	5	1051	<7	23
397	3.91	0.20	0.09	179	82	44	60	16	81	24	181	188	390	23	831	84	18
398	3.64	0.12	0.07	104	82	44	60	10	29	19	138	188	136	12	679	<7	16
399	3.43	0.09	0.06	92	82	39	60	10	25	16	119	176	79	10	656	11	17
400	3.32	0.08	0.05	70	82	64	60	10	18	16	114	173	87	10	683	<7	12
AV87	2.09	0.53	0.04	419	161	34	60	35	126	21	87	756	378	41	931	72	13
AV88	2.75	0.37	0.05	265	131	39	60	27	99	23	160	500	239	25	953	46	17
AV118	3.61	0.16	0.06	101	82	44	60	12	94	11	161	217	113	12	884	57	23
AV119	2.75	0.24	0.03	205	97	51	60	12	156	12	112	309	260	19	871	79	23
AV81	3.32	0.08	0.08	68	82	50	60	13	28	13	141	167	80	11	899	26	18
AV67	2.91	0.23	0.03	263	82	56	60	20	101	20	149	289	214	20	821	57	21
AV29	2.71	0.23	0.06	137	82	13	60	17	49	14	116	337	152	19	920	66	13
AV30	2.90	0.22	0.06	132	82	47	60	19	51	14	120	312	142	22	930	48	11
AV13	3.15	0.20	0.07	78	82	60	60	17	33	12	132	283	88	11	952	47	16
AV14	3.25	0.24	0.06	139	82	73	60	18	49	13	132	323	130	20	934	64	22
AV136	2.79	0.30	0.05	285	82	41	60	10	66	15	110	394	163	16	1104	65	35
AV158	2.71	0.37	0.06	333	82	42	60	10	17	16	102	523	216	18	1246	80	33
AV159	2.72	0.32	0.05	382	82	55	60	10	16	15	104	458	182	16	1116	74	31
AV160	2.54	0.34	0.05	411	82	57	60	10	18	14	91	490	280	21	1093	65	36
AV161	2.88	0.27	0.05	244	82	61	60	10	12	14	114	401	183	16	1063	58	35
AV28	2.68	0.30	0.06	126	82	36	60	19	26	15	94	435	161	21	943	44	16
AV174	2.84	0.32	0.06	64	82	64	60	10	<12	13	138	192	126	12	987	46	40
AV175	**2.79**	**0.32**	**0.06**	**<68**	**82**	**78**	**60**	**10**	**<12**	**10**	**147**	**128**	**98**	**10**	**1068**	**58**	**38**
AV176	3.29	0.27	0.07	83	62	82	60	<6	24	13	119	261	130	<2	569	25	35
AV177	3.29	0.24	0.08	88	55	29	54	10	25	15	119	270	123	3	605	31	37
AV197	3.07	0.22	0.07	85	55	24	50	10	26	14	105	285	120	7	557	25	36
AV198	3.07	0.20	0.08	74	53	34	51	<6	26	13	108	270	115	6	588	22	30
AV199	3.09	0.25	0.07	79	49	17	40	9	21	13	114	286	120	3	616	35	37
AV200	3.28	0.17	0.08	66	45	40	52	<6	26	13	114	283	117	5	619	28	31
AV202	2.73	0.32	0.07	123	73	16	62	19	46	12	90	381	144	5	544	34	30
AV204	2.97	0.27	0.08	123	63	22	47	10	36	15	98	340	144	5	618	32	25

Sample Name	Location	x-coord	y-coord	Terrace	Alt	Relalt	Depth	UpstrMedian	SiO2	TiO2	Al2O3	Fe2O3	MnO	MgO	CaO	Na2O
AV205	La Claire	536.900	5097.300	Fx4	271	10	2.00	-2.5	1200	74.22	0.85	11.45	3.58	0.05	1.57	1.78	1.38
AV206	La Claire	536.900	5097.300	Fx4	271	10	2.50	-2.5	1400	76.21	0.68	10.85	3.07	0.04	1.40	1.54	1.32
AV207	La Claire	536.900	5097.300	Fx4	271	10	3.00	-2.5	1500	75.02	0.70	11.25	3.19	0.04	1.39	2.17	1.48
AV208	La Claire	536.900	5097.300	Fx4	271	10	3.00	-2.5	1000	76.18	0.68	10.85	2.96	0.03	1.36	2.14	1.48
AV209	La Claire	536.900	5097.300	Fx4	271	10	3.50	-2.5	1600	75.41	0.74	10.51	3.32	0.04	1.70	2.32	1.35
AV210	La Claire	536.900	5097.300	Fx4	271	10	3.75	-2.5	1100	69.10	1.33	11.02	6.20	0.08	2.95	3.45	1.33
AV211	La Claire	536.900	5097.300	Fx4	271	10	3.75	-2.5	1100	70.88	1.01	11.78	4.77	0.06	2.34	2.80	1.43
AV212	La Claire	536.900	5097.300	Fx4	271	10	4.00	-2.5	1000	72.59	1.04	10.51	4.69	0.06	2.51	3.17	1.33
AV213	La Claire	536.900	5097.300	Fx4	271	10	3.75	-2.5	1000	73.88	0.92	10.35	3.71	0.05	1.75	2.64	1.36
AV214	La Claire	536.900	5097.300	Fx4	271	10	3.50	-2.5	1400	74.89	0.78	11.82	3.03	0.03	1.35	1.87	1.29
AV217	Petit Bardins	537.500	5092.500	Fx4	271	10	3.30	3.5	1200	70.23	1.38	11.20	6.39	0.09	2.47	2.45	1.37
AV218	Petit Bardins	537.500	5092.500	Fx4	271	10	3.30	3.5	1500	75.42	0.75	11.22	3.23	0.04	1.54	1.97	1.45
AV219	Petit Bardins	537.500	5092.500	Fx4	271	10	3.50	3.5	800	68.36	1.28	11.11	5.84	0.08	3.49	3.29	1.39
AV226	M Curacon route	535.600	5088.300	Fx4	283	10	2.50	6.5	600	81.75	0.11	10.09	0.18	0.00	0.06	0.00	1.04
AV227	M Curacon route	535.600	5088.300	Fx4	283	10	2.50	6.5	1000	84.27	0.09	9.73	0.16	0.00	0.06	0.00	0.90
AV228	M Curacon route	535.600	5088.300	Fx4	283	10	2.60	6.5	<16	79.67	0.27	11.37	0.28	0.00	0.09	0.06	1.18
AV229	M Curacon route	535.600	5088.300	Fx4	283	10	2.60	6.5	1500	82.86	0.05	9.96	0.12	0.00	0.04	0.00	0.86
AV230	M Curacon route	535.600	5088.300	Fx4	283	10	2.70	6.5	1200	81.73	0.08	10.73	0.13	0.00	0.03	0.00	0.99
AV249	Luzillat NE	531.200	5089.000	Fx4	290	10	2.50	10.0	1000	69.32	1.24	11.12	5.57	0.08	3.35	4.08	1.51
AV250	Luzillat NE	531.200	5089.000	Fx4	290	10	2.50	10.0	800	71.08	0.91	12.16	4.37	0.06	2.43	2.80	1.64
AV251	Luzillat NE	531.200	5089.000	Fx4	290	10	2.50	10.0	1000	69.28	1.23	11.21	5.08	0.07	3.24	4.53	1.58
AV252	Luzillat NE	531.200	5089.000	Fx4	290	10	2.50	10.0	1600	69.43	1.18	11.31	5.07	0.07	3.15	4.21	1.68
AV253	Luzillat NE	531.200	5089.000	Fx4	290	10	2.00	10.0	1100	71.81	1.01	11.29	4.64	0.06	2.71	3.35	1.51
AV254	Luzillat NE	531.200	5089.000	Fx4	290	10	2.00	10.0	700	72.06	0.91	12.09	4.22	0.05	2.23	2.75	1.52
AV255	Limons/poyet	533.700	5090.600	Fx4	281	10	2.00	6.0	900	71.55	1.02	12.02	3.80	0.04	1.42	2.94	1.65
AV273	Hauterive Sabli	533.900	5090.700	Fx4	262	9	2.00	-8.8	900	72.46	1.10	10.99	5.20	0.07	2.19	2.52	1.40
AV274	Hauterive Sabli	533.900	5090.700	Fx4	262	9	2.00	-8.8	1000	72.73	1.05	10.88	4.73	0.06	2.25	2.63	1.41
AV275	Hauterive Sabli	533.900	5090.700	Fx4	262	9	2.50	-8.8	1000	74.45	0.78	10.76	3.49	0.04	1.82	2.30	1.39
AV276	Hauterive Sabli	533.900	5090.700	Fx4	262	9	3.00	-8.8	1300	78.28	0.59	10.50	2.50	0.03	1.60	1.81	1.34
AV277	Hauterive Sabli	533.900	5090.700	Fx4	262	9	3.00	-8.8	1400	76.35	0.62	10.50	2.66	0.03	1.27	1.72	1.36
AV278	Hauterive Sabli	533.900	5090.700	Fx4	262	9	3.00	-8.8	1100	76.49	0.43	11.81	1.81	0.02	0.52	1.45	1.70
AV287	La grand Domain	534.500	5103.600	Fx4	263	9	2.00	-8.0	1400	76.99	0.65	10.23	3.06	0.04	1.27	1.87	1.30
AV288	La grand Domain	534.500	5103.600	Fx4	263	9	2.00	-8.0	1200	72.89	0.89	11.23	4.37	0.05	1.84	2.40	1.30
AV289	La grand Domain	534.500	5103.600	Fx4	263	9	2.00	-8.0	1400	78.10	0.63	10.25	2.76	0.03	1.20	1.89	1.34
AV290	La grand Domain	534.500	5103.600	Fx4	263	9	2.00	-8.0	1100	78.44	0.59	10.45	2.60	0.03	1.08	1.66	1.37
AV291	La grand Domain	534.500	5103.600	Fx4	263	9	2.00	-8.0	800	75.40	0.83	10.96	3.50	0.04	1.25	1.84	1.41
AV317	La Latte	533.900	5099.300	Fx4	271	10	4.00	-3.8	700	70.93	0.94	12.35	4.50	0.06	2.27	2.78	1.69
AV318	La Latte	533.900	5099.300	Fx4	271	10	3.00	-3.8	800	70.80	0.99	11.79	4.47	0.06	2.51	3.33	1.66
AV319	La Latte	533.900	5099.300	Fx4	271	10	3.00	-3.8	500	68.32	1.10	12.34	5.21	0.07	2.76	3.60	1.69
AV320	La Latte	533.900	5099.300	Fx4	271	10	3.50	-3.8	1200	71.02	1.04	10.98	4.64	0.06	2.77	3.56	1.57
AV321	La Latte	533.900	5099.300	Fx4	271	10	3.50	-3.8	1400	73.31	0.80	11.30	3.40	0.05	1.86	2.77	1.62
AV322	La Latte	533.900	5099.300	Fx4	271	10	4.00	-3.8	1300	72.00	0.92	11.44	4.02	0.06	2.41	3.26	1.63
AV454	Longues plac	516.000	5057.400	Fx4	350	10	3.00	48.5	1400	61.94	1.80	12.82	8.54	0.08	2.63	5.71	1.84
AV455	Longues plac	516.000	5057.400	Fx4	350	10	1.50	48.5	1600	61.06	1.81	12.19	9.82	0.08	3.02	5.75	1.80
AV456	Longues plac	516.000	5057.400	Fx4	350	10	4.00	48.5	1300	68.64	1.28	13.14	6.43	0.06	1.34	2.32	1.27
AV457	Longues plac	516.000	5057.400	Fx4	350	10	4.00	48.5	800	71.81	1.19	11.61	5.03	0.06	1.65	3.17	1.30
AV459	Longues plac	516.000	5057.400	Fx4	350	10	4.00	48.5	700	70.92	0.80	11.45	5.46	0.04	1.43	2.34	1.51
AV460	Longues plac	516.000	5057.400	Fx4	350	10	4.00	48.5	400	73.85	0.68	10.69	4.45	0.03	1.15	2.02	1.43
AV489	Lempdes Abat	517.200	5067.400	Fx4	330	10	6.00	22.5	800	72.20	0.67	12.08	3.05	0.04	1.68	2.07	1.69
AV491	Lempdes Abat	517.200	5067.400	Fx4	330	10	6.00	22.5	20	53.62	1.65	16.92	8.54	0.18	3.18	6.38	3.25
AV162	Saladis	517.100	5058.000	Fx4	342	8	4.00	47.5	1400	78.65	0.50	9.67	3.50	0.02	0.71	1.06	1.32
AV163	Saladis	517.100	5058.000	Fx4	342	8	4.00	47.5	1900	75.84	0.55	10.03	4.55	0.03	0.90	1.55	1.38
AV164	Saladis	517.100	5058.000	Fx4	342	8	1.00	47.5	1600	66.26	1.48	11.59	6.00	0.08	3.39	4.53	1.75
AV448	Lempdes Abat	517.200	5067.400	Fx4	330	10	4.80	22.5	1500	43.87	0.99	11.87	5.76	0.10	3.93	14.76	1.60
AV449	Lempdes Abat	517.200	5067.400	Fx4	330	10	10.00	22.5	800	75.98	0.57	11.26	2.62	0.03	0.98	1.28	1.32
AV450	Lempdes Abat	517.200	5067.400	Fx4	330	10	4.00	22.5	300	56.48	1.56	16.27	8.05	0.15	3.10	6.03	2.76
AV451	Lempdes Abat	517.200	5067.400	Fx4	330	10	2.00	22.5	400	67.06	1.01	13.79	4.85	0.07	2.34	3.18	1.64
AV486	Joze	524.400	5079.800	Fx3	313	12	3.00	10.5	800	79.29	0.58	9.65	2.25	0.03	1.02	1.69	1.31
AV487	Joze	524.400	5079.800	Fx3	313	12	3.00	10.5	1100	80.09	0.59	9.63	2.05	0.02	0.95	1.94	1.32
AV488	Joze	524.400	5079.800	Fx3	313	12	3.20	10.5	1200	75.80	0.80	9.66	3.42	0.05	1.37	2.16	1.28
AV77	Ouillandre	528.100	5022.000	Fx3	420	14	2.50	89.5	2000	70.65	0.68	14.48	3.92	0.05	0.84	0.91	1.22

Sample	K2O	P2O5	BaO	V	Cr	Co	Ni	Cu	Zn	Ga	Rb	Sr	Zr	Nb	Ba	La	Pb
AV205	3.31	0.22	0.07	92	57	23	54	<6	33	12	118	224	147	6	630	23	37
AV206	3.35	0.20	0.08	77	45	20	45	9	24	10	115	230	114	<2	631	24	37
AV207	3.26	0.24	0.08	82	46	33	53	11	29	14	108	317	123	4	695	17	34
AV208	3.22	0.22	0.08	71	48	37	59	6	25	12	102	312	122	3	623	32	33
AV209	3.02	0.24	0.08	84	44	34	62	<6	30	15	98	311	130	4	666	21	30
AV210	2.41	0.34	0.06	186	95	32	67	10	54	14	81	354	176	9	520	41	34
AV211	2.97	0.29	0.07	124	76	23	57	7	44	14	100	327	155	<2	567	33	35
AV212	2.65	0.29	0.08	126	91	31	66	<6	37	14	82	249	148	4	573	32	40
AV213	2.96	0.25	0.07	112	63	28	60	<6	32	16	97	335	167	6	557	30	29
AV214	3.38	0.26	0.08	83	52	14	36	6	20	13	116	277	121	4	661	41	36
AV217	3.15	0.29	0.06	173	86	38	69	<6	65	13	115	257	181	7	499	48	36
AV218	3.52	0.29	0.08	85	48	28	48	<6	22	10	126	262	124	2	607	24	36
AV219	2.68	0.36	0.06	175	109	39	141	60	100	15	93	323	167	8	555	31	38
AV226	5.78	0.02	0.08	<5	10	44	49	<6	10	10	254	107	112	7	631	28	45
AV227	5.71	0.01	0.08	7	5	43	45	11	<3	12	257	98	69	3	622	<12	39
AV228	6.46	0.02	0.08	17	11	34	38	<6	<3	12	322	111	181	8	623	24	48
AV229	6.28	0.01	0.07	<5	5	61	59	20	<3	13	308	86	64	<2	566	12	46
AV230	6.64	0.01	0.07	<5	8	52	46	14	<3	12	324	89	81	<2	574	15	47
AV249	2.39	0.38	0.07	171	99	42	76	11	47	16	79	421	168	6	581	42	27
AV250	3.14	0.28	0.08	109	69	28	66	8	39	16	111	347	144	7	640	36	30
AV251	2.35	0.38	0.07	149	88	34	68	9	39	15	73	470	171	4	528	37	24
AV252	2.51	0.36	0.07	141	87	30	65	8	40	13	78	451	169	6	590	37	26
AV253	2.77	0.33	0.08	131	81	37	64	<6	36	12	91	365	148	3	612	40	36
AV254	2.93	0.20	0.06	103	72	26	52	<6	36	14	117	325	142	5	513	26	32
AV255	2.65	0.27	0.08	131	79	>400	>500	<6	274	25	92	351	161	3	720	32	19
AV273	2.94	0.26	0.07	143	84	36	62	<6	48	14	98	296	159	7	520	44	32
AV274	2.91	0.27	0.07	125	70	32	62	<6	44	12	97	315	156	7	522	18	30
AV275	3.04	0.24	0.08	93	59	28	58	<6	27	14	103	288	131	7	547	28	29
AV276	3.20	0.19	0.07	65	38	80	61	9	23	14	112	268	109	4	609	<12	34
AV277	3.30	0.20	0.08	61	37	29	49	<6	19	13	113	266	117	4	651	29	35
AV278	3.44	0.12	0.09	38	15	31	46	<6	13	14	108	341	119	2	693	24	28
AV287	3.22	0.26	0.08	64	43	35	49	9	27	10	111	262	120	4	642	20	42
AV288	3.10	0.26	0.07	101	64	20	50	<6	35	13	117	272	144	5	556	39	41
AV289	3.29	0.22	0.09	65	44	53	64	<6	25	11	112	282	116	<2	690	25	42
AV290	3.59	0.20	0.08	60	33	38	54	<6	18	15	120	257	109	5	643	23	37
AV291	3.34	0.20	0.07	86	61	23	43	<6	31	13	120	263	130	5	558	31	37
AV317	3.07	0.26	0.08	104	60	24	49	<6	37	14	107	348	163	8	578	42	31
AV318	2.94	0.31	0.08	118	66	29	57	8	35	14	99	403	166	7	625	51	28
AV319	2.85	0.31	0.07	127	84	34	62	<6	46	15	96	387	171	5	523	42	33
AV320	2.68	0.31	0.07	123	75	38	68	<6	36	12	86	374	152	5	549	42	32
AV321	3.12	0.25	0.09	86	55	23	48	<6	20	14	99	355	145	7	705	28	31
AV322	2.99	0.29	0.08	101	58	25	51	<6	28	13	93	384	153	8	618	33	31
AV454	2.11	0.52	0.06	252	122	40	47	8	52	17	72	545	248	6	489	43	173
AV455	1.77	0.49	0.05	252	131	28	55	<6	54	15	58	524	248	4	414	46	182
AV456	2.52	0.26	0.04	156	100	20	45	<6	47	15	91	287	187	6	453	25	106
AV457	2.43	0.31	0.06	143	81	36	43	<6	44	15	83	327	163	7	504	38	58
AV459	3.00	0.21	0.07	89	63	24	27	<6	24	12	114	254	129	7	524	25	121
AV460	3.03	0.19	0.09	78	44	18	24	<6	14	14	116	257	118	6	584	28	140
AV489	3.44	0.20	0.08	70	46	12	32	<6	18	17	125	293	117	8	648	17	34
AV491	2.61	0.73	0.08	211	29	23	21	7	92	16	74	730	307	12	578	67	35
AV162	3.06	0.05	0.07	75	34	13	20	13	10	12	135	225	113	6	602	<12	172
AV163	3.02	0.12	0.07	90	37	7	20	14	17	11	139	280	119	3	701	21	318
AV164	2.43	0.23	0.05	263	97	15	60	9	52	15	90	548	214	3	506	40	64
AV448	2.41	0.46	0.09	128	57	17	23	<6	52	11	90	736	175	9	524	34	47
AV449	3.49	0.08	0.08	54	51	31	40	<6	20	14	122	207	128	7	636	22	42
AV450	2.68	0.75	0.07	218	46	32	27	9	79	20	88	656	303	14	584	64	26
AV451	3.30	0.31	0.08	118	70	24	51	<6	64	16	129	295	273	15	565	61	50
AV486	2.91	0.16	0.08	57	38	26	59	<6	18	12	94	248	112	4	588	22	28
AV487	2.72	0.19	0.07	58	29	12	29	<6	<3	11	84	272	111	3	612	19	22
AV488	2.73	0.20	0.07	91	69	19	48	<6	20	12	87	277	124	6	564	15	29

Sample	labnr	Location	x-coord	y-coord	Terrace	Alt	RelAlt	Depth	UpstrMedian	SiO2	TiO2	Al2O3	Fe2O3	MnO	MgO	CaO	Na2O
AV292		La Merlaude	534.400	5102.200	Fx3	265	12	2.00	-6.8	1800	66.91	1.41	11.93	6.19	0.07	2.83	4.41	1.40
AV293		La Merlaude	534.400	5102.200	Fx3	265	12	2.00	-6.8	700	73.20	0.93	11.12	3.86	0.05	1.59	2.57	1.48
AV294		La Merlaude	534.400	5102.200	Fx3	265	12	2.00	-6.8	1600	69.65	1.58	10.89	7.36	0.09	2.66	3.43	1.38
AV360		La Varrenne	520.400	5072.800	Fx3	311	15	7.00	29.8	250	65.01	1.12	14.38	5.68	0.07	2.27	2.77	1.79
AV361		La Varrenne	520.400	5072.800	Fx3	311	15	7.00	29.8	500	66.67	1.32	12.09	6.49	0.09	2.72	2.96	1.58
AV362		La Varrenne	520.400	5072.800	Fx3	311	15	7.00	29.8	700	65.78	1.48	11.72	7.05	0.10	2.92	3.13	1.56
AV363		Sabl Rulhat	520.400	5073.600	Fx3	315	15	4.00	27.6	600	65.40	1.18	12.24	5.74	0.08	3.65	4.02	1.56
AV364		Sabl Rulhat	520.400	5073.600	Fx3	315	15	4.00	27.6	900	68.97	1.23	11.73	5.29	0.07	2.84	3.85	1.57
AV365		Sabl Rulhat	520.400	5073.600	Fx3	315	15	6.00	27.6	1200	70.94	1.21	11.04	5.94	0.09	1.99	2.19	1.38
AV366		Sabl Rulhat	520.400	5073.600	Fx3	315	15	6.00	27.6	1200	71.80	1.09	10.77	4.81	0.07	2.10	2.80	1.43
AV367		Les Genevriers	520.500	5074.000	Fx3	317	16	4.00	27.0	1600	70.63	1.10	11.45	4.70	0.07	2.56	3.45	1.66
AV368		Les Genevriers	520.500	5074.000	Fx3	317	16	4.00	27.0	1400	64.88	1.57	11.42	7.06	0.11	3.78	4.50	1.61
AV280		Fontsalive	533.800	5103.500	Fx3	282	12	2.00	-7.8	800	74.47	0.81	11.54	3.49	0.04	1.67	2.62	1.56
AV281		Fontsalive	533.800	5103.500	Fx3	282	12	2.00	-7.8	900	72.30	0.89	12.15	4.50	0.05	1.93	2.78	1.51
AV282		Fontsalive	533.800	5103.500	Fx3	282	12	2.00	-7.8	600	69.01	1.38	11.69	6.23	0.07	3.18	3.72	1.37
AV283		Fontsalive	533.800	5103.500	Fx3	282	12	2.00	-7.8	1600	53.73	2.25	13.62	10.28	0.13	6.01	7.42	1.49
AV284		Fontsalive	533.800	5103.500	Fx3	282	12	2.50	-7.8	1800	66.39	1.32	12.85	5.71	0.07	2.62	4.35	1.65
AV285		Fontsalive	533.800	5103.500	Fx3	282	12	2.50	-7.8	1300	62.02	1.67	12.36	7.58	0.10	4.48	5.66	1.61
AV286		Fontsalive	533.800	5103.500	Fx3	282	12	1.50	-7.8	1500	69.43	1.23	11.49	5.16	0.07	2.84	3.86	1.49
AV244		Sanat	527.800	5086.700	Fx3	293	12	2.00	13.8	900	63.89	1.78	11.96	7.83	0.11	4.15	5.27	1.88
AV245		Sanat	527.800	5086.700	Fx3	293	12	2.00	13.8	1400	68.79	1.26	11.91	5.62	0.08	2.86	3.78	1.79
AV246		Sanat	527.800	5086.700	Fx3	293	12	2.00	13.8	1500	61.56	1.95	11.84	8.67	0.13	4.64	5.88	1.90
AV247		Sanat	527.800	5086.700	Fx3	293	12	2.00	13.8	1000	66.95	1.37	11.88	6.20	0.09	3.50	4.03	1.79
AV248		Sanat	527.800	5086.700	Fx3	293	12	2.00	13.8	600	67.62	1.34	11.94	5.99	0.09	3.27	4.03	1.76
AV170		Mariol	537.800	5097.000	Fx3	283	15	2.80	-1.8	700	65.87	1.38	13.07	6.82	0.09	2.80	3.46	1.65
AV171		Mariol	537.800	5097.000	Fx3	283	15	2.80	-1.8	600	68.83	1.04	13.71	4.74	0.06	2.07	2.71	1.89
AV172		Mariol	537.800	5097.000	Fx3	283	15	2.70	-1.8	800	67.99	1.13	13.31	5.26	0.07	2.44	3.32	1.67
AV173		Mariol	537.800	5097.000	Fx3	283	15	2.70	-1.8	900	69.29	1.16	12.72	5.35	0.07	2.19	2.93	1.67
294	164	CulhatB	525.275	5078.675	Fx3	302	12	4.75	21.0	380	66.06	1.59	12.34	6.68	0.09	4.00	4.18	2.29
295	165	CulhatB	525.275	5078.675	Fx3	302	12	4.30	21.0	600	69.46	1.20	11.86	4.95	0.06	2.81	3.69	2.15
296	166	CulhatB	525.275	5078.675	Fx3	302	12	4.50	21.0	800	69.46	1.35	12.51	5.03	0.06	2.66	3.81	2.36
365	233	Rulhat	521.000	5073.550	Fx3	318	17	13.00	27.6	370	71.17	0.97	12.29	4.12	0.05	2.08	2.45	2.37
366	234	Rulhat	521.000	5073.550	Fx3	318	17	13.30	27.6	620	73.42	0.92	11.20	3.60	0.05	1.94	2.65	2.28
367	235	Rulhat	521.000	5073.550	Fx3	318	17	13.00	27.6	1050	70.66	1.06	11.77	4.22	0.05	2.21	3.32	2.43
311	180	Mortaix	519.400	5070.825	Fx3	328	15	4.00	30.9	280	63.55	1.50	13.65	6.68	0.09	4.51	4.70	2.41
312	181	Mortaix	519.400	5070.825	Fx3	328	15	4.00	30.9	950	63.01	1.68	12.89	6.74	0.09	3.98	5.38	2.56
313	182	Mortaix	519.400	5070.825	Fx3	328	15	7.00	30.9	440	69.44	1.17	12.71	4.92	0.06	2.84	3.35	2.23
304	174	Perignat	517.625	5063.325	Fx3	336	12	8.50	38.9	460	69.70	1.14	13.30	4.76	0.06	2.33	3.01	2.27
305	175	Perignat	517.625	5063.325	Fx3	336	12	8.50	38.9	350	64.38	1.78	12.09	7.87	0.10	4.38	4.28	2.03
306	176	Perignat	517.625	5063.325	Fx3	336	12	9.30	38.9	620	65.26	1.64	11.91	6.99	0.09	4.60	5.35	2.05
307	177	Perignat	517.625	5063.325	Fx3	336	12	8.50	38.9	440	68.44	1.36	12.24	5.46	0.07	3.12	4.08	2.17
308	178	Perignat	517.625	5063.325	Fx3	336	12	8.50	38.9	1060	68.66	1.35	12.10	5.61	0.07	2.97	4.34	2.25
309	179	Perignat	517.625	5063.325	Fx3	336	12	9.00	38.9	180	69.05	1.03	15.03	4.85	0.06	2.05	2.21	2.32
AV147		Les Montagniers	536.100	5088.700	Fx3	228	15	2.30	6.5	1500	60.89	1.90	12.07	7.80	0.12	5.00	6.00	1.70
AV148		Les Montagniers	536.100	5088.700	Fx3	228	15	2.30	6.5	1400	61.06	1.84	12.01	7.62	0.11	5.04	6.13	1.73
AV149		Les Montagniers	536.100	5088.700	Fx3	228	15	2.50	6.5	2000	67.63	1.36	11.57	5.45	0.08	3.39	4.13	1.66
AV150		Les Montagniers	536.100	5088.700	Fx3	228	15	1.80	6.5	800	70.40	1.01	11.58	4.16	0.06	2.47	3.18	1.65
AV151		Les Montagniers	536.100	5088.700	Fx3	228	15	1.80	6.5	2000	66.09	1.43	11.89	5.62	0.08	3.35	4.63	1.76
AV33		Les Montagniers	536.100	5088.700	Fx3	288	15	1.50	6.5	1000	72.99	1.07	11.56	3.82	0.06	2.35	3.13	1.78
AV34		Les Montagniers	536.100	5088.700	Fx3	288	15	1.80	6.5	500	70.40	1.20	11.91	4.16	0.06	2.54	3.56	1.89
AV369		Les Genevriers	520.500	5074.000	Fx2	317	15	6.00	27.0	1300	70.14	1.03	11.17	4.49	0.06	2.42	3.49	1.50
AV370		Les Genevriers	520.500	5074.000	Fx2	317	15	6.00	27.0	1000	74.43	0.72	11.07	3.22	0.04	1.50	2.23	1.49
AV323		La Latte W	533.800	5099.300	Fx2	275	15	2.00	-3.8	1300	78.83	0.80	9.70	3.14	0.05	0.68	1.31	1.21
AV324		La Latte W	533.800	5099.300	Fx2	275	15	2.00	-3.8	800	79.12	0.45	10.73	1.53	0.02	0.67	1.38	1.42
AV325		La Latte W	533.800	5099.300	Fx2	275	15	2.00	-3.8	1300	81.93	0.24	9.69	0.81	0.01	0.28	0.61	1.23
AV326		La Latte W	533.800	5099.300	Fx2	275	15	2.00	-3.8	800	80.59	0.35	10.68	1.36	0.02	0.50	0.99	1.36
AV327		La Latte W	533.800	5099.300	Fx2	275	15	2.50	-3.8	1600	81.90	0.45	9.31	1.78	0.02	0.60	1.12	1.20
AV328		La Latte W	533.800	5099.300	Fx2	275	15	2.50	-3.8	700	79.40	0.51	11.06	1.85	0.03	0.53	1.12	1.46
AV142		Les Montagniers	536.100	5088.700	Fx2	288	14	3.00	6.5	1400	75.95	0.26	12.52	1.20	0.01	0.57	0.72	1.96
AV143		Les Montagniers	536.100	5088.700	Fx2	288	14	3.00	6.5	1000	77.35	0.24	12.30	1.03	0.01	0.50	0.68	1.87
AV144		Les Montagniers	536.100	5088.700	Fx2	288	14	3.00	6.5	1400	77.14	0.25	12.46	1.02	0.01	0.50	0.72	1.99

Sample	K2O	P2O5	BaO	V	Cr	Co	Ni	Cu	Zn	Ga	Rb	Sr	Zr	Nb	Ba	La	Pb
AV292	2.55	0.40	0.07	192	114	25	54	9	56	15	90	441	181	4	509	38	34
AV293	3.10	0.25	0.08	99	65	26	52	<6	32	13	103	317	148	8	560	24	35
AV294	2.45	0.34	0.06	217	108	33	61	<6	70	13	79	359	207	9	437	29	50
AV360	3.03	0.33	0.07	155	80	26	50	14	63	21	122	337	257	15	583	52	43
AV361	2.78	0.28	0.07	167	100	25	55	<6	67	15	96	301	255	13	546	55	37
AV362	2.64	0.30	0.06	210	113	39	61	<6	74	16	92	305	264	18	542	72	35
AV363	2.50	0.34	0.07	158	103	40	85	13	48	15	94	405	206	7	588	33	31
AV364	2.49	0.30	0.06	147	87	28	59	<6	39	15	87	390	180	4	514	45	28
AV365	2.91	0.24	0.07	158	70	33	48	<6	63	15	104	256	181	9	609	49	32
AV366	2.66	0.26	0.07	144	70	28	46	12	40	14	92	306	162	<2	553	43	29
AV367	2.52	0.34	0.07	136	70	31	55	7	35	16	88	390	172	<2	552	44	26
AV368	2.35	0.38	0.06	225	115	37	73	10	61	14	78	422	200	6	522	45	31
AV280	3.06	0.27	0.08	90	56	20	49	10	24	13	106	342	134	4	665	30	34
AV281	3.05	0.28	0.08	105	63	28	49	<6	30	15	107	347	143	5	609	24	37
AV282	2.54	0.32	0.05	170	114	33	85	<6	56	15	89	365	179	6	460	32	35
AV283	1.57	0.67	0.06	346	193	41	116	14	90	17	44	636	260	12	488	56	44
AV284	2.62	0.43	0.09	161	89	27	64	<6	50	14	80	480	183	8	634	35	37
AV285	2.13	0.52	0.06	241	136	34	89	12	65	15	67	539	222	7	522	50	43
AV286	2.71	0.36	0.07	161	86	38	69	10	45	13	91	439	166	4	593	35	30
AV244	2.17	0.43	0.05	259	142	45	74	9	75	15	74	483	220	8	423	38	28
AV245	2.64	0.36	0.07	153	82	40	71	8	55	16	89	387	187	10	534	40	33
AV246	2.06	0.50	0.06	293	151	39	76	7	83	14	60	522	222	8	501	59	25
AV247	2.56	0.33	0.05	173	102	31	89	17	71	15	92	385	197	10	475	38	30
AV248	2.48	0.34	0.06	179	95	35	69	10	60	13	85	405	182	6	494	33	30
AV170	2.95	0.38	0.07	208	95	43	74	14	79	17	117	377	229	9	560	51	34
AV171	3.68	0.20	0.06	127	67	32	78	12	52	16	156	337	190	2	536	45	41
AV172	3.25	0.30	0.07	148	77	55	69	8	48	15	123	385	161	9	619	39	34
AV173	3.19	0.28	0.07	152	89	34	64	<6	48	16	125	342	194	7	520	46	41
294	2.22	0.34	0.05	364	181	59	88	44	78	16	90	497	221	24	692	46	16
295	2.52	0.35	0.07	223	97	64	57	16	38	18	90	472	217	19	773	56	5
296	2.50	0.37	0.06	283	88	40	41	22	47	16	91	503	211	22	801	46	8
365	2.88	0.20	0.06	252	48	35	31	8	59	21	115	348	162	17	749	<7	14
366	2.72	0.22	0.06	239	28	39	29	<4	34	16	92	363	174	19	771	<7	12
367	2.80	0.29	0.08	224	48	34	23	8	41	19	87	449	192	21	877	30	5
311	2.17	0.35	0.06	319	196	52	100	24	83	19	104	551	259	28	684	80	3
312	2.22	0.44	0.07	350	163	45	70	28	69	19	80	628	291	30	765	40	5
313	2.70	0.31	0.08	252	76	38	49	21	55	18	148	439	207	21	789	17	12
304	2.72	0.27	0.07	201	92	44	49	10	79	19	140	429	206	20	785	37	7
305	2.18	0.33	0.06	415	216	47	104	21	95	18	100	481	267	27	683	47	<1
306	1.92	0.43	0.07	352	201	43	98	23	74	18	59	583	278	29	647	61	5
307	2.27	0.34	0.07	330	132	40	60	17	61	19	94	502	232	24	705	46	8
308	2.28	0.39	0.08	288	124	38	49	15	54	18	76	526	236	24	781	51	12
309	3.01	0.22	0.07	240	91	46	35	17	75	19	205	345	247	21	782	29	12
AV147	2.05	0.50	0.03	538	150	44	31	13	115	17	66	705	311	25	1182	103	60
AV148	2.22	0.49	0.05	541	168	60	21	13	112	14	81	710	327	24	1132	130	34
AV149	2.83	0.35	0.05	354	80	29	<10	<6	83	16	120	504	208	18	1138	72	40
AV150	3.28	0.29	0.07	251	52	39	<10	<6	64	18	133	455	193	17	1106	51	35
AV151	2.85	0.41	0.06	405	91	48	<10	<6	83	19	118	594	256	21	1200	64	32
AV33	3.14	0.27	0.07	126	82	28	60	20	33	16	130	419	135	16	980	72	17
AV34	3.08	0.31	0.06	144	82	37	60	19	42	19	132	481	175	21	912	51	19
AV369	2.50	0.32	0.08	133	72	20	47	13	28	15	83	388	156	5	560	32	36
AV370	2.92	0.22	0.08	77	41	23	41	7	23	13	100	298	136	3	651	29	31
AV323	**3.55**	**0.05**	**0.07**	**78**	**26**	**26**	**28**	**<6**	**22**	**12**	**118**	**199**	**130**	**2**	**527**	**29**	**28**
AV324	3.72	0.11	0.09	43	23	34	39	<6	8	12	127	238	101	<2	626	22	29
AV325	4.06	0.07	0.09	14	10	27	35	<6	<3	8	137	190	75	2	714	<12	29
AV326	3.84	0.11	0.09	22	26	25	34	<6	6	12	129	220	100	2	649	16	29
AV327	3.34	0.10	0.07	42	24	30	38	<6	8	14	116	191	102	3	581	19	30
AV328	3.81	0.11	0.09	43	27	31	39	<6	12	12	130	244	145	4	672	43	29
AV142	4.48	0.09	0.08	38	<82	27	<60	<6	30	15	210	241	60	10	1022	47	47
AV143	4.52	0.08	0.08	22	<82	36	<60	<6	21	17	206	251	72	8	1099	60	44
AV144	4.49	0.09	0.08	16	<82	21	<60	<6	26	14	204	250	62	9	1035	34	50

Sample	labnr	Location	x-coord	y-coord	Terrace	Alt	RelAlt	Depth	UpstrMedian	SiO2	TiO2	Al2O3	Fe2O3	MnO	MgO	CaO	Na2O
AV145		Les Montagniers	536.100	5088.700	Fx2	288	14	2.70	6.5	1000	76.67	0.40	11.63	1.64	0.02	0.95	1.17	1.79
AV146		Les Montagniers	536.100	5088.700	Fx2	288	14	2.60	6.5	1500	76.90	0.37	11.23	1.44	0.02	0.80	1.05	1.65
AV31		Les Montagniers	536.100	5088.700	Fx2	288	15	2.50	6.5	1400	80.52	0.19	10.69	0.82	0.01	0.44	0.59	1.60
AV32		Les Montagniers	536.100	5088.700	Fx2	288	15	2.80	6.5	710	78.93	0.28	12.18	1.23	0.02	0.59	0.78	2.03
AV152		Hauterive	534.000	5104.000	Fx2	265	10	5.00	-9.0	600	73.47	0.91	12.69	3.65	0.05	1.53	1.53	1.92
AV153		Hauterive	534.000	5104.000	Fx2	265	10	4.70	-9.0	300	68.65	1.07	14.63	4.18	0.05	1.47	2.14	1.88
AV154		Hauterive	534.000	5104.000	Fx2	265	10	4.60	-9.0	500	69.09	0.96	14.15	4.21	0.05	1.74	2.52	1.92
AV155		Hauterive	534.000	5104.000	Fx2	265	10	4.30	-9.0	2000	79.86	0.49	9.81	1.91	0.02	0.79	1.46	1.35
AV156		Hauterive	534.000	5104.000	Fx2	265	10	4.20	-9.0	1400	76.23	0.63	10.97	2.55	0.03	1.21	1.97	1.47
AV157		Hauterive	534.000	5104.000	Fx2	265	10	4.10	-9.0	2000	74.71	0.69	11.46	2.71	0.03	1.25	1.93	1.56
AV8		Hauterive	534.000	5104.000	Fx2	265	10	4.00	-9.0	2000	79.11	0.63	9.89	2.06	0.03	1.03	1.56	1.47
AV25		Hauterive	534.000	5104.000	Fx2	265	10	4.50	-9.0	1000	79.18	0.48	10.59	1.68	0.02	0.80	1.10	1.55
AV26		Hauterive	534.000	5104.000	Fx2	265	10	4.70	-9.0	710	76.98	0.68	11.61	2.53	0.03	1.09	1.73	1.73
AV27		Hauterive	534.000	5104.000	Fx2	265	10	5.00	-9.0	500	75.96	0.85	11.99	3.14	0.04	1.32	1.72	1.69
AV425a		Les Pinots	536.800	5097.200	Fx1	272	10	5.00	-1.8	400	72.80	0.51	14.59	2.27	0.03	0.81	1.03	1.81
AV425b		Les Pinots	536.800	5097.200	Fx1	272	10	5.00	-1.8	1400	80.33	0.19	10.97	0.76	0.01	0.29	0.44	1.32
AV426		Les Pinots	536.800	5097.200	Fx1	272	10	5.00	-1.8	1200	79.45	0.36	11.11	1.33	0.01	0.45	0.80	1.35
AV236		Le bas Lachamp	524.500	5084.500	Fx1	305	20	2.50	17.0	500	78.07	0.41	11.31	2.18	0.02	0.63	1.09	1.49
AV237		Le bas Lachamp	524.500	5084.500	Fx1	305	20	4.00	17.0	1200	80.32	0.52	9.88	2.16	0.02	0.78	1.39	1.29
AV238		Le bas Lachamp	524.500	5084.500	Fx1	305	20	4.00	17.0	1200	81.45	0.43	9.90	1.78	0.02	0.65	1.35	1.33
AV239		Le bas Lachamp	524.500	5084.500	Fx1	305	20	4.00	17.0	1400	79.53	0.49	10.01	2.06	0.03	0.94	1.61	1.34
AV240		Le bas Lachamp	524.500	5084.500	Fx1	305	20	4.00	17.0	1400	79.00	0.60	9.66	2.52	0.03	1.00	2.16	1.16
AV241		Le bas Lachamp	524.500	5084.500	Fx1	305	20	4.40	17.0	420	78.54	0.43	11.17	1.76	0.02	0.81	1.46	1.59
AV242		Le bas Lachamp	524.500	5084.500	Fx1	305	20	4.40	17.0	600	82.75	0.35	11.71	1.48	0.01	0.57	1.06	1.61
AV243		Le bas Lachamp	524.500	5084.500	Fx1	305	20	4.40	17.0	700	69.99	0.53	15.27	3.06	0.03	1.50	1.05	1.48
AV220		M Curacon ch fe	535.500	5088.400	Fx1	283	10	3.00	6.3	1400	81.47	0.63	9.46	2.50	0.03	0.47	0.75	1.13
AV221		M Curacon ch fe	535.500	5088.400	Fx1	283	10	3.00	6.3	900	76.08	1.50	9.76	6.16	0.10	0.71	0.92	1.12
AV222		M Curacon ch fe	535.500	5088.400	Fx1	283	10	3.10	6.3	1200	82.34	0.37	9.61	1.66	0.02	0.47	0.84	1.14
AV223		M Curacon ch fe	535.500	5088.400	Fx1	283	10	3.30	6.3	900	82.56	0.34	9.93	1.29	0.02	0.47	0.79	1.29
AV224		M Curacon ch fe	535.500	5088.400	Fx1	283	10	3.30	6.3	900	82.35	0.38	9.73	1.38	0.02	0.45	0.69	1.25
AV225		M Curacon ch fe	535.500	5088.400	Fx1	283	10	3.50	6.3	1000	81.18	0.32	9.99	1.35	0.02	0.38	0.63	1.29
AV215		La Claire	536.900	5097.300	Fx1	271	10	4.10	-2.5	1300	74.18	0.83	12.03	3.45	0.04	0.83	1.24	1.26
AV216		La Claire	536.900	5097.300	Fx1	271	10	4.00	-2.5	600	78.54	0.40	11.53	1.73	0.01	0.34	0.34	0.49
297	167	CulhatO	525.275	5079.350	Fx1	302	12	5.70	21.0	800	77.24	0.72	10.94	2.88	0.03	1.64	2.39	1.79
298	168	CulhatO	525.275	5079.350	Fx1	302	12	6.40	21.0	330	73.05	0.75	12.68	3.18	0.04	1.66	1.94	2.34
299	169	CulhatO	525.275	5079.350	Fx1	302	12	5.70	21.0	1050	74.17	0.79	12.24	3.31	0.04	1.82	2.64	2.40
349	217	Beissat	524.650	5083.225	Fx1	309	18	2.00	18.0	250	75.73	0.61	12.39	2.21	0.02	0.76	1.28	2.64
350	218	Beissat	524.650	5083.225	Fx1	309	18	2.00	18.0	340	77.42	0.51	11.44	1.73	0.02	0.69	1.31	2.51
351	219	Beissat	524.650	5083.225	Fx1	309	18	2.20	18.0	620	81.73	0.42	9.57	1.35	0.01	0.56	1.17	1.91
352	220	Beissat	524.650	5083.225	Fx1	309	18	1.80	18.0	980	84.04	0.58	7.84	2.04	0.02	0.63	1.42	1.50
345	213	TissonnieresW	523.700	5081.325	Fx1	312	21	1.50	19.6	300	78.35	0.35	12.05	1.36	0.01	0.44	0.62	2.60
346	214	TissonnieresW	523.700	5081.325	Fx1	312	21	1.80	19.6	440	79.50	0.43	10.96	1.71	0.02	0.70	0.84	2.23
347	215	Tissonnieres W	523.700	5081.325	Fx1	312	21	2.30	19.6	600	79.45	0.50	10.15	1.87	0.02	0.73	1.05	2.10
348	216	TissonnieresW	523.700	5081.325	Fx1	312	21	2.10	19.6	710	80.77	0.36	10.08	1.32	0.01	0.46	0.81	2.07
AV126		Les jarrauds A	536.200	5099.300	Fx1	271	10	7.00	-3.5	400	76.96	0.41	12.00	1.63	0.02	0.52	0.84	1.85
AV127		Les jarrauds A	536.200	5099.300	Fx1	271	10	7.00	-3.5	1000	77.29	0.45	10.74	1.91	0.02	0.85	1.27	1.54
AV128		Les jarrauds A	536.200	5099.300	Fx1	271	10	7.00	-3.5	800	77.84	0.45	10.89	1.87	0.02	0.81	1.42	1.59
AV129		Les jarrauds A	536.200	5099.300	Fx1	271	10	5.50	-3.5	500	77.45	0.48	11.36	1.78	0.02	0.73	1.27	1.66
AV130		Les jarrauds A	536.200	5099.300	Fx1	271	10	5.50	-3.5	100	64.00	1.03	17.12	5.11	0.04	1.42	1.44	1.67
AV131		Les jarrauds A	536.200	5099.300	Fx1	271	10	5.50	-3.5	150	65.83	0.79	16.44	4.53	0.04	1.28	1.47	1.98
AV132		Les jarrauds A	536.200	5099.300	Fx1	271	10	7.00	-3.5	300	73.80	0.48	13.44	2.42	0.02	0.66	0.96	1.98
AV133		Les jarrauds A	536.200	5099.300	Fx1	271	10	4.30	-3.5	75	71.38	0.76	14.32	2.23	0.03	0.69	0.89	2.05
AV134		Les jarrauds A	536.200	5099.300	Fx1	271	10	3.00	-3.5	1400	77.09	0.48	10.32	2.04	0.03	0.84	1.15	1.62
AV135		Les jarrauds A	536.200	5099.300	Fx1	271	10	3.00	-3.5	1000	75.91	0.54	11.20	2.51	0.03	1.12	1.42	1.63
AV483		Joze	524.000	5079.800	Fx1	313	12	4.00	10.5	700	78.60	0.46	9.56	1.77	0.02	0.86	1.55	1.34
AV484		Joze	524.000	5079.800	Fx1	313	12	4.00	10.5	1400	82.08	0.48	9.01	1.65	0.02	0.72	1.46	1.23
AV485		Joze	524.000	5079.800	Fx1	313	12	4.00	10.5	420	71.85	0.53	13.79	2.50	0.03	0.95	0.93	1.71
AV91		Coudes N9	516.600	5051.000	Fwb	363	20	5.00	54.8	1400	63.28	3.15	10.69	13.55	0.21	1.38	2.47	1.81
AV92		Coudes N9	516.600	5051.000	Fwb	363	20	10.00	54.8	1000	66.51	1.74	12.04	7.01	0.12	1.92	3.86	2.33
AV93		Coudes N9	516.600	5051.000	Fwb	363	20	15.00	54.8	1400	70.96	1.04	10.82	4.26	0.07	1.35	3.92	1.53
AV434		Coudes N9	516.600	5051.000	Fwb	363	20	6.00	54.8	400	52.33	0.20	9.15	0.68	0.02	0.36	17.12	1.26

Sample	K2O	P2O5	BaO	V	Cr	Co	Ni	Cu	Zn	Ga	Rb	Sr	Zr	Nb	Ba	La	Pb
AV145	3.93	0.13	0.07	63	<82	21	<60	<6	34	14	181	278	87	10	970	25	44
AV146	4.19	0.14	0.09	64	<82	29	<60	<6	27	15	175	272	81	10	1091	70	40
AV31	4.19	0.08	0.09	68	<82	42	<60	10	12	11	162	225	40	13	971	31	29
AV32	4.10	0.10	0.08	68	<82	15	<60	14	17	16	176	256	66	8	921	66	29
AV152	3.45	0.23	0.06	225	<82	59	<60	<6	67	17	150	300	235	17	1074	63	36
AV153	3.50	0.25	0.07	261	<82	50	<60	6	91	17	184	350	293	20	1169	95	36
AV154	3.31	0.25	0.07	274	<82	44	<60	<6	87	19	145	403	212	17	1200	79	34
AV155	3.06	0.15	0.07	101	<82	61	<60	<6	26	15	113	276	118	12	968	40	38
AV156	3.19	0.21	0.08	180	<82	53	<60	<6	43	19	123	304	116	11	1101	68	38
AV157	3.31	0.19	0.08	183	<82	41	<60	<6	12	18	130	323	148	13	1126	62	39
AV8	3.17	0.17	0.07	68	<82	29	<60	11	12	16	122	264	86	9	1058	42	22
AV25	3.71	0.12	0.08	68	<82	48	<60	<6	12	17	148	238	73	13	988	48	24
AV26	3.39	0.18	0.07	75	<82	22	<60	13	32	20	138	316	112	13	982	37	16
AV27	3.47	0.19	0.07	109	<82	36	<60	10	21	17	154	291	195	18	955	70	15
AV425a	4.49	0.14	0.07	35	31	25	35	<6	29	19	214	208	216	12	606	37	40
AV425b	4.54	0.08	0.09	35	12	33	35	<6	<3	14	180	186	75	5	716	15	40
AV426	4.12	0.09	0.09	41	19	38	41	<6	<3	15	164	194	104	6	662	<12	39
AV236	3.29	0.14	0.08	39	27	39	54	9	29	14	113	211	95	3	624	26	29
AV237	2.99	0.14	0.07	50	38	46	59	8	25	10	98	228	105	4	602	18	28
AV238	3.16	0.16	0.09	40	21	49	54	<6	14	13	101	241	95	5	684	<12	31
AV239	3.03	0.19	0.08	45	34	33	49	10	17	11	95	240	96	3	625	<12	26
AV240	2.69	0.39	0.08	66	41	49	50	9	19	10	84	275	108	8	625	20	32
AV241	3.21	0.15	0.08	39	28	42	54	<6	18	15	108	238	100	<2	653	<12	28
AV242	4.44	0.12	0.08	27	19	34	44	<6	7	11	119	227	100	5	732	<12	28
AV243	3.04	0.17	0.08	51	34	25	40	<6	19	12	103	231	111	6	605	18	30
AV220	3.28	0.06	0.08	61	41	34	43	<6	15	14	113	171	192	9	574	21	27
AV221	3.00	0.13	0.05	200	66	33	33	<6	65	13	110	166	209	9	435	50	30
AV222	3.09	0.12	0.08	32	42	24	35	6	5	10	114	173	95	7	646	17	31
AV223	3.50	0.08	0.09	22	33	28	46	<6	4	10	116	173	107	4	645	19	31
AV224	3.43	0.08	0.08	29	28	36	51	<6	17	12	114	166	107	<2	611	18	29
AV225	3.71	0.07	0.08	25	23	48	55	<6	20	14	124	167	91	5	669	15	31
AV215	3.52	0.17	0.07	95	73	18	38	<6	39	14	143	190	188	8	585	39	39
AV216	5.31	0.11	0.07	41	43	33	42	9	18	13	250	127	255	15	578	34	89
297	2.64	0.21	0.07	179	14	44	20	<4	5	18	98	331	120	12	749	<7	18
298	3.17	0.17	0.07	166	31	44	19	15	34	17	145	318	136	15	710	40	14
299	2.71	0.22	0.06	172	<14	30	31	11	18	17	88	361	135	15	737	34	11
349	3.23	0.15	0.07	123	<14	45	7	<4	19	14	147	286	162	14	719	<7	8
350	3.16	0.13	0.05	116	<14	52	6	<4	13	21	120	272	104	12	741	<7	14
351	2.94	0.12	0.06	114	<14	41	<2	<4	7	16	98	246	80	9	740	<7	12
352	2.18	0.15	0.04	107	<14	39	6	<4	9	13	70	246	90	12	565	19	13
345	3.47	0.08	0.07	80	<14	52	3	<4	<1	16	130	211	79	11	742	43	18
346	3.13	0.10	0.07	116	<14	92	10	<4	<1	14	109	211	79	10	709	10	10
347	3.13	0.14	0.06	112	<14	63	12	<4	<1	18	105	246	83	10	746	<7	12
348	3.32	0.12	0.06	99	<14	36	2	<4	<1	15	111	218	71	8	790	13	13
AV126	3.97	0.11	0.08	68	10	40	<2	<4	<1	11	162	240	132	12	953	55	21
AV127	3.74	0.13	0.08	68	10	33	<2	<4	<1	13	148	240	99	11	979	44	24
AV128	3.58	0.14	0.08	87	10	30	<2	<4	<1	16	136	245	101	12	1056	49	37
AV129	3.42	0.13	0.07	102	10	38	<2	<4	<1	17	136	244	93	10	1037	65	42
AV130	3.81	0.25	0.04	274	17	147	<2	<4	<1	18	312	251	399	23	1063	123	45
AV131	3.69	0.23	0.06	234	14	126	<2	<4	<1	17	278	263	438	25	1066	124	42
AV132	4.11	0.13	0.06	105	10	61	<2	<4	<1	18	198	252	169	14	998	51	34
AV133	4.36	0.16	0.07	180	10	71	<2	<4	<1	18	229	243	659	32	1293	113	43
AV134	**4.10**	**0.14**	**0.06**	**118**	**10**	**36**	**<2**	**<4**	**<1**	**14**	**190**	**251**	**108**	**12**	**968**	**32**	**43**
AV135	4.04	0.16	0.07	121	10	40	<2	<4	<1	12	184	270	125	13	1047	67	40
AV483	2.94	0.16	0.07	44	33	24	44	<6	<3	11	95	240	98	<2	602	15	29
AV484	3.00	0.16	0.08	39	24	30	36	<6	<3	10	88	244	95	<2	649	16	31
AV485	4.32	0.14	0.09	49	36	16	34	8	32	17	196	214	136	6	654	31	34
AV91	2.78	0.30	0.01	460	82	35	60	12	262	18	141	381	782	50	833	76	16
AV92	3.12	0.34	0.06	239	82	39	60	12	114	19	134	467	463	31	1103	83	15
AV93	2.65	0.20	0.07	133	82	41	60	12	65	16	154	408	253	18	859	59	15
AV434	3.32	0.20	0.11	21	9	17	14	<6	<3	9	109	569	131	9	593	30	34

Sample	labnr	Location	x-coord	y-coord	Terrace	Alt	RelAlt	Depth	UpstrMedian	SiO2	TiO2	Al2O3	Fe2O3	MnO	MgO	CaO	Na2O
AV435		Coudes N9	516.600	5051.000	Fwb	363	20	10.00	54.8	1500	77.95	0.62	10.09	2.50	0.03	0.72	1.10	1.11
AV436		Coudes N9	516.600	5051.000	Fwb	363	20	8.00	54.8	200	68.15	0.92	11.78	7.40	0.06	1.19	2.21	1.33
AV437		Coudes N9	516.600	5051.000	Fwb	363	20	6.00	54.8	1000	70.06	0.95	12.11	4.29	0.07	1.49	3.22	1.95
AV438		Coudes N9	516.600	5051.000	Fwb	363	20	4.00	54.8	900	63.11	2.24	12.44	10.40	0.16	1.65	3.37	1.94
AV439		Coudes N9	516.600	5051.000	Fwb	363	20	2.00	54.8	1700	63.60	2.13	11.11	11.36	0.16	1.41	2.65	1.60
AV469		Coudes N9	516.600	5051.000	Fwb	363	20	6.00	54.8	400	74.07	0.58	11.50	3.40	0.03	0.94	1.49	1.54
AV470		Coudes N9	516.600	5051.000	Fwb	363	20	9.00	54.8	1100	80.92	0.32	9.14	2.62	0.01	0.49	0.85	1.21
AV471		Coudes N9	516.600	5051.000	Fwb	363	20	8.00	54.8	300	59.55	1.13	14.50	6.54	0.05	1.53	4.67	1.47
AV472		Coudes N9	516.600	5051.000	Fwb	363	20	8.00	54.8	300	68.52	1.01	14.57	4.03	0.03	1.23	1.41	1.61
AV473		Coudes N9	516.600	5051.000	Fwb	363	20	10.00	54.8	1000	75.67	0.47	8.89	5.69	0.02	0.81	1.47	1.39
AV474		Coudes N9	516.600	5051.000	Fwb	363	20	8.00	54.8	1500	69.60	1.11	11.30	6.20	0.07	1.54	3.33	1.84
AV475		Coudes N9	516.600	5051.000	Fwb	363	20	10.00	54.8	<16	71.68	0.39	10.88	0.89	0.02	0.37	5.57	1.46
AV476		Coudes N9	516.600	5051.000	Fwb	363	20	10.00	54.8	900	73.26	0.58	10.65	6.47	0.03	0.75	1.09	1.50
AV108		Les Gaves	517.300	5050.400	Fwb	365	20	10.00	55.3	2000	65.21	2.07	11.69	9.39	0.13	2.15	2.51	1.40
AV115		Les Varennes	516.300	5055.900	Fwb	370	20	2.40	50.2	1000	68.45	1.44	12.32	6.91	0.09	1.52	1.79	1.50
AV62		Labinet	528.600	5022.000	Fwb	454	30	3.00	94.0	1000	80.14	0.33	10.82	1.85	0.02	0.48	0.35	1.17
AV63		Labinet	528.600	5022.000	Fwb	454	30	1.50	94.0	500	72.52	1.02	12.39	4.64	0.07	0.67	0.53	1.28
AV258		Bois Relais	532.700	5091.000	Fwb	297	30	2.00	5.0	1300	74.00	0.71	11.50	3.42	0.04	1.19	1.51	1.36
AV259		Bois Relais	532.700	5091.000	Fwb	297	30	2.00	5.0	600	75.52	0.62	12.23	3.02	0.03	0.91	1.00	1.32
AV260		Bois Relais	532.700	5091.000	Fwb	297	30	2.00	5.0	1300	66.64	2.29	11.61	11.34	0.14	1.90	1.65	1.04
AV440		Saladis haute	516.600	5057.700	Fwb	349	25	4.00	47.5	1200	68.20	1.90	10.26	8.75	0.13	1.51	2.26	1.31
AV441		Saladis haute	516.600	5057.700	Fwb	349	25	4.00	47.5	600	76.75	0.39	10.15	3.24	0.02	0.64	1.10	1.32
AV442		Saladis haute	516.600	5057.700	Fwb	349	25	2.50	47.5	500	71.65	1.00	11.40	5.23	0.06	1.27	1.53	1.44
AV443		Saladis haute	516.600	5057.700	Fwb	349	25	4.50	47.5	1000	69.84	1.36	10.98	6.02	0.08	1.48	2.81	1.25
AV444		Saladis haute	516.600	5057.700	Fwb	349	25	5.00	47.5	1200	74.91	0.68	11.36	3.79	0.04	0.62	0.84	0.95
AV445		Saladis haute	516.600	5057.700	Fwb	349	25	6.00	47.5	1400	76.18	0.77	11.01	4.39	0.05	0.67	0.92	1.08
AV446		Saladis haute	516.600	5057.700	Fwb	349	25	7.00	47.5	1400	76.15	0.55	10.13	4.62	0.04	0.70	1.09	1.23
AV461		Coudes haute	516.100	5051.900	Fwa	400	45	6.00	53.0	600	65.75	2.19	13.34	6.46	0.12	1.64	3.25	2.32
AV463		Coudes haute	516.100	5051.900	Fwa	400	45	2.00	53.0	1200	84.99	0.31	5.69	1.44	0.01	0.27	1.42	0.84
AV35		St.Priest	534.575	5096.100	Fwa	294	31	7.00	0.0	710	77.82	1.33	9.61	5.24	0.08	0.52	0.66	1.37
AV36		St.Priest	534.575	5096.100	Fwa	294	31	6.50	0.0	1400	84.78	0.25	8.52	1.47	0.01	0.29	0.37	1.22
AV37		St.Priest	534.575	5096.100	Fwa	294	31	8.00	0.0	1000	79.28	0.88	10.17	3.10	0.05	0.55	0.94	1.44
AV38		St.Priest	534.575	5096.100	Fwa	294	31	6.00	0.0	710	77.34	0.59	10.78	2.31	0.03	0.59	1.02	1.50
327	196	St.Priest	534.575	5096.100	Fwa	294	31	5.00	0.0	600	80.84	0.28	9.91	1.29	0.01	0.36	0.53	1.86
328	197	St.Priest	534.575	5096.100	Fwa	294	31	5.00	0.0	1250	83.69	0.19	9.39	0.82	0.00	0.27	0.43	1.71
AV39		Les Rondeaux	533.700	5101.100	Fwa	293	29	7.00	-5.3	355	78.63	0.82	10.82	2.23	0.03	0.42	0.80	1.67
AV40		Les Rondeaux	533.700	5101.100	Fwa	293	29	7.50	-5.3	1000	79.20	0.64	10.41	2.04	0.03	0.35	0.57	1.53
AV41		Vilena	533.500	5101.400	Fwa	290	27	4.50	-5.4	710	80.33	0.65	10.02	2.66	0.04	0.33	0.54	1.40
AV42		Vilena	533.500	5101.400	Fwa	290	27	4.00	-5.4	710	82.66	0.28	9.93	0.99	0.01	0.22	0.37	1.40
AV43		Vilena	533.500	5101.400	Fwa	290	27	2.50	-5.4	355	74.34	0.59	13.26	2.84	0.03	0.77	0.82	2.08
AV7		Le Debat	533.500	5102.900	Fwa	295	27	3.00	-5.6	1400	69.30	1.41	12.03	5.16	0.06	2.48	3.33	1.81
AV256		Limons	533.500	5090.700	Fwa	308	35	2.50	5.3	900	66.70	1.28	14.58	6.07	0.08	1.87	1.92	1.41
AV257		Limons	533.500	5090.700	Fwa	308	35	2.50	5.3	1000	68.46	1.09	14.93	5.16	0.06	1.70	1.99	1.24
AV295		Bois Laurent	534.300	5096.700	Fwa	290	30	6.00	-0.8	300	70.48	0.71	15.20	3.26	0.03	1.10	1.06	1.53
AV296		Bois Laurent	534.300	5096.700	Fwa	290	30	6.00	-0.8	900	81.46	0.26	10.30	1.13	0.01	0.32	0.41	1.31
AV297		Bois Laurent	534.300	5096.700	Fwa	290	30	6.00	-0.8	1200	80.63	0.40	10.07	1.70	0.02	0.39	0.42	1.27
AV298		Bois Laurent	534.300	5096.700	Fwa	290	30	3.00	-0.8	800	77.71	0.41	12.89	1.66	0.02	0.42	1.22	1.89
AV299		Bois Laurent	534.300	5096.700	Fwa	290	30	3.00	-0.8	1100	77.07	0.62	11.44	2.58	0.04	0.63	1.43	1.65
AV300		Bois Laurent	534.300	5096.700	Fwa	290	30	4.00	-0.8	1100	78.72	0.45	11.06	1.88	0.02	0.48	1.14	1.45
AV301		Ch Maulmont	534.400	5096.200	Fwa	290	30	6.00	-0.5	500	73.60	0.59	13.30	3.03	0.03	0.76	0.74	1.54
AV302		Ch Maulmont	534.400	5096.200	Fwa	290	30	6.00	-0.5	1300	75.60	0.66	10.41	2.69	0.04	1.36	1.97	1.35
AV303		Ch Maulmont	534.400	5096.200	Fwa	290	30	6.00	-0.5	600	73.79	0.52	13.72	2.18	0.02	0.60	1.42	1.83
AV304		Ch Maulmont	534.400	5096.200	Fwa	290	30	7.00	-0.5	400	81.72	0.15	10.95	0.41	0.00	0.13	0.00	0.82
AV313		Les Gilberts	533.800	5099.100	Fwa	295	32	4.00	-3.8	1200	79.77	0.38	10.30	1.96	0.01	0.33	0.40	0.85
AV314		Les Gilberts	533.800	5099.100	Fwa	295	32	4.00	-3.8	500	78.24	0.36	11.70	1.58	0.01	0.46	0.62	1.47
AV315		Les Gilberts	533.800	5099.100	Fwa	295	32	4.00	-3.8	500	78.45	0.32	12.04	1.62	0.01	0.44	0.51	1.42
AV316		Les Gilberts	533.800	5099.100	Fwa	295	32	3.00	-3.8	900	80.03	0.39	11.29	1.51	0.02	0.38	0.62	1.42
AV329		L'etang Garmy	529.400	5083.800	Fwa	326	40	4.00	11.0	500	80.00	0.37	11.62	2.00	0.02	0.70	0.81	1.41
AV330		L'etang Garmy	529.400	5083.800	Fwa	326	40	4.00	11.0	1200	81.95	0.27	9.35	1.38	0.01	0.49	0.72	1.22
AV331		L'etang Garmy	529.400	5083.800	Fwa	326	40	3.00	11.0	420	73.46	0.68	13.80	3.33	0.04	1.00	1.19	1.70
AV332		L'etang Garmy	529.400	5083.800	Fwa	326	40	3.00	11.0	1000	80.51	0.35	10.15	1.73	0.02	0.66	0.83	1.29

Sample	K2O	P2O5	BaO	V	Cr	Co	Ni	Cu	Zn	Ga	Rb	Sr	Zr	Nb	Ba	La	Pb
AV435	2.76	0.14	0.08	60	40	29	31	<6	18	13	114	198	121	6	576	28	83
AV436	3.05	0.18	0.07	123	84	24	33	<6	52	15	159	199	325	20	569	61	98
AV437	3.09	0.33	0.10	115	32	36	29	<6	38	17	112	387	207	5	682	53	74
AV438	2.89	0.37	0.06	350	53	42	18	<6	128	17	105	381	510	15	547	75	59
AV439	2.75	0.30	0.04	327	51	31	13	<6	125	16	101	300	408	12	444	65	83
AV469	3.15	0.10	0.08	55	52	18	30	<6	23	14	205	222	176	10	595	42	51
AV470	3.01	0.12	0.08	26	26	19	33	<6	<3	11	117	178	89	4	601	16	79
AV471	3.27	0.39	0.07	146	101	18	39	8	64	19	181	278	358	21	502	85	182
AV472	3.68	0.18	0.06	109	84	34	44	<6	51	18	197	192	354	20	563	82	84
AV473	2.54	0.17	0.07	49	40	13	23	<6	<3	8	107	200	111	6	535	13	96
AV474	2.82	0.35	0.06	124	37	16	18	<6	27	14	104	366	213	2	554	40	98
AV475	3.91	0.85	0.12	27	17	30	33	<6	<3	11	135	436	306	17	863	48	44
AV476	3.39	0.15	0.07	67	42	25	26	<6	11	16	152	189	137	6	614	33	360
AV108	2.86	0.29	0.01	414	145	45	60	12	189	18	141	309	524	31	903	103	15
AV115	2.91	0.24	0.01	286	82	33	60	12	134	14	167	278	311	24	822	65	15
AV62	4.04	0.08	0.08	68	82	48	60	12	17	15	184	161	65	12	975	34	16
AV63	3.74	0.12	0.06	72	82	22	60	22	91	18	230	161	325	27	941	83	14
AV258	3.05	0.23	0.08	71	39	22	44	<6	21	12	106	247	114	<2	602	31	35
AV259	3.24	0.19	0.08	60	34	24	47	6	29	14	117	193	119	5	621	22	34
AV260	2.45	0.30	0.03	363	132	47	42	<6	127	16	85	202	283	9	293	58	31
AV440	2.81	0.22	0.04	271	140	32	24	<6	84	14	98	204	342	18	4227	73	96
AV441	3.19	0.12	0.08	37	33	9	19	<6	<3	11	108	189	97	7	598	<12	>500
AV442	2.93	0.18	0.08	112	76	19	35	<6	36	12	117	67	304	22	554	89	299
AV443	2.48	0.28	0.06	173	88	25	28	<6	54	16	85	310	187	8	512	39	97
AV444	2.71	0.14	0.06	69	36	16	26	<6	23	15	108	164	108	5	505	28	126
AV445	2.68	0.14	0.07	84	68	24	30	<6	28	13	100	175	141	4	485	26	103
AV446	2.92	0.14	0.07	58	49	21	25	<6	9	12	108	182	106	7	573	17	180
AV461	3.39	0.14	0.04	261	52	26	23	<6	77	18	107	388	476	11	398	35	37
AV463	1.65	0.57	0.07	17	133	94	246	64	46	8	77	385	183	8	565	18	79
AV35	3.41	0.09	0.04	159	82	28	60	10	71	16	138	190	152	18	871	52	19
AV36	3.31	0.09	0.07	68	82	41	60	10	12	10	136	180	46	8	946	32	23
AV37	3.76	0.11	0.06	121	82	36	60	10	40	15	155	241	122	25	864	37	27
AV38	3.35	0.12	0.07	68	82	31	60	12	31	14	130	224	65	14	989	37	21
327	3.34	0.07	0.07	68	82	54	60	10	12	15	139	207	65	9	773	8	11
328	3.69	0.06	0.08	68	82	63	60	10	12	15	137	199	57	7	852	15	17
AV39	3.58	0.10	0.11	68	82	42	60	10	17	15	141	235	204	19	1469	74	20
AV40	3.80	0.08	0.08	68	82	45	60	10	22	15	165	244	197	21	854	66	18
AV41	3.74	0.09	0.07	86	82	36	60	10	12	11	146	191	107	18	899	58	17
AV42	3.97	0.06	0.08	68	82	4	60	10	14	15	150	190	39	10	1062	48	18
AV43	4.06	0.13	0.08	68	82	25	60	15	47	16	179	254	189	16	1092	56	16
AV7	2.76	0.31	0.05	227	82	21	60	22	64	17	109	470	215	31	902	84	13
AV256	2.69	0.36	0.08	156	77	24	56	7	55	15	101	244	212	11	608	51	33
AV257	2.55	0.36	0.08	134	72	18	53	7	44	20	96	248	167	5	648	40	35
AV295	4.10	0.13	0.08	76	50	16	23	10	56	18	189	217	339	18	671	66	36
AV296	4.12	0.07	0.10	20	13	31	41	<6	4	11	148	177	96	3	707	19	32
AV297	3.95	0.07	0.08	34	26	37	56	<6	20	13	144	171	106	5	651	20	30
AV298	3.89	0.13	0.10	38	22	35	47	<6	14	17	138	345	108	3	739	20	30
AV299	3.49	0.11	0.08	54	24	29	34	<6	21	14	115	292	116	<2	599	25	27
AV300	3.69	0.09	0.09	39	26	26	37	<6	11	13	129	260	99	<2	635	35	30
AV301	4.27	0.13	0.10	61	38	23	37	10	43	18	180	175	293	16	693	60	36
AV302	3.15	0.21	0.08	57	36	26	45	<6	13	11	102	281	119	2	579	29	29
AV303	3.82	0.12	0.09	46	21	23	35	<6	20	19	137	332	131	6	667	28	32
AV304	**6.16**	**0.01**	**0.09**	**<5**	**13**	**32**	**35**	**11**	**<3**	**11**	**298**	**103**	**78**	**<2**	**659**	**13**	**39**
AV313	3.54	0.09	0.07	27	16	7	14	<6	13	11	140	134	95	11	600	<12	33
AV314	4.00	0.09	0.09	23	25	26	35	<6	15	14	143	189	138	14	711	19	33
AV315	4.21	0.05	0.09	24	22	23	34	<6	10	13	163	189	99	13	730	33	39
AV316	3.94	0.09	0.09	31	17	36	45	<6	16	13	136	197	139	13	693	32	31
AV329	3.57	0.12	0.08	30	29	26	50	<6	15	15	126	203	104	3	614	18	37
AV330	3.17	0.11	0.08	14	20	36	53	<6	8	13	101	176	80	4	666	14	31
AV331	3.63	0.17	0.08	65	46	26	45	6	40	17	142	247	228	10	661	36	37
AV332	3.44	0.11	0.08	28	23	34	51	<6	10	13	113	189	90	3	657	18	36

Sample	labnr	Location	x-coord	y-coord	Terrace	Alt	RelAlt	Depth	UpstrMedian	SiO2	TiO2	Al2O3	Fe2O3	MnO	MgO	CaO	Na2O
AV333		L'etang Garmy	529.400	5083.800	Fwa	326	40	3.00	11.0	600	79.67	0.34	10.95	1.68	0.02	0.58	0.78	1.35
317	186	Crevant-la-Vein	529.375	5084.000	Fwa	326	41	3.60	14.2	300	73.88	0.53	14.33	2.51	0.02	0.93	0.82	2.49
318	187	Crevant-la-Vein	529.375	5084.000	Fwa	326	41	4.10	14.2	650	83.22	0.24	9.19	1.16	0.01	0.36	0.50	1.61
319	188	Crevant-la-Vein	529.375	5084.000	Fwa	326	41	3.85	14.2	1400	85.02	0.26	9.43	1.17	0.01	0.36	0.49	1.73
300	170	Culhat-E	526.900	5079.350	Fwa	330	40	6.60	19.7	210	72.58	0.71	15.19	2.76	0.03	0.82	1.70	3.15
301	171	Culhat-E	526.900	5079.350	Fwa	330	40	6.70	19.7	360	76.72	0.54	12.59	2.04	0.03	0.82	1.51	2.57
302	172	Culhat-E	526.900	5079.350	Fwa	330	40	6.90	19.7	500	79.27	0.43	11.29	1.70	0.02	0.70	1.18	2.06
303	173	Culhat-E	526.900	5079.350	Fwa	330	40	6.55	19.7	1200	79.66	0.32	11.02	1.27	0.01	0.47	0.81	2.05
362	230	Les Arrats	521.825	5073.175	Fwa	340	36	2.60	28.1	230	72.53	0.61	14.27	2.67	0.03	0.94	0.95	2.67
363	231	Les Arrats	521.825	5073.175	Fwa	340	36	2.90	28.1	520	80.13	0.40	10.48	1.63	0.01	0.64	0.98	1.97
364	232	Les Arrats	521.825	5073.175	Fwa	340	36	2.40	28.1	940	82.60	0.40	9.99	1.65	0.02	0.55	0.89	1.88
323		Perigere	533.000	5093.500	Fvb	324	55	2.85	4.7	420	76.40	0.43	13.17	1.51	0.02	0.40	1.07	3.14
324		Perigere	533.000	5093.500	Fvb	324	55	2.80	4.7	930	79.73	0.27	11.25	1.06	0.01	0.26	0.58	2.47
325		Perigere	533.000	5093.500	Fvb	324	55	2.85	4.7	190	72.08	0.50	15.58	2.04	0.02	0.58	1.08	3.63
326		Perigere	533.000	5093.500	Fvb	324	55	3.30	4.7	1580	80.76	0.27	10.72	0.96	0.01	0.22	0.54	2.29
AV9		Perigere	533.000	5093.500	Fvb	324	55	3.50	4.7	500	74.25	0.63	13.75	2.42	0.03	0.61	1.50	2.48
AV10		Perigere	533.000	5093.500	Fvb	324	55	3.50	4.7	500	73.86	0.51	13.36	1.92	0.02	0.44	1.29	2.37
AV11		Perigere	533.000	5093.500	Fvb	324	55	3.00	4.7	1000	75.07	0.59	13.13	2.03	0.02	0.44	1.12	2.06
AV96		Neschers	513.200	5049.800	VCC	466	78	3.00	46.0	1400	63.11	0.93	16.84	3.81	0.10	0.98	2.75	4.00
AV97		Neschers	513.200	5049.800	VCC	466	78	4.00	46.0	710	63.60	0.88	17.00	3.34	0.09	1.10	3.29	4.09
AV113		Brolac	516.600	5055.200	Fva	375	26	5.00	50.6	1400	80.23	0.36	10.25	1.66	0.01	0.40	0.60	1.28
AV114		Brolac	516.600	5055.200	Fva	375	26	6.00	50.6	2000	78.05	0.39	10.99	2.21	0.02	0.52	0.63	1.31
AV1		Puel Chauvin	533.200	5096.400	Fva	325	53	2.00	0.0	1400	80.16	0.35	10.85	1.24	0.01	0.27	0.55	1.60
AV2		Puel Chauvin	533.200	5096.400	Fva	325	53	2.00	0.0	355	73.09	0.52	14.56	1.82	0.02	0.30	1.00	2.59
AV3		Puel Chauvin	533.200	5096.400	Fva	325	53	4.00	0.0	710	81.48	0.37	10.56	1.23	0.02	0.25	0.57	1.51
AV3		Puel Chauvin	533.200	5096.400	Fva	325	53	5.10	0.0	1000	79.23	0.50	10.68	1.88	0.02	0.41	0.74	1.53
AV180		Puel Chauvin	533.200	5096.400	Fva	325	53	4.70	0.0	1000	78.53	0.43	11.20	1.78	0.02	0.45	0.86	1.56
AV188		Puel Chauvin	533.200	5096.400	Fva	325	53	4.50	0.0	40	74.84	0.64	12.99	2.03	0.02	0.88	0.75	1.45
AV191		Puel Chauvin	533.200	5096.400	Fva	325	53	5.00	0.0	1800	71.12	1.32	10.95	8.26	0.08	1.19	1.41	1.08
AV464		Puel Chauvin	533.200	5096.400	Fva	325	53	1.50	0.0	1200	73.54	0.93	12.39	3.79	0.05	0.38	0.77	1.55
AV465		Ornon	528.700	5078.825	Fva	360	53	6.00	19.1	120	67.49	1.05	14.97	4.75	0.06	1.09	2.29	1.52
359		Ornon	528.700	5078.825	Fva	360	64	8.00	19.1	450	69.11	1.39	11.97	6.21	0.09	1.76	2.78	2.24
360		Ornon	528.700	5078.825	Fva	360	64	2.50	19.1	700	81.47	0.48	9.08	1.84	0.02	0.79	1.10	1.69
361		Ornon	528.700	5078.825	Fva	360	64	2.60	19.1	930	80.43	0.42	9.59	1.72	0.02	0.61	0.99	1.78
342		Fouilhouze	527.125	5077.475	Fva	362	64	2.60	21.2	200	68.79	0.85	15.61	3.88	0.03	1.16	1.02	2.70
343		Fouilhouze	527.125	5077.475	Fva	362	64	3.00	21.2	400	77.29	0.72	11.19	2.85	0.03	0.72	1.19	2.10
344		Fouilhouze	527.125	5077.475	Fva	362	64	3.00	21.2	800	77.02	0.93	10.61	3.75	0.04	0.96	1.59	2.13
AV231		Chez Faure	532.000	5085.900	Fva	341	63	2.50	11.5	600	68.66	0.70	16.40	2.83	0.05	0.38	1.55	3.26
AV232		Chez Faure	532.000	5085.900	Fva	341	63	2.50	11.5	500	68.66	0.65	16.84	2.50	0.04	0.34	1.60	3.21
AV233		Chez Faure	532.000	5085.900	Fva	341	63	2.50	11.5	1200	72.70	0.54	14.84	2.03	0.03	0.35	1.37	2.97
AV261		Rigaudanches	533.000	5095.100	Fva	325	60	8.00	2.0	400	73.75	0.53	13.44	2.54	0.03	0.53	1.00	1.87
AV262		Rigaudanches	533.000	5095.100	Fva	325	60	8.00	2.0	1200	78.54	0.28	11.14	1.37	0.01	0.29	0.59	1.38
AV263		Rigaudanches	533.000	5095.100	Fva	325	60	10.00	2.0	300	73.80	0.54	13.58	2.50	0.02	0.55	0.88	1.69
AV264		Rigaudanches	533.000	5095.100	Fva	325	60	10.00	2.0	210	67.65	0.74	16.30	3.69	0.03	0.92	1.18	2.10
AV265		Rigaudanches	533.000	5095.100	Fva	325	60	10.00	2.0	2000	83.70	0.31	9.71	1.38	0.01	0.33	0.49	1.06
AV266		Rigaudanches	533.000	5095.100	Fva	325	60	6.00	2.0	400	69.58	1.76	12.19	7.78	0.12	0.66	1.43	1.66
AV267		Rigaudanches	533.000	5095.100	Fva	325	60	6.00	2.0	800	77.03	0.64	11.26	2.89	0.04	0.45	1.00	1.60
AV268		Rigaudanches	533.000	5095.100	Fva	325	60	4.00	2.0	900	73.79	0.63	13.50	2.71	0.04	0.36	1.10	2.17
AV269		Rigaudanches	533.000	5095.100	Fva	325	60	4.00	2.0	600	74.10	0.78	12.64	3.20	0.06	0.40	1.14	2.00
AV270		Rigaudanches	533.000	5095.100	Fva	325	60	3.00	2.0	500	69.57	1.59	12.62	7.03	0.13	0.41	0.97	1.97
AV271		Rigaudanches	533.000	5095.100	Fva	325	60	10.00	2.0	900	76.42	1.00	9.31	4.55	0.06	0.78	1.07	1.05
AV340		Drevoux	535.500	5085.900	Fva	330	66	2.00	8.5	400	72.29	0.44	14.60	3.14	0.01	0.55	0.83	1.62
AV341		Drevoux	535.500	5085.900	Fva	330	66	2.00	8.5	800	72.59	0.56	13.15	4.37	0.02	0.56	0.67	1.48
AV342		Drevoux	535.500	5085.900	Fva	330	66	3.00	8.5	900	78.71	0.61	11.01	2.68	0.04	0.43	0.79	1.36
AV343		Drevoux	535.500	5085.900	Fva	330	66	2.50	8.5	600	80.47	0.33	10.98	1.51	0.01	0.31	0.65	1.30
AV344		Drevoux	535.500	5085.900	Fva	330	66	4.00	8.5	600	79.33	0.28	11.00	1.40	0.01	0.27	0.62	1.55
AV345		Drevoux	535.500	5085.900	Fva	330	66	5.00	8.5	1400	83.39	0.25	9.62	1.06	0.01	0.28	0.50	1.04
AV346		Bogros	527.900	5079.700	Fva	359	70	2.00	18.8	500	66.67	1.23	15.99	5.73	0.08	0.71	1.80	2.49
AV347		Bogros	527.900	5079.700	Fva	359	70	2.50	18.8	800	71.92	0.66	14.23	2.89	0.05	0.78	2.08	2.43
AV348		Bogros	527.900	5079.700	Fva	359	70	3.00	18.8	900	77.47	0.51	11.74	2.27	0.02	0.58	1.05	1.46
AV349		Bogros	527.900	5079.700	Fva	359	70	3.00	18.8	1000	80.17	0.39	10.59	1.63	0.02	0.46	0.88	1.45

Sample	K2O	P2O5	BaO	V	Cr	Co	Ni	Cu	Zn	Ga	Rb	Sr	Zr	Nb	Ba	La	Pb
AV333	3.60	0.11	0.07	24	23	31	52	<6	14	14	121	194	95	2	688	12	34
317	3.62	0.07	0.06	110	<14	49	9	6	38	19	184	257	112	11	778	37	7
318	3.01	0.08	0.07	39	<14	75	<2	<4	<1	12	105	176	53	8	809	22	10
319	3.13	0.09	0.07	56	<14	60	<2	<4	<1	13	108	185	44	7	740	10	14
300	2.99	0.12	0.08	162	33	38	8	6	34	18	150	444	287	23	845	44	11
301	2.91	0.09	0.07	125	<14	47	9	<4	10	16	117	343	136	15	771	18	16
302	3.01	0.09	0.06	114	25	52	5	<4	<1	12	113	276	83	12	799	<7	9
303	3.50	0.09	0.09	59	<14	49	<2	<4	<1	13	126	256	87	11	982	10	13
362	3.58	0.10	0.07	122	<14	58	15	5	40	17	238	245	136	12	732	32	16
363	3.04	0.10	0.06	84	<14	48	3	<4	6	14	116	215	70	11	690	12	18
364	2.85	0.11	0.07	64	<14	34	7	<4	11	11	99	228	89	12	808	17	14
323	3.67	0.11	0.09	70	82	33	60	10	12	18	135	376	144	16	903	35	13
324	3.64	0.08	0.08	68	82	58	60	10	12	13	128	289	99	13	928	19	14
325	3.80	0.10	0.08	101	82	44	60	10	25	19	192	393	195	20	942	35	13
326	3.55	0.05	0.08	68	82	65	60	10	12	17	132	259	112	14	874	20	19
AV9	3.88	0.17	0.09	68	82	31	60	12	26	19	141	359	152	19	1221	73	9
AV10	3.92	0.14	0.10	68	82	5	60	10	18	18	142	372	144	21	1277	24	18
AV11	3.76	0.13	0.08	78	82	52	60	14	18	17	145	305	128	20	1157	39	20
AV96	4.66	0.23	0.12	127	82	8	60	12	101	20	157	567	482	32	1601	74	19
AV97	4.51	0.27	0.14	95	82	27	60	12	84	19	144	624	394	28	1743	86	9
AV113	3.27	0.09	0.07	68	82	47	60	12	44	9	165	190	67	10	877	57	14
AV114	3.49	0.10	0.07	68	82	39	60	12	78	13	202	205	88	11	1031	47	19
AV1	3.92	0.08	0.10	68	82	47	60	10	12	14	149	241	105	16	1168	49	19
AV2	4.22	0.09	0.11	68	82	45	60	12	27	19	171	389	195	26	1390	62	16
AV3	4.18	0.09	0.07	68	82	93	60	10	12	15	171	267	105	14	1014	27	19
AV3	3.63	0.08	0.08	68	82	73	60	11	12	16	147	232	94	13	1022	24	16
AV180	3.76	0.13	0.10	35	32	27	46	6	10	13	133	233	133	4	727	23	32
AV188	4.14	0.14	0.09	64	38	25	19	16	43	15	240	173	472	27	649	57	37
AV191	2.75	0.17	0.05	189	81	40	39	<6	62	16	115	179	248	12	419	42	32
AV464	3.51	0.06	0.08	93	27	11	21	<6	42	16	120	248	248	6	615	39	30
AV465	2.87	0.27	0.12	119	34	17	39	<6	39	16	98	424	202	5	943	40	30
359	2.97	0.16	0.07	291	23	45	11	7	72	18	99	456	234	23	765	24	3
360	2.84	0.08	0.06	112	<14	41	<2	<4	<1	13	91	218	67	11	636	9	10
361	3.30	0.12	0.07	114	<14	10	<2	<4	<1	16	101	258	81	12	779	16	10
342	3.46	0.15	0.06	168	26	28	18	14	71	21	212	304	214	21	700	24	11
343	3.32	0.13	0.07	170	<14	37	<2	<4	31	13	124	306	154	18	863	33	21
344	2.89	0.15	0.07	203	<14	55	<2	<4	19	15	100	344	215	21	770	25	12
AV231	4.33	0.13	0.13	68	15	34	47	20	53	17	129	534	307	12	1037	41	27
AV232	4.35	0.12	0.13	58	17	34	50	9	37	19	124	555	268	8	682	46	24
AV233	4.09	0.11	0.12	47	35	33	70	<6	30	17	113	450	217	2	857	38	24
AV261	4.52	0.15	0.09	52	26	35	44	8	34	18	186	277	196	8	683	38	34
AV262	4.45	0.10	0.09	19	12	24	31	<6	5	12	166	226	90	3	719	23	31
AV263	4.43	0.12	0.10	52	39	23	35	11	29	15	187	238	218	9	719	36	36
AV264	4.37	0.18	0.08	85	42	28	38	11	55	20	226	310	230	8	629	59	39
AV265	4.11	0.08	0.09	21	14	41	48	<6	9	11	145	180	105	3	727	17	34
AV266	3.35	0.28	0.06	240	58	34	27	<6	91	14	131	262	766	36	513	103	27
AV267	3.72	0.15	0.07	65	27	36	46	9	32	15	139	256	222	5	609	48	29
AV268	4.05	0.12	0.10	63	20	32	35	<6	31	15	132	341	173	3	764	38	29
AV269	3.91	0.12	0.09	78	23	27	38	<6	43	14	124	323	203	3	692	34	28
AV270	3.88	0.14	0.07	225	54	32	41	<6	110	16	129	300	346	13	615	59	28
AV271	3.56	0.10	0.07	114	45	32	37	<6	46	11	113	182	179	5	524	22	28
AV340	3.79	0.09	0.09	48	35	20	41	11	36	17	181	220	153	4	761	34	33
AV341	3.74	0.09	0.08	67	28	17	24	<6	34	18	175	188	227	9	727	39	35
AV342	3.78	0.11	0.09	70	41	34	37	11	28	14	131	212	215	10	756	19	32
AV343	3.50	0.09	0.09	24	19	44	53	7	14	15	128	197	130	6	709	23	28
AV344	4.00	0.08	0.09	18	20	49	50	8	6	12	132	210	97	<2	770	<12	34
AV345	3.79	0.08	0.09	18	31	31	55	15	<3	13	131	177	99	4	738	27	33
AV346	3.59	0.14	0.09	170	73	30	26	20	84	20	136	431	538	21	755	78	36
AV347	3.99	0.18	0.11	63	27	28	30	<6	30	16	118	435	216	6	883	41	26
AV348	3.45	0.08	0.08	51	26	38	33	14	19	16	122	237	117	6	696	20	30
AV349	3.53	0.14	0.09	32	20	32	35	14	5	14	114	237	102	4	803	27	29

Sample	labnr	Location	x-coord	y-coord	Terrace	Alt	RelAlt	Depth	UpstrMedian	SiO2	TiO2	Al2O3	Fe2O3	MnO	MgO	CaO	Na2O
AV350		Bogros	527.900	5079.700	Fva	359	70	4.00	18.8	600	75.69	0.94	10.95	4.02	0.07	1.10	1.94	1.33
AV351		Bogros	527.900	5079.700	Fva	359	70	4.00	18.8	450	75.75	0.42	13.45	2.03	0.02	0.47	0.83	1.76
AV352		Bogros	527.900	5079.700	Fva	359	70	4.00	18.8	1400	66.62	1.76	11.92	8.30	0.18	1.63	2.78	1.93
AV178		Bogros	527.900	5079.700	Fva	359	70	4.00	18.8	400	67.36	0.77	16.20	3.63	0.06	0.71	1.72	2.55
AV179		Bogros	527.900	5079.700	Fva	359	70	4.10	18.8	500	68.44	0.87	14.49	4.01	0.08	1.05	2.22	2.46
AV353		Beauregard	523.300	5075.400	Fva	371	72	2.00	24.0	1500	67.63	1.49	12.69	7.49	0.14	1.06	2.03	1.84
AV354		Beauregard	523.300	5075.400	Fva	371	72	2.00	24.0	1000	65.32	1.52	14.03	7.98	0.14	1.01	2.16	2.08
AV355		Beauregard	523.300	5075.400	Fva	371	72	2.00	24.0	900	72.36	0.66	12.97	3.29	0.05	0.81	1.63	1.87
AV356		Beauregard	523.300	5075.400	Fva	371	72	5.00	24.0	1000	62.78	1.97	12.69	10.06	0.20	1.47	2.68	1.96
AV357		Beauregard	523.300	5075.400	Fva	371	72	5.00	24.0	900	70.98	0.65	15.03	2.88	0.04	0.62	1.79	2.58
AV358		Beauregard	523.300	5075.400	Fva	371	72	3.50	24.0	500	70.49	0.88	12.42	4.44	0.07	1.41	1.75	1.62
AV359		Beauregard	523.300	5075.400	Fva	371	72	3.50	24.0	1000	76.21	0.43	11.67	2.11	0.02	0.62	1.04	1.60
AV272		Rigaudanches	533.000	5095.100	Fva	325	60	3.00	2.0	900	33.60	9.43	6.66	41.46	0.84	1.42	0.90	0.67
AV111		Cote de Sagnes	517.200	5055.400	Lh	421	72	10.00	50.5	1000	69.84	1.37	13.03	4.24	0.06	0.90	2.09	1.46
AV112		Cote de Sagnes	517.200	5055.400	Lh	421	72	11.00	50.5	500	78.27	0.19	10.48	1.32	0.01	0.19	0.73	0.12
AV89		Lair	518.300	5047.100	Fu	470	100	1.00	59.8	1000	81.21	0.37	9.95	2.42	0.02	0.31	0.32	1.37
AV90		Lair	518.300	5047.100	Fu	470	100	1.40	59.8	710	73.71	0.37	8.92	9.62	0.03	0.25	0.25	1.07
AV101		Issoire W	518.600	5044.300	Fu	423	60	0.50	63.5	500	65.09	1.17	14.38	5.72	0.11	1.83	3.27	2.40
AV102		Issoire W	518.600	5044.300	Fu	423	60	1.10	63.5	1000	64.66	0.70	18.21	2.78	0.06	0.72	2.41	4.20
AV103		Issoire W	518.600	5044.300	Fu	423	60	2.20	63.5	710	62.19	0.93	17.94	3.78	0.09	0.91	3.02	4.22
AV100		Boulade	518.400	5044.400	FuCP	430	65	1.00	62.5	1400	79.25	0.32	8.35	4.89	0.02	0.26	0.52	1.23
AV49		Beaulieu Haute	522.000	5032.900	Ft	480	86	4.00	76.5	710	81.78	0.54	9.06	2.15	0.02	0.51	0.86	1.28
AV50		Beaulieu Haute	522.000	5032.900	Ft	480	86	6.00	76.5	355	76.67	1.08	9.92	3.59	0.05	0.86	1.37	1.32
AV124		Lherat	529.400	5096.000	Ft	379	115	3.00	-1.0	1000	75.80	1.23	9.39	5.12	0.06	1.01	1.57	1.36
AV58		Ouillandre	528.100	5022.000	Fs	420	14	3.75	89.5	710	93.47	0.10	3.08	0.12	0.00	0.08	0.00	0.01
AV59		Ouillandre	528.100	5022.000	Fs	420	14	3.50	89.5	500	93.69	0.05	3.73	0.14	0.00	0.09	0.00	0.04
AV60		Ouillandre	528.100	5022.000	Fs	420	14	3.00	89.5	200	91.69	0.14	4.09	0.19	0.00	0.10	0.00	0.01
AV61		Ouillandre	528.100	5022.000	Fs	420	14	4.00	89.5	250	93.39	0.14	4.06	0.16	0.00	0.16	0.00	0.11
314	183	Girauds Faures	531.150	5079.450	Fs	390	100	2.00	17.7	160	83.10	0.24	9.47	1.06	0.00	0.38	0.50	1.69
315	184	Girauds Faures	531.150	5079.450	Fs	390	100	2.00	17.7	600	91.96	0.05	5.04	0.36	0.00	0.03	0.00	0.20
316	185	Girauds Faures	531.150	5079.450	Fs	390	100	2.00	17.7	1600	97.08	0.03	2.44	0.36	0.00	0.04	0.00	0.03
AV181		Girauds Faures	531.150	5079.450	Fs	390	100	2.00	17.7	900	92.00	0.07	4.29	0.09	0.00	0.11	0.00	0.14
AV182		Girauds Faures	531.150	5079.450	Fs	390	100	2.00	17.7	900	92.97	0.07	4.36	0.09	0.00	0.12	0.00	0.14
AV183		Ch eau Lezoux	530.600	5077.800	Fs	407	115	3.00	18.6	600	90.24	0.14	5.40	0.37	0.00	0.19	0.14	0.28
AV184		Ch eau Lezoux	530.600	5077.800	Fs	407	115	3.00	18.6	300	85.31	0.39	7.00	1.35	0.00	0.48	1.01	0.55
AV185		Ch eau Lezoux	530.600	5077.800	Fs	407	115	3.00	18.6	1000	88.31	0.15	6.40	0.37	0.00	0.18	0.12	0.33
AV73		Mont Celet	520.100	5026.300	Fs	620	224	17.00	81.0	180	78.07	0.51	10.89	1.85	0.01	0.45	0.45	1.00
AV74		Mont Celet	520.100	5026.300	Fs	620	224	16.00	81.0	1000	86.25	0.37	6.37	2.05	0.13	0.31	0.22	0.69
AV75		Mont Celet	520.100	5026.300	Fs	620	224	17.00	81.0	710	86.03	0.50	6.99	1.74	0.02	0.27	0.24	0.64
AV5		Les Poiliers	526.600	5097.700	Fl	393	130	4.00	-1.0	1400	82.63	0.14	9.64	0.21	0.00	0.06	0.00	0.32
AV6		Les Poiliers	526.600	5097.700	Fl	393	130	1.50	-1.0	710	86.36	0.05	8.03	0.38	0.00	0.08	0.00	0.21

Sample	K2O	P2O5	BaO	V	Cr	Co	Ni	Cu	Zn	Ga	Rb	Sr	Zr	Nb	Ba	La	Pb
AV350	2.93	0.22	0.08	110	52	32	40	12	48	16	104	246	170	4	614	38	27
AV351	3.83	0.09	0.10	41	26	32	42	14	24	15	143	254	121	6	723	21	32
AV352	3.48	0.28	0.07	252	75	42	35	<6	119	19	103	324	319	6	587	58	33
AV178	4.37	0.19	0.12	86	25	29	52	8	47	19	147	403	301	8	945	58	37
AV179	4.22	0.22	0.09	98	43	25	37	<6	54	16	129	397	233	6	781	39	29
AV353	3.76	0.28	0.07	222	44	33	32	7	100	16	113	324	283	6	684	49	29
AV354	3.54	0.23	0.07	230	61	36	31	14	116	18	109	382	346	6	658	63	36
AV355	3.96	0.24	0.10	71	35	20	34	9	25	15	121	317	153	4	753	32	32
AV356	3.34	0.29	0.06	302	66	36	26	<6	139	19	98	352	369	11	581	51	30
AV357	4.14	0.11	0.09	63	26	16	21	<6	19	21	123	452	195	4	761	26	31
AV358	3.34	0.21	0.07	106	53	31	49	14	58	18	130	271	184	6	597	31	37
AV359	3.58	0.14	0.08	41	23	34	48	10	17	16	127	248	131	5	670	32	33
AV272	1.40	0.24	0.01	>1000	242	286	<8	<6	597	20	60	97	1024	<2	<24	154	20
AV111	2.66	0.21	0.02	244	82	53	60	12	85	17	130	316	383	25	807	66	10
AV112	6.07	0.10	0.09	68	82	52	60	12	25	7	219	135	67	9	1081	60	31
AV89	3.71	0.07	0.06	68	82	50	60	12	17	16	179	131	99	14	804	76	17
AV90	3.54	0.20	0.06	71	82	17	60	12	67	9	166	130	84	9	826	49	18
AV101	3.04	0.27	0.06	201	82	28	60	12	129	23	125	488	365	26	1093	106	9
AV102	5.03	0.17	0.07	78	82	24	60	12	67	17	154	558	431	29	1110	79	15
AV103	4.69	0.18	0.08	141	82	45	60	12	88	20	130	612	674	41	1167	112	15
AV100	2.88	0.19	0.08	78	82	41	60	12	46	8	102	185	96	12	966	45	17
AV49	2.56	0.09	0.07	68	82	52	60	10	17	12	84	258	93	12	898	32	8
AV50	2.53	0.08	0.06	153	82	49	60	15	40	18	90	332	146	20	981	51	16
AV124	3.25	0.15	0.03	227	149	38	60	10	73	15	117	271	169	16	867	63	14
AV58	2.08	0.03	0.03	68	82	107	60	10	12	5	69	54	53	10	361	32	13
AV59	2.51	0.02	0.04	68	82	139	60	10	12	5	79	60	26	4	562	24	9
AV60	2.59	0.03	0.04	68	82	155	60	10	12	7	87	63	46	15	478	31	23
AV61	2.54	0.05	0.05	68	82	85	60	10	12	7	88	54	80	12	490	40	8
314	3.18	0.07	0.07	68	82		60	10	12	10	182	155	136	10	993	39	21
315	3.21	0.02	0.07	68	82		60	10	12	8	111	105	18	5	739	24	20
316	1.33	0.01	0.01	68	82		60	10	12	9	43	51	12	4	320	24	7
AV181	2.98	0.04	0.04	68	82		60	10	12	12	147	97	8	6	771	26	25
AV182	2.99	0.04	0.07	68	82		60	10	12	12	138	89	4	7	770	16	26
AV183	3.43	0.05	0.05	68	82		60	10	12	11	147	144	66	9	971	51	29
AV184	3.66	0.13	0.06	68	82		60	10	12	13	101	192	126	12	987	46	40
AV185	3.86	0.07	0.04	68	82		60	10	12	10	106	128	98	10	1068	58	38
AV73	4.04	0.13	0.07	68	82	28	60	10	31	17	277	127	380	24	948	80	17
AV74	2.50	0.06	0.07	68	82	73	60	13	12	13	140	90	90	14	963	50	15
AV75	2.75	0.09	0.04	68	82	31	60	14	20	8	171	91	114	14	654	65	19
AV5	6.44	0.02	0.04	68	82	81	60	10	12	12	369	69	155	17	562	48	38
AV6	5.36	0.02	0.03	68	82	47	60	10	12	13	285	56	26	13	385	47	31

DORE DATA

Sample	labnr	Location	x-coord	y-coord	Terrace	Alt	Relalt	depth	Upstr	Median	SiO2	TiO2	Al2O3	Fe2O3	MnO	MgO	CaO	Na2O
AV337		Ferrat	535.70	5084.00	FzD	281	0.0	0.00	12.5	1200	81.65	0.08	10.78	0.25	0.00	0.09	0.21	1.39
AV338		Ferrat	535.70	5084.00	FzD	281	0.0	0.00	12.5	1000	77.68	0.28	12.65	1.13	0.01	0.43	0.43	1.61
AV339		Ferrat	535.70	5084.00	FzD	281	0.0	0.00	12.5	900	83.85	0.07	9.81	0.28	0.00	0.13	0.23	1.29
AV452		Bas de Chabanne	534.90	5088.10	FzD	275	0.0	0.00	8.0	500	78.75	0.28	11.61	0.77	0.02	0.30	0.52	1.58
AV453		Bas de Chabanne	534.90	5088.10	FzD	275	0.0	0.00	8.0	300	78.26	0.32	11.74	0.87	0.02	0.33	0.51	1.53
AV466		Puy Guillaume	536.10	5090.10	FzD	271	0.0	0.00	5.5	2000	84.89	0.13	8.43	0.49	0.00	0.22	0.28	0.99
AV467		Puy Guillaume	536.10	5090.10	FzD	271	0.0	0.00	5.5	500	78.77	0.30	11.53	0.88	0.01	0.32	0.61	1.54
AV468		Puy Guillaume	536.10	5090.10	FzD	271	0.0	0.00	5.5	1200	83.14	0.19	8.85	0.64	0.01	0.31	0.39	1.01
AV427		La GArde	537.00	5091.70	FzD	269	0.0	0.00	4.0	300	75.97	0.49	12.71	1.65	0.02	0.53	0.80	1.73
AV428		Grand bardins	536.70	5093.00	FzD	267	0.0	0.00	2.8	400	76.16	0.32	12.20	1.02	0.02	0.44	0.69	1.70
AV429		Grand bardins	536.70	5093.00	FzD	267	0.0	0.00	2.8	300	74.54	0.31	13.15	1.14	0.01	0.48	0.68	1.86
AV430		La GArde	537.00	5091.70	FzD	269	0.0	0.00	4.0	420	75.73	0.63	11.53	2.32	0.04	0.64	0.86	1.53
AV405		114	537.00	5094.40	FzD	267	0.0	0.00	1.0	420	76.87	0.31	12.35	1.02	0.01	0.39	0.66	1.70
AV305		Charnat	537.00	5094.70	FzD	266	0.0	0.00	0.3	300	74.99	0.39	12.89	1.43	0.02	0.54	0.72	1.74
AV306		Charnat	537.00	5094.70	FzD	266	0.0	0.00	0.3	600	77.20	0.39	11.79	1.49	0.02	0.52	0.67	1.46
AV307		Charnat	537.00	5094.70	FzD	266	0.0	0.00	0.3	800	75.70	0.77	11.27	3.07	0.05	0.77	0.86	1.36
AV373		Charnat 105	536.70	5095.00	FzD	265	0.0	0.00	~0	400	77.35	0.29	12.21	1.08	0.01	0.38	0.67	1.66
AV374		Charnat 105	536.70	5095.00	FzD	265	0.0	0.00	~0	1500	82.18	0.23	9.04	0.80	0.01	0.32	0.50	1.08
AV375		Charnat 105	536.70	5095.00	FzD	265	0.0	0.00	~0	250	73.86	0.38	13.22	1.43	0.02	0.52	0.71	1.81
AV376		Charnat 105	536.70	5095.00	FzD	265	0.0	0.00	~0	400	75.81	0.48	12.03	1.80	0.03	0.58	0.70	1.62
AV377		Charnat 105	536.70	5095.00	FzD	265	0.0	0.00	~0	1200	82.33	0.25	9.29	1.09	0.01	0.75	0.77	1.08
420	122	Peschadoires	538.40	5074.95	FzD	295	0.0	0.00	22.0	600	78.18	0.13	11.50	0.71	0.01	0.31	0.34	2.25
421	123	Peschadoires	538.40	5074.95	FzD	295	0.0	0.00	22.0	210	69.42	0.53	16.36	1.91	0.02	0.95	0.98	3.42
422	124	Peschadoires	538.40	5074.95	FzD	295	0.0	0.00	22.0	1400	81.36	0.06	9.89	0.58	<0.00	0.27	0.23	1.83
AV20		Noalhat	535.10	5084.40	FzD	279	0.0	0.00	11.3	355	78.82	0.17	11.53	0.63	0.01	0.30	0.40	1.75
AV21		Noalhat	535.10	5084.40	FzD	279	0.0	0.00	11.3	2000	82.63	0.08	9.92	0.36	0.00	0.17	0.22	1.42
AV51		Marsac en Livra	557.10	5037.20	Fyz	535	3.0	1.00	69.0	1400	80.94	0.13	10.55	0.64	0.01	0.28	0.50	2.02
AV52		Brugeailles z	557.60	5038.00	Fz	535	0.0	0.00	68.3	500	77.06	0.45	12.34	1.95	0.07	0.63	0.96	2.20
AV53		Brugeailles z	557.60	5038.00	Fyz	535	2.0	0.50	68.3	710	78.55	0.31	11.71	1.50	0.03	0.54	0.84	2.12
AV54		Brugeailles z	557.60	5038.00	Fyz	535	2.0	0.50	68.3	1000	80.63	0.19	10.89	1.14	0.02	0.40	0.60	1.95
79	527	Peschadoires	538.40	5074.95	FyzD	296	1.0	1.00	22.0	1000	79.70	0.06	10.73	0.46	0.00	0.20	0.16	1.89
430	132	Les Ogheards	534.60	5085.93	FyzD	283	1.0	1.15	11.0	600	79.97	0.09	10.99	0.46	0.00	0.22	0.29	2.16
431	133	Les Ogheards	534.60	5085.93	FyzD	283	1.0	1.00	11.0	420	78.15	0.15	12.42	0.66	0.01	0.32	0.52	2.60
432	134	Les Ogheards	534.60	5085.93	FyzD	283	1.0	1.30	11.0	1000	82.05	0.20	9.78	0.58	0.02	0.19	0.21	1.86
410	112	Lastioulas	542.30	5065.80	FyzD	315	1.5	1.10	32.0	420	74.03	0.22	13.50	1.18	0.01	0.64	0.69	2.71
411	113	Lastioulas	542.30	5065.80	FyzD	315	1.5	1.25	32.0	1000	75.51	0.24	12.75	1.17	0.01	0.65	0.61	2.54
412	114	Lastioulas	542.30	5065.80	FyzD	315	1.5	1.00	32.0	600	76.00	0.19	12.64	1.04	0.01	0.56	0.63	2.60
357	225	Dorat-Gare	537.40	5081.35	FyD	283	2.0	1.00	15.5	400	80.81	0.22	10.90	0.60	0.01	0.23	0.29	2.24
358	226	Dorat-Gare	537.40	5081.35	FyD	283	2.0	1.00	15.5	780	82.46	0.09	10.39	0.40	0.00	0.16	0.15	1.87
218	59	Dorat-Gare	537.40	5081.35	FyD	283	2.0	1.50	15.5	600	82.19	0.03	9.20	0.27	<0.01	0.13	0.14	1.65
416	118	Neronde	540.80	5071.80	FyD	309	7.0	1.40	25.5	600	78.74	0.10	11.66	0.68	0.01	0.38	0.49	2.53
417	119	Neronde	540.80	5071.80	FyD	309	7.0	0.75	25.5	300	71.56	0.36	14.55	1.83	0.02	0.95	0.86	3.02
418	120	Neronde	540.80	5071.80	FyD	309	7.0	2.00	25.5	420	78.01	0.19	12.52	0.94	0.01	0.50	0.57	2.66
419	121	Neronde	540.80	5071.80	FyD	309	7.0	1.90	25.5	1400	82.64	0.08	9.70	0.60	0.00	0.29	0.26	1.81
AV57		Chambouffe	556.70	5041.30	Fx	535	5.0	1.00	64.8	1400	82.91	0.18	9.74	0.99	0.01	0.43	0.52	1.63
353	221	W Dorat	536.40	5082.45	FxD	290	10.0	3.50	13.5	300	76.23	0.31	12.64	1.45	0.01	0.71	0.54	2.46
354	222	W Dorat	536.40	5082.45	FxD	290	10.0	4.00	13.5	620	78.64	0.18	11.89	0.96	0.01	0.44	0.31	2.39
355	223	W Dorat	536.40	5082.45	FxD	290	10.0	4.10	13.5	760	81.91	0.16	10.74	0.82	0.01	0.36	0.25	2.10
356	224	W Dorat	536.40	5082.45	FxD	290	10.0	4.20	13.5	1240	80.95	0.11	10.95	0.64	0.00	0.24	0.21	2.02
413	115	Limarie	541.20	5069.65	FxD	320	15.0	6.10	27.5	1000	81.73	0.06	9.66	0.47	<0.01	0.19	0.10	1.39
414	116	Limarie	541.20	5069.65	FxD	320	15.0	5.75	27.5	420	79.73	0.19	10.37	0.72	0.01	0.34	0.21	1.51
415	117	Limarie	541.20	5069.65	FxD	320	15.0	5.45	27.5	1400	83.77	0.07	8.31	0.50	<0.00	0.23	0.10	1.25
AV19		Goutet	535.70	5082.50	FxD	299	20.0	2.00	14.0	500	87.54	0.11	6.97	0.31	0.01	0.12	0.04	0.51
AV55		Brugeailles	557.90	5038.70	Fw	550	15.0	3.00	68.0	710	77.29	0.30	12.75	0.78	0.01	0.16	0.59	2.13

Sample	K2O	P2O5	BaO	V	Cr	Co	Ni	Cu	Zn	Ga	Rb	Sr	Zr	Nb	Ba	La	Pb
AV337	4.98	0.05	0.10	<5	6	41	41	16	<3	14	176	180	66	7	861	14	44
AV338	4.71	0.08	0.10	14	40	15	27	16	22	17	200	181	208	11	785	25	45
AV339	4.23	0.04	0.08	<5	11	50	56	19	<3	14	154	161	62	<2	724	12	39
AV452	4.66	0.09	0.10	14	22	34	36	<6	<3	13	178	175	271	11	742	56	44
AV453	4.48	0.11	0.09	17	27	37	44	<6	6	14	168	177	292	19	765	69	44
AV466	3.67	0.06	0.08	<5	10	29	33	<6	<3	10	135	137	95	5	659	<12	33
AV467	4.67	0.09	0.10	16	20	33	39	<6	<3	14	178	183	217	11	744	40	39
AV468	3.84	0.06	0.09	10	15	76	46	<6	<3	12	139	145	100	4	633	17	36
AV427	4.79	0.11	0.08	44	36	28	36	<6	15	14	193	188	293	18	675	50	40
AV428	4.81	0.10	0.09	21	25	31	35	<6	7	15	196	184	261	16	712	41	41
AV429	4.98	0.09	0.09	28	33	39	43	<6	19	17	211	189	227	13	690	41	43
AV430	4.40	0.11	0.09	60	40	42	46	<6	26	15	170	181	250	15	679	62	36
AV405	4.72	0.08	0.08	23	20	40	41	<6	<3	16	199	180	241	14	673	33	44
AV305	5.40	0.11	0.09	30	37	29	41	<6	14	15	255	165	301	18	722	48	46
AV306	5.45	0.09	0.10	29	33	43	56	<6	25	14	258	151	204	10	700	21	46
AV307	4.90	0.11	0.12	85	53	29	40	<6	34	13	233	153	342	22	947	48	45
AV373	4.87	0.09	0.09	26	20	24	30	<6	<3	17	206	174	235	5	695	23	42
AV374	3.86	0.04	0.08	15	13	39	41	<6	<3	12	149	148	99	3	600	25	34
AV375	5.04	0.10	0.09	36	39	31	38	12	17	16	230	180	292	18	696	59	51
AV376	4.84	0.11	0.10	40	33	34	41	8	20	14	206	170	274	18	729	61	44
AV377	3.99	0.09	0.08	25	24	32	43	<6	<3	13	151	163	77	<2	625	<12	35
420	4.56	0.07	0.07	68	82	30	60	10	12	16	165	199	78	7	737	<7	24
421	4.38	0.13	0.09	101	82	25	60	10	100	24	216	246	471	25	894	85	31
422	4.10	0.06	0.06	68	82	16	60	10	12	15	143	172	50	4	687	28	22
AV20	4.75	0.07	0.10	68	82	93	60	10	12	13	198	204	103	15	1066	68	26
AV21	4.45	0.05	0.10	68	82	98	60	10	12	13	175	183	26	8	1027	24	24
AV51	3.48	0.05	0.07	68	82	23	60	10	12	15	107	219	40	7	937	52	20
AV52	2.98	0.12	0.10	68	82	40	60	10	12	15	110	233	222	22	1082	104	17
AV53	3.04	0.08	0.08	68	82	41	60	10	12	17	109	217	134	13	945	83	21
AV54	3.12	0.06	0.09	68	82	61	60	10	12	13	96	207	48	8	1012	34	22
79	5.17	0.07	0.08	68	82	48	60	10	12	11	179	209	31	4	865	<7	108
430	4.66	0.05	0.06	68	82	27	60	10	12	16	167	202	71	7	729	23	19
431	4.50	0.07	0.07	68	82	32	60	10	12	17	156	214	111	7	757	20	18
432	4.19	0.05	0.06	68	82	28	60	10	12	13	133	177	44	8	710	39	26
410	4.43	0.11	0.08	68	82	58	60	10	12	17	153	224	136	9	802	<7	26
411	4.38	0.09	0.07	68	82	18	60	10	17	18	169	212	127	8	737	20	22
412	4.42	0.10	0.09	68	82	23	60	10	13	17	146	215	91	5	831	24	22
357	4.07	0.06	0.07	68	82	35	60	10	12	14	167	177	200	13	927	68	12
358	4.38	0.03	0.07	68	82	53	60	10	12	16	178	187	45	6	840	14	24
218	4.22	0.04	0.06	68	82	25	60	10	12	14	135	163	25	<4	661	10	23
416	4.09	0.06	0.06	68	82	23	60	10	12	15	134	216	47	6	689	<7	24
417	4.29	0.11	0.07	77	82	40	60	10	36	23	184	246	195	11	775	30	21
418	4.22	0.08	0.06	68	82	15	60	10	14	17	151	230	99	8	715	30	16
419	3.50	0.05	0.07	68	82	32	60	10	12	16	114	190	48	5	685	<7	14
AV57	2.62	0.05	0.07	68	82	75	60	10	12	15	86	179	83	14	859	54	21
353	3.99	0.09	0.06	80	82	33	60	10	25	19	182	205	114	10	753	46	21
354	4.26	0.05	0.07	68	82	51	60	10	12	18	185	200	52	8	759	29	19
355	3.87	0.05	0.05	68	82	60	60	10	12	17	173	169	86	8	653	9	28
356	4.53	0.05	0.07	68	82	28	60	10	12	15	172	215	54	5	853	<7	22
413	4.76	0.06	0.07	68	82	22	60	10	12	18	178	166	29	4	749	32	29
414	4.53	0.06	0.07	68	82	18	60	10	12	15	181	174	80	6	747	17	28
415	3.77	0.06	0.06	68	82	23	60	10	12	12	135	134	32	<4	649	<7	20
AV19	4.14	0.04	0.08	68	82	40	60	10	12	13	143	135	31	9	1000	38	33
AV55	4.88	0.06	0.14	68	82	48	60	10	12	17	172	311	269	22	1467	61	29

Sample	labnr	Location	x-coord	y-coord	TerraceAlt	Relalt	depth	Upstr	Median	SiO2	TiO2	Al2O3	Fe2O3	MnO	MgO	CaO	Na2O
AV56		Brugeailles	557.90	5038.70	Fw	550	15.0	2.00	68.0	500	75.54	0.16	14.17	0.54	0.01	0.18	0.80	2.67
AV16		Les Raveaux	536.30	5078.20	FwD	320	40.0	3.00	17.8	1000	80.17	0.18	11.38	0.81	0.01	0.31	0.20	1.20
Av18		Les Gaillards	536.30	5080.50	FwD	310	35.0	3.00	15.8	500	82.70	0.09	7.58	0.20	0.00	0.10	0.64	0.64
AV22		Chamonel	535.00	5082.10	FwD	308	35.0	2.00	14.0	1000	83.33	0.29	9.09	0.94	0.02	0.32	0.18	0.89
AV23		Chamonel	535.00	5082.10	FwD	308	35.0	2.10	14.0	1400	84.74	0.22	8.84	0.79	0.01	0.28	0.14	0.83
AV24		Chamonel	535.00	5082.10	FwD	308	35.0	2.30	14.0	1000	80.06	0.31	10.84	1.06	0.02	0.36	0.23	1.21
426	128	Rapine	535.90	5076.50	FvD	350	62.0	0.68	19.5	1000	85.05	0.14	6.95	0.24	<0.00	0.08	<0.00	0.46
427	129	Rapine	535.90	5076.50	FvD	350	62.0	0.82	19.5	2000	84.72	0.03	8.71	0.22	<0.00	0.08	<0.00	0.72
428	130	Rapine	535.90	5076.50	FvD	350	62.0	0.85	19.5	600	82.88	0.13	8.48	0.85	<0.00	0.07	<0.00	0.83
429	131	Rapine	535.90	5076.50	FvD	350	62.0	0.85	19.5	420	81.19	0.18	10.76	0.74	0.00	0.30	0.14	1.27
137	216	Rapine	535.90	5076.50	FvD	350	62.0	0.85	19.5	1600	84.06	0.04	8.25	0.22	<0.01	0.06	<0.01	0.88
423	125	Bourson	538.20	5074.75	FvD	362	70.0	1.70	22.5	420	86.33	0.27	6.41	0.43	0.00	0.10	<0.0	0.40
424	126	Bourson	538.20	5074.75	FvD	362	70.0	1.60	22.5	1000	88.08	0.04	6.14	0.15	<0.00	0.08	<0.00	0.31
425	127	Bourson	538.20	5074.75	FvD	362	70.0	1.90	22.5	300	87.21	0.03	6.05	0.15	<0.00	0.07	<0.00	0.32
136	215	Le Pialoux	537.60	5068.80	FsD	403	100.0	1.60	26.5	900	87.68	0.06	7.73	0.18	<0.01	0.09	<0.01	0.61
407	109	Le Pialoux	537.60	5068.80	FsD	403	100.0	1.60	26.5	420	83.83	0.12	9.06	0.26	<0.01	0.14	<0.01	0.85
408	110	Le Pialoux	537.60	5068.80	FsD	403	100.0	1.70	26.5	600	86.96	<0.02	6.31	0.08	<0.01	0.06	<0.01	0.53
409	111	Le Pialoux	537.60	5068.80	FsD	403	100.0	2.00	26.5	1400	86.26	<0.02	7.10	0.13	<0.01	0.08	<0.01	0.72
111	208	Chau La Garde	535.35	5070.85	FrD	415	110.0	2.00	24.0	1500	89.00	0.06	5.25	0.15	<0.01	0.07	<0.01	0.28

Sample	K2O	P2O5	BaO	V	Cr	Co	Ni	Cu	Zn	Ga	Rb	Sr	Zr	Nb	Ba	La	Pb
AV56	4.69	0.03	0.10	68	82	76	60	10	12	19	205	382	123	16	1074	57	30
AV16	4.71	0.05	0.09	68	82	45	60	10	12	15	210	177	54	13	1125	24	34
Av18	4.53	0.04	0.09	68	82	67	60	10	12	9	177	153	33	7	1055	54	22
AV22	3.94	0.04	0.08	68	82	27	60	10	12	13	147	145	111	17	941	51	22
AV23	3.90	0.04	0.08	68	82	23	60	10	12	10	146	130	33	10	916	49	20
AV24	4.33	0.05	0.09	68	82	35	60	11	12	13	183	170	82	12	1080	43	26
426	4.38	0.05	0.07	68	82	12	60	10	12	11	144	128	234	12	859	33	12
427	5.22	0.02	0.06	68	82	46	60	10	12	15	200	117	20	4	671	<7	26
428	4.65	0.05	0.07	68	82	19	60	10	12	12	186	125	56	6	727	7	26
429	5.04	0.04	0.06	68	82	14	60	10	15	15	208	145	57	7	695	<7	26
137	4.90	0.03	0.06	68	82	19	60	10	12	11	170	122	16	4	647	<7	29
423	4.09	0.04	0.07	68	82	41	60	10	12	13	128	121	118	12	726	40	20
424	3.94	0.04	0.06	68	82	43	60	10	12	10	134	124	74	7	686	12	20
425	4.14	0.03	0.07	68	82	40	60	10	12	7	131	122	56	5	691	<7	14
136	4.32	0.03	0.06	68	82	14	60	10	12	11	156	123	13	<4	638	13	18
407	4.71	0.04	0.08	68	82	32	60	10	12	12	180	134	46	6	708	24	23
408	3.87	0.03	0.06	68	82	30	60	10	12	13	135	112	9	5	623	13	25
409	3.85	0.03	0.06	68	82	23	60	10	12	13	134	120	15	4	617	8	14
111	3.21	0.03	0.04	68	82	21	60	10	12	8	116	89	83	8	497	34	11

APPENDIX II

```
(*****************************************************************)
(*                                                               *)
(*   Module Global: definition and declaration of the global     *)
(*         variables of the LIMTER program                       *)
(*        - Time                                                 *)
(*        - Entity RIVER                                         *)
(*        - Entity LANDSCAPE                                     *)
(*        - The processes                                        *)
(*   Date first version as TERRAS program 21-05-1987             *)
(*   Authors TERRAS version: A. Veldkamp en S.E.J.W. Vermeulen   *)
(*   Date first LIMTER program 02-05-1990,                       *)
(*   DEFINITE VERSION (D2)  30-05-1990 copyright A. Veldkamp     *)
(*****************************************************************)

(*****************************************************************)
(*                                                               *)
(*   Constant variables which have be determined for each        *)
(*        simulation:                                            *)
(*   - Initial relief: ZMID is initial altitude valley floor     *)
(*                     INIHOOGTE initial altitude highest terrace*)
(*   - Scale of LANDSCAPE:                                       *)
(*                     XMETER width of LANDSCAPE in kilometres   *)
(*                     YMETER length of LANDSCAPE in kilometres  *)
(*                     ZMETER max altitude in metres             *)
(*   - TECTONISM:                                                *)
(*                     QTEKGEM is uplift rate in m/ky            *)
(*                     QTEKHOEK in UNEQUAL_UPLIFT rate in m/ky   *)
(*   - Discharge Allier:                                         *)
(*                     QGEM is average discharge in m3/ky        *)
(*                     QAMPL is amplitude in discharge in m3/ky  *)
(*   - Sediment load Allier:                                     *)
(*                     INLGEM average input sediment load m3/ky  *)
(*                     INLAMP amplitude sediment input load m3/ky*)
(*   - Periodicical cycli of Milankovitch curve:                 *)
(*                     PRECC, ECC, TILT                          *)
(*   - Amplitudes of Milankovitch curve:                         *)
(*                     A,B,C                                     *)
(*****************************************************************)

[ENVIRONMENT('GLO.BAL')]MODULE GLOBAL;

CONST
        TMAX=601; (* ending time in ky of simulation            *)
        TMIN=1;   (* starting time of simulation in ky          *)
                  (* TMIN <= simulation time (ky) <= TMAX       *)

        XMAX=100; (* amount of grid cells in width relief       *)
        YMAX=100; (* amount of grid cells in length relief      *)
        ZMAX=500; (* amount of maximum grid cells in altitude   *)
        XMIN=1;   (* XMIN <= X <= XMAX                          *)
        YMIN=1;   (* YMIN <= Y <= YMAX                          *)
        ZMIN=1;   (* ZMIN <= Z <= ZMAX                          *)

        XMID=50;  (* The centre of the Valley, this is where the *)
                  (* Allier flows and where the lowest place of  *)
                  (* the cross-section is situated.             *)
```

```
(*****************************************************************)
(*                                                               *)
(* Simulation constant variables                                 *)
(*****************************************************************)

        ZMID=270;     (* initial altitude of RELIEF at XMIN,YMIN *)
        INIHOOGTE = 30; (* ZMID - INIHOOGTE = initial altitude   *)
                        (* of valley slope altitude at XMID,YMIN *)

        XMETER = 10000; (* cross-section in metre               *)
        YMETER = 10000; (* longitudinal section in metres       *)
        ZMETER = 500;   (* Altitude in metres                   *)

        QTEKGEM = 0.1;  (* uplift rate in m/ky                  *)
        QTEKHOEK = 0.01;(* unequal-uplift rate in m/ky          *)

        QGEM = 150;     (* average discharge in m3/sec          *)
        QAMP = 130;     (* amplitude in discharge in m3/sec     *)

        INLGEM = 0.5E-3;(* average sediment load in m3/sec      *)
        INLAMP = 1.5E-3;(* amplitude in sediment load in m3/sec *)
        FLUX = 4;       (* relative increase in sediment load   *)
                        (* due to glacier melting after prolonged*)
                        (* glacial (> 10ky)                     *)

        PRECC = 96;     (* Preccision earth orbit in ky         *)
        ECC = 41;       (* Ecc earth orbit in ky                *)
        TILT = 23;      (* Tilt earth orbit in ky               *)
        A = 1;          (* amplitude of PRECC                   *)
        B =1;           (* amplitude of ECC                     *)
        C = 1;          (* amplitude of TILT                    *)

        (* Constant variables to calculate the maximum sediment *)
        (* load  of the Allier.                                 *)
           MB= 7.96E-5; (* meander bedload                      *)
           MS= 2.2E-8;  (* meander suspended load               *)
           MD= 3E-6;    (* meander dissolved load               *)
           VB= 5.23E-4; (* braided bed load                     *)
           VS= 1.9E-8;  (* braided suspended load               *)
           VD= 3.2E-6;  (* braided dissolved load               *)

        CHEMIN = 1;     (* minimal geochemical class sediment   *)
        CHEMAX = 11;    (* maximal geochemical class sediment   *)

        UIT1MAX = 5;    (* time lapse (ky) after which cross-   *)
                        (* section is stored in a file          *)
        UIT2MAX = 50;   (* idem for a x,y,z     releif          *)

(*****************************************************************)

TYPE
     (*       error notifications                                *)
              (* ZETMIN= true if Z = ZMIN at XMID,YMAX          *)
              (* ZETMAX= true if Z = ZMAX at XMID,YMIN          *)
              (* DWARSERO= true if XMID is not the lowest place *)
              (* in a cross-section during the erosion process. *)
              (* DWARSSED: true if XMID is not the lowest place *)
              (* in a cross-section during sedimentation        *)
              (* DUMERO= true if DUMEROSIE the amount of        *)
```

```
            (* remaining erosion capasity is too large          *)
            (* OKAY= true if there not error notify             *)
      FOUTRIJ = (ZETMIN,ZETMAX, DWARSERO, DWARSSED,DUMERD,OKAY);

VAR
      X,          (* X is cross-section in grid cells            *)
      Y,          (* Y is longitudinal profile in grid cells     *)
      Z,          (* Z is altitude in grid cells                 *)
      OUD,        (* erosion capacity reminder, takes care for   *)
                  (* gradual erosion or sedimentation            *)
      GLACIAAL, (* variable to determine length of a glacial in ky *)
      TIJD: INTEGER;  (*  TIME in thousands of years (ky)        *)

      (* Entity RIVER with Attributes                           *)
      RIVIER :RECORD
           Q:    REAL;           (* discharge in m3/sec          *)
           INLAST:    REAL;      (* input sediment load in m3/sec *)
           CHEM:      INTEGER;   (* geochemical class sediment   *)
           MEANDER: BOOLEAN;     (* River has meandering         *)
                                 (* characteristics              *)
           VERWILDERD: BOOLEAN; (* River has braided            *)
                                 (* characteristics              *)
           M50: REAL;            (* mean grain size sediment in mm *)
           S:    REAL;           (* slope of riverbed in m/m     *)
           BREEDTE:REAL;         (* width of flood plain in m    *)
           MAXLAST:REAL;         (* Max load of river in m3/sec  *)
           QEROSIE:REAL;         (* Erosion capasity in m3/sec   *)
           END;

      (* Entity LANDSCAPE with attributes                       *)
      LANDSCHAP:  RECORD
           QTEKTONIEK: REAL;     (* Uplift rate in m/ky          *)
           HOOGTE :INTEGER;      (* difference in altitude between *)
                                 (* highest terrace level XMIN,YMIN *)
                                 (* and riverbed (XMID,YMIN) in grid *)
                                 (* cells                        *)
           DALBREEDTE:INTEGER;   (* valley width in grid cells   *)
           S:    INTEGER;        (* Slope valley downstream in grids *)
                                 (* (xmid,ymin) - relief(xmid,ymax) *)
           QEROSIE:INTEGER;      (* Erosion for a timestep of one ky *)
                                 (* in grid cells                *)
           END;


      RELIEF: ARRAY[XMIN..XMAX,YMIN..YMAX] OF
           RECORD
                ZET: INTEGER;    (* altitude of a grid  cell     *)
                STRATIG: PACKED ARRAY[1..10] OF TMIN..TMAX;
                                 (* stratigraphy for each grid cell *)
                GEOCHEM: PACKED ARRAY[1..10] OF CHEMIN..CHEMAX;
                                 (* chemostratigraphy for each grid *)
           END;

      (* The PROCESSES                                          *)
      TEKTONIEK,
      EROSIE,
      INSNIJDING,
      KANT,
      SEDIMENTATIE:  BOOLEAN;
      FOUT:       FOUTRIJ;       (* error variable              *)
```

```
END (* GLOBAL *).

(*****************************************************************)
(*   PROGRAM LIMTER: calculates relief changes over a timespan of  *)
(*                   0.6 MA caused by fluvial erosion and sedimen- *)
(*                   tation as a result of climate and tectonism,  *)
(*                   with timesteps of 1000 years (ky)             *)
(*   input: Gradual but unequal Tectonism                          *)
(*          Climate controlled discharge and sediment load  inputs *)
(*   Output:RELIEF1: Cross-section development in time             *)
(*          RELIEF2: simulated relief: x,y,z-coordinates           *)
(*          UITSTRATIG: stratigraphy of cross-sections in time     *)
(*          UITSTRATIS: surface stratigraphy of RELIEF2            *)
(*          LOGBOEK: values of the global variables                *)
(*          UITFOUT: errors during simulation                      *)
(*          GEOCHEMIG: chemostratigraphy cross-sections  RELIEF1   *)
(*          GEOCHEMIS: surface chemostratigraphy of RELIEF2        *)
(*   Date first TERRAS version: 19 maart 1987                      *)
(*   Authors TERRAS: S.E.J.W. Vermeulen and A. Veldkamp            *)
(*   Date first Allier version: 21-05-1990                         *)
(*   Author LIMTER: A. VELDKAMP                                    *)
(*   VERSION LIMTER D2          COPYRIGHT A. VELDKAMP              *)
(*****************************************************************)

(*****************************************************************)
(*   programm characteristics:                                     *)
(*   output files:  RELIEF1.DAT                                    *)
(*                  RELIEF2.DAT                                    *)
(*                  UITSTRATIG.DAT                                 *)
(*                  LOGBOEK.DAT                                    *)
(*                  UITSTRATIS.DAT                                 *)
(*                  UITFOUT.DAT                                    *)
(*                  CHEMIS.DAT                                     *)
(*                  CHEMIG.DAT                                     *)
(*   Amount of procedures: five                                    *)
(*****************************************************************)

[INHERIT('GLD.BAL')]PROGRAM TERRAS(RELIEF1,RELIEF2,UITSTRATIG,LOGBOEK,
GEOCHEMIS, GEOCHEMIG, SINUS, UITSTRATIS, UITFOUT);
VAR
     (* file variables                                          *)

     RELIEF1,       (* Cross-section at y=90 for each UIT1MAX   *)
                    (* timesteps                                *)
     RELIEF2,       (* RELIEF x,y,z for each UIT2MAX timesteps  *)
     UITSTRATIG,    (* Stratigraphy of RELIEF1                  *)
     UITSTRATIS,    (* Stratigraphy of RELIEF2                  *)
     LOGBOEK,       (* Global variables for each timestep       *)
     SINUS,         (* Local and input variables for each timestep *)
     GEOCHEMIS,     (* Chemostratigraphy at RELIEF2             *)
     GEOCHEMIG,     (* Chemostratigraphy at RELIEF1             *)
     UITFOUT:       (* Error notifications during simulation    *)

               TEXT;

     (* Local variables                                         *)

     HOOGTE,        (* Total amount of uplift in grid cells     *)
     TEKTILT,       (* Total amont of unequal uplift in metres  *)
```

```
      VERHANG,          (* Slope of river in grid cells                *)
      REROSIE,          (* sum of LANDSCHAP.QEROSIE en DUMEROSIE       *)
      DUMEROSIE,        (* residue of LANDSCHAP.QEROSIE                *)
      SOMEROSIE,        (* cumulated erosion during the simulation in  *)
                        (* grid cells                                  *)
      SMIN,             (* altitude relief according VERHANG           *)
      XBREEDTEMIN,      (* smallest X-coordinate for RIVIER.BREEDTE    *)
                        (* in grid cells; control variable             *)
      XBREEDTEMAX,      (* larges X-coordinaat; control variable       *)
      UIT1,UIT2,UIT3,   (* loop counters for writing data to files      *)
      TEL1,TEL2,TEL3,
      ZRAND,            (* Altitude of valley scarp in grid cells      *)
      ZVALLEI,          (* altitude valley floor in grid cells         *)
      LUI,              (* test variable - REROSIE                     *)
                        (* prevents never ending loop, 15 mei 1987     *)
      I,                (* loop counters                               *)
      K:    INTEGER;

      DUM,              (* calculates landschap.qerosie rivier.qerosie *)
      DALS,             (* slope valley floor in m/m                   *)
      VORMCONST,        (* constant dtermines river characteristic     *)
      OUDQ,             (* river.discharge at time - t-1 m3/sec        *)
      OUDINLAST,        (* river.inlast at time - t-1  m3/sec          *)
      PI,               (* constant                                    *)
      HOEK,             (* counter of unequal-uplift                   *)
      QTEKHOOGTE:       (* Total amount of LANDSCHAP.QTEKTONIEK        *)
           REAL;

      OUDVORM,          (* rivier.vorm at time - t-1; if true than     *)
                        (* Allier is meandering                        *)
      RAND,             (* If true than erosding valleyslope           *)
      AF,               (* If true than landschap.s - rivier.s         *)
      GRENS,            (* If true than error motification and         *)
                        (* simulation is stopped                       *)
      DUMMY:            (* Is always true during simulation            *)
           BOOLEAN;

         PAD:ARRAY[1..45] OF INTEGER;
                        (* test variable                               *)

(*****************************************************************)
(*                                                               *)
(* procedure: FLUSS                                              *)
(*   Calculates the attributes of entity RIVER and translates    *)
(*   these properties to landscape properties in grid cell units *)
(*    local variables:DALS,VORMCONST,DUM                         *)
(*                                                               *)
(*****************************************************************)

PROCEDURE FLUSS;
BEGIN

              (* 1 calculates slope-valley in grid cells to slope  *)
              (*   of valley in m/m. slope of valley is not within *)
              (*   domain than valley slope is 1E-4 m/m            *)

        DALS := LANDSCHAP.S * ZMETER/(YMETER * ZMAX);
      IF DALS < 1E-4 THEN DALS := 1E-4;

              (* 2 If RIVER at time is t-1 is Meandering than      *)
              (*   slope of river is 0.5 slope valley              *)
      IF OUDVORM = TRUE THEN
      BEGIN
        PAD[6] := 1;
        DALS := 0.5 * DALS;
      END;

              (* 3 calculates discharge and input load of the      *)
              (*   RIVER in m3/sec. QGEM and QAMP determine the    *)
              (*   domain of both discharge and input load         *)
              (*   PRECC, ECC, TILT descripe Milankovitch  curve   *)
              (*   INLAST is  /2 out of phase with discharge       *)

RIVIER.Q := QGEM + QAMP/(A+B+C)*(A*SIN(2*PI*TIJD/PRECC) +
          B*SIN(2*PI*TIJD/ECC) + C*SIN(2*PI*TIJD/TILT));
RIVIER.INLAST := INLGEM + INLAMP/(A+B+C)*(A*COS(2*PI*TIJD/PRECC)+
          B*COS(2*PI*TIJD/ECC) + C*COS(2*PI*TIJD/TILT));


  IF DUMMY THEN
    BEGIN
      PAD[3] := 1;

              (* 4.1 determine RIVER characteristic                *)
              (*     debiet at t-1 -OUDQ and inlast at t-1-OUDINL  *)
              (*     + means increase                              *)
              (*     - means descrease                             *)
              (*     If Q- and Inlast+ then verwilderd (braided)   *)
              (*     If Q+ and Inlast- then meander (meandering)   *)
              (*     If Q+ and Inlast+ then no change in           *)
              (*     RIVER characteristics,                        *)
              (*     If Q- and Inlast- then no change in           *)
              (*     RIVER characteristics                         *)

            (* 4.1.1 If Q- and Inlast+ then verwilderd             *)
        IF (OUDQ - RIVIER.Q > 0)  AND
             (OUDINLAST - RIVIER.INLAST < 0)  THEN
        BEGIN
             PAD[8] := 1;
             RIVIER.VERWILDERD := TRUE;
          END (*IF*);

            (* 4.1.2 If Q+ and Inlast- then meander                *)
        IF (OUDQ - RIVIER.Q < 0)  AND
             (OUDINLAST - RIVIER.INLAST > 0)  THEN
        BEGIN
             PAD[13] := 1;
          RIVIER.MEANDER := TRUE;
          END(* if *);

            (* 4.1.3 If Q+ and Inlast+ then vorm of t-1            *)
        IF (OUDQ - RIVIER.Q < 0)  AND
             (OUDINLAST - RIVIER.INLAST < 0)  THEN
        BEGIN
          IF RIVIER.INLAST <= INLGEM THEN OUDVORM := TRUE;
          IF RIVIER.INLAST > INLGEM THEN OUDVORM := FALSE;
             PAD[4] := 1;
          IF OUDVORM = TRUE THEN
          BEGIN
               PAD[14] := 1;
```

```
            RIVIER.MEANDER :=  TRUE;
         END (* if *)
         ELSE
            BEGIN
              PAD[9] := 1;
                RIVIER.VERWILDERD := TRUE;
         END; (* else *)
       END (* if *);

         (* 4.1.4 If Q- and Inlast- then vorm of t-1          *)
    IF (OUDQ - RIVIER.Q > 0)  AND
         (OUDINLAST - RIVIER.INLAST > 0)  THEN
    BEGIN
         IF RIVIER.INLAST <= INLGEM THEN OUDVORM := TRUE;
         IF RIVIER.INLAST > INLGEM THEN OUDVORM := FALSE;
              PAD[5] := 1;
         IF OUDVORM = TRUE THEN
         BEGIN
              PAD[15] := 1;
              RIVIER.MEANDER :=  TRUE;
         END
         ELSE
         BEGIN
              PAD[10] := 1;
              RIVIER.VERWILDERD := TRUE;
         END;
    END (* if *);
END (* if dummy *);

(* 5.0 *)
(* Determination of duration of a Glacial. If Glacial is      *)
(* longer then 10.000 years a larger sediment flux is         *)
(* released into the Allier which is FLUX times normal        *)
(* and has compositional class 4                              *)
IF RIVIER.VERWILDERD THEN
BEGIN
    GLACIAAL := GLACIAAL +1;
    RIVIER.CHEM := 3;
END;


IF RIVIER.MEANDER THEN
BEGIN
    IF GLACIAAL <= 8 THEN
    BEGIN
         GLACIAAL := 0;
         RIVIER.CHEM := 2;
    END;
    IF GLACIAAL > 9 THEN
    BEGIN
         RIVIER.INLAST := FLUX * (INLGEM + INLAMP);
         GLACIAAL := 0;
         RIVIER.CHEM := 4;
    END;

END;

         (* 5 determine OUDQ and OUDINLAST                    *)
OUDQ := RIVIER.Q;
OUDINLAST := RIVIER.INLAST;

         (* 6 If meander, calculate slope, maxlast and the    *)
         (*   width of the floodplain                         *)
IF RIVIER.MEANDER = TRUE THEN
   BEGIN
     PAD[16] := 1;

         (* 6.1 control: If meander than verwilderd=false     *)
     RIVIER.VERWILDERD := FALSE;

         (* 6.2 determine grain size in mm                    *)
         RIVIER.M50 := 0.35;

         (* 6.3 put oudvorm on true; meander                  *)
     OUDVORM := TRUE;

         (* 6.4 calculate slope of river surface in m/m       *)
         (*     use formula from Bloom 19??                   *)
         RIVIER.S := 2 * 0.005 * (RIVIER.Q/0.028)**(-0.37);

         (* 6.5 Discharge increases in the simulated LAND-    *)
         (*     SCAPE due to rain. This causes an increase    *)
         (*     of 1 per cent m3/sec for the simulated area   *)
         RIVIER.Q := RIVIER.Q + 0.01*RIVIER.Q;

         (* 6.6 calculates the maximum load of a meandering   *)
         (*     RIVER. The constants are from Lit.            *)

         RIVIER.MAXLAST := MB * RIVIER.Q * DALS / RIVIER.M50 +
               MS * (RIVIER.Q)**2 + MD * RIVIER.Q;

         (* 6.7 Calculates the river-width in metres          *)
     RIVIER.BREEDTE := 15 * (RIVIER.Q/0.028)**(0.5);


   END;

         (* 7 If verwilderd (braided) calculate slope and     *)
         (* and maxlast as in 6                               *)

IF RIVIER.VERWILDERD = TRUE THEN
   BEGIN
     PAD[11] := 1;
         RIVIER.M50 := 2.0;
     OUDVORM := FALSE;
         RIVIER.S := 0.325 * (RIVIER.Q/0.028)**(-0.56);
         RIVIER.Q := RIVIER.Q + 0.01*RIVIER.Q;
         RIVIER.MAXLAST := VB * RIVIER.Q * DALS / RIVIER.M50 +
                   VS * (RIVIER.Q)**2 + VD * RIVIER.Q;

END;

         (* 8 Convert River slope into grid cells             *)
VERHANG :=TRUNC( RIVIER.S * YMETER * ZMAX / ZMETER);

         (* 9 Convert rivier.breedte into grid cells          *)
LANDSCHAP.DALBREEDTE := TRUNC( RIVIER.BREEDTE * XMAX / XMETER);

         (* 10 Calculate the amount to erode in m3/sec        *)
RIVIER.QEROSIE := (RIVIER.MAXLAST - RIVIER.INLAST);
```

```
            (* 11 Convert QEROSIE into grid cells per time step *)
            (*    If qerosie > 0 then erosion                   *)
            (*    If qerosie < 0 then sedimentation             *)
     DUM :=  (3.154E10 * RIVIER.QEROSIE) /
            (XMETER/XMAX * YMETER/YMAX * ZMETER/ZMAX);

     LANDSCHAP.QEROSIE := TRUNC (DUM) +OUD;
     IF ABS(LANDSCHAP.QEROSIE) < ABS(LANDSCHAP.DALBREEDTE * 100) THEN

     BEGIN
          OUD := LANDSCHAP.QEROSIE;
          LANDSCHAP.QEROSIE := 1;
     END;
     IF ABS(LANDSCHAP.QEROSIE) >= ABS(LANDSCHAP.DALBREEDTE * 100) THEN

     BEGIN
          OUD := 0;
     END;


WRITELN(UITFOUT,TIJD,OUD,GLACIAAL,LANDSCHAP.QEROSIE,RIVIER.CHEM,hoek:5);

     IF LANDSCHAP.QEROSIE > 0 THEN
     BEGIN
          EROSIE := TRUE;
     END;

     IF LANDSCHAP.QEROSIE < 0 THEN
     BEGIN
          SEDIMENTATIE := TRUE;
     END;

 END (* procedure river *);

(*********************************************************************)
(*                                                                   *)
(*   procedure OPHEFFING (UPLIFT): Changes relief by tectonism       *)
(*                                 (UPLIFT)                          *)
(*   local variables: HOOGTE, QTEKHOOGTE, TEKTILT                    *)
(*   date: 29-05-1990                                                *)
(*                                                                   *)
(*********************************************************************)
PROCEDURE OPHEFFING;
BEGIN

            (* 1. Tectonism as uplift rate in m/1000 years (ky) *)
     LANDSCHAP.QTEKTONIEK := QTEKGEM;
     QTEKHOOGTE := QTEKHOOGTE + LANDSCHAP.QTEKTONIEK;

            (* 2. calculate the sum of uplift for a timestep in *)
            (*    in  grid cells                                *)
     HOOGTE := TRUNC(QTEKHOOGTE);
     HOEK := HOEK + QTEKHOEK;
     TEKTILT := TRUNC(HOEK);
            (* 3. If the incision m/timestep is less then the   *)
            (*    amount of uplift then tektoniek (tectonism)   *)
            (*    is true. These differences in uplift and in-  *)
            (*    cision are determined relative to the upper   *)
            (*    terrace level.                                *)
                  IF LANDSCHAP.HOOGTE < HOOGTE + INIHOOGTE THEN
     BEGIN
          PAD[1] := 1;
          TEKTONIEK := TRUE;
     END;

            (* 4. If altitude of highest terrace is less then   *)
            (*    the initial altitude + tectonism(uplift) then *)
            (*    rise all grid cells with one grid unit (1 m)  *)
     IF RELIEF[XMIN,YMIN].ZET < ZMID + HOOGTE THEN
     BEGIN
          FOR Y := YMIN TO YMAX DO
          BEGIN
               PAD[2] := 1;
               FOR X := XMIN TO XMID+2 DO
               BEGIN
               RELIEF[X,Y].ZET := RELIEF[X,Y].ZET + 1;
               END;
               FOR X := XMID+3 TO XMAX DO
               BEGIN
               RELIEF[X,Y].ZET := RELIEF[X,Y].ZET + 1 + TEKTILT;
               END;
          END;
          IF TEKTILT >= 1 THEN HOEK := 0;
     END;
END; (* procedure opheffing *)


(*********************************************************************)
(*                                                                   *)
(*   procedure BLOK: determines relief changes for each timestep     *)
(*   input: The entity LANDSCAPE                                     *)
(*          The processes                                            *)
(*          local variables                                          *)
(*   output: The entity LANDSCAPE                                    *)
(*   local variables : REROSIE, XBREEDTEMIN, XBREEDTEMAX,            *)
(*                     LUI,SMIN,TEL1,K,ZRAND, ZVALLEI, AF,RAND,      *)
(*                     LABEL 999: When relief is changed             *)
(*                     LANDSCHAP.QEROSIE than the erosion or         *)
(*                     sedimentation process stops                   *)
(*   local procedures: HAALEENLAAGWEG: erodes a cross-section        *)
(*                     ZETEENLAAGBIJ: sedimentates a cross-section   *)
(*********************************************************************)

PROCEDURE BLOK;

LABEL 999;      (* exit label                                        *)

(*********************************************************************)
(*                                                                   *)
(*   procedure HAALEENLAAGWEG (remove_one_layer)                     *)
(*   erodes one cross-section                                        *)
(*                                                                   *)
(*********************************************************************)

PROCEDURE HAALEENLAAGWEG;
BEGIN
            (* 1 erode to the left valley scarp and erode then  *)
            (* to the right valley scarp                        *)
     FOR TEL1 := 1 TO 2 DO
```

```
BEGIN

        (* 2 RAND indicates the valley scarp, at start is   *)
        (*   RAND false                                     *)
    RAND := FALSE;
    PAD[23] := 1;

        (* 3 XMID is middle of valley where eroding starts  *)
    X := XMID;
    K := 1;

        (* 4 If erosion has reached right valley scarp move *)
        (*   then one grid cell down stream xmid = xmid + 1 *)
    IF TEL1 = 2 THEN
    BEGIN
        PAD[24] := 1;
        K := -1;
        X := XMID - K;
    END;

        (* 5 Search for valley scarp or untill the calcula  *)
        (*   ted rivier.breedte  is reached                 *)
    REPEAT
        PAD[25] := 1;

        (* 5.1 determine altitude of scarp                  *)
        Z := RELIEF[X,Y].ZET;

        (* 5.2 If z=1 then error and exit                   *)
        IF Z=1 THEN
        BEGIN
            PAD[43] := 1;
            FOUT := ZETMIN;
            GOTO 999;
        END
        ELSE
        BEGIN
            PAD[26] := 1;

        (* 5.3 If insnijding (incision) lower relief with   *)
        (*     one grid unit (1 m). this grid cell is re-   *)
        (*     moved from the system. Change also the       *)
        (*     stratigraphy and the chemostratigraphy from  *)
        (*     the eroded grid cell. and decrease the value *)
        (*     of rerosie with one grid cell                *)
        IF INSNIJDING THEN
            BEGIN
                PAD[27] := 1;
                RELIEF[X,Y].ZET := Z-1;
                FOR TEL2 := 1 TO 9 DO
    RELIEF[X,Y].STRATIG[TEL2]:=RELIEF[X,Y].STRATIG[TEL2+1];
    RELIEF[X,Y].STRATIG[10] := 1;
                FOR TEL2 := 1 TO 9 DO
    RELIEF[X,Y].GEOCHEM[TEL2]:=RELIEF[X,Y].GEOCHEM[TEL2+1];
    RELIEF[X,Y].GEOCHEM[10] := 1;
                REROSIE := REROSIE - 1;
            END (* if *);
        END (* else *);

        (* 5.4 shift x positions                            *)
        (* check the valleirand (valley scarp) and the      *)
        (* valleibodem (valley bottom)                      *)
        X := X-K;
        IF RELIEF[X,Y].ZET > Z THEN RAND := TRUE;
        IF RELIEF[X,Y].ZET < Z THEN FOUT := DWARSERO;
    UNTIL RAND OR (X=XBREEDTEMIN) OR (X = XBREEDTEMAX);

        (* 6 If RAND (lateral erosion) remove the valley    *)
        (*   scarp (valleirand)                             *)
    IF RAND AND KANT THEN
    BEGIN
        PAD[28] := 1;

        (* 6.1 determine valley scarp ZRAND, determine the  *)
        (*     the altitude of valley bottom ZVALLEI        *)
        ZRAND := RELIEF[X,Y].ZET;
        ZVALLEI := RELIEF[X+K,Y].ZET;

        (* 6.2 Remove the valley scarp ZZRAND               *)
        FOR Z := ZRAND DOWNTO ZVALLEI + 1 DO
        BEGIN

        (* 6.3 check if z > 1                               *)
            IF Z > 1 THEN
            BEGIN
                PAD[29] := 1;

        (* 6.4 see for 5.3                                  *)
                RELIEF[X,Y].ZET := Z-1;
                FOR TEL2 := 1 TO 9 DO
    RELIEF[X,Y].STRATIG[TEL2]:=RELIEF[X,Y].STRATIG[TEL2+1];
    RELIEF[X,Y].STRATIG[10]:=1;
                FOR TEL2 := 1 TO 9 DO
    RELIEF[X,Y].GEOCHEM[TEL2]:=RELIEF[X,Y].GEOCHEM[TEL2+1];
    RELIEF[X,Y].GEOCHEM[10]:=1;
                REROSIE := REROSIE - 1;
            END (* if *);
        END (* for *);
    END (* if rand and kant *);
END (* for *);

        (* 7 when one cross-section is eroded it is checked *)
        (*   whether the erosion capacity has been used     *)
        (*   If erosion capacity <= 0 then exit             *)
IF REROSIE <= 0 THEN GOTO 999;

END (* procedure haaleenlaagweg *);

(*****************************************************************)
(*                                                               *)
(*   procedure ZETEENLAAGBIJ (Add_a_layer_to_it)                 *)
(*   sedimentates one cross-section                              *)
(*                                                               *)
(*****************************************************************)

PROCEDURE ZETEENLAAGBIJ;
BEGIN
```

```
          (* 1 This procedure has an a almost exactly similar *)
          (*   structures as the procedure HAALEENLAAGWEG see *)
          (*   for more explanation that procdure. The major  *)
          (*   difference is that this procedures adds new    *)
          (*   gridd cells while the other removes them       *)
    FOR TEL1 := 1 TO 2 DO
    BEGIN
         RAND := FALSE;
         PAD[36] := 1;
         X:= XMID;
         K := 1;
         IF TEL1 = 2 THEN
         BEGIN
              PAD[37] := 1;
              K := -1;
              X := XMID -K;
         END;

         REPEAT
              PAD[38] := 1;

              Z := RELIEF[X,Y].ZET;

              (* 5.2 If highest terrace equals ZMAX then exit     *)
              IF RELIEF[XMIN,YMIN].ZET >= ZMAX THEN
              BEGIN
                   PAD[44] := 1;
                   FOUT := ZETMAX;
                   GOTO 999;
              END
              ELSE
              BEGIN
                   PAD[39] := 1;

              (* 5.3 Increase grid cell with one unit (1 m) this  *)
              (*     new grid cell has the age age of the time    *)
              (*     step and the chemostratigraphy of the class  *)
              (*     which is deposited that time step            *)
                   RELIEF[X,Y].ZET := RELIEF[X,Y].ZET + 1;
                   FOR TEL2 := 10 DOWNTO 2 DO
         RELIEF[X,Y].STRATIG[TEL2]:=RELIEF[X,Y].STRATIG[TEL2-1];
         RELIEF[X,Y].STRATIG[1] := TIJD;
                   FOR TEL2 := 10 DOWNTO 2 DO
         RELIEF[X,Y].GEOCHEM[TEL2]:=RELIEF[X,Y].GEOCHEM[TEL2-1];
         RELIEF[X,Y].GEOCHEM[1] := RIVIER.CHEM;
                   REROSIE := REROSIE + 1;
                   X := X-K;
                   IF RELIEF[X,Y].ZET > Z+1 THEN RAND := TRUE;
                   IF RELIEF[X,Y].ZET < Z THEN FOUT := DWARSSED;
              END (* else *);
         UNTIL RAND OR (X=XBREEDTEMIN) OR (X=XBREEDTEMAX);

    END (* for *);

              (* 6 If erosion = 0 then exit                       *)
    IF REROSIE >= 0 THEN GOTO 999;
999; (* zeteenlaagbij *)
```

```
(*****************************************************************)
(* begin blok                                                    *)
(*****************************************************************)
BEGIN (* blok *)

              (* 1. put AF on false                               *)

    AF := FALSE;

              (* 2. determine the total amount to erode including *)
              (*    the remaining erosioncapacity of the prece-   *)
              (*    ding timestep                                 *)

    SOMEROSIE := SOMEROSIE + LANDSCHAP.QEROSIE;
    REROSIE := LANDSCHAP.QEROSIE + NUMEROSIE;

              (* 3. Check landschap.dalbreedte. a cross-section   *)
              (*    cannot be wider than 94 grid cells.           *)

    IF LANDSCHAP.DALBREEDTE > 94 THEN LANDSCHAP.DALBREEDTE := 94;

    IF KANT OR SEDIMENTATIE THEN LANDSCHAP.DALBREEDTE := 94;
    XBREEDTEMIN := TRUNC(XMID -LANDSCHAP.DALBREEDTE/2);
    XBREEDTEMAX := XBREEDTEMIN + LANDSCHAP.DALBREEDTE;

              (* 4. If erosion change relief from downstream to   *)
              (*    upstrea, (from ymax to ymin)                  *)

IF EROSIE THEN
BEGIN
    PAD[17] := 1;

              (* 4.1 Check if value of erosion is positive if not *)
              (*     then exit                                    *)

    IF REROSIE <= 0 THEN GOTO 999;

              (* 4.2 YSTOP is place where process stopped during  *)
              (*     the preceeding timestep                      *)

              (* 4.3 If slope river < slope valley erode until    *)
              (*     slope river = slope valley                   *)
    WHILE (VERHANG < LANDSCHAP.S) AND NOT AF DO
    BEGIN
         PAD[18] := 1;

              (* 4.3.1 make AF = true; if nothing erodes leave    *)
              (*       the loop.                                  *)
              (* LUI is a control variable; LUI = REROSIE         *)
         LUI := REROSIE;
         AF := TRUE;

              (* 4.3.2 Move along axis valley from YMIN to YMAX   *)
         FOR Y := YSTOP DOWNTO YMIN DO
         BEGIN

              (* 4.3.3 If relief[xmid,y] above slope line then    *)
              (*       remove at theat Y the cross-section        *)
              (*       (xmid,ymax) is staedy point                *)
              SMIN := TRUNC(VERHANG*(YMAX - Y)/YMAX);
```

```
            IF RELIEF[XMID,Y].ZET > RELIEF[XMID,YMAX].ZET+SMIN THEN

            BEGIN
                 PAD[19] := 1;
                 HAALEENLAAGWEG;

            (* 4.3.4 If value rerosie decreased then AF = false *)
                 IF REROSIE < LUI THEN
                 AF := FALSE;
            END;
       END;

            (* 4.3.5 ystop equals ymax; do to new cross-section *)
       YSTOP := YMAX;
  END (* while *);

            (* 4.4 If rivier.verhang > landschap.s then erode   *)
            (*     untill untill new slope is made              *)
            (*     see also 4.3                                 *)
  WHILE (VERHANG > LANDSCHAP.S) AND NOT AF DO
  BEGIN
       PAD[20] := 1;
       AF := TRUE;
       LUI := REROSIE;
       FOR Y := YSTOP DOWNTO YMIN DO
       BEGIN

            (* 4.4.3 see 4.3.3 but xmid,ymin is steaady point   *)

            SMIN := TRUNC(VERHANG*(-Y)/YMAX);
            IF RELIEF[XMID,Y].ZET > RELIEF[XMID,YMIN].ZET+SMIN THEN

            BEGIN
                 PAD[21] := 1;
                 HAALEENLAAGWEG;
                 IF REROSIE < LUI THEN
                 AF := FALSE;
            END;
       END;
       YSTOP := YMAX;
  END (* while *);

            (* 4.5 If slope river is slope valley or if new     *)
            (*     slope is made erode all cross-sections       *)
            (*     see action 4.3                               *)
  WHILE (VERHANG = LANDSCHAP.S) OR AF DO
  BEGIN
       PAD[22] := 1;
       LUI := REROSIE;
       FOR Y := YSTOP DOWNTO YMIN DO
       BEGIN
            HAALEENLAAGWEG;
       END;

            (* 4.5.2 If nothing eroded than exit                *)
       IF REROSIE >= LUI THEN GOTO 999;
       YSTOP := YMAX;
  END  (* while *);
END (* if erosie *);
```

```
            (* 5 If sedimentation change relief from upstream   *)
            (*   downstream from ymin to ymax, see action 4     *)
IF SEDIMENTATIE THEN
BEGIN
     PAD[30] := 1;

            (* 5.1 check if rerosie is not  negative,else exit  *)
     IF REROSIE >= 0 THEN GOTO 999;

            (* 5.2 control see 4.2                              *)

     WHILE (VERHANG < LANDSCHAP.S) AND NOT AF DO
     BEGIN
          PAD[31] := 1;
          AF := TRUE;
          LUI := REROSIE;

            (* 5.3.2 see 4.3.2 go from ystop to ymax            *)
          FOR Y := YSTOP TO YMAX DO
          BEGIN

            (* 5.3.3 If relief(xmid,y) below slope line then    *)
            (*       sedimentate at that y, relief(xmid,ymin)   *)
            (*        is steady point                           *)
            SMIN := TRUNC(VERHANG*(-Y)/YMAX);
            IF RELIEF[XMID,Y].ZET < RELIEF[XMID,YMIN].ZET+SMIN THEN

            BEGIN
                 PAD[32] := 1;
                 ZETEENLAAGBIJ;
                 IF REROSIE > LUI THEN
                 AF := FALSE;
            END;
          END;
          YSTOP := YMIN;
     END (* while *);

            (* 5.4 see 4.4 for sedimentation                    *)
     WHILE (VERHANG > LANDSCHAP.S) AND NOT AF DO
     BEGIN
          PAD[33] := 1;
          AF := TRUE;
          LUI := REROSIE;
          FOR Y := YSTOP TO YMAX DO
          BEGIN
            (* 5.4.3 see 5.3.3 but relief[xmid,ymax] is  steady *)
            SMIN := TRUNC(VERHANG*(YMAX-Y)/YMAX);
            IF RELIEF[XMID,Y].ZET < SMIN+RELIEF[XMID,YMAX].ZET THEN
            BEGIN
                 PAD[34] := 1;
                 ZETEENLAAGBIJ;
                 IF REROSIE > LUI THEN
                 AF := FALSE;
            END;
          END;
          YSTOP := YMIN;
     END (* while *);

            (* 5.5 see 4.5 for sedimentation                    *)
```

```
     WHILE (VERHANG = LANDSCHAP.S) OR AF DO
     BEGIN
          PAD[35] := 1;
          LUI := REROSIE;
          FOR Y := YSTOP TO YMAX DO
          BEGIN
               ZETEENLAAGBIJ;
          END;
          IF REROSIE <= LUI THEN GOTO 999;
          YSTOP := YMIN;
     END (* while *);

END (* if sedimentatie *);

               (* 6. exit label                                    *)
999:
     PAD[42] := 1;

               (* 6.1 Dumerosie becomes rerosie                    *)
               (*     in case of large dumerosie a error notify    *)

     DUMEROSIE :=REROSIE;
     IF DUMEROSIE > 1E5 THEN FOUT := DUMERO;

               (* 6.2 determine new slope of valley, determine     *)
               (*     difference between highhest terrace and val- *)
               (*     ley bottom                                   *)
     LANDSCHAP.S := RELIEF[XMID,YMIN].ZET - RELIEF[XMID,YMAX].ZET;
     LANDSCHAP.HOOGTE := RELIEF[XMIN,YMIN].ZET-RELIEF[XMID,YMIN].ZET;

     YSTOP := Y;

END (* blok *);


(*********************************************************************)
(*                                                                   *)
(*   begin of main Program LIMTER                                    *)
(*   date: 30-05-1990                                                *)
(*                                                                   *)
(*********************************************************************)

BEGIN (* LIMTER *);

               (* 1. Open the files                                 *)
     OPEN(RELIEF1,'RELIEF1.DAT',NEW);
     REWRITE(RELIEF1);
     OPEN(RELIEF2,'RELIEF2.DAT',NEW);
     REWRITE(RELIEF2);
     OPEN(UITSTRATIG,'STRATIG.DAT',NEW);
     REWRITE(UITSTRATIG);
     OPEN(GEOCHEMIG,'CHEMIG.DAT',NEW);
     REWRITE(GEOCHEMIG);
     OPEN(LOGBOEK,'LOGBOEK.DAT',NEW);
     REWRITE(LOGBOEK);
     OPEN(UITFOUT,'FOUT.DAT',NEW);
     REWRITE(UITFOUT);
     OPEN(UITSTRATIS,'STRATIS.DAT',NEW);
     REWRITE(UITSTRATIS);
     OPEN(GEOCHEMIS,'CHEMIS.DAT',NEW);
     REWRITE(GEOCHEMIS);
     OPEN(SINUS,'SINUS.DAT',NEW);
     REWRITE(SINUS);

               (* 2. Initialise variables                          *)
     OUDQ := 0;
     OUDINLAST := 0;
               (* 2.1 make OUDVORM is meander                      *)
     OUDVORM := TRUE;
     GLACIAAL := 0;
     GRENS := FALSE;
     LANDSCHAP.S := 7;
     DUMMY := TRUE;
     SOMEROSIE := 0;
     TEKTILT := 0;
     PI := 4*ARCTAN(1);
     LANDSCHAP.HOOGTE := INIHOOGTE;
     UIT1 := 0;
     UIT2 := 0;
     UIT3 := 0;
     VERHANG := 10;
     YSTOP := 1;
     OUD := 0;
               (* 2.2 Make initial relief, with intial strati-     *)
               (* graphy of one                                    *)
     FOR Y := YMIN TO YMAX DO
     BEGIN
          FOR X := XMIN TO 23 DO
          BEGIN
               RELIEF[X,Y].ZET := ZMID;
               FOR K := 1 TO 10 DO
               RELIEF[X,Y].STRATIG[K] := 1;
               FOR K := 1 TO 10 DO
               RELIEF[X,Y].GEOCHEM[K] := 1;
          END;
          FOR X := 24 TO 77 DO
          BEGIN
               RELIEF[X,Y].ZET := ZMID - LANDSCHAP.HOOGTE;
               FOR K := 1 TO 10 DO
               RELIEF[X,Y].STRATIG[K] := 1;
               FOR K := 1 TO 10 DO
               RELIEF[X,Y].GEOCHEM[K] := 1;
          END;
          FOR X := 78 TO XMAX DO
          BEGIN
               RELIEF[X,Y].ZET := ZMID;
               FOR K := 1 TO 10 DO
               RELIEF[X,Y].STRATIG[K] := 1;
               FOR K := 1 TO 10 DO
               RELIEF[X,Y].GEOCHEM[K] := 1;
          END;
     END (* for *);


               (* 3. Time loop. Time in thousand years (ky)        *)
               (* Repeat loop until tijd=tmax                      *)
               (* Or until relief is too high or too low           *)
TIJD := TMIN;
REPEAT
BEGIN
```

```
            (* 3.1 Initial processes                              *)

    RIVIER.MEANDER := FALSE;
    RIVIER.VERWILDERD := FALSE;
    TEKTONIEK := FALSE;
    EROSIE := FALSE;
    INSNIJDING := FALSE;
    KANT := FALSE;
    SEDIMENTATIE := FALSE;
    FOUT := OKAY;

       FOR I := 1 TO 45 DO
    BEGIN
          PAD[I] := 0;
       END;

            (* 3.2 Calculate entity RIVER                         *)
    FLUSS;


            (* 3.3 Determine tectonism                            *)
    OPHEFFING;

            (* 3.4 Decission rules                                *)

IF TEKTONIEK AND EROSIE AND RIVIER.MEANDER    THEN INSNIJDING := TRUE;
IF     TEKTONIEK AND EROSIE     AND RIVIER.VERWILDERD THEN
                            BEGIN
                                 INSNIJDING := TRUE;
                                 KANT := TRUE;
                            END;
IF     TEKTONIEK AND SEDIMENTATIE AND RIVIER.MEANDER THEN DUMMY := TRUE;
IF     TEKTONIEK AND SEDIMENTATIE AND RIVIER.VERWILDERD THEN DUMMY:= TRUE;
IF NOT TEKTONIEK AND EROSIE       AND RIVIER.MEANDER THEN
                            BEGIN
                                  INSNIJDING := TRUE;
                                 KANT := TRUE;
                            END;
IF NOT TEKTONIEK AND EROSIE       AND RIVIER.VERWILDERD THEN KANT := TRUE;
IF NOT TEKTONIEK AND SEDIMENTATIE AND RIVIER.MEANDER THEN DUMMY := TRUE;
IF NOT TEKTONIEK AND SEDIMENTATIE AND RIVIER.VERWILDERD THEN DUMMY := TRUE;

            (* 3.5 Change relief                                  *)
    BLOK;

            (* 3.6 storing orders by write commandos              *)




            (* 3.6.1 determine errors. Stop simulation if         *)
            (*   ZETMAX or SETMIN, report error in error notify   *)
            (*   file                                             *)
    CASE FOUT OF
         ZETMIN:
              BEGIN
                   WRITELN(UITFOUT,FOUT,TIJD);
                   GRENS := TRUE;
              END;
         ZETMAX:
              BEGIN
                   WRITELN(UITFOUT,FOUT,TIJD);
                   GRENS := TRUE;
              END;
         DWARSERO: WRITELN(UITFOUT,FOUT,TIJD);
         DWARSSED:  WRITELN(UITFOUT,FOUT,TIJD);
         DUMERO: WRITELN(UITFOUT,FOUT,TIJD);
         OKAY:
    END;

, WRITE(SINUS,TIJD,RIVIER.Q:8,RIVIER.INLAST:8,RIVIER.QEROSIE:8);
 WRITELN(SINUS,TEKTONIEK,EROSIE,RIVIER.MEANDER,INSNIJDING,KANT);

            (* 3.6.2 If time is UITlMAX or a multiply of it       *)
            (* store cross-section, stratigraphy, and most        *)
            (* important variables to LOGBOEK                     *)

    UIT1 := UIT1 + 1;
    IF UIT1 = UIT1MAX THEN
    BEGIN
         UIT1 := 0;

            (* 3.6.2.1 In LOGBOEK are listed on the first line    *)
            (* time and entity RIVER, on the second line the      *)
            (* entity LANDSCAPE and some local variables. on      *)
            (* third line are the process booleans  listed        *)

         WRITELN(LOGBOEK, TIJD:5,RIVIER.Q:9,RIVIER.INLAST:9,
              RIVIER.S:6,RIVIER.BREEDTE:9,
              RIVIER.MAXLAST:9,RIVIER.QEROSIE:9);

         WITH LANDSCHAP DO
         BEGIN
              WRITE(LOGBOEK,QTEKTONIEK:8,HOOGTE:5,
                   QEROSIE:6,DUMEROSIE:6,SOMEROSIE:8,
                   S:5,VERHANG:5);
         END;

         Z:=RELIEF[XMID,YMAX].ZET;
         WRITELN(LOGBOEK,Z,RELIEF[XMID,YMIN].ZET:5);
         WRITELN(LOGBOEK, TEKTONIEK,RIVIER.MEANDER,RIVIER.VERWILDERD,

                   EROSIE,SEDIMENTATIE,INSNIJDING,KANT);


            (* 3.6.2.2 write cross-section at y = 90 to RELIEF1 *)
            (* On each line are 24 z-coordinates. four line is  *)
            (* one cross-section                                *)
         Y := 90;
         FOR X := XMIN TO 25 DO
              WRITE(RELIEF1,RELIEF[X,Y].ZET:5);
         WRITELN(RELIEF1);
         FOR X := 26 TO XMID DO
              WRITE(RELIEF1,RELIEF[X,Y].ZET:5);
         WRITELN(RELIEF1);
         FOR X := XMID + 1 TO 75 DO
              WRITE(RELIEF1,RELIEF[X,Y].ZET:5);
         WRITELN(RELIEF1);
         FOR X := 76 TO XMAX DO
              WRITE(RELIEF1,RELIEF[X,Y].ZET:5);
```

```
     WRITELN(RELIEF1);

          (* 3.6.2.3 Write stratigraphy of cross-section      *)
          (* to UITSTRATIS.   Each line contains the time     *)
          (* a z-coordinate, and the relative ages of the     *)
          (* sediments in the upper ten grid cells for each   *)
          (* z-coordinate, 100 lines is one cross-section     *)
     FOR X:= XMIN TO XMAX DO
     BEGIN
          Z := RELIEF[X,Y].ZET;
          WRITE(UITSTRATIS,Z:5,X:5,TIJD:5);
          FOR TEL2 := 1 TO 10 DO
          BEGIN
               TEL3 := RELIEF[X,Y].STRATIG[TEL2];
               WRITE(UITSTRATIS,TEL3:5);
          END;
          WRITELN(UITSTRATIS);
     END;
     FOR X:= XMIN TO XMAX DO
     BEGIN
          Z:= RELIEF[X,Y].ZET;
          WRITE(GEOCHEMIS,Z:5,X:5,TIJD:5);
          FOR TEL2 := 1 TO 10 DO
          BEGIN
               TEL3 := RELIEF[X,Y].GEOCHEM[TEL2];
               WRITE(GEOCHEMIS,TEL3:5);
          END;
          WRITELN(GEOCHEMIS);
     END;

END; (* if uitlmax *)

          (* 3.6.3 If time is a multiple of UIT2MAX or if     *)
          (* GRENS (error) than write releif to file and      *)
          (* write stratigraphy to relief2.                   *)
UIT2 := UIT2 + 1;
IF (UIT2 = UIT2MAX) OR GRENS THEN
BEGIN
     UIT2 := 0;

          (* 3.6.3.1 each lines contain 25 z-coordinaten.     *)
          (* four lines is one cross-section and              *)
          (* 25 cross-sections are one relief                 *)
     FOR TEL1 := 1 TO 25 DO
     BEGIN
          Y := 4*TEL1;
          FOR X := XMIN TO 25 DO
          WRITE(RELIEF2,RELIEF[X,Y].ZET:5);
          WRITELN(RELIEF2);
          FOR X := 26 TO XMID DO
          WRITE(RELIEF2,RELIEF[X,Y].ZET:5);
          WRITELN(RELIEF2);
          FOR X := XMID + 1 TO 75 DO
          WRITE(RELIEF2,RELIEF[X,Y].ZET:5);
          WRITELN(RELIEF2);
          FOR X := 76 TO XMAX DO
          WRITE(RELIEF2,RELIEF[X,Y].ZET:5);
          WRITELN(RELIEF2);

     END;
```

```
WRITELN(RELIEF2);

     (* 3.6.3.2 write stratigraphy of RELIEF2 in         *)
     (* UITSTRATIG. only surface stratigraphy is stored  *)
     (* Each line contains the stratigraphy for each 4X  *)
     (* 25 lines ois one relief                          *)
FOR TEL1 := 1 TO 25 DO
BEGIN
     Y := 4*TEL1;
     FOR X := 1 TO 25 DO
          WRITE(UITSTRATIG,RELIEF[X,Y].STRATIG[1]:5);
     WRITELN(UITSTRATIG);
     FOR X := 26 TO 50 DO
          WRITE(UITSTRATIG,RELIEF[X,Y].STRATIG[1]:5);
     WRITELN(UITSTRATIG);
     FOR X := 51 TO 75 DO
          WRITE(UITSTRATIG,RELIEF[X,Y].STRATIG[1]:5);
     WRITELN(UITSTRATIG);
     FOR  X := 76 TO 100 DO
          WRITE(UITSTRATIG,RELIEF[X,Y].STRATIG[1]:5);
     WRITELN(UITSTRATIG);
END;
WRITELN(UITSTRATIG);

FOR TEL1 := 1 TO 25 DO
BEGIN
     Y := 4*TEL1;
     FOR X := 1 TO 25 DO
          WRITE(GEOCHEMIG,RELIEF[X,Y].GEOCHEM[1]:5);
     WRITELN(GEOCHEMIG);
     FOR X := 26 TO 50 DO
          WRITE(GEOCHEMIG,RELIEF[X,Y].GEOCHEM[1]:5);
     WRITELN(GEOCHEMIG);
     FOR X := 51 TO 75 DO
          WRITE(GEOCHEMIG,RELIEF[X,Y].GEOCHEM[1]:5);
     WRITELN(GEOCHEMIG);
     FOR X := 76 TO 100 DO
          WRITE(GEOCHEMIG,RELIEF[X,Y].GEOCHEM[1]:5);
     WRITELN(GEOCHEMIG);
END;
WRITELN(GEOCHEMIG);

     (* DUMMY always true                                *)
IF NOT DUMMY THEN
BEGIN
     FOR TEL1 := 1 TO 3 DO
     BEGIN
          CASE TEL1 OF
               1: Y := 10;
               2: Y := 50;
               3: Y := 90;
          END;

          FOR X := XMIN TO XMAX DO
          BEGIN
               Z := RELIEF[X,Y].ZET;
               WRITE(UITSTRATIG,X:5,Z:5);
               FOR TEL2 := 1 TO 10 DO
               BEGIN
                    TEL3 := RELIEF[X,Y].STRATIG[TEL2];
```

```
                        WRITE(UITSTRATIG,TEL3:5);
                    END;
                    WRITELN(UITSTRATIG);
                END (* for *);
            END (* for *);
        END (* not dummy *);
    END (* if uit2max *);
END (* time loop *);

            (* 4 Go to the next timestep                    *)
TIJD := TIJD + 1;
UNTIL (TIJD = TMAX + 1) OR GRENS;


            (* 5. Close files                               *)
    CLOSE(RELIEF1);
    CLOSE(RELIEF2);
    CLOSE(UITSTRATIG);
    CLOSE(GEOCHEMIG);
    CLOSE(LOGBOEK);
    CLOSE(UITFOUT);
    CLOSE(UITSTRATIS);
    CLOSE(GEOCHEMIS);
    CLOSE(SINUS);

END (* LIMTER *).
```